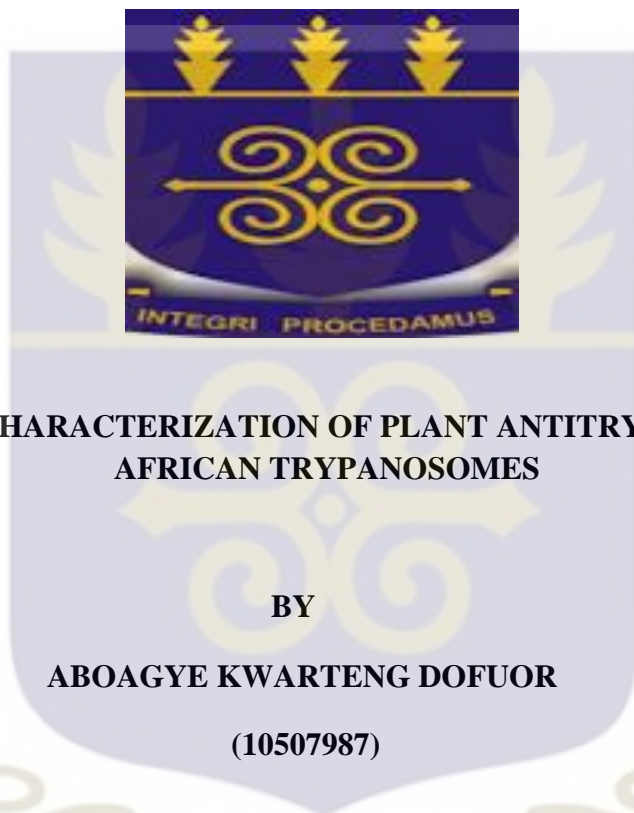


WEST AFRICA CENTRE FOR CELL BIOLOGY OF INFECTIOUS PATHOGENS
DEPARTMENT OF BIOCHEMISTRY, CELL AND MOLECULAR BIOLOGY
SCHOOL OF BIOLOGICAL SCIENCES
COLLEGE OF BASIC AND APPLIED SCIENCES
UNIVERSITY OF GHANA, LEGON



**ISOLATION AND CHARACTERIZATION OF PLANT ANTITRYPANOSOMALS FOR
AFRICAN TRYPANOSOMES**

BY

ABOAGYE KWARTENG DOFUOR

(10507987)

**THIS THESIS IS SUBMITTED TO THE DEPARTMENT OF BIOCHEMISTRY, CELL
AND MOLECULAR BIOLOGY, COLLEGE OF BASIC AND APPLIED SCIENCES,
UNIVERSITY OF GHANA, LEGON, IN PARTIAL FULFILMENT OF THE
REQUIREMENT FOR THE AWARD OF PHD MOLECULAR CELL BIOLOGY OF
INFECTIOUS DISEASES DEGREE**

JULY, 2018

DECLARATION

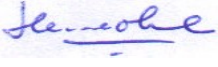
I, Aboagye Kwarteng Dofuor, do hereby declare that except for references to other people's work, for which I have acknowledged, this report is the product of my own research carried out at the West African Centre for Cell Biology of Infectious Pathogens (WACCBIP), Department of Biochemistry, Cell and Molecular Biology, University of Ghana, Legon, Ghana, Centre for Plant Medicine Research, Mampong-Akuapem, Ghana, Noguchi Memorial Institute for Medical Research (NMIMR) Department of Parasitology, University of Ghana, Legon, Ghana, Department of Chemistry, University of Ghana, Legon, Ghana and the Department of Pathogen Molecular Biology, London School of Hygiene and Tropical Medicine, University of London, United Kingdom, under the supervision of Prof. Laud Kenneth Okine, Prof. Mitsuko Ohashi, Dr. Theresa Manful Gwira, Dr. Kwaku Kyeremeh and Dr. Sam Alford.

ABOAGYE KWARTENG DOFUOR (STUDENT)

SIGNATURE: 

DATE: 31/07/2018

PROF. LAUD KENNETH OKINE (PRINCIPAL SUPERVISOR)

SIGNATURE: 

DATE: 31/07/2018

PROF. MITSUKO OHASHI (CO-SUPERVISOR)

SIGNATURE: 大橋 光子

DATE: 31/07/2018

DR. THERESA MANFUL GWIRA (CO-SUPERVISOR)

SIGNATURE: 

DATE: 31/07/2018

DR. KWAKU KYEREMEH (CO-SUPERVISOR)

SIGNATURE: 

DATE: 31/07/2018

DR. SAM ALSFORD (CO-SUPERVISOR)

SIGNATURE: 

DATE: 31/07/2018

DEDICATION

This thesis is dedicated to the Almighty God, my family and all friends for their support and loyalty.

ACKNOWLEDGMENT

I acknowledge all my supervisors for their guidance and encouragement throughout the research period. I am grateful to Dr. Alfred Ampomah Appiah, Frederick Ayertey, Peter Bola, Herone Blagogee and Henry Brew-Daniels of the Centre for Plant Medicine Research, Mampong-Akuapem, Ghana, for their expertise with respect to the identification of plant species, collection of plant materials, preparation of crude extracts or fractions and the chromatography of selected fractions. I acknowledge the laboratory assistance of Michael Amoa-Bosompem, Gina I. Djameh, Thelma Tetteh, Faustus Akankperiwen Azerigyik, Kofi Baffour-Awuah Owusu, as well as all colleagues and staff of the Department of Parasitology, Noguchi Memorial Institute for Medical Research, University of Ghana, Legon, Ghana, with respect to the screening of antitrypanosomal activities of plant fractions and isolated compounds. I would like to acknowledge the immense technical support of Enoch Osei, Samuel Kwain and Gilbert Tetevi Kwami Mawuli of the Department of Chemistry, University of Ghana, Legon, Ghana, concerning the purification and identification of antitrypanosomal compounds from selected plant fractions. Sanger sequencing was performed at Source BioScience (<https://www.sourcebioscience.com>), UK. Mass spectrometry was performed at the Sanger Building, Department of Biochemistry, University of Cambridge. I am highly grateful to Prof. (Mrs.) Regina Appiah-Opong, NMIMR, University of Ghana for the generous provision of Jurkat and Chang liver (HeLa derivative) cell lines. I am grateful to Prince Berko Nyarko, WACCBIP, University of Ghana, Legon, Ghana, for his practical assistance in flow cytometry. I would also like to thank Dr. Juan Macedo, London School of Hygiene and Tropical Medicine, University of London, UK, for the immense laboratory and technical expertise concerning RNA interference library screening of selected antitrypanosomal compounds.

TABLE OF CONTENTS

DECLARATION.....	ii
DEDICATION.....	iv
ACKNOWLEDGMENT.....	v
LIST OF TABLES.....	xii
LIST OF FIGURES.....	xiii
ABBREVIATIONS AND ACRONYMS.....	xvi
ABSTRACT.....	xxii
CHAPTER ONE	1
1.0 INTRODUCTION.....	1
1.1 BACKGROUND	1
1.2 PROBLEM STATEMENT AND JUSTIFICATION	4
1.3 HYPOTHESIS.....	6
1.4 CONCEPTUAL FRAMEWORK.....	6
1.5 AIM/SPECIFIC OBJECTIVES	7
1.5.1 Aim.....	7
1.5.2 Specific Objectives	7
CHAPTER TWO	8
2.0 LITERATURE REVIEW	8
2.1 MEDICINAL VALUES OF PLANTS	8
2.2 CLASSIFICATION AND BOTANICAL DESCRIPTION OF <i>ZANTHOXYLUM</i>	9
2.3 TRADITIONAL USES OF <i>ZANTHOXYLUM</i>.....	11
2.4 PHYTOCHEMISTRY OF <i>ZANTHOXYLUM</i>.....	12
2.5 PHARMACOLOGY OF <i>ZANTHOXYLUM</i>.....	13

2.6 CLASSIFICATION AND BOTANICAL DESCRIPTION OF <i>BIDENS</i>	17
2.7 TRADITIONAL USES OF <i>BIDENS</i>	18
2.8 PHYTOCHEMISTRY OF <i>B. PILOSA</i>	19
2.9 PHARMACOLOGY OF <i>B. PILOSA</i>	19
2.10 <i>TRYPANOSOMATIDAE</i>: CLASSIFICATION AND BIOLOGICAL DESCRIPTION	25
2.11 GENOME ORGANIZATION OF <i>T. BRUCEI</i>	28
2.12 CELL DEATH IN <i>TRYPANOSOMATIDAE</i>	29
2.13 CELL CYCLE IN <i>TRYPANOSOMATIDAE</i>	33
2.14 CONTROL OF AFRICAN TRYPANOSOMIASIS	40
2.14.1 Vector control of African trypanosomiasis	41
2.14.2 Vaccine development for African trypanosomiasis	45
2.14.3 Chemotherapeutic control of African trypanosomiasis	47
2.15 CHALLENGES IN THE CONTROL OF AFRICAN TRYPANOSOMIASIS	51
2.16 RNA INTERFERENCE IN <i>T. BRUCEI</i>	52
CHAPTER THREE	57
3.0 MATERIALS AND METHODS	57
3.1 CULTURE OF PARASITES AND HUMAN CELL LINES	57
3.2 CRUDE EXTRACTION AND FRACTIONATION OF PLANTS	57
3.3 CHROMATOGRAPHIC AND SPECTROSCOPIC ANALYSIS	60
3.4 ISOLATION AND STRUCTURE ELUCIDATION OF ANTITRYPANOSOMALS ..	61
3.5 CELL VIABILITY ASSAY	63
3.6 CELL DEATH ASSAY	63

3.7 CELL CYCLE ASSAY.....	64
3.8 FLUORESCENCE MICROSCOPY	64
3.9 ANTITRYPANOSOMAL SENSIVITY ASSAY	65
3.10 INDUCTION OF RNAI LIBRARY STRAINS.....	65
3.11 INDUCIBILITY ASSAY	66
3.12 EXTRACTION OF GENOMIC DNA FROM LIBRARY STRAINS	67
3.13 AMPLIFICATION AND ELECTROPHORESIS OF RNAI TARGET FRAGMENTS	67
3.14 PURIFICATION OF RNAi TARGET AMPLICONS.....	68
3.15 MOLECULAR CLONING OF RNAI TARGET AMPLICONS.....	69
3.16 PURIFICATION OF LIGATION PRODUCT	69
3.17 RESTRICTION DIGESTION OF RECOMBINANT PLASMIDS.....	70
3.18 SANGER SEQUENCING	71
3.19 STATISTICAL ANALYSIS	71
CHAPTER FOUR.....	72
4.0 RESULTS	72
4.1 ANTITRYPANOSOMAL ACTIVITY OF KUPCHAN FRACTIONS.....	72
4.2 EFFECT OF KUPCHAN FRACTIONS ON CELL DEATH/CELL CYCLE OF <i>T. BRUCEI</i> <i>BRUCEI</i>	74
4.3 EFFECTS OF KUPCHAN FRACTIONS ON CELL MORPHOLOGY OF <i>T. BRUCEI</i>	76
4.4 EFFECT OF COLUMN FRACTIONS ON CELL VIABILITY OF <i>T. BRUCEI</i>	78
4.5 HIGH RESOLUTION ELECTROSPRAY IONIZATION MASS SPECTROMETRY ANALYSIS OF KUPCHAN FRACTIONS	79

4.6 STRUCTURE DETERMINATION OF A NOVEL COMPOUND FROM Z. ZANTHOXYLOIDES	89
4.7 ISOLATION AND IDENTIFICATION OF THE STRUCTURAL FUNCTIONALITY OF ZR-FD-C4-C3	93
4.8 ISOLATION AND IDENTIFICATION OF THE STRUCTURAL FUNCTIONALITY OF BP-FD-HB and BP-FD-HC.....	97
4.9 EFFECTS OF COMPOUNDS ON CELL VIABILITY OF <i>T. BRUCEI</i>	100
4.10 EFFECTS OF COMPOUNDS ON CELL CYCLE OF <i>T. BRUCEI</i>.....	101
4.11 GROWTH INHIBITION OF <i>T. BRUCEI</i> BY COMPOUNDS	102
4.12 EFFECTS OF COMPOUNDS ON INDUCTION OF RNAI LIBRARY	103
4.13 ANTITRYPANOSOMAL SENSITIVITY OF SELECTED COMPOUNDS	106
4.14 CLONING AND SEQUENCING OF RNAI FRAGMENTS.....	107
4.15 INDUCIBILITY ANALYSIS OF COMPOUNDS.....	109
CHAPTER FIVE	111
5.0 DISCUSSION, CONCLUSIONS AND RECOMMENDATIONS	111
5.1 DISCUSSION	111
5.2 CONCLUSIONS	118
5.3 RECOMMENDATIONS.....	118
REFERENCES.....	120
APPENDICES.....	172
Appendix 1: Full ¹³C-NMR spectrum of zanthoxylamide.....	172
Appendix 2: gHSQC NMR spectrum of zanthoxylamide	173
Appendix 3: gHSQC NMR spectrum of zanthoxylamide	174

Appendix 4: Expanded ¹ H-NMR spectrum of zanthoxylamide, version 1	175
Appendix 5: Expanded ¹ H-NMR spectrum of zanthoxylamide, version 2	176
Appendix 6: Expanded ¹ H-NMR spectrum of zanthoxylamide, version 3	177
Appendix 7: Expanded ¹ H-NMR spectrum of zanthoxylamide, version 4	178
Appendix 8: Expanded COSY-NMR spectrum of zanthoxylamide, version 1	179
Appendix 9: Expanded COSY-NMR spectrum of zanthoxylamide, version 2	180
Appendix 10: Expanded COSY-NMR spectrum of zanthoxylamide, version 3	181
Appendix 11: Expanded COSY-NMR spectrum of zanthoxylamide, version 4	182
Appendix 12: Expanded HMBC-NMR spectrum of zanthoxylamide, version 1	183
Appendix 13: Expanded HMBC-NMR spectrum of zanthoxylamide, version 2	184
Appendix 14: Expanded HMBC-NMR spectrum of zanthoxylamide, version 3	185
Appendix 15: Expanded HMBC-NMR spectrum of zanthoxylamide, version 4	186
Appendix 16: Expanded HMBC-NMR spectrum of zanthoxylamide, version 5	187
Appendix 17: Expanded HSQCTOCSY-NMR spectrum of zanthoxylamide.....	188
Appendix 18: HSQCTOCSY-NMR spectrum of zanthoxylamide	189
Appendix 19: Expanded HSQCTOCSY-NMR spectrum of zanthoxylamide, version 1 ...	190
Appendix 20: Expanded HSQCTOCSY-NMR spectrum of zanthoxylamide, version 2 ...	191
Appendix 21: Expanded HSQCTOCSY-NMR spectrum of zanthoxylamide, version 3 ...	192
Appendix 22: Expanded HSQCTOCSY-NMR spectrum of zanthoxylamide, version 4 ...	193
Appendix 23: Expanded HSQCTOCSY-NMR spectrum of zanthoxylamide, version 5 ...	194
Appendix 24: Expanded HSQCTOCSY-NMR spectrum of zanthoxylamide, version 6 ...	195
Appendix 25: Expanded HSQCTOCSY-NMR spectrum of zanthoxylamide, version 7 ...	196
Appendix 26: Expanded NOESY-NMR spectrum of zanthoxylamide, version 1.....	197

Appendix 27: Expanded NOESY-NMR spectrum of zanthoxylamide, version 2.....	198
Appendix 28: ¹ H NMR spectrum of ZRFD-C4-C3.....	199
Appendix 29: ¹³ C NMR spectrum of ZRFD-C4-C3.....	200
Appendix 30: ¹ H NMR spectrum of BPDFD-HC.....	201
Appendix 31: gHSQC spectrum of BP-FD-HC.....	202
Appendix 32: ¹ H NMR spectrum of BPDFD-HB.....	203
Appendix 33: Dose-response curves of Kupchan fractions.....	204
Appendix 34: Effects of Kupchan fractions on cell cycle of <i>T. brucei</i>	205
Appendix 35: Effects of Kupchan fractions on induction of cell death in <i>T. brucei</i>	206
Appendix 36: Effects of compounds on cell cycle of <i>T. brucei</i>	207
Appendix 37: Protein sequence: Tb927.4.2100, hypothetical	208
Appendix 38: Protein sequence: Tb927.3.1490, leucine-rich repeat protein, putative.....	209
Appendix 39: Protein sequence: Tb927.4.3880, receptor-type adenylate cyclase GRESAG 4, putative.....	210
Appendix 40: Protein sequence: Tb927.11.9770, hypothetical, conserved	211
Appendix 41: Protein sequence: Tb927.11.1640, stumpy formation signaling pathway, putative.....	212

LIST OF TABLES

Table 2.1: Pharmacology of <i>Z. zanthoxyloides</i>	16
Table 2.2: Pharmacology of <i>B. pilosa</i>	24
Table 3.1: PCR protocol for amplification of RNAi target fragments.....	68
Table 3.2: PCR cycle reactions for amplification of RNAi target fragments.....	68
Table 4.1: Effect of Kupchan fractions on cell viability of <i>T. brucei</i> , Jurkat and Chang liver cells.....	73
Table 4.4: Effect of column chromatographic fractions on cell viability of <i>T. brucei</i>	79
Table 4.6.1: NMR analysis of zanthoxylamide.....	90
Table 4.9: Effect of compounds on cell viability of <i>T. brucei</i> and Chang liver cells.....	100

LIST OF FIGURES

Figure 2.1: A picture of <i>Z. zanthoxyloides</i> at the environs of Center for Plant Medicine Research, Mampong-Akuapem, Ghana.....	10
Figure 2.2: A picture of <i>B. pilosa</i> at the environs of Center for Plant Medicine Research, Mampong-Akuapem, Ghana.....	18
Figure 2.3: A diagram depicting the cellular mechanisms of apoptosis and necrosis in eukaryotes	33
Figure 2.4: A schematic diagram depicting the cell cycle phases in <i>T. brucei</i>	40
Figure 2.5: Chemotherapeutic control of AAT.....	50
Figure 2.6: Chemotherapeutic control of HAT.....	50
Figure 2.7: A schematic diagram of RNA interference target sequencing (RITseq).....	56
Figure 3.1: Schematic for modified Kupchan method of liquid-liquid extraction.....	59
Figure 3.2: A simplified diagram of the genetic constitution of the RNAi library.....	66
Figure 4.2.1: Effect of selected fractions on induction of cell death in <i>T. brucei</i>	74
Figure 4.2.2: Effect of selected fractions on cell cycle of <i>T. brucei</i>	76
Figure 4.3: Effect of selected fractions on cell morphology and structure of <i>T. brucei</i>	77
Figure 4.5.1: HRESI-LC-MS ⁿ analysis of ZRFH.....	81
Figure 4.5.2A: HRESI-LC-MS ⁿ analysis of ZRFD, version 1.....	82

Figure 4.5.2B: HRESI-LC-MS ⁿ analysis of ZRFD, version 2.....	83
Figure 4.5.3: HRESI-LC-MS ⁿ analysis of ZRFM.....	84
Figure 4.5.4: HRESI-LC-MS ⁿ analysis of ZRWB.....	85
Figure 4.5.5: HRESI-LC-MS ⁿ analysis of BPFH.....	86
Figure 4.5.6: HRESI-LC-MS ⁿ analysis of BPFD.....	87
Figure 4.5.7: HRESI-LC-MS ⁿ analysis of BPFM.....	87
Figure 4.6.1: HRESI-LC-MS ⁿ analysis of zanthoxylamide showing various fragmentation peaks.....	90
Figure 4.6.2: Structure of zanthoxylamide showing COSY, TOCSY, HMBC and NOESY correlations.....	91
Figure 4.6.3: Fragmentation of zanthoxylamide via labile bond cleavage.....	92
Figure 4.7.1: HPLC profile of ZR-FD fraction showing the peak that yielded the compound ZR-FD-C4-C3.....	93
Figure 4.7.2: HPLC-UV spectrum of ZRFD-C4-C3	94
Figure 4.7.3: HRESI-LC-MS ⁿ analysis of ZRFD-C4-C3.....	95
Figure 4.7.4: Fragmentation pattern of ZRFD-C4-C3 via labile bond cleavage analysis.....	96
Figure 4.8.1: HPLC profile of BPFD fraction	97
Figure 4.8.2: HPLC-UV spectrum of BPFD-HB.....	98

Figure 4.8.3: HRESI-LC-MS ⁿ analysis of BPFH-HB.....	99
Figure 4.8.4: Fragmentation pattern of BPFH-HB and BPFH-HC via labile bond cleavage..	99
Figure 4.10: Effect of compounds on cell cycle of <i>T. brucei</i>	101
Figure 4.11: Inhibition of growth of <i>T. brucei</i> by compounds.....	103
Figure 4.12.1: Induction of RNAi by antitrypanosomal compounds.....	105
Figure 4.12.2: PCR of selected RNAi library strains.....	106
Figure 4.13.1: Antitrypanosomal sensitivity of compounds.....	107
Figure 4.14.1: Cloning of selected RNAi fragments.....	108
Figure 4.14.2: Capillary sequencing of RNAi fragments.....	109
Figure 4.15: Inducibility analysis of selected compounds.....	110

ABBREVIATIONS AND ACRONYMS

AAT: Animal African trypanosomiasis

AdoMetDC: S-adenosyl methionine decarboxylase

Apaf-1: Apoptotic protease activating factor 1

Asf1: Nucleosome assembly factor

AT: African trypanosomiasis

Bax/Bak: Bcl-2 associated X/Bcl-2 antagonist

Bcl-2: B-cell lymphoma-2

BLAST: Basic local alignment search tool

BP: *Bidens pilosa* L.

BUB1: Spindle checkpoint serine/threonine protein kinase

CAK: CDK-activating kinase

Cdc: Cell division cycle

CDK: Cyclin dependent kinase

Cdt 1: Chromatin licensing and DNA replication factor- 1

CenH3: Centromeric histone

COSY: Correlation Spectroscopy

CP: Cysteine protease

CRK: Cdc2-related kinase

DAPI: 4', 6-diamidino-2-phenylindole

DCM: Dichloromethane

DGCR8: DiGeorge syndrome critical gene 8

Dpb11: DNA replication initiation protein

DPF2: Doubled PHD finger 2 protein

dsRBD: Double stranded RNA-binding domain

EC₅₀: Half-maximal effective concentration

ESAG6/7: Expression site associated genes

FAZ: Flagellar attachment zone

FD: Dichloromethane fraction

FH: Hexane fraction

FM: Methanol fraction

GPI: Glycosylphosphatidylinositol

HAT: Human African trypanosomiasis

HMBC: Heteronuclear multiple bond correlation

HPLC: High performance liquid chromatography

HRESI-LC-MSⁿ: High resolution electrospray ionization mass spectrometry

HsIV/U: Heat shock protease/ATPase system

HSQC: Heteronuclear single quantum coherence

IC50: Half-maximal inhibition concentration

IFN: Interferon

Ig: Immunoglobulin

I κ B: inhibitor of kappa B

IL: Interleukin

kDNA: Kinetoplast DNA

LC-MS: Liquid chromatography-mass spectrometry

Mcm 2-7: Hexameric minichromosome maintenance complex

MEN: Mitotic exit network

MeOH: Methanol

miRNA: microRNA

mRNA: Messenger RNA

MS: Mass spectrometry

MTT: 3-(4,5-dimethylthiazol-2-yl)-2,5-diphenyltetrazolium bromide

Myt-1: Myelin transcription factor

NDR: Nuclear dbf2-related kinase

NF κ B: Nuclear factor kappa B

NMR: Nuclear magnetic resonance

NOESY: Nuclear Overhauser Effect Spectroscopy

NRK: NIMA-related kinase

ORC: Origin of replication

PACRG: Parkin coregulated gene

PARP: Procylic acidic repetitive protein

PAZ: PIWI/Argonaute/Zwinkle

PCNA: Proliferating cell nuclear antigen

PHD: Plant homeodomain

PI3K/AKT/MAPK/ERK/JNK: Phosphatidylinositol-3 kinase/protein kinase B/mitogen-activated protein kinase/ extracellular signal-regulated kinase/ c-jun N-terminal kinase

piRNA: Piwi interacting RNA

PP1: Protein phosphatase 1

PP2A: Protein phosphatase 2A

Pre-miRNA: Precursor miRNA

Pre-RC: Prereplicative complex

Pri-miRNA: Primary miRNA

Rb: Retinoblastoma

RISC: RNAi-induced silencing complex

RITseq: RNAi target sequencing

RLC-RISC-double stranded RNA

RNAi: RNA interference

S-CDK: S phase CDK

siRNA: Short interfering RNA

SIN: Septum initiation network

TCE: Total Crude Extract

TNF: Tumor necrosis factor

TOCSY: Total Correlation Spectroscopy

TLK: Serine/threonine-protein kinase tousled-like

TLC: Thin layer chromatography

Vps34: Class III PI3K

VSG: Variant surface glycoprotein

WB: Water/Sec-butanol fraction

XTT: 2,3-bis(2-methoxy-4-nitro-5-sulfophenyl)-5-[(phenylamino)carbonyl]-2H-tetrazolium
hydroxide

ZR: *Zanthoxylum zanthoxyloides* (Lam.) Zepern. & Timler (root)

ABSTRACT

African trypanosomiasis is a disease caused by the parasitic protozoans of African trypanosomes. Despite several efforts at chemotherapeutic interventions, the disease poses serious health and economic concerns to humans and animals of various sub-Saharan African countries. Commercially available drugs such as suramin, eflornithine, pentamidine, melarsoprol and nifurtimox have reported cases of undesirable side effects, drug resistance, and difficulty in regimen application. Studies have reported on the antitrypanosomal activities of several medicinal plants although their mechanisms of action remain poorly understood. *Zanthoxylum zanthoxyloides* (Lam.) Zepern. & Timler (*Z. zanthoxyloides*) and *Bidens pilosa* L. (*B. pilosa*) are plant species of important phytochemical and pharmacological relevance found in several tropical and temperate zones. However, their effects and mechanisms of antitrypanosomal action in African trypanosomes remain largely unknown. The aim of this study was thus to isolate antitrypanosomals from these plants and determine the effects and mechanisms of action of selected antitrypanosomals in *Trypanosoma brucei* (*T. brucei*). The Kupchan method of solvent extraction was used to prepare crude extracts and fractions from the air-dried pulverized plant material of *Z. zanthoxyloides* (root) and *B. pilosa* (whole), thereby giving rise to methanol (ZRFM, BPFM), dichloromethane (ZRFD, BPDF), hexane (ZRFH, BPFH) and butanol (ZRWB, BPWB) fractions from the respective plants. Effects and mechanisms of action of selected fractions were determined through analysis of cell viability, cell death, cell cycle, fluorescence microscopy and RNA interference target sequencing. The fractions ZRFD, ZRFM, ZRWB, BPDF and BPFM were selectively active against *T. brucei* with respective half-maximal inhibitory concentrations of 5.70, 3.89, 4.02, 3.29, and 5.86 $\mu\text{g/ml}$. Fractions ZRFD, ZRFM, ZRWB, BPDF, BPFM and BPFH caused a significant induction of apoptosis-like cell death. The ZRFD, ZRFM, ZRWB, BPDF and

BPFM fractions caused significant inhibition and arrest of the G0-G1 and G2-M cell cycle phases respectively, while ZRFD and ZRFM resulted in a significant increase in the S phase of *T. brucei*. Fractions ZRFD, ZRFM, BPDF, and BPFM also induced distortion and aggregation of the parasites. Antitrypanosomal compounds were isolated from the dichloromethane fraction of both plant species in a bioactivity-guided process using high performance liquid chromatography. Isolated compounds were identified through mass spectrometry, ultraviolet spectroscopy and nuclear magnetic resonance spectroscopy as aromatic nitrogen-containing alkaloids. Promising compounds included new and known alkaloids from *Z. zanthoxyloides* (root), as well as esters of tryptophan from *B. pilosa* (whole plant). Compounds exhibited selective activities, significant induction of apoptosis-like cell death and a marked alteration of cell cycle in *T. brucei*. Through an RNA interference target sequencing, putative forms of leucine-rich repeat proteins, stumpy formation signaling pathway proteins, receptor-type adenylate cyclase and other hypothetically conserved proteins were identified for the most promising compounds, thereby suggesting the potential interference of pathogenesis, growth, development and secretory pathways of *T. brucei*. Taken together, the results indicate that *Z. zanthoxyloides* (root) and *B. pilosa* (whole plant) have promising antitrypanosomal activities with implications for novel therapeutic interventions in African trypanosomiasis.

CHAPTER ONE

1.0 INTRODUCTION

1.1 BACKGROUND

African trypanosomiasis (AT) is a tsetse-transmitted disease of humans and livestock caused by the parasitic protozoan of the genus *Trypanosoma*. Human African trypanosomiasis (HAT) and Animal African trypanosomiasis (AAT) are the two main types of AT (Raper et al., 2001; Simarro et al., 2012). HAT afflicts an estimated 70 million population in about 36 countries of sub-Saharan Africa (Simarro et al., 2012). A large number of the most vulnerable people in HAT-affected countries also engage in activities such as agriculture, animal husbandry and hunting as a means of sustenance, thereby leading to significant losses in respect of health, economy and productivity of livestock. Moreover, AAT, which continues to threaten the lives of several million herds of cattle every year, is in need of new approaches to combat the disease (Morrison et al., 2016).

Type HAT is mainly transmitted in sub-Sahara Africa by at least 30 species and subspecies of the tsetse fly vector (Simarro et al., 2012). It is caused by two human-infective subspecies of *Trypanosoma brucei* (*T. brucei*): *T. b. gambiense* and *T. b. rhodesiense*. Unlike HAT, AAT affects several animal species such as deer, duikers, antelopes, buffalos, equidae, lions, leopards, warthogs, capybaras and elephants. Moreover, several species of the parasite such as *T. vivax*, *T. brucei* and *T. congolense* are capable of causing AAT.

T. brucei is a species of *Trypanosoma* with about 35 megabase of haploid genome organised into about 10,000 predicted genes and pseudogenes (Berriman et al., 2005; Daniels et al., 2010). The species possesses 11 principal diploid nuclear chromosomes, several intermediate-sized chromosomes of 300–900 kb and many minichromosomes of 50–100 kb. The intermediate and minichromosomes serve as repositories of variant surface glycoproteins (VSG) genes (Horn and

McCulloch, 2010). Among the three major genetically related subspecies of *T. brucei*, *T.b. brucei* rarely infects humans due to its susceptibility to the innate immune system, thereby making the subspecies a safe model organism for genetic studies (Barrett, 2003; Deborggraeve et al., 2008).

The prospect of vaccine development for African trypanosomiasis is beset with various challenges partly due to several immune evasion strategies adopted by the parasite (Xong et al, 1998; Oli et al, 2006; Kieft et al, 2010; Capewell, 2013). Currently, the most efficient and economically viable option is chemotherapy (Steверding, 2010). However, there are challenges associated with drug resistance, undesirable side effects, and difficulty in regimen application (Scott et al., 1996; Matovu et al., 2001; Baker et al., 2011; Barrett et al, 2011; Franco et al., 2012). In order to meet the urgent need for novel, less toxic and more efficient chemotherapy for African trypanosomiasis, an understanding of metabolic pathways associated with the action of antitrypanosomals in the parasites is required.

About two-thirds of the world population depends on traditional medicinal products because pharmaceutical products are not readily affordable and available (Tagboto and Townson, 2001). Several studies have reported on the antitrypanosomal activities of various herbal extracts in different parts of the world (Hoet et al., 2004; Al-Musayeib et al., 2012; Ibrahim et al., 2012; Norhayati et al., 2013). However, most of these studies did not investigate potential mechanisms of action of the active antitrypanosomal agents. Insights into the mode of action of antitrypanosomals are required if novel drugs that may outwit resistance to commercially available antitrypanosomal drugs are to be developed.

Zanthoxylum is a genus of mostly deciduous and evergreen trees and shrubs that comprises at least 500 species (Patino et al., 2012). It is a widely distributed plant genus native to most temperate

and sub-tropical zones of Africa, Asia, North America, South America and Australia. Traditionally, the leaves, stem and roots of many species are employed in medicinal preparations for the treatment of diseases such as coli, toothache, stomachache and oral infections (Adesina, 2005). Many of the species are also used in the building of houses, construction of talking drums and decorative paneling (Adesina, 2005). Hence, the genus is considered to be of an important medicinal and economical value. *Zanthoxylum zanthoxyloides* (Lam.) Zepern. & Timler (*Z. zanthoxyloides*) is one of the most important species of *Zanthoxylum* on the African continent.

Bidens is an annual or perennial herbaceous genus that consists of at least 200 species (Karis and Rydin, 1994; Pozharitskaya, 2010). Species are distributed in different parts of Africa, America, Polynesia, Europe and Asia (Ganders et al., 2000). Botanically, *Bidens pilosa* L (*B. pilosa*) remains one of the most well characterized species of *Bidens*. It is currently found in most temperate and tropical zones though it is thought to have originated from South America (Ge, 1990).

Zanthoxylum and *Bidens* have been reported to exhibit several pharmacological properties such as antidiabetic, anticancer, antiinflammatory, antioxidant, immunomodulatory, antibacterial, antiparasitic and antihelminthic activities (Patino et al., 2012; Bartolome et al., 2013; Medhi et al., 2013). Phytochemically, about 200 secondary metabolites have been isolated from *Bidens pilosa* (Silva et al., 2011). These compounds include aliphatics, flavonoids, terpenoids, phenyl propanoids, aromatics and porphyrins (Bartolome et al., 2013). Secondary metabolites have also been isolated from *Z. zanthoxyloides* with acridones, citronellol and divanilloylquinic acids being prominent examples (Ngassoum et al., 2003; Ouattara et al., 2004; Wouatsa et al., 2013). However, the antitrypanosomal effects of these plants have been reported in only a few studies (Ogiti et al., 2009; Mann et al., 2011; Mann et al., 2012; Mwaniki et al., 2017). Even so, the potential mechanisms of such antitrypanosomal effects remain to be elucidated. The present study,

therefore, sought to isolate, characterize and determine the effects and mode of action of antitrypanosomals from these plants in *T. b. brucei*.

1.2 PROBLEM STATEMENT AND JUSTIFICATION

Types HAT and AAT afflict an estimated number of 70 million humans and 50 million cattle respectively (Raper et al., 2001; Simarro et al., 2012). The prospect of vaccine development against AT is beset with various challenges partly due to several immune evasion strategies adopted by the parasite (Xong et al., 1998; Oli et al., 2006; Kieft et al., 2010; Capewell, 2013). Therefore, the most efficient and economically viable option is chemotherapy (Steverding, 2010). However, commercially available drugs that are used to treat AT possess undesirable side effects, physicochemical limitations, drug resistance and difficulty in regimen application (Fairlamb, 2003; Steverding, 2010). This necessitates the search for new antitrypanosomals that may overcome these challenges.

Several studies about the potential antitrypanosomal activities of herbal extracts have been reported (Hoet et al., 2004; Al-Musayeb et al., 2012; Ibrahim et al., 2012; Norhayati et al., 2013). However, little is known about the identity as well as the mode of action of the active antitrypanosomals in these extracts. Insights into the identities, effects, and mechanisms of action of such antitrypanosomal agents is required if novel drugs that can outwit the challenges associated with commercially available antitrypanosomal drugs are to be developed.

Z. zanthoxyloides and *B. pilosa* have been reported to possess useful phytochemical and pharmacological properties (Silva et al., 2011; Patino et al., 2012; Bartolome et al., 2013; Medhi et al., 2013). However, little is known about their potential antitrypanosomal effects (Ogiti et al., 2009; Mann et al., 2011; Mann et al., 2012; Mwaniki et al., 2017). Thus, the present study aimed

to identify, characterize and determine the mechanisms of action of selected antitrypanomals from these plants to facilitate drug discovery in African trypanosomiasis.

1.3 HYPOTHESIS

If natural products of plants are potential sources of promising antitrypanosomal chemotherapy, then the isolation, structure determination and target identification of plant antitrypanosomal compounds in African trypanosomes will provide insights into their mechanisms of action and facilitate the development of novel chemotherapy for the treatment of African trypanosomiasis.

1.4 CONCEPTUAL FRAMEWORK

Several studies have reported on the potential antitrypanosomal activities of plants (Hoet et al., 2004; Al-Musayeb et al., 2012; Ibrahim et al., 2012; Norhayati et al., 2013). Yet, very little is known about the identity and mechanisms of action of the antitrypanomals. It is within this framework that *B. pilosa* and *Z. zanthoxyloides* were considered for the purpose of drug discovery in African trypanosomiasis. The present study aimed to apply the principles of target-based drug discovery towards the isolation, structure determination, characterization and determination of the mechanisms of action of promising antitrypanomals from these plants.

Even though plants synthesize a large number of phytochemicals, only a limited number of them may be pharmacologically relevant to the control of African trypanosomiasis. The isolation and structure determination of active antitrypanosomal compounds are therefore critical to the identification of relevant antitrypanomals. Chromatographic and spectroscopic approaches are immensely useful in the isolation and structure elucidation of many phytochemicals, and may therefore be applicable to *B. pilosa* and *Z. zanthoxyloides* as well.

Subsequent to structural identification, mechanisms of action are elucidated in order to facilitate the identification of potential targets. Target identification is crucial at an early stage in the drug discovery process, because it may pave the way for further optimization of the structure, potency, toxicity and stability of the antitrypanosomals, thereby facilitating entry into preclinical and clinical stages. Elucidation of mechanisms of action and identification of targets may be achieved through a number of molecular, cellular and computational approaches (Schenone et al., 2013).

Effects on cell viability, cell death and cell cycle are particularly important to consider due to the central role they play in the life of eukaryotes (Vaughan and Gull, 2008; Vega-Avila and Pugsley, 2011; Berghe et al., 2015). Moreover, advances in genomics, transcriptomics, proteomics and bioinformatics have proven to be very important in the identification of targets (Schenone et al., 2013). In this context, RNA interference target sequencing is an immensely useful loss-of-function approach capable of elucidating metabolic mechanisms of a drug resistance and action in trypanosomes (Alsford et al., 2012; Alsford et al., 2013). Moreover, properties of targets such as essentiality, druggability, assayability, resistance potential, toxicity potential and structural information are critical qualities of varying importance in drug discovery for African trypanosomiasis (Gilbert, 2014). Hence, the application of these concepts, principles and methods would enable a test of the hypothesis and a subsequent address of the challenges captured in the problem statement.

1.5 AIM/SPECIFIC OBJECTIVES

1.5.1 Aim

To isolate and determine the effects and mechanisms of action of *Z. zanthoxyloides* and *B. pilosa* antitrypanosomals in *T. b. brucei*.

1.5.2 Specific Objectives

1. To determine the effects and mechanisms of action of antitrypanosomal fractions (cell viability, cell death, cell cycle, fluorescence microscopy).
2. To isolate and determine the structures of antitrypanosomal compounds of selected fractions (chromatography, spectroscopy).
3. To determine the effects and mechanisms of action of selected antitrypanosomal compounds (cell viability, cell cycle, RNA interference target sequencing).

CHAPTER TWO

2.0 LITERATURE REVIEW

2.1 MEDICINAL VALUES OF PLANTS

The potential medicinal effects of natural products from plants continue to receive an increasing level of research and medical attention. These effects are largely due to the pharmacological and phytochemical properties of several organic compounds synthesized by the plants. Herbs and spices of plants such as garlic, thyme, mustard, and rosemary have been shown to be of considerable medicinal and therapeutic values (Lai and Roy, 2004).

Traditionally, organic compounds of plants are classified into two main groups. The first class of organic compounds that are involved in essential roles such as respiration, growth, photosynthesis and development are referred to as primary metabolites. These include amino acids, nucleotides, carbohydrates and lipids. The second group of compounds are not directly involved in these essential roles, and may be referred to as secondary metabolites or phytochemicals. Major secondary metabolites of plants include terpenoids, alkaloids (mainly containing nitrogen), phenylpropanoids and related phenolics.

The medicinal properties of plants originate from the combined effects of primary and secondary metabolites, with the latter involved in crucial pharmacological roles. These pharmacological functions include antidiabetic, antibacterial, anti-inflammatory, antiparasitic, antiviral, antitumor, antihelmitic and antinociceptive effects. Though secondary metabolites of plants are structurally and functionally diverse, many also serve as protective barriers against pathogens, attractants for pollinators and seed-dispersing animals, UV protectants and allelopathic agents (Croteau et al.,

2000; Dewick 2002). They are also employed in the production of dyes, waxes, flowering agents, drugs and perfumes (Croteau et al., 2000; Dewick 2002).

2.2 CLASSIFICATION AND BOTANICAL DESCRIPTION OF ZANTHOXYLUM

Zanthoxylum, also known as the prickly ash or Hercules club, is a genus of mostly deciduous and evergreen trees and shrubs that belongs to the subfamily of *Toddalioideae* comprising at least 500 species (Figure 2.1) (Patino et al., 2012). Members of *Toddalioideae* belong to the family of *Rutaceae* and the order of *Sapindales*. Species are natives to the middle latitudes of both temperate and subtropical zones in Australia, Africa, South America, Asia and North America. Many species are of yellow heartwood from which the genus name originates etymologically. Notable species include *Z. americanum*, *Z. flavum*, *Z. acanthopodium*, *Z. ailanthoides*, *Z. armatum*, *Z. avicennae*, *Z. capense*, *Z. fagara*, *Z. monophyllum*, *Z. rhoifolium* and *Z. zanthoxyloides* (Patino et al., 2012).

Z. zanthoxyloides, commonly known as the Senegal prickly-ash, remains one of the most important species of *Zanthoxylum* as far as the African continent is concerned. The species is native to many countries in West Africa such as Benin, The Gambia, Ghana, Guinea, Ivory Coast, Mali and Nigeria. In Ghana, it is known as ‘Okanto’ (or Kanto), ‘Xeti’ (or Xetsi), ‘haatso’, ‘hantso’, and ‘kanfu’ by the Akans, Ewes, Gas, Ga-Dangmes and Fantes respectively (Mshana et al., 2000). The shrubs and trees of *Z. zanthoxyloides* are spiny and somewhat scandent in nature, ranging between 6 and 12 m in height (Nacoulma, 1996; Arbonnier, 2004). The bark is of a grey to beige color with fine vertical fissures and woody prickly-bearing protuberances. The slash is odorous, yellow and orange-mottled beneath while the stem is glabrous and grey with solitary prickles (Nacoulma, 1996; Arbonnier, 2004). The leaves are usually alternate, glabrous or imparipinnately compound and are arranged in about 5 to 11 opposite leaflets. Leaflets may be obovate, elliptical, apiculate or notched with cuneate to rounded base and obtuse to rounded apex.

Leaflets are also endowed with many glandular dots. These dots are pinnately veined with about 10-14 pairs of lateral veins that are rigidly papery and smell of lemon or pepper when crushed. Petioles are glabrous and spiny beneath with about 2 to 5 cm in length with recurved prickles (Nacoulma, 1996; Arbonnier, 2004).

The inflorescence of *Z. zanthoxyloides* consists of a lax terminal or axillary panicle of 5-25 cm long with short branches (Nacoulma, 1996; Arbonnier, 2004). The white or greenish flowers themselves could be regular or unisexual with a sessile nature. Male flowers possess stamens that are slightly exerted while female flowers consist of a one-celled superior ovary and a short style (Nacoulma, 1996; Arbonnier, 2004). Fruits of *Z. zanthoxyloides* are in the form of brown, dehiscent and one-seeded ovoid follicles of about 5-6 mm in diameter. Seeds may be black to bluish in appearance (Nacoulma, 1996; Arbonnier, 2004).



Figure 2.1: A picture of *Z. zanthoxyloides* at the environs of Center for Plant Medicine Research, Mampong-Akuapem, Ghana.

2.3 TRADITIONAL USES OF ZANTHOXYLUM

Traditionally, many *Zanthoxylum* species find various economical and medicinal uses in different parts of the world. The construction of houses, boats, talking drums, decorative paneling and the making of industrial paper and pulp involve timber obtained from *Zanthoxylum* species such as *Z. lemairi*, *Z. tessmannii*, *Z. gillettii*, and *Z. leprieurii* (Dalziel, 1937; Oliver-Bever, 1982). The leaves, stem and roots of many species are used in medicinal preparations to treat coli, toothache, stomachache, rheumatism, lumbago, leprosy ulcerations and oral infections (Oliver-Bever, 1982; Olatunji, 1983). Their medicinal properties are also employed in antiplasmodial, analgesic, and antiseptic preparations. The stem bark and root of some species are utilized as piscicides, vermifuges and febrifuges.

Macerations, decoctions and infusions of the root and stem bark of *Z. zanthoxyloides* are traditionally taken to treat malaria, paralysis, oedema, fever, sickle cell anemia and body weakness (Nacoulma, 1996). They are also used in the treatment of intestinal problems such as colic, dysentery and worm infestations. Preparations from the bark of stems and roots are used as an emmenagogue and stimulant, as well as to treat neuralgia and migraine (Nacoulma, 1996). Particularly, the roots may be applied to wounds, sores, ulcers, swellings, abscesses, bites and yaws to facilitate healing (Nacoulma, 1996). When chewed, the bark of roots and stems tend to provide the palate with a warm, pungent and numbing effect, thereby finding applications in the treatment of oral infections, sore gums, toothache and dental caries. The root decoction is also used to help fight sore throat (Nacoulma, 1996).

In Ghana, the root and the powder of the stem bark are used to treat whooping cough (Arbonnier, 2004). In Ivory Coast, sap of the bark may be applied in the treatment of conjunctivitis (Arbonnier, 2004). In the southern part of Nigeria, a decoction prepared from the stem bark and roots is used

as an anticancer preparation (Arbonnier, 2004). The pulped bark of the stem and roots may also be used as piscicides to stupefy fish (Arbonnier, 2004). In many parts of West Africa, *Z. zanthoxyloides* is planted as a hedge due to its impenetrable nature (Arbonnier, 2004). The timber is used for firewood and building purposes due to its hard and termite-resistant nature (Arbonnier, 2004). The roots, shoots, and twigs may be useful as chew-sticks (Arbonnier, 2004). The young branches and bark of *Z. zanthoxyloides* may be used as torches on special occasions due to their high quantity of resins (Arbonnier, 2004). Moreover, the leaves and seeds are commonly used in the seasoning of food, as well as in feeding livestock (Arbonnier, 2004). The species of *Z. zanthoxyloides* is believed to possess spiritual benefits thereby serving as a fetish plant in some parts of West Africa (Arbonnier, 2004).

2.4 PHYTOCHEMISTRY OF ZANTHOXYLUM

Zanthoxylum is endowed with a vast array of diverse phytochemicals from all the major groups of secondary metabolites. These include terpenes, sterols, flavonoids, amides, alkaloids, lignans and coumarins (Patino et al., 2012; Medhi et al., 2013). Sabinene, elemol, β -myrcene, isobutyl amides, benzohenanthridines, benzyloisoquinoline alkaloids, berberine, aporphine alkaloids, quinolone alkaloids, furcocoumarins, and diarylbutirolactones are specific examples of these secondary metabolites isolated from *Zanthoxylum* (Adesina, 2005; Patino et al., 2012; Medhi et al., 2013). *Z. simulans*, *Z. integrifoliolum*, *Z. rugosum*, *Z. chiloperone*, *Z. monophyllum*, *Z. integrifoliolum*, *Z. shinifolium*, *Z. liebmannianum*, *Z. monophyllum*, and *Z. fagara* are some of the species from which these compounds were isolated (Patino et al., 2012). Particularly, various secondary metabolites have also been isolated from *Z. zanthoxyloides*. For instance, citronellol, citronellyl acetate, α -terpinolene, α -pinene, limonene, trans- β -ocimene, geraniol, and β -myrcene were isolated from the fruits of *Z. zanthoxyloides* (Ngassoum et al., 2003). Moreover, 3-hydroxy-1,5,6-trimethoxy-9-

acridone, 1,6-dihydroxy-3-methoxy-9-acridone, 3,4,5,7-tetrahydroxy-1-methoxy-10-methyl-9-acridone and 4-hydroxyzanthacridone (and related zanthacridones) were purified from the fruits of *Z. zanthoxyloides* (Wouatsa et al., 2013). Again, citronellol, geraniol, citronellyl acetate, limonene, citronellal, (E)- β -ocimene, myrcene, limonene and α -pinene were also purified from the fruits of *Z. zanthoxyloides* (Fogang et al., 2012). Finally, three divanilloylquinic acid isomers (burkinabines A, B and C) were isolated from the root bark of the same species (Ouattara et al., 2004).

2.5 PHARMACOLOGY OF ZANTHOXYLUM

Different species of *Zanthoxylum* exhibit various biological activities, namely, antimicrobial, insecticidal, anti-inflammatory, antioxidant, antiparasitic, antitumor, antihelmitic, antinociceptive and antiviral activities (Patino et al., 2012). Studies of circulatory systems, central nervous systems and enzyme inhibition have been employed to characterize the biological properties of members of *Zanthoxylum* (Patino et al., 2012). Xanthoxyline, which is known to be allelopathic to various plant species such as *Amaranthus tricolor* and *Echinochloa crus-galli* was isolated from the fruit extract of *Z. limonella* (Charoenying et al., 2010). The methanol extracts of *Z. capense* exhibited anticonvulsant activities in mice (Amabeoku and Kinyua, 2010). Leaf and bark extracts of ethanol, hexane and ethyl-acetate from *Z. fagara*, *Z. elephantiasis*, *Z. martinicense*, *Z. coriaceum* and *Z. chiloperone* exhibited promising anti-inflammatory activities (Bastos, 2001; Márquez et al., 2005; Villalba et al., 2007). Dibenzylbutirolactonic lignin that was isolated from *Z. naranjillo* also possessed anti-inflammatory properties (Bastos, 2001). Benzophenanthridine alkaloids, quinolone alkaloids, lignans and coumarins from *Z. nitidum* gave rise to promising anti-inflammatory activities (Chen et al., 2011). The triterpene lupeol found in many species of *Zanthoxylum* is known to possess *in vitro* and *in vivo* inhibitory effects against inflammation (Saleem, 2009). The

compounds 3β , 16β -hydroxybetulinic acid, 3β -acetoxy- 16β -hydroxybetulinic acid and 2,6-dimethoxy-1,4-benzoquinone that were isolated from *Z. tessmannii* gave rise to antimicrobial activities against *Chlorella sorokiniana*, *Mucor miehei*, *Escherichia coli*, *Bacillus subtilis*, *Staphylococcus aureus*, *Streptomyces viridochromogenes*, *Candida albicans*, *Chlorella vulgaris*, and *Scenedesmus subspicatus* (Mbaze et al., 2007). The fruit extract of *Z. armatum* was shown to exhibit antibacterial activities against *Staphylococcus aureus*, *Escherichia coli*, *Pseudomonas aeruginosa* and *Shigella boydii* (Panthi and Chaudhary, 2006). The hexane, ethyl acetate and ethanol extracts of *Z. chilipiron*, as well as the lupeol of *Z. rhoifolium* were shown to be antinociceptive (Villalba et al., 2007; Pereira et al., 2010). Antioxidant activities were also exhibited by the fruits and seeds of *Z. alatum*, *Z. bungeanum*, *Z. piperitum*, and *Z. achanthopodium* (Hisatomi et al., 2000; Lee and Lim, 2008; Batool et al., 2010; Xia et al., 2011). *Z. chalybeum*, *Z. syncarpum*, *Z. gillettii*, *Z. limonella*, *Z. rhoifolium* and *Z. usambarense* have been shown to have antiplasmodial activities (Ross et al., 2004; Bertani et al., 2005; Ross et al., 2005; Jullian et al., 2006; Charoenying et al., 2008; Kaur et al., 2009; Zirihi et al., 2009; Were et al., 2010). Antitrypanosomal activities have been demonstrated in *Z. naranjillo* and *Z. chiloperone* (Bastos et al., 1999; Ferreira et al., 2007; Ferreira et al., 2011). Canthin-6-one alkaloids and meglumine antimonate of *Z. chiloperone* were shown to have activities against *Leishmania* (Ferreira et al., 2002; Sen and Chatterjee, 2011). The methanolic stem extract of *Z. beecheyanum* possesses strong antiplatelet activity (Patino et al., 2012). *Z. coreanum*, *Z. planispinum*, *Z. schinifolium*, *Z. ailanthoides* and *Z. integrifoliolum* are known to possess antiviral properties (Patino et al., 2012). Terpenoids isolated from *Z. rhoifolium* were shown to have antitumor activities (Da Silva et al., 2007a, b). The chloroform fraction of *Z. ailanthoides* showed cytotoxic activity against human promyelocytic and myelomonocytic leukemia cells (Chou et al., 2011). Pyranoquinoline alkaloids

(zanthosimuline and huajiaosimulin) isolated from *Z. simulans* were active against thirteen human cancer cell lines (Chen et al., 1994b). Berberine, an alkaloid isolated from the bark of *Z. monophyllum* showed activity against colorectal cancer, breast cancer, larynx cancer and gastric cancer cell lines (Cordero et al., 2004). Benzophenanthridine alkaloids such as fagaronine and nitidine that are commonly isolated from most species of *Zanthoxylum* were characterized to possess potent antitumor activity (Tillequin, 2007).

The plant species of *Z. zanthoxyloides* has been shown to possess analgesic, antidiabetic, hypolipidaemic, hypotensive, gastroprotective, antiproliferative, antioxidant, antihelminthic, antimicrobial and antiparasitic effects. The aqueous root extract of *Z. zanthoxyloides* was shown to possess analgesic properties probably via the inhibition of prostaglandin (Prempeh and Mensah-Attipoe, 2008). Aqueous and ethanolic extracts from the leaves of *Z. zanthoxyloides* exhibited antihelminthic activities against *Asaris lumbricoides*, *Haemonchus contortus* and *Trichostrongylus colubriformis* (Azando et al., 2011; Barnabas et al., 2011). The essential oils of *Z. zanthoxyloides* were found to be active against bacteria and fungi (Ngane et al., 2000; Tatsadjieu et al., 2003; Anne et al., 2013, Misra et al., 2013). The alkaloid extract of *Z. zanthoxyloides*, as well as the benzophenanthridine alkaloid fagaronine obtained from the root extract inhibited the growth of *Plasmodium falciparum* (Gansane et al., 2010; Adebayo and Krettli, 2011). Purified and semi-purified root extracts also inhibited the growth of *Plasmodium falciparum* (Kassim et al., 2005). The root extracts of *Z. zanthoxyloides* were found to be active against *Leishmania* (Ahua et al., 2007). The leaf extracts were shown to have hypolipidaemic and antidiabetic properties (Aloke et al., 2012). Stem extracts were shown to possess radical-scavenging and iron-chelating effects with or without hydrogen peroxide, thereby demonstrating the antioxidant activities of the plant species (Adekunle et al., 2012). The extract from the bark of the root of *Z. zanthoxyloides* was also shown

to exhibit hypotensive effects (Zahoui et al., 2010). The extract of *Z. zanthoxyloides* reduced vasodilatation and permeability of the capillaries during inflammation (Prempeh et al., 2009). The ethanolic root bark extract was shown to exhibit gastroprotective effects in Sprague-Dawley rats, and this might have occurred through antimuscarinic or antihistaminic mechanisms (Boye et al., 2012). By employing the 3-(4,5-dimethylthiazol-2-yl)-2,5-diphenyltetrazolium bromide (MTT) assay, the oils of *Z. zanthoxyloides* were shown to have antiproliferative effects (Fogang et al., 2012). These pharmacological properties of *Z. zanthoxyloides* have been summarized in Table 2.1 below.

Table 2.1 Pharmacology of *Z. zanthoxyloides*

Pharmacological properties	Plant part used	References
Analgesic	Root	Prempeh and Mensah-Attipoe, 2008
Antihelmintic	Leaves	Azando et al., 2011; Barnabas et al., 2011
Antifungal	Essential oil	Ngane et al., 2000
Antibacterial	Essential oil	Misra et al., 2013
Antiplasmodial	Root	Gansane et al., 2010; Adebayo and Krettli, 2011
Gastroprotective	Root	Boye et al., 2012
Antiproliferative	Oil	Fogang et al., 2012
Antileishmania	Root	A hua et al., 2012
Antioxidant	Stem	Adekunle et al., 2012
Hypotensive	Root	Zahoui et al., 2010

The root, stem and leaves are pharmacologically useful parts of *Z. zanthoxyloides*. Oil extracts have also been reported to exhibit antifungal, antibacterial and antiproliferative activities. Further details have been provided in the text.

2.6 CLASSIFICATION AND BOTANICAL DESCRIPTION OF *BIDENS*

Bidens, commonly known as the beggarticks or black jack, is a genus of mostly annual or perennial herbaceous plants (Figure 2.2). The genus belongs to the subfamily of *Asteroideae* and consists of at least 200 species (Karis and Rydin, 1994; Pozharitskaya, 2010). Members of the *Asteroideae* subfamily belong to the family of *Asteraceae* and the order of *Asterales*. Species may be found in different parts of Africa, America, Polynesia, Europe and Asia (Ganders et al., 2000). Well-known species include *B. tripartita*, *B. aurea*, *B. pilosa*, *B. subalternans* and *B. bipinnata*. Botanically, *B. pilosa* remains one of the most well characterized species of *Bidens*. Though South America may be considered as the original source, the plant may currently be found in different temperate and tropical zones (Ge, 1990). Several varieties may be recognized, namely, *B. pilosa* var. *pilosa*, var. *minor*, var. *radiata* and var. *bisetosa*. In Ghana, it is referred to as ‘dwirentwi’ and ‘dzanikpikpi’ by the Akans and Ewes, respectively (Mshana et al., 2000).

B. pilosa are usually glabrous or hairy. The leaves may be lobbed, serrate or dissected while petioles could be slightly winged (Figure 2.2). It may possess white or yellow flowers that are displayed in small heads with somewhat long peduncles. In favorable environmental conditions, it may grow to a maximum height of 150 cm. Species are fast-growing, with individual plants capable of producing between 3,000 and 60,000 seeds. Fruits may be slightly curved and stiff with rough blackrods. The infructescence also forms spherical burrs about one to two centimeters in diameter arranged in a radiating starlike pattern. Seeds are narrow or ribbed and may consist of two to four barbed spines. Seeds usually germinate within 3 to 4 days when planted under favorable climate, and are dispersed by the process of zoochory. The species is generally considered to be a weed due to its invasive nature (Young et al., 2010).



Figure 2.2: A picture of *B. pilosa* at the environs of Center for Plant Medicine Research, Mampong-Akuapem, Ghana.

2.7 TRADITIONAL USES OF *BIDENS*

From the traditional point of view, *Bidens* has many ethnomedical values most of which may be attributed to *B. pilosa*. These traditional values usually originate from the medicinal and nutritional significance of the plant (Geissberger and Sequin, 1991; Noumi et al., 1999; Tan et al., 2000; Cano and Volpato, 2004; Ayyanar and Ignacimuthu, 2005; Lans, 2007; Hsu et al., 2009; Namukobe et al., 2011). The whole plant is used in various forms to treat snake bite, stomach ulcers, nose bleeds, hemorrhoids, morning sickness, menstrual irregularities, sore throat, renal infections, bacterial infections and malaria in different parts of Asia, Africa and Central America (Geissberger and Sequin, 1991; Noumi et al., 1999; Tan et al., 2000; Cano and Volpato, 2004; Ayyanar and Ignacimuthu, 2005; Lans, 2007; Hsu et al., 2009; Namukobe et al., 2011). It is also valued as an anti-inflammatory, antidiabetic, antirheumatic and a potent hypotensive (Geissberger and Sequin, 1991; Noumi et al., 1999; Tan et al., 2000; Cano and Volpato, 2004; Ayyanar and Ignacimuthu, 2005; Lans, 2007; Hsu et al., 2009; Namukobe et al., 2011).

2.8 PHYTOCHEMISTRY OF *B. PILOSA*

Most of the secondary metabolites known in *Bidens* were isolated from *B. pilosa* (Silva et al., 2011; Bartolome et al., 2013). Phytochemically, about 200 secondary metabolites have been isolated from *B. pilosa* (Silva et al., 2011; Bartolome et al., 2013). Isolated compounds consist of at least 25 terpenoids, 19 phenyl propanoids, 13 aromatics, 70 aliphatics, 60 flavonoids, 8 porphyrins and a few other compounds (Bartolome et al., 2013).

Specific examples of these classes of compounds include ferulic acid, caffeic acid, eugenol, 4-O-caffeoylquinic acid, pyrocatechin, pyrocatechol, p-vinylguaiacol, vanillin, bidenphytin A, pheophytin A, α -tocopheryl quinone, 2-acetyl-thiophene, gallic acid, salicylic acid, chlorogenic acid, squalene, lupeol, β -amyrin, stigmasterol, phytanic acid, campesterol, phytol, bicyclogermacrene, quercetin, isoquercitrin, luteoside, myristic acid, palmitic acid, butein and okanin (Silva et al., 2011; Bartolome et al., 2013).

2.9 PHARMACOLOGY OF *B. PILOSA*

Most of the pharmacological and biological importance of *Bidens* is attributed to *B. pilosa* because it is perhaps the most studied species in the genus. Many studies have reported on the pharmacological properties of the extracts or compounds of *B. pilosa*. These include antibacterial, antifungal, antihypertensive, antitumor, anti-inflammatory, antidiabetic, antihyperglycemic, antioxidant, immunomodulatory, antimalarial, vasodilatory and anti-ulcerative activities (Bartolome et al., 2013).

The cytotoxic activities of chloroform, hydroethanolic, ethyl-acetate, and methanol fractions of *B. pilosa* were demonstrated in different types of assays including brine shrimp, MTT and neutral red uptake assays (Chiang et al., 2005). In the study, chloroform fraction stood out as the most toxic

with IC₅₀ values of 97 and 83 µg/ml in neural red uptake and MTT assay, respectively (Chiang et al., 2005). Phenyl-1, 3, 5-heptatriene from *B. pilosa* leaves was identified as the cytotoxic agent in different human cancer lines (Kumari et al., 2009). The ethyl acetate fraction of the methanol extract of *B. pilosa* was shown to have the highest cytotoxicity against HeLa and KB cells (Sundararajan et al., 2006). The antileukemic effect of hot water extract of *B. pilosa* var. *minor* Sheriff assessed on several types of leukemia cells using the 2,3-bis (2-methoxy-4-nitro-5-sulfophenyl)-5-[(phenylamino) carbonyl]-2H-tetrazolium hydroxide (XTT)-based colorimetric assays was demonstrated in all cell types (Chang et al., 2001). Luteolin, a well-known phytochemical of *B. pilosa* was shown to prevent tumor cells from proliferating (Lee et al., 2006; Seelinger et al., 2008). The regulation of topoisomerase I and II, PI3K/Akt/MAPK/ERK/JNK pathways (phosphatidylinositol-3 kinase/protein kinase B/mitogen-activated protein kinase/ extracellular signal-regulated kinase/c-Jun N-terminal kinase), apoptosis, cell cycle arrest and fatty acid synthase were identified as the main mechanisms by which luteolin might exhibit its anti-tumor activity (Lee et al., 2006; Seelinger et al., 2008). The cytotoxic effect on human colon cancer of butein, another flavonoid from *B. pilosa*, was shown to occur by affecting the incorporation of ¹⁴C-labeled amino acids or nucleosides, thereby inhibiting the synthesis of DNA, RNA or protein (Yit and Das, 1994). The anticancer activity of centaureidin, another flavonoid from *B. pilosa* has been reported in CA46 Burkitt lymphoma and NCI60 human tumor cell lines (Beutler et al., 1993; Beutler et al., 1998). Polyne aglycones from *B. pilosa* exhibited significant antiproliferative effects in primary human umbilical vein endothelial cells (Wu et al., 2004).

B. pilosa is also reported to exhibit several anti-inflammatory properties. The aqueous extracts of *B. pilosa* suppressed the activation and production of p38, JNK, ERK1/2, cyclooxygenase-2 and prostaglandin (Yoshida et al., 2006). The oral administration of *B. pilosa* treated with cellulose

reduced the level of serum immunoglobulin E (IgE) in mice 10 days after immunization with dinitrophenylated *Ascaris* (Horiuchi et al., 2008). The phenolic luteolin was shown to inhibit the release of tumor necrosis factor α (TNF- α) and interleukin-6 (IL-6) in RAW 264.7 cells, as well as to suppress the degradation of inhibitor of kappa B (I κ B- α) and the expression of nitric oxide synthase in microglia (Kim et al., 2006). Ethyl caffeate exerted a nitric oxide synthase-mediated anti-inflammatory effect in RAW 246.7 cells (Chiang et al., 2005). The methanol extract of *B. pilosa*, and a polyene isolated from *B. pilosa* were reported to suppress immune response and inflammation in mice (Pereira et al., 1999).

The antidiabetic properties of *B. pilosa* have been reported in many parts of Asia, Africa and America. The butanol fraction respectively inhibited and stimulated the proliferation of T-helper cells thereby preventing type 1 diabetes in non-obese diabetic mice (Chang et al., 2004). Cytopiloyne, a polyene found in *B. pilosa*, was shown to exhibit potent activity against type 1 diabetes (Chang et al., 2007). Cytopiloyne was also demonstrated to reduce postprandial levels of blood glucose, increase levels of blood insulin, improve glucose tolerance, suppress glycosylated haemoglobin level and protect pancreatic islets in type 2 diabetes mouse models (Chang et al., 2013). The aqueous ethanol extract of *B. pilosa* lowered the level of blood glucose in a type 2 diabetes mouse model (Ubillas et al., 2000). The aqueous extract of *B. pilosa* also exhibited an antihyperglycemic effect in type 2 diabetes mouse models through an increase in the levels of serum insulin (Hsu et al., 2009). A study about the antidiabetic properties of *B. pilosa* varieties in type 2 diabetes mouse models demonstrated that the crude extracts of these varieties decreased postprandial levels of blood glucose (Chien et al., 2009).

B. pilosa is known to exhibit several antioxidant properties in terms of its scavenging effects. A study about the free radical scavenging effect of *B. pilosa* using 1, 1-diphenyl-2-picrylhydrazyl

(DPPH) and hypoxanthine-xanthine oxidase assays resulted in the determination of at least nine compounds with free radical scavenging effects (Chiang et al., 2004). The crude extract, as well as the ethyl acetate, butanol and water fractions were also found to have free radical scavenging effects in the same study. The methanol extract of *B. pilosa* that contained several compounds such as hydroxybenzaldehyde, caffeic acid, coumaric acid, and ferulic acid also gave rise to DPPH radical scavenging effects (Muchuweti et al., 2007). The essential oils of *B. pilosa* also exhibited protective effects and antioxidant properties (Deba et al., 2008).

B. pilosa may also possess immunomodulatory properties. The hot water and butanol extracts of *B. pilosa* displayed varying interferon gamma (IFN- γ) promoter activities (Chang et al., 2007). In the same study, centaurein and centaureidin isolated from the butanol fraction also gave rise to IFN- γ promoter activity (Chang et al., 2007). Three polyynes isolated from *B. pilosa* were shown to regulate the differentiation and production of helper T cells and associated cytokines (Chang et al., 2004). Butanol extracts of *B. pilosa* exacerbated pulmonary inflammation in mice thereby affecting the infiltration of white blood cells (Chang et al., 2005). Cytopyloyne from *B. pilosa* also decreased the levels of IFN- γ -producing type 1 helper T cells (Chiang et al., 2007).

Hypotensive and vasodilatory properties have also been reported for *B. pilosa*. The vasodilation-mediated hypotensive effect of *B. pilosa* leaves was demonstrated in normotensive and hypertensive rat models (Dimo et al., 1999; Hsu et al., 2009). In the same study, *B. pilosa* leaves were found to exert an insulin-independent hypotensive effect in rat models. In another study on rat aorta, *B. pilosa* relaxed the rat aorta previously contracted by potassium chloride (Nguelefack et al., 2005). The ethanol extract of the plant was also shown to facilitate wound healing in Wistar rats (Hassan et al., 2011). *B. pilosa* also inhibited gastric ulcers in Wistar rats through the synthesis

of prostaglandins (Tan et al., 2000). Nine hydroxychalcones of *B. pilosa* were reported to possess gastric cytoprotective properties (Kandaswami and Middleton, 1994).

Finally, *B. pilosa* has been reported to possess antiplasmodial, antibacterial and antifungal activities (Bartolome et al., 2013). The leaf extracts of *B. pilosa* was found to exhibit antiplasmodial activity in two different strains of *Plasmodium falciparum* (Kumari et al., 2009). The same active agent also resulted in the reduction of average parasitemia in red blood cells infected with *Plasmodium berghei* (Tobinaga et al., 2009). Centaurein and centaureidin were reported to enhance antilisterial activity in macrophages through the expression of IFN- γ (Chiang et al., 2004; Chang et al., 2007; Chang et al., 2007). A polyene was reported to suppress bacterial growth minimum inhibitory concentration similar to that of several commercially available antibiotics (Tobinaga et al., 2009). Water and methanol extracts of the plant also exhibited antifungal activities against several species of fungi (Deba et al., 2007; Ashafa and Afolayan, 2009). These properties have been summarized in Table 2.2.

Table 2.2 Pharmacology of *B. pilosa*

Pharmacological properties	Plant extract or compound used	References
Anticancer	Chloroform, ethanol, aqueous, methanol, ethylacetate (phenyl-1,3,5 heptatriene, luteolin, butein, centaureidin, polyne, aglycone)	Beutler et al., 1993; Beutler et al., 1998; Chang et al., 2001; Chiang et al., 2015; Kumari et al., 2009; Lee et al., 2006; Seelinger et al., 2008; Yit and Das, 1994; Wu et al., 2004
Anti-inflammatory	Aqueous, methanol, luteolin	Pereira et al., 1999; Kim et al., 2006; Yeshida et al., 2006
Anti-diabetic	Butanol, cytopiloyne, aqueous-ethanol, aqueous	Ubillas et al., 2000; Chang et al., 2004; Chang et al., 2007; Hsu et al., 2009
Antioxidant	Ethyl-acetate, butanol, aqueous, methanol, essential oil	Chiang et al., 2004; Muchuweti et al., 2007; Deba et al., 2008
Immunomodulatory	Aqueous, butanol, centaurein, centaureidin, polyne	Chang et al., 2004; Chang et al., 2005, Chang et al., 2007; Chiang et al., 2007
Hypotensive	Ethanol, hydroxychalcone	Kandaswami and Middleton, 1994; Hassan et al., 2011
Antibacterial	Centaurein, centaureidin, polyne	Chang et al., 2007; Chiang et al., 2004; Tobinaga et al., 2009
Antifungal	Aqueous, methanol	Deba et al., 2007; Ashafa and Afolayan, 2009

Different solvent extracts of *B. pilosa* have been reported to exhibit several pharmacological properties. Activities have also been linked to phytochemicals such as centaurein, centaureidin, polyne, luteolin, butein and cytopiloyne. Detailed descriptions have been provided in the text.

2.10 TRYPANOSOMATIDAE: CLASSIFICATION AND BIOLOGICAL DESCRIPTION

Trypanosomiasis may be described as a broad group of protozoan diseases caused by the family of *Trypanosomatidae*. Since the history of trypanosomatids dates back to about 100 million years ago, trypanosomiasis is probably a very ancient group of diseases (Poinar and Poinar, 2004; Poinar and Poinar, 2005; Simpson et al., 2006). The family of *Trypanosomatidae* belongs to the order of *Trypanosomatida* and the class of *Kinetoplastea*. In accordance with morphological features and host relationships, nine genera of trypanosomatids are generally recognized. These include both monoxenous forms (*Crithidia*, *Blastocrithidia*, *Herpetomonas*, *Leptomonas* and *Wallaceina*) and heteroxenous genera (*Trypanosoma*, *Leishmania*, *Endotrypanum* and *Phytomonas*) (Lopes et al., 2010). Morphotypes by which trypanosomatids are commonly recognised include promastigotes, opisthomastigotes, amastigotes, epimastigotes, trypomastigotes, choanomastigotes and spheromastigotes (Lopes et al., 2010).

A set of features common or peculiar to the larger group of eukaryotes may be used to describe trypanosomatids. Generally, the cell surfaces of all trypanosomatids are coated with glycosylphosphatidylinositol (GPI)-anchored proteins or free GPI glycolipids that serve to protect the surface layers or mediate host-parasite interactions (Ilgoutz and McConville, 2001; Nakayasu et al., 2009). They also consist of membrane transporters that perform critical roles that include the uptake of nutrients, expelling of metabolites, establishment of ion gradients, translocation of compounds and the export of drugs (Landfear et al., 2004; Landfear, 2008; Dean et al., 2009; Gaur et al., 2009; Landfear, 2010). Membrane transporters may constitute about 2-2.5% of proteins encoded in the genome of trypanosomatids (Landfear et al., 2004; Landfear, 2008; Dean et al., 2009; Gaur et al., 2009; Landfear, 2010).

Trypanosomatids consist of flagella that help to propel the parasite forward through wave-like beats of the microtubule-based flagellar axoneme (Landfear and Ignatushchenko, 2001; Gull, 2003; Ralston et al., 2009). The flagellum and cell body are held in close proximity by a network of cytoskeletal and membranous connections called the flagellum attachment zone (FAZ). It also consists of a fibrillar structure known as a paraflagellar or paraxial rod that is made of a matrix of filaments connected to the axoneme (Portman and Gull, 2010). The flagellum is also involved in motility, host-parasite interactions, morphogenesis, cell division and evasion from the host immune system (Landfear and Ignatushchenko, 2001; Gull, 2003; Ralston et al., 2009).

Most trypanosomatids possess sub-pellicular microtubules distributed throughout the entire cell body with the exception of the flagellar pocket region (Gull, 1999). These microtubules constitute an axial helical pattern that underlies the plasma membrane together with a uniformly spaced intermicrotubule. Even though microfilaments have not yet been observed in the cytoplasm of *T. cruzi*, there is a possible role for an actin-myosin system in this species based on biochemical and genomic analyses (Corrêa et al., 2007; Corrêa et al., 2008; De Melo and Sant'Anna, 2008).

Most trypanosomatids also possess cytoplasmic organelles called acidocalcisomes which contain several ions, amino acids and enzymes on the basis of X-ray microanalysis, NMR spectroscopy and biochemical analyses (Moreno et al., 2000; Ruiz et al., 2001; Rohloff et al., 2003; Fang et al., 2007). Acidocalcisomes, therefore, are critical for the storage of ions and pH homeostasis. They possess a nucleolus-containing nucleus that is enveloped by a porous membrane (De Souza and Meyer, 1974; Solari, 1995). The nucleus also encloses a condensed chromatin dispersed throughout the nucleoplasm (De Souza and Meyer, 1974; Solari, 1995; Elias et al., 2001). During cell division, intranuclear microtubules appear and the chromatin disperses while the nuclear membrane remains intact (De Souza and Meyer, 1974; Solari, 1995; Elias et al., 2001).

Most trypanosomatids contain bacterial endosymbionts that play important roles in the biosynthetic pathways of the host protozoan (Gray, 1992; Motta, 1999). Members of the class *Kinetoplastea* possess spherical structures called glycosomes, which harbor the glycolytic pathway. Indeed, the glycosomal proteome of *T. brucei*, *L. major*, and *T. cruzi* showed that the glycosome is a critical site for several important glycolytic enzymes in these species (Parsons, 2004; Waller et al., 2004; Opperdoes and Szikora, 2006). Glycosomes also function in purine salvage pathways, biosynthesis of pyrimidines, synthesis of ether lipids and β -oxidation of fatty acids (Vickerman, 1994; Michels et al., 2000; Moyersoen et al., 2004).

Trypanosomatids possess mitochondria that are distributed in branches under the sub-pellicular microtubules while appearing to dilate in regions of disk-like structures called kinetoplasts. The kinetoplast DNA (kDNA) consists of circular topologically relaxed and interlocked network of minicircles and maxicircles (Stuart and Panigrahi, 2002; Liu and Englund, 2007; Schneider et al., 2008). There is a unique form of kinetoplast RNA editing mediated by short overlapping complementary minicircle-encoded guide RNAs that provide the information for uridylyate insertion and deletion on messenger RNA (mRNAs) through a series of enzyme-mediated cleavage-ligation steps (Blum and Simpson, 1990; Blum et al., 1990; Stuart and Panigrahi, 2002).

Trypanosomatids transcribe all protein-encoding genes polycistronically (Martinez-Calvillo et al., 2010). Generally, they utilize both cis- and trans-RNA splicing for the processing and maturation of pre-mRNAs although cis-splicing rarely removes introns due to the scarcity of intron-containing genes in trypanosomatid genome (Cordingley, 1985; Stuart et al., 2005). Trans-splicing of a 39-nucleotide spliced leader exon and 3'-end polyadenylation are particularly important for the maturation of translatable monocistronic units (Boothroyd and Cross 1982; Liang et al., 2003; Zamudio et al., 2009).

2.11 GENOME ORGANIZATION OF *T. BRUCEI*

T. brucei are single-celled extracellular species of trypanosomatids that can live freely in the bloodstream, lymph or cerebrospinal fluid. As in most trypanosomatids, the species possesses both a nuclear and a mitochondrial genome. There are 11 principal diploid nuclear chromosomes, several intermediate-sized chromosomes of 300–900 kb and many minichromosomes of 50–100 kb. The intermediate and mini-chromosomes serve as repositories of VSG genes (Horn and McCulloch, 2010). Generally, the intermediate and mini-chromosomes are not diploid in nature. Overall, the total genome size of *T. brucei* is about 35 Mb per haploid genome.

The surface of *T. brucei* is covered with a highly dense layer of approximately 10^8 molecules of VSG homodimers attached to the cell membrane via GPI anchors. The species has about 1000 VSG genes and pseudogenes even though transcription proceeds monocistronic at a time from one of multiple telomeric VSG expression sites. Antigenic variation in trypanosomes involves the random switching of VSG genes in a continuous manner, and this enables the parasite to maintain a state of chronic infection in the host (Horn and McCulloch, 2010). Gene conversion also leads to the production of multiple chimeric genes thereby resulting in the rapid evolution of the VSG family. As in most members of the trypanosomatids, the kinetoplast genome also contributes to genome plasticity via RNA editing using a complex structure called editosome (Carnes et al., 2011). Trypanosomes employ an extensive RNA editing process that appears to be unique to these parasites.

2.12 CELL DEATH IN *TRYPANOSOMATIDAE*

Observations in rat embryos exposed to toxicants were initially used as a system of morphological classification of cell death (Schweichel and Merker, 1973). Subsequent to this, different types of cell death have been observed in eukaryotes. Even though some studies have even described more

than five pathways of cell death (Melino et al., 2005), three main types are recognized in trypanosomatids: apoptosis (type I), autophagy (type II) and necrosis (type III).

Apoptosis is probably the best understood mechanism of cell death. Primarily, it is defined by shrinkage of the cell, formation of apoptotic bodies, blebbing of the plasma membrane and characteristic changes in nuclear morphology such as the condensation or fragmentation of chromatin (Taylor et al., 2008). If the integrity of the plasma membrane is severely affected, early apoptosis may eventually develop into late apoptosis.

In most mammalian cells, two main routes of apoptosis are recognized: the extrinsic death receptor pathway and the intrinsic mitochondrial pathway (Debatin and Krammer, 2004; Green and Kroemer 2004; Jiang and Wang 2004; Peter et al., 2007). The intrinsic pathway responds to various forms of cellular stress that activates proapoptotic Bcl-2 homology (BH3-only) proteins in order to sense death stimuli thereby relieving the inhibitory action of other antiapoptotic Bcl-2 proteins. The activation of BH3-proteins oligomerizes Bcl-2 associated X (Bax) and Bcl-2 antagonist/killer (Bak) proteins that may lead to the formation of pores in the outer mitochondrial membrane causing the release of cytochrome c. Cytosolic cytochrome c binds to the adaptor protein called apoptotic protease activating factor 1 (Apaf-1) thereby initiating the formation of the apoptosome and subsequent activation mechanisms. The extrinsic death receptor pathway is initiated by binding of death ligands to cognate death receptors and subsequent recruitment of adaptor proteins and death-inducing signaling complexes (DISC). In metazoans, the caspase family of proteases such as caspase 3, 8, and 9 form part of the central machinery of apoptosis activation in both intrinsic and extrinsic pathways (Los et al., 1999; Fuentes-Prior and Salvesen, 2004). However, in most protozoans such as trypanosomatids, the set of specific proteases responsible for the caspase-independent mechanisms in both pathways have not yet been characterized.

As in apoptosis, autophagy is a genetically regulated type of cell death. Classically, autophagy is activated during cellular development and differentiation, as well as in various conditions of environmental stress. Autophagy is a catabolic process by which proteins and other biomolecules are directed to lysosomes for recycling. It is characterized by the apparent encapsulation of cytosolic materials by autophagosomes and the subsequent fusion of autophagosomes with lysosomes. This fusion then triggers the degradation of autophagosomal contents in an autophagic process of cell death (Levine and Yuan, 2005; Levine and Kroemer, 2008).

At normal physiological conditions, autophagy occurs at low basal levels that contribute to the turnover of cytoplasmic components. Therefore, excess autophagy is usually the cause of autophagic cell death. Autophagy and apoptosis are interrelated in that autophagy may both promote and inhibit apoptotic cell death. In fact, regulators of apoptosis may also interfere with the process of autophagy (Maiuri et al., 2007). Therefore, further studies are required to characterize autophagy in the context of mechanism and interactions with other cell death pathways.

Necrosis is characterized by swelling of the cytoplasm, rupture of the plasma membrane, moderate condensation of the chromatin and the dilation of organelles such as mitochondria, endoplasmic reticulum and Golgi apparatus (Festjens et al., 2006). Initially thought to be a form of unregulated type of cell death, it is increasingly becoming clear that necrosis is more highly regulated than previously thought (Berghe et al., 2015). The process leads to a substantial rise in mitochondrial calcium overload that can depolarize the inner mitochondrial membrane and reduce ATP production (Orrenius et al., 2003). Regulated necrosis may be categorized into multiple cell death subclasses such as necroptosis, parthanatos, ferroptosis, netosis, pyroptosis, and ischemia reperfusion injury-mediated necrosis (Berghe et al., 2015).

A complex interaction also appears to occur between necrosis and other mechanisms of cell death. Inhibition of regulators of apoptosis or autophagy may affect the mechanism of necrosis. For instance, in most mammals, if phagocytes do not rapidly engulf apoptotic bodies during apoptosis, they may undergo late apoptosis, also known as secondary necrosis, during which the integrity of the plasma membrane can reduce significantly thereby triggering an inflammatory response (Berghe et al., 2015). Necrosis may, therefore, serve as a backup mechanism when apoptosis or autophagy fails.

All the canonical hallmarks of apoptosis, necrosis and autophagy have been reported in trypanosomatids (Welburn et al., 1996; Schmidt and Bütikofer, 2014; De Silva Rodrigues et al., 2016; Sousa et al., 2017). However, the underlying mechanisms of cell death remain poorly understood in trypanosomatids. Trypanosomatids, as in all protozoans, do not encode caspases in their genome (Kaczanowski et al, 2011). In metazoans, caspases play important roles in apoptosis, necrosis and autophagy because the major types of cell death overlap at the molecular level. The absence of caspases in trypanosomatids, therefore, raises interesting questions about how the underlying mechanisms are initiated and regulated in a caspase-independent manner in these protozoans.

Evolutionarily distant homologues of caspases called metacaspases are found in trypanosomatids (Vercammen et al., 2007). Five metacaspases are known to be encoded in the genome of *T. brucei* (Szallies et al., 2002). However, none of these has been clearly shown to be responsible for cell death in the parasite. Moreover, prostaglandin induced cell death in *T. brucei* occurred independently of three of the five known metacaspases (Helms et al., 2006). In *T. cruzi*, even though two metacaspases were reported to play a role in human serum induced cell death, an enzymatic function for these enzymes was not demonstrated (Kosec et al., 2006). In *L. major*, a

metacaspase was shown to be involved in the segregation of the nucleus and kinetoplast rather than apoptosis (Ambit et al., 2008). Hence, much remains to be understood as far as cell death pathways in trypanosomatids are concerned. Figure 2.3 summarizes the cellular mechanism of apoptosis and necrosis as observed in most eukaryotes include trypanosomes.

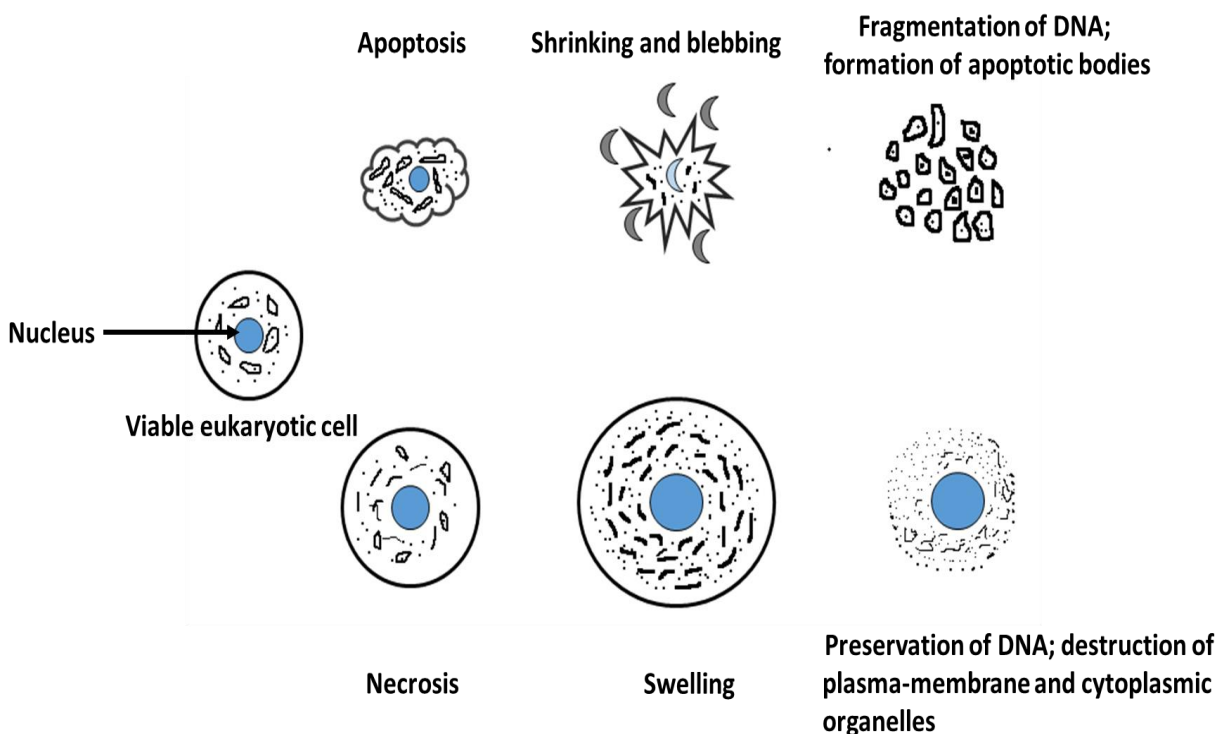


Figure 2.3: A diagram depicting the cellular mechanisms of apoptosis and necrosis in eukaryotes. In most eukaryotes, apoptosis is identified by shrinkage of the cell, formation of apoptotic bodies, blebbing of the plasma membrane and characteristic changes in nuclear morphology such as the condensation or fragmentation of chromatin. Necrosis is characterized by swelling of the cytoplasm, rupture of the plasma membrane, moderate condensation of the chromatin and the dilation of organelles such as mitochondria, endoplasmic reticulum and Golgi apparatus. Apoptosis and necrosis are the best understood types of cell death in most eukaryotes (Berghe et al., 2015).

2.13 CELL CYCLE IN *TRYPANOSOMATIDAE*

As in most eukaryotic cells, there are 4 canonical phases of the cell cycle in trypanosomatids: first gap phase (G₀-G₁), synthesis phase (S), second gap phase (G₂) and mitosis phase (M). During the

G₀-G₁ phase, the cell ensures that energy and nutrients are available for entry into a new round of DNA synthesis. The synthesis or replication of DNA takes place in the S-phase. During the G₂ phase, the cell ensures that there are sufficient nutrients for the division of the nucleus (karyokinesis) and cytoplasm (cytokinesis) during the subsequent M phase (Vaughan and Gull, 2008) (Figure 2.4).

In most eukaryotes, the molecular regulation of the cell cycle involves a set of key proteins with cyclin-dependent kinases (CDKs) and associated cyclins playing central roles. The interaction between cyclins and CDKs regulates the progression of the cell cycle. Different types of cyclins and CDKs are responsible for the regulation of distinct phases of the cell cycle (Murray, 2004; Hammarton, 2007). For instance, in mammalian cells, the activation of CDK4 and CDK6 through their interaction with cyclin D regulates the progression of the G₁ phase by inhibiting the retinoblastoma (Rb) protein (a repressor of transcription of cyclin E) (Murray, 2004; Hammarton, 2007). Also, cyclins E and A interact with CDK2 to regulate progression through the S phase while a complex of CDK1, cyclin A and cyclin B regulates the progression of mitosis (Murray, 2004; Hammarton, 2007). In most eukaryotic cells, the activity of CDKs is also regulated by phosphorylation. For instance, in mammals, phosphorylation of a threonine residue by the CDK-activating kinase (CAK) activates the CDK:cyclin complex (Hammarton, 2007). Protein phosphatases (PP) are also critical in the regulation of the cell cycle. For example, in mammals, protein phosphatase 2A (PP2A) regulates the cohesion of sister chromatids and subsequent mitotic exit while protein phosphatase 1 (PP1) controls the structure of chromatids and chromosomes during mitosis (Trinkle-Mulcahy and Lamond, 2006; Hammarton, 2007). Moreover, the cell division cycle (*cdc25*) phosphatases activate CDKs while *cdc14* phosphatases are involved in the

maturation of the centrosome, stability of the spindle and cytokinesis (Trinkle-Mulcahy and Lamond, 2006).

However, trypanosomatids regulate the cell cycle in uniquely conserved and divergent ways. Orthologs of conserved protein kinases such as MAPKs, CDKs, aurora and polo-like kinases (PLK) are present in *T. brucei*, albeit with divergent functions (Hammarton et al., 2003; Hammarton et al., 2005; Kumar and Wang, 2006). Moreover, checkpoint regulators such as the spindle checkpoint serine/threonine protein kinase (BUB1), centromeric histone (CenH3) and Rho GTPases have not yet been reported in trypanosomatids (Hammarton et al., 2003; McKean, 2003). Furthermore, receptor-linked tyrosine kinases have not yet been reported in trypanosomatids. Approximately 30 putative protein phosphatases are important in cell cycle regulation (Hammarton, 2007), thereby providing an explanation to the inhibition of kinetoplast segregation in procyclic forms of trypanosomatids (Das et al., 1994).

Regulation of the G1 phase in trypanosomes is different from that of most metazoans. In mammals, the ERK/Ras and PI3K pathways act to promote the progression of the G1 phase in mammals while the interactions of CRKs with CYC2, CYC4 and CYCE3 regulate G1 progression in trypanosomatids (Hammarton, 2007). RNA interference (RNAi) of the *CYC2* gene arrested both bloodstream and procyclic forms of *T. brucei* during the G1 phase (Li and Wang, 2003; Hammarton et al., 2004). Depletion of *CYC2* resulted in active microtubule extensions at the posterior end of the cell in procyclic forms of the parasite (Hammarton et al., 2004). RNAi of *CRK1* in blood stream and procyclic forms enriched G1 phase cells, an observation which was further enhanced by the co-downregulation of *CRK2* (Tu and Wang, 2004, 2005).

Aside the interaction between specific CRKs and CYCs, other G1 events such as the duplication of the flagellum, basal body and Golgi apparatus are also regulated by unique proteins (Hammarton, 2007). The γ/δ -tubulins, TbCentrin1/2 and the NIMA-related kinase (NRKC) have all been implicated in the regulation of the duplication of the basal body and flagellum in trypanosomes (He et al., 2005; Gadelha et al., 2006; Pradel et al., 2006). Moreover, depletion of PLK by RNAi in *T. brucei* may result in the production of aberrant cells thereby suggesting the importance of PLK in the G1 phase (Hammarton, 2007). MAPKs regulate flagellar length in *Leishmania* (Erdmann et al., 2006), while Parkin coregulated gene (PACRG) proteins maintain outer microtubule doublets along the axoneme (Dawe et al., 2005). TbCentrin2 may be required for the duplication of the Golgi apparatus (He et al., 2005), while the class III PI3K (Vps34) facilitates the segregation of the basal body.

The regulation of the S phase in trypanosomatids has also evolved different molecular pathways. In most eukaryotes, preparation towards the regulation of the S phase starts during the G1 phase. This is achieved through the assembling of a highly intricate replication licensing system known as the pre-replicative complex (pre-RC). The pre-RC comprises about 6 origin of recognition complexes (ORC), cdc6, chromatin licensing and DNA replication factor-1 (Cdt1) and the hexameric minichromosome maintenance complex (Mcm2-7) (D'Amours and Amon, 2004; Blow and Dutta, 2005). DNA replication is initiated by the S-phase CDK (S-CDK) and regulatory subunit [(Dbf4)-dependent kinase (DDK)] or the Dbf4-Cdc7 complex (Labib, 2010). S-CDK may phosphorylate two replication factors (Sld2 and Sld3) in order to generate binding sites for the DNA replication initiation protein (Dpb11), an important component of the pre-loading complex (pre-LC) (Araki et al., 1995; Tanaka et al., 2007; Zegerman and Diffley, 2007). Sld3 complexes with cdc45 for recruitment onto replication origins by interacting with the Mcm2-7 complex (Zou

and Stillman, 2000; Masai et al., 2006; Sheu and Stillman, 2006). The Dbf4-Cdc7 complex phosphorylates the N-terminal tails of several subunits in the Mcm2-7 complex, thereby forming the Cdc45-Mcm2-7 complex that can subsequently function as components of the replication fork to help unwind the duplex DNA (Calzada et al., 2005; Gambus et al., 2006; Moyer et al., 2006; Ilves et al., 2010; Sheu and Stillman, 2010).

About five ORC proteins are expressed in trypanosomes, namely, TbOrc1/Cdc6, TbOrc1b, TbOrc4, Tb3120, and Tb7980, which appear to be fundamental to the S phase progression. However, most of these are distantly related to the metazoan orthologs. Homologs of Cdt1, Sld2, Sld3, and the Cdc7-Dbf4 complex have not yet been reported in trypanosomes (Berriman et al., 2005). Although Mcm3 may interact with both TbOrc1/Cdc6 and TbOrc1b, recruitment towards the origins of replication is still poorly understood in trypanosomes (Dang and Li, 2011). Additionally, even though Mcm2-7 is exported from the nucleus after DNA replication in yeasts (Nguyen et al., 2000; Blow and Dutta, 2005), it appears to remain in the nucleus throughout the cell cycle in trypanosomes (Dang and Li, 2011). It appears to be Cdc45 that is exported out of the nucleus instead of Mcm2-7 (Dang and Li, 2011). Interestingly, homologs of serine/threonine-protein kinase tousel-like (TLK), nucleosome assembly factor (Asf1), and proliferating cell nuclear antigen (PCNA) proteins have been shown to be essential for DNA replication in trypanosomes (Li et al., 2007; Kaufmann et al., 2012). Moreover, an analogous DNA replication licensing system regulates the replication of kDNA (Klingbeil and Shapiro, 2009). Furthermore, it was shown that the heat shock protease/ATPase system (HslVU) regulates kDNA replication in the mitochondrion by controlling the abundance of the mitochondrial helicase TbPIF2 (Li et al., 2008; Liu et al., 2009).

Progression through the G2-M boundary in metazoans involves interactions between CDKs and the associated B-type cyclins. In the budding yeast, at least four B-type cyclins (Clb1 to Clb4) activate Cdc28 to facilitate the progression of G2-M transition while two B-type cyclins (Cig1 and Cdc13) are involved in the same process in the fission yeast (Humphrey and Pearce, 2005). In mammals, Cdk1 interacts with A- and B-type cyclins to regulate the G2-M transition (Harper and Brooks, 2005). In the G2 phase of mammals, Cdk1, which appears to be in an inactive state via its association with Wee1- and Myt1-mediated phosphorylation, might be activated by Cdc25-mediated dephosphorylation to stimulate mitotic entry (Harper and Brooks, 2005). Cdc25 may in turn be activated by PLK, which is an effective regulator of M phase (Archambault and Glover, 2009). PLK is also involved in the degradation of the Cdk1 inhibitor Wee1 (Van Vugt et al., 2004). In human cells, Aurora A kinase activates PLK1 in the G2 phase through phosphorylation of a threonine residue of PLK1 to help facilitate the G2-M transition (Seki et al., 2008). Moreover, Aurora A kinase may activate Cdc25 via phosphorylation at a site distinct from that of PLK (Dutertre et al., 2004).

In trypanosomes, G2-M transition is primarily regulated by the CRK3 and CYC6 pair (Hammarton et al., 2003; Li and Wang, 2003; Tu and Wang, 2004). Moreover, CRK3 also interacts with the primary trypanosomal G1 cyclin (CYC2) (Van Hellemond et al., 2000; Gourguechon et al., 2007), suggesting that CYC2 plays an important role in the G2-M transition. CYC6 may also form a complex with CRK9 to help regulate G2-M progression (Gourguechon and Wang, 2009). Furthermore, RNAi of CYC8 was reported to delay the G2-M transition in the procyclic form of *T. brucei* (Li and Wang, 2003). Interestingly, even though trypanosomes encode the homolog of Wee1 kinase, homologs of Myt1 kinase and Cdc25 phosphatase have not yet been found in the genome. Again, trypanosomes do express the PLK homolog (TbPLK) although it is not required

for mitosis due to its exclusion from the nucleus (Kumar and Wang, 2006; Hammarton et al., 2007; De Graffenried et al., 2008).

Cytokinesis initiation in mammals involves cooperation between Aurora B kinase and PLK to regulate the centralspindlin complex. The centralspindlin complex recruits the guanine nucleotide exchange factor (Ect2) to the mid-body, which then activates the small GTPase RhoA to further activate the actomyosin contractile ring (Glotzer, 2005; Carmena, 2008). Moreover, a system of septum initiation network (SIN) or mitotic exit network (MEN) is essential for cytokinesis even though how they interact with PLKs is not fully understood (Gruneberg and Nigg, 2003; D'Amours and Amon, 2004).

The regulation of cytokinesis in trypanosomatids is also different from that observed in most metazoans. In trypanosomes, cytokinesis is initiated at the anterior portion of the newly formed FAZ and progresses posteriorly via an ingression of a cleavage furrow (Kohl et al., 2003; Vaughan and Gull, 2008; Vaughan et al., 2008). Homologs of Aurora B kinase (TbAUK1) and PLK (TbPLK) may play important roles in cytokinesis initiation, furrow ingression, and abscission regulation (Kumar and Wang, 2006; Li and Wang, 2006; Tu et al., 2006; Hammarton et al., 2007). However, trypanosomatids appear to lack homologs of interacting partners of Aurora B and Polo-like kinases such as those found in other eukaryotes, which suggests that these protozoans have evolved distinct TbAUK1- and TbPLK-mediated pathways for the initiation of cytokinesis. Trypanosomes do express SIN/MEN pathway proteins such as homologs of monopolar spindle (Mps) one binder 1 (MOB1), yeast double PHD (plant homeodomain) fingers 2 (DPF2) kinase and human nuclear DPF2-related (NDR1) kinase (PK50 and PK53). While MOB1 helps to complete the cytokinesis in bloodstream forms, it positions the cleavage furrow in procyclic forms (Hammarton et al., 2005). Additional proteins that are also important for cytokinesis include the

type III phosphatidylinositol 4-kinase (Rodgers et al., 2007), KMP-11 (Li and Wang, 2008), arginine methyltransferase (Fisk et al., 2010), the small GTPase ARL2 (Price et al., 2010), Katanin and Spastin (Benz et al., 2012), the F-box protein CFB2 (Benz and Clayton, 2007), the microtubule-associated protein AIR9 (May et al., 2012), adenylyl cyclase (Salmon et al., 2012) and the kinetoplast-specific kinesin TbKIN-C together with its partner TbKIN-D (Humphrey and Pearce, 2005; Hu et al., 2012). Hence, cytokinesis appears to involve an intimate coordination between cell morphogenesis and cell division. The cellular mechanism of the cell cycle in *T. brucei* is summarized schematically in Figure 2.4.

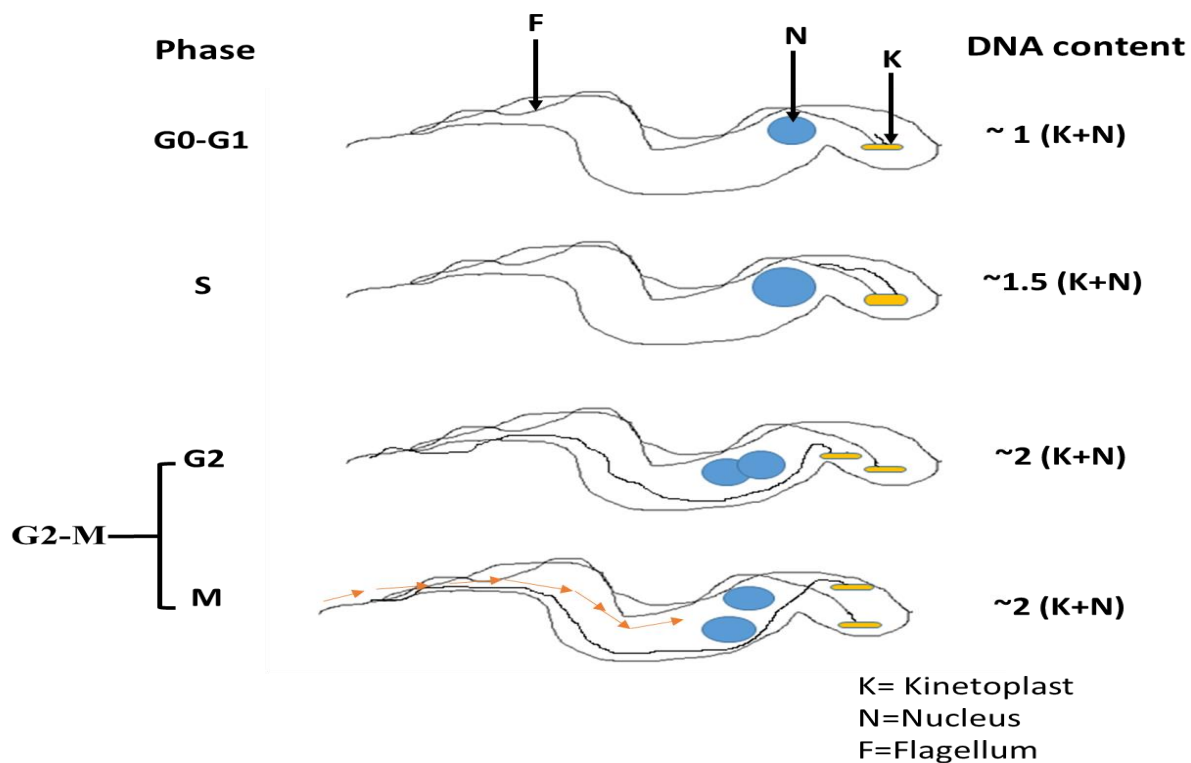


Figure 2.4: A schematic diagram depicting the cell cycle phases in *T. brucei*. There are 4 canonical phases of the cell cycle in *T. brucei*: first gap phase (G0-G1), synthesis phase (S), second gap phase (G2) and mitosis phase (M) (Vaughan and Gull, 2008). During the G0-G1 phase, the cell ensures that energy and nutrients are available for entry into a new round of DNA synthesis. The synthesis or replication of DNA takes place in the S-phase. During the G2 phase, the cell ensures that there are sufficient nutrients for the division of the nucleus (karyokinesis) and cytoplasm (cytokinesis) during the subsequent M phase. Morphology and intracellular organelles are intact during G0-G1 phase, while DNA synthesis leads to an increase in the size of the kinetoplast and nucleus during the S-phase. By the end of the G2 phase, division of the kinetoplast is complete while karyokinesis is about half-way through. During the M phase, karyokinesis is complete as cytokinesis begins by the indication of the orange arrows. In terms of DNA content, the G2 and M phases are almost indistinguishable [$\sim 2 (K+N)$], thereby essentially forming a single G2-M phase.

2.14 CONTROL OF AFRICAN TRYPANOSOMIASIS

The two main types of AT are HAT and AAT (Raper et al., 2001; Simarro et al., 2012). While HAT afflicts an estimated 70 million populations in about 36 sub-Saharan African countries (Simarro et al., 2012), AAT continues to threaten the lives of several million herds of cattle every year and requires new approaches of combating the disease (Morrison et al., 2016). Moreover, even though there is no reported case of HAT in Ghana, AAT remains a burden albeit with scanty reported data (Mahama et al., 2003). Through parasitological and serological detection methods, bovine trypanosomiasis was characterized in the West Mamprusi (16% and 53%, respectively) and Savelugu districts of Ghana (8% and 24%, respectively) (Mahama et al., 2004). In addition, distinct parasite prevalence in tsetsefly (17.4%), cattle (57.5%) and pigs (28.6%) was characterized in the Adidome and Koforidua regions of Ghana using molecular epidemiology (Nakayima et al., 2012).

The most comprehensive way to control AT involves an all-encompassing approach of different strategies: vector control, reservoir control, vaccination and chemotherapy. Each control strategy has its own set of advantages, strengths and limitations. Moreover, as far as prevention is concerned, it is noteworthy that general hygiene procedures may also be helpful in the control of AT. Furthermore, strategies may overlap or exert considerable impact on each other. For instance, an effective diagnosis or detection of the parasite may be essential to the success of chemotherapy for the host or reservoir. In Ghana, the use of insecticide-impregnated traps and blue screens, as well as prophylactics and curative drugs may remain the most popular vector control and chemotherapeutic strategies for AAT (Mahama et al., 2003).

2.14.1 Vector control of African trypanosomiasis

Tsetse flies belong to the *Glossina* genus, *Glossinidae* family and the order of *Diptera*. Classification of *Glossina* depends on external morphological characteristics such as color, shape of antennae, nature of bristles on thoracic pleura, shape of genitalia, geographical distribution and other bioecological features (Newstead, 1911). *Nemorhina*, *Glossina* sensu stricto (*Glossina* s.str.) and *Austenina* form the three main subgenera of *Glossina*. *Glossina Nemorhina palpalis* (*G. n. palpali*), *Glossina Glossina longipalpis* (*G. g. longipalpis*) and *Glossina Austenina brevipalpis* (*G. a. brevipalpi*) are the standard subspecies of *Nemorhina*, *Glossina* s.str. and *Austenina*, respectively (Newstead, 1911).

The only known cyclical vectors of human and animal trypanosomes are tsetse flies. The life cycle of tsetse flies is a typical example of adenotrophic viviparity that involves the development of a single larva in the uterus of the female fly. Infection of tsetseflies by trypanosomes can occur at any time in the life of the fly. Both female and male flies are potential vectors since both do feed on vertebrate blood. Generally, vegetation-determined climate and host availability determine the density of tsetse fly populations. Moreover, there has not been any reported case of resistance to insecticides in tsetse flies. Thus, effective vector control can have a positive impact on the overall effort towards AT control.

Vector control remains crucial to the fight against AT because it is currently the only strategy that is capable of protecting against the acquisition of infection. There are two main objectives behind vector control: one objective is to reduce the density of tsetse flies thereby reducing the risk of transmission to an acceptable level, while the other objective involves the complete eradication of tsetse flies from a given area irrespective of the geographical scale (Knipling, 1955). In either case,

preliminary surveys to help determine the spatial distribution of fly, species identity and critical tsetse–human points of interaction are crucial to the success of the vector control strategy.

An integrated strategy that can exploit all the weaknesses in fly behavior as well as promote synergy of different methods is the best approach towards vector control. Strategies commonly applied include bush clearing (Ford et al., 1970), elimination of wild animal hosts (Potts and Jackson, 1952; Robertson, 1983), autonomous control of tsetse flies (Courtin et al., 2009, 2010), indigenous control of tsetse flies, spraying techniques (Jordan, 1986; Adam et al., 2013), zero grazing practices (Bauer et al., 2006, 2011), bait methods (Challier and Laveissiere, 1973; Challier et al., 1977; Hargrove and Vale, 1979; Green and Cosens, 1983) and other forms of sterile insect techniques.

Bush clearing and elimination of wild animal hosts are gradually fading off as large-scale vector control methods due to environmental concerns. For instance, even though extensive bush clearing is currently not commonly practised due to environmental concerns, local farmers still practise it at least on a small scale. Clearing of vegetation is probably the oldest way of reducing vector population (Ford et al., 1970). However, when the vegetation reappears, flies can invade. In the same way, when games recover, fly populations may naturally be restored.

Autonomous control of tsetse flies refers to the spontaneous reduction of fly populations as the influence, pressure or impact of the human factor increases. Typical examples of such pressures include economic growth, deforestation, hunting and expansion of agriculture (Courtin et al., 2009, 2010). Furthermore, indigenous practices have been used by farmers and pastoralists to help limit contact between tsetse and herds. Most farmers also tend to avoid tsetse-infested areas during grazing. However, in the dry season, livestock may still be exposed to tsetse bites at infested areas.

Ground and aerial insecticide spraying are also useful vector control techniques (Jordan, 1986; Adam et al., 2013). In the twentieth century, ground spraying was useful for controlling tsetse population in many African countries. For example, in Nigeria, about 200,000 km² of land was eradicated of tsetse flies through the application of dichlorodiphenyltrichloroethane, dieldrin and endosulfan between 1955 and 1978 (Jordan, 1986). Aerial spraying is accomplished in the form of a sequential aerosol technique using fixed-wing aircrafts and helicopters. This approach has been applied in different African countries such as Ghana, Angola, Botswana, Burkina Faso, Namibia and Zambia (Kgori et al., 2006, 2009; Adam et al., 2013). However, spraying techniques have certain limitations and disadvantages. First, it may have several adverse effects on non-target organisms such as reptiles, mammals, fish, birds and other insects. In addition, as the use of sequential aerosol technique depends on the landscape, it is generally difficult for aircraft to operate in hilly areas. Again, the possibility of resistance to insecticides may exist.

In the method of zero grazing, livestock is constrained and fed in an enclosed and shaded area without being allowed to roam about. In this approach, mosquito netting impregnated with synthetic pyrethroids may be placed at a reasonable height around grazing units to protect the animals from tsetse bites while simultaneously serving as a form of bait to attract and kill the flies. Attracted flies are then captured by the netting, from where they pick up toxic or lethal doses of insecticides (Bauer et al., 2006, 2011).

Bait instruments are available as less damaging, simpler and cheaper techniques for controlling tsetse flies (Challier and Laveissiere, 1973; Challier et al., 1977; Hargrove and Vale, 1979; Green and Cosens, 1983). The methods involve the use of well-designed traps or screens for catching tsetse flies. Bait screens are particularly useful for drastically reducing fly populations. Biconical,

monoconical, vavoua, lancien, pyramidal, epsilon, F-3, ngu and H-traps are common examples of such screens. Efficiency of screens can increase several fold via the utilization of chemicals that attract tsetse to their hosts. Attractants such as 1-octen-3-ol, 4-methylphenol, 3-n-propylphenol, 2-butanone, carbondioxide and para-cresol have been identified as promising attractants for different species of *Glossinidae* (Hall et al., 1984; Hassanali et al., 1986; Saini, 1990, 1992; Saini et al., 1993; Tour et al., 1995). Moreover, instead of using traps, host animals themselves may be used as live baits to control tsetse fly populations. Animals can serve as mobile baits to capture and kill flies when they are sprayed with insecticides (Bauer et al., 1995).

The sterile insect approach involves the sterilization of male tsetse with gamma radiation before releasing them into the population of wild tsetse. Hence, females inseminated by sterile males would produce no viable offspring thereby leading to a gradual decline of wild population. The sterile insect approach is only useful if the targeted area is isolated in order to prevent reinvasion. Moreover, in practice, the technique is usually preceded by methods such as live baits, traps, targets and insecticide spraying, which may help to increase the efficiency of the control method. The sterile insect technique was employed to eradicate *G. austeni* on Unguja Island, Zanzibar (Vreysen et al., 2000; Hendrichs et al., 2005), after initial suppression of the fly population with bait targets and insecticide-treated cattle (Vreysen, 1996, 2005). However, the production and logistics involved in the sterile insect approach are complicated and expensive (Shaw et al., 2013). Moreover, it may not be feasible in areas of multiple species of tsetse fly.

2.14.2 Vaccine development for African trypanosomiasis

If the ultimate goal is the prevention of AT, then vaccination remains one of the most effective options. It also remains a powerful approach to potentially eradicate AT from affected regions. Even though no commercially available antitrypanosomal vaccine exists, several biomolecules of

the parasite are potential targets for the research and development of effective vaccines against AT. These include the expression site associated genes (ESAG6/7) transferrin receptor, actin, tubulin, cation pump, sialidase, cysteine protease (CP), GPI and flagellar pocket antigens (La Greca and Magez, 2011).

The flagellar pocket is a membrane invagination at the base of the parasite's flagellum that plays important roles in exocytosis, endocytosis, cell division, protein trafficking, virulence and immune evasion (La Greca and Magez, 2011). Thus, invariant trypanosome antigens of the flagellar pocket are potential candidates for vaccine development. Immunization of cattle with invariant antigens of the flagellar pocket conferred a partial protection (Mkunza et al., 1995). Also, mice immunized with preparations of flagellar pocket proteins provided partial protection of about 60% (Radwanska et al., 2000). In a similar approach, vaccination with a DNA plasmid that encodes a bloodstream form of invariant surface glycoproteins resulted in about 40% protection of mice with a corresponding increase in IgG2a antibodies (Lança et al., 2011). However, in most cases, subsequent challenges with higher load of the parasite suggested that the induced protection was short-term. Thus, only a marginal protection towards low-dose infections was probably induced (Radwanska et al., 2000).

Actin is involved in cell division, motility and formation of coated vesicles (García-Salcedo et al., 2004). Mice immunized with actin displayed varying extents of protective immunity towards *T. evansi*, *T. equiperdum* and *T.b. brucei* (Li et al., 2009). Mice immunized with recombinant β -tubulin were also protected from lethal challenge with trypanosomes through an antibody-mediated response mechanism (Li et al., 2007). Moreover, tubulin immunization protected about 60–80% of mice in a parasite challenge of *T. brucei*, *T. congolense* and *T.b. rhodesiense* (Lubega

et al., 2002). However, a short-term parasite challenge was utilized in all the studies, thereby making it difficult to assess the functional implementation of immunological memory.

Trans-sialidases and cation pumps are membrane-associated proteins that also serve as potential candidates for vaccine development. Sialidases are enzymes involved in the transfer of sialic acid of sialylated glycoconjugates from the surface of the host cell to acceptor molecules on the surface of the parasite (Schenkman et al., 1991). Immunization with a plasmid that encodes the catalytic and N-terminal domains of sialidase provided about 60% protection to mice challenged with a low dose of 500 *T. b. brucei* parasites (Silva et al., 2009). With respect to cation pumps, which are essential for cation homeostasis in the parasites, vaccination was shown to cause a biased stimulation of pro-inflammatory cytokines (Ramey et al., 2009). However, only a short-term induction of the cytokines was observed.

Anti-disease approaches towards vaccine development may provide alternatives to anti-parasite methods. GPIs and CPs are prominent examples of candidates utilized in anti-disease approaches of vaccine development. Liposome-based GPI treatment of mice previously challenged with parasites increased the expression of the anti-inflammatory cytokines while impairing the secretion of pro-inflammatory mediators (Stijlemans et al., 2007). The treatment also prolonged the survival of mice, as well as alleviated the clinical symptoms of infection such as liver damage, anemia and weight loss. In addition, trypano-susceptible animals immunized with predominant families of congopain (CP1 and CP2) displayed characteristics of weight gain and less severe anemia (Boulangé et al., 2001). Particularly, CP2 might have been involved in immunosuppression based on the prominent IgG responses developed by the animals, which mimicked responses of a trypano-tolerant animal (Boulangé et al., 2001). However, as in most cases of anti-parasite candidates, short-term induction of immunity might have been the norm.

2.14.3 Chemotherapeutic control of African trypanosomiasis

Currently, the most economically viable means of parasite control is chemotherapy. Different drugs are used in the treatment of AAT and HAT (Figures 2.5, 2.6). AAT may be treated with isometamidium, homidium, diminazine, pyritidium and quinapyramine (Melaku and Birasa, 2013). Species that may be treated with AAT drugs include *T. vivax*, *T. brucei*, *T. congolense* and *T. evansi* (Melaku and Birasa, 2013). Pentamidine, eflornithine and nifurtimox are used in the treatment of *T. b. gambiense* HAT while melarsoprol and suramin are involved in the treatment of *T. b. rhodesiense* HAT (Fairlamb, 2003). Moreover, pentamidine and suramin are useful for early-stage HAT while nifurtimox, eflornithine and melarsoprol are employed in the treatment of late-stage HAT (Fairlamb, 2003). Elucidation of the action and resistance mechanisms of antitrypanosomals is critical to drug discovery. Even though nucleoside transporters and changes in mitochondrial electrical potential might be closely associated with antitrypanosomal activities of AAT drugs, their exact action and resistance mechanisms remain largely unexplored (Melaku and Birasa, 2013). However, the mechanisms of action for most of the HAT drugs have been fairly studied, albeit poorly understood.

Suramin is a colorless, highly soluble polyanionic sulfonated naphthylamine that is given intravenously by injection. The action mechanism of suramin might be linked to the inhibition of various glycolytic enzymes (Fairlamb and Bowman, 1980). Suramin might also affect the biosynthesis of polyamine with regards to its potential synergy with eflornithine (Clarkson et al., 1984). Moreover, it might be capable of interacting with multiple targets thereby providing an explanation as to why no significant resistance has yet been associated with its usage (Fries and Fairlamb, 2003).

The uptake of pentamidine may be linked to several receptors (De Koning, 2001). Pentamidine was shown to disrupt the structure of kDNA possibly through the inhibition of topoisomerase II (Shapiro and Englund, 1990). It was also reported to inhibit the catalytic activity of group I intron in *Candida albicans* and *Pneumocystis carinii* (Liu et al., 1994; Zhang et al., 2002). Pentamidine may exhibit an *in vitro* effect on S-adenosylmethionine decarboxylase (AdoMetDC), and thus may be involved in the inhibition of polyamine biosynthesis (Fairlamb, 2003). However, pentamidine did not cause any changes in the levels of putrescine or spermidine in *T. b. brucei in vivo* (Berger et al., 1993). Other potential targets of pentamidine may also involve the plasma membrane Ca^{2+} ATPase and the mitochondrial membrane potential (Vercesi and Docampo, 1992; Benaim et al., 1993).

Melarsoprol is administered intravenously when dissolved in propylene glycol due to its poor solubility in water. It is administered as a prodrug that is rapidly converted to the pharmacologically active form called melarsen oxide (Keiser et al., 2000). P2 purine transporters are mainly involved in the uptake of trivalent arsenicals including melarsoprol (Carter and Fairlamb, 1993). Melarsen oxide forms a stable but reversible product by reacting with trypanothione. This product is competitively inhibited by trypanothione reductase, an enzyme involved in maintaining the balance of thiol-redox within the parasite (Fairlamb and Cerami 1992).

Nifurtimox and eflornithine are typically used together in a combination therapy. Eflornithine is an irreversible inhibitor of ornithine decarboxylase (ODC) within the first committed step of polyamine biosynthesis. This may in turn cause a reduction in the levels of spermidine, putrescine or trypanothione. It may also result in a disturbance of AdoMet metabolism (Fairlamb, 2003). These may ultimately interfere with the biosynthesis of DNA, RNA or protein, as well as potential morphological effects on the parasite (Fairlamb, 2003). Nifurtimox is a 5-nitrofurantoin that is

administered orally. The cyclical oxido-reduction of nifurtimox's nitro group produces superoxides, hydrogen peroxides and free radicals that may result in the damage of the DNA, lipids and proteins in the parasites (Docampo, 1990).

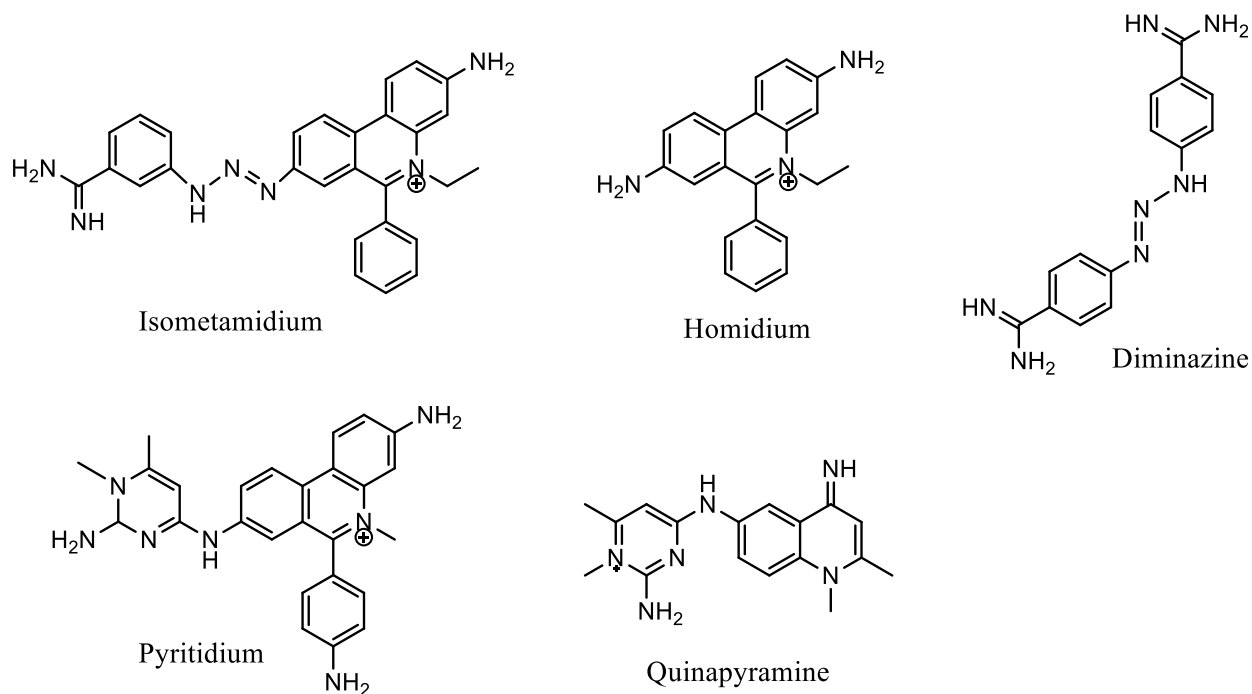


Figure 2.5: Chemotherapeutic control of AAT: AAT is treated with isometamidium, homidium, diminazine, pyritidium or quinapyramine. Species that may be treated include *T. vivax*, *T. brucei*, *T. congolense* and *T. evansi*.

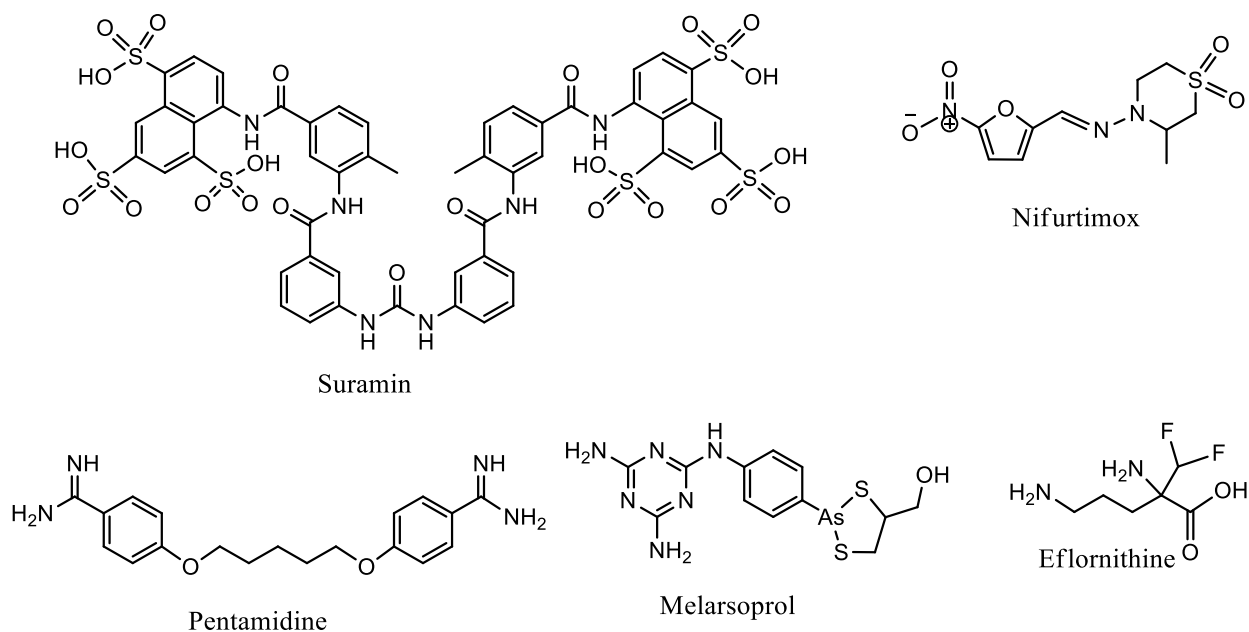


Figure 2.6: Chemotherapeutic control of HAT: Suramin and pentamidine are used to treat early-stage *T. b rhodesiense* and *T. b gambiense* HAT respectively. Melarsoprol is used to treat late-stage *T. b rhodesiense* HAT while nifurtimox and eflornithine are mainly employed in the treatment of late-stage *T. b gambiense* HAT. Currently, nifurtimox and eflornithine are used collectively as a combination therapy.

2.15 CHALLENGES IN THE CONTROL OF AFRICAN TRYPANOSOMIASIS

There are challenges associated with the various strategies of vector control. Whenever vegetation reappears, flies and games usually re-invade an initially cleared area. Livestock are re-exposed to tsetse bites when taken back to infested areas, thereby making an autonomous control of fly population impractical. Spraying techniques may have inadvertent adverse effects on reptiles, mammals, fish, birds and other insects. Sequential aerosol techniques depend on the landscape, thereby making it difficult to operate in mountainous areas. The production and logistics involved in the release of sterile insects are complicated and expensive to use, thereby limiting the utilization of the sterile insect approach.

The control of AT via vaccination also comes with its own challenges. In most cases of vaccination studies involving mammals, subsequent challenges with higher loads of parasites or their antigens

show that only a short-term protection is induced. The limitation associated with vaccination is mainly due to certain immune evasion strategies evolved by trypanosomes. The most important immune evasion strategy appears to be the antigenic variation involving the VSGs. However, other pathogenically useful strategies involve the trypanolytic factor defense, use of adenylate cyclase to inhibit parts of the innate response and immune modulation of the death and proliferation of B or T cells (Cnops et al., 2015).

Even though chemotherapy is currently the most economically viable mode of parasite control, there are limitations associated with the commercially available antitrypanosomal drugs. These challenges mainly originate from issues of side effects, drug resistance and physicochemical limitations (Fairlamb, 2003). Side effects of suramin include exfoliative dermatitis, agranulocytosis, haemolytic anaemia, nausea, vomiting, kidney damage and diarrhea. Due to its large size, suramin has difficulties in penetrating the blood-brain barrier. Side effects of pentamidine may include hypotensive reactions, liver damage, kidney damage and damage to the pancreas. Moreover, pentamidine exhibits poor availability because it is highly protonated at physiological pH. The use of melarsoprol may result in reactive encephalopathy, vomiting, abdominal colic, peripheral neuropathy, arthralgia, thrombophlebitis, acute haemolysis. Aside from being difficult to administer, eflornithine may cause bone marrow suppression. Moreover, the superoxides, free radicals and hydrogen peroxides that result from the oxido-reduction of nifurtimox may cause damage to host cells (Fairlamb, 2003).

2.16 RNA INTERFERENCE IN *T. BRUCEI*

RNAi is the regulation of gene expression by an array of approximately 20- to 30-nucleotide non-coding small RNAs and their associated set of proteins in most eukaryotic cells. The process involves the association of a small non-coding RNA with a class of proteins to form a gene-silencing ribonucleoprotein called RNAi-induced silencing complex (RISC). The base pairing between a target mRNA of a gene and RISC then provides the specificity to regulate the level of mRNA via degradation or transcriptional repression. RNAi controls critical processes such as cell growth, tissue differentiation, heterochromatin formation and cell proliferation (Lu et al., 2008; Carthew and Sontheimer, 2009; Berezikov, 2011).

At least 3 non-coding small RNAs are central to the formation of RISCs during RNAi in most eukaryotes. These include microRNA (miRNA), short interfering RNA (siRNA), and piwi interacting RNA (piRNA). The biogenesis of miRNA, which is the best understood noncoding small RNA, starts from the nucleus as a primary miRNA (pri-miRNA). A pri-miRNA is at least 1000 nucleotides and may possess single or clustered double-stranded hairpins with single-stranded 5'-and 3'-terminal overhangs together with approximately 10-nucleotide distal loops (Saini et al., 2007). A pri-miRNA is processed by a complex of an RNase III family enzyme (Drosha) and the vertebrate DiGeorge syndrome critical region gene 8 (DGCR8) protein (or the orthologous invertebrate Pasha), a protein with two double-stranded RNA-binding domains (dsRBDs) (Kim and Kim, 2007). The cropped approximately 70-nucleotide precursor miRNA (pre-miRNA) associates with specific proteins to be exported to the cytoplasm (Lund and Dahlberg, 2006). While miRNA is mostly endogenous in biogenesis, siRNA could be endogenous or exogenous in origin. Furthermore, while siRNA precursor duplexes involve nearly perfect base-pairing, that of miRNA helices contain mismatches and relatively extended terminal loops.

However, once the processed RNA assembles into the RISC, subsequent molecular pathways of miRNA and siRNA converge considerably. Moreover, despite the fact that piRNA is mostly endogenous, its biogenesis pathway remains poorly understood except for a proposed ping-pong mechanism (Brennecke et al., 2007; Aravin et al., 2008).

In the cytoplasm of eukaryotes, at least three proteins are responsible for the processing of the precursor small RNA and the subsequent incorporation into RISC: dicer, Argonaute and dsRNA-binding protein (dsRBP). These proteins essentially constitute a RISC-loading complex (RLC) that generates a diced double-stranded RNA (dsRNA) to be loaded onto Argonaute (MacRae et al., 2008). The dsRNA that is produced is a duplex of about 21 to 25 nucleotides with a 2-nucleotide overhang at the 3'-terminus and a phosphate group at the 5'-terminus (Schwarz et al., 2003). The process of loading a RISC involves a strand selection step, in which one strand (guide strand) of the duplex is bound to Argonaute to direct silencing while the other strand (passenger strand) is discarded. Once a dsRNA helix is bound to Argonaute, the 3'-terminus and 5'-phosphate of the guide strand also bind to PAZ (PIWI/Argonaute/Zwille) and MID (middle) domains of Argonaute, thereby forming RISC.

RISC examines the extent of complementarity between a target mRNA and Argonaute's guide RNA. Nucleotides 2 to 8 of the guide RNA constitute the critical seed sequence to initiate binding to a target mRNA. The extent of complementarity and base pairing may influence the nature of subsequent silencing pathways. If the complementarity is perfect, direct cleavage of the mRNA may be triggered through the catalytic activity of Argonaute. However, RISC can also trigger a translational repression before or after initiation which may be followed by deadenylation or degradation. Moreover, extra downstream pathways may be involved in subsequent silencing processes of the target mRNA. These include the recruitment of additional components to RISC

as well as the localization of silencing activity to cytoplasmic loci known as processing bodies (Eulalio et al., 2008).

The molecular mechanism of RNAi in *T. brucei* involves a similar level of detail and complexity. *T. brucei* is probably the only parasitic protozoan in which RNAi has been demonstrated to occur in a canonical and fully functional manner. In other parasitic protozoans such as *Plasmodium* and *Leishmania*, RNAi may only occur in relatively non-canonical pathways (Mueller et al., 2014). RNAi in *T. brucei* was first observed when a plasmid bearing a portion of α -tubulin mRNA was transfected into *T. brucei* (Ngo et al., 1998; Ullu et al., 2002). Since the discovery of the phenomenon, it has been immensely useful in the study of gene function in *T. brucei*.

The study of RNAi in *T. brucei* began with the utilization of two types of vectors, namely, hairpin and double promoter vector cassettes (Ullu et al., 2002). The hairpin construct utilized a pLew79 vector backbone in which a luciferase gene is replaced by a cassette of two inverted repeats of the mRNA target sequence separated by a stuffer sequence (Wirtz et al., 1999). In this construct, RNA transcription occurs by tetracycline-inducible procyclic acidic repetitive protein (PARP) promoter to produce a hairpin-like molecule of RNA (Shi et al., 2000). The double promoter vector employed two opposing tetracycline-inducible T7 RNA polymerase promoters flanking the mRNA target sequence (Shi et al., 2000). Although the double promoter vector has the advantage of requiring only a single cloning step to insert the target mRNA between the promoters, there is the possibility of leaky transcription of dRNA in the absence of tetracycline (Wirtz et al., 1999). To a large extent, modern *T. brucei* RNAi vectors are improved inversions of both constructs.

RNAi is immensely useful in the study of gene function and subsequent validation of potential drug targets in *T. brucei*. Through the construction of a library of genomic fragments in the

appropriate vector and the subsequent generation of a library of transgenic trypanosomes, it is possible to screen for mutant phenotypes of interest in *T. brucei*. This approach has proven to be immensely valuable in the identification of potential targets and subsequent elucidation of mechanisms of action of antitrypanosomals (Figure 2.7). For instance, it was utilized to screen for potential genes involved in the action and resistance of HAT drugs (Alsford et al., 2012). The possible existence of multiple targets was brought to light in the detection of about 28 genes in an RNAi library screening of suramin in *T. brucei* (Alsford et al., 2012). Moreover, a screening of pentamidine in *T. brucei* identified about 9 genes which may be involved in the resistance mechanism of pentamidine, with the P-type ATPase and aquaglyceroporin-2 being important candidates (Alsford et al., 2012). The approach also identified the amino acid transporter 6 (AAT6) as a useful importer of eflornithine (Alsford et al., 2012). A flavin-dependent nitroreductase, putative flavokinase and proteins for ubiquinone biosynthesis were identified as potential candidates for the mode of action of nifurtimox. Aside trypanothione reductase, the screening of melarsoprol also detected genes such as aquaglyceroporin-2 and large tumor suppressor (LATS1)-related protein (Alsford et al., 2012). Therefore, RNAi promises to be a valuable tool for drug discovery in AT.

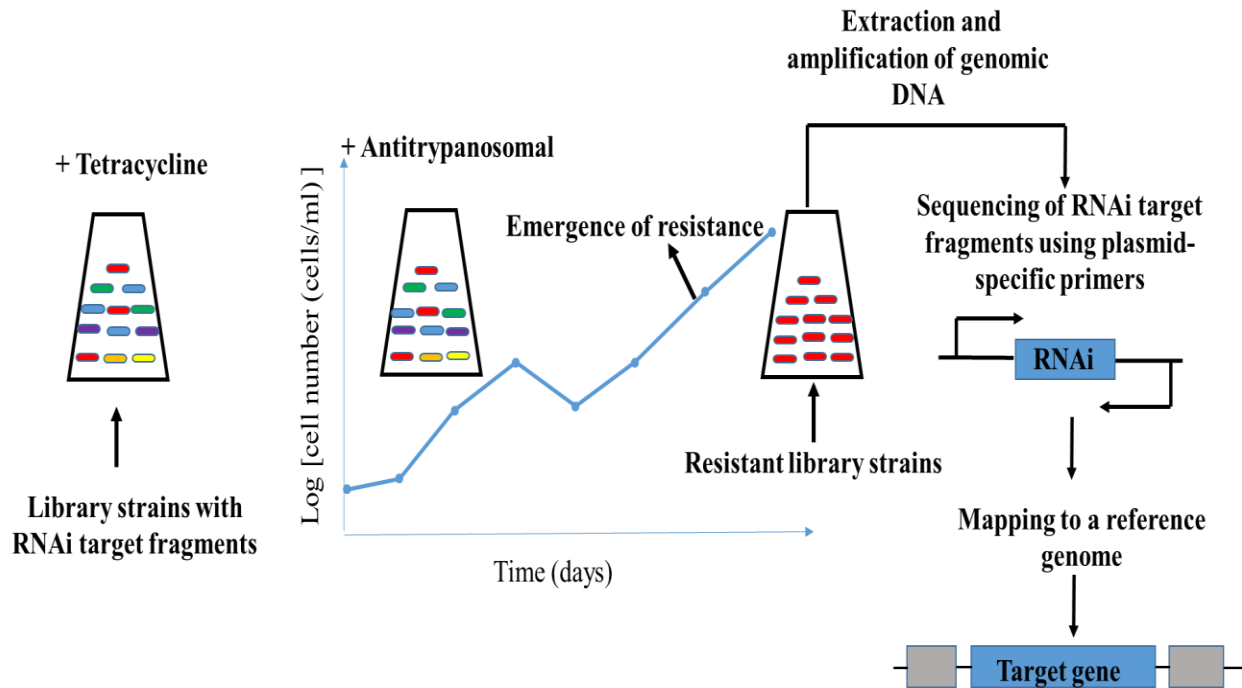


Figure 2.7: A schematic diagram of RNA interference target sequencing (RITseq). When RNAi library that contains RNAi target fragments are induced with tetracycline and subsequently exposed to an antitrypanosomal agent, RNAi fragments are downregulated thereby leading to the reduction in the sensitivity of library strains to the antitrypanosomal (Alsford et al., 2013). This facilitates the emergence of resistant strains. These strains can be extracted, purified, PCR-amplified, sequenced and mapped to a reference genome to identify RNAi target fragments involved in the mode of action and resistance of the antitrypanosomal agent under investigation.

CHAPTER THREE

3.0 MATERIALS AND METHODS

3.1 CULTURE OF PARASITES AND HUMAN CELL LINES

Wildtype *T. brucei* blood-stream forms of the subspecies *T. b. brucei* (GUTat 3.1 strains) and Jurkat cells were cultivated *in vitro* to the logarithmic phase using Iscoves Modified Dubelco's Media (IMDM, Thermo Fisher Scientific) with 10% foetal bovine serum (Thermo Fisher Scientific) at 5% CO₂ and 37°C. Wildtype blood stream forms of the subspecies *T. b. brucei* (2T1 strains) (Alsford et al., 2005), as well as mutant RNAi library strains were cultivated *in vitro* to the logarithmic phase using Hirus's Modified Iscove's medium (HMI-9, Life Technology) supplemented with 10% foetal bovine serum (Sigma-Aldrich) at 5% CO₂ and 37°C. Chang liver (HeLa derivatives) cell lines were cultivated *in vitro* to the logarithmic phase using Minimum Essential Medium (MEM, Thermo Fisher Scientific) with 10% foetal bovine serum at 5% CO₂ and 37°C.

3.2 CRUDE EXTRACTION AND FRACTIONATION OF PLANTS

Plant species were collected from an arboretum and the environs of the Center for Plant Medicine Research (CPMR), Mampong-Akuapem, Ghana. It was authenticated by Herone Blagooee, a Senior Botanist at the Plant Development Department of CPMR and given the voucher specimen numbers of CPMR 4120/4121/4122 (*Z. zanthoxyloides*) and CPMR 4123/4124/4125 (*B. pilosa*). Crude extracts and fractions were prepared from the air-dried pulverized plant material using the modified Kupchan method (Kupchan et al., 1973) of solvent extraction (Figure 3.1). Briefly, 250 g each of the pulverized air-dried plant materials was soaked in dichloromethane and left in the cold to percolate for one week. The dichloromethane extracts were decanted and filtered through a mixture of cotton and glass wool. The plant materials were then soaked in methanol for one week

and the methanol extract was decanted and filtered. The methanol and dichloromethane extracts were combined and dried under vacuum with a Heidolph Rotavap at 40 °C and 1 atm pressure to give 1.5 g of total crude extract (TCE) for *Z. zanthoxyloides* and 1.0 g TCE for *B. pilosa*. The TCEs were suspended in 200 ml water and extracted three times with dichloromethane. The remaining aqueous layer was then extracted once with *sec*-butanol and the butanol fraction was dried under vacuum to give the WB fraction (0.5 g for *Z. zanthoxyloides* and 0.4 g for *B. pilosa*). The dichloromethane layer was dried under vacuum to give 0.9 g of extract which was suspended in a 1:9 mixture of water and methanol (200 ml). This fraction was then extracted three times with hexane (200 ml) after which the hexane layer was dried under vacuum to give an FH fraction (0.2 g for *Z. zanthoxyloides* and 0.2 g for *B. pilosa*). The remaining 1:9 mixture of water and methanol layer was phase adjusted to a 1:1 mixture and extracted three times with dichloromethane and dried under vacuum to give an FD fraction (0.6 g for *Z. zanthoxyloides* and 0.3 g for *B. pilosa*). The 1:1 water methanol layer was also dried under vacuum to give an FM fraction (0.1 g for both *Z. zanthoxyloides* and *B. pilosa*) (Figure 3.1.).

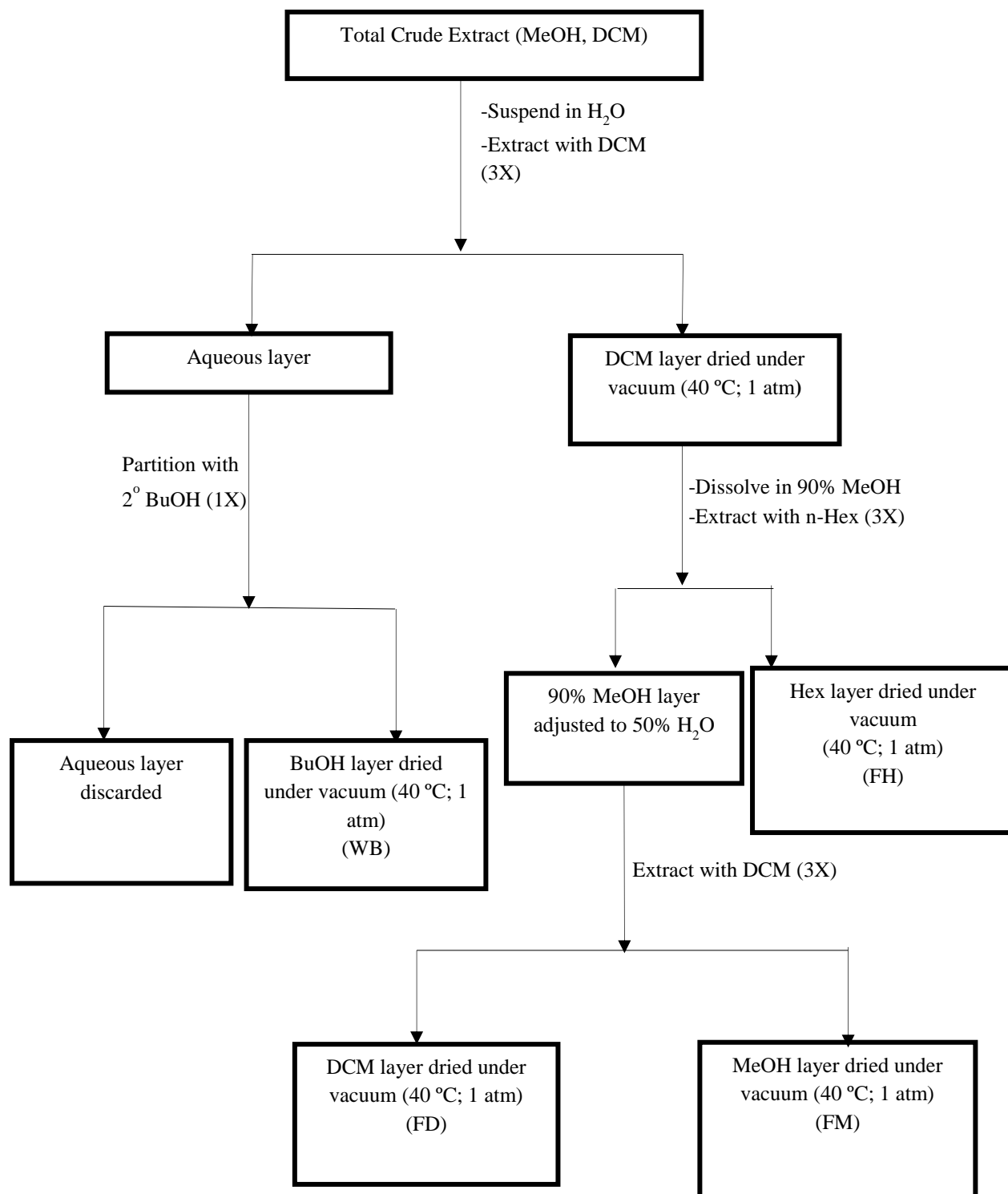


Figure 3.1: Schematic for modified Kupchan method of liquid-liquid extraction: The method gave rise to 4 fractions per plant sample: butanol fraction (WB), hexane fraction (FH), dichloromethane fraction (FD) and methanol fraction (FM). In all, the 8 fractions prepared from both plant samples were BPWB, BPFH, BPDF, BPFM, ZRWB, ZRFH, ZRFD and ZRFM. MeOH=methanol; DCM=dichloromethane, BuOH=butanol; Hex=n-hexane.

3.3 CHROMATOGRAPHIC AND SPECTROSCOPIC ANALYSIS

Analytical normal phase silica-coated thin layer chromatography (TLC) was repeatedly run on both Kupchan and gravity column fractions to estimate the levels of polarity and purity of all fractions, as well as to determine the appropriate solvent systems for silica gel gravity column chromatography. The solvent systems used in TLCs were selected based on the Kupchan fractions (FH, FD, FM, and WB). For the FD fractions, the solvents used were ethylacetate, dichloromethane, hexane and occasionally methanol to facilitate the movement of highly polar compounds on normal phase. The data obtained from TLC runs were used to set up gravity column chromatography. Apart from observing TLC plates under both long (365 nm) and short (254 nm) UV wavelengths, phytochemical screening of TLC spots was conducted using a number of reagents such as iodine, ninhydrin, Dragendorff and antimony (III) chloride. For the ninhydrin and antimony (III) chloride tests, TLC spots were developed in 10% H₂SO₄ with heating at 110°C. Appropriate solvent systems for silica gel gravity column chromatography were selected following successful TLC runs. Silica gel gravity column chromatography was used in the further purification of plant extracts following Kupchan solvent partitioning. The column used for this chromatographic step was 120 cm long and 2.5 cm wide with ethylacetate, hexane and methanol routinely used as mobile phases.

A Thermo Instrument MS system (LTQ XL/LTQ Orbitrap Discovery) coupled to a Thermo Instruments high pressure liquid chromatography (HPLC) system (Accela PDA detector, Accela PDA autosampler and Accela pump) was used to obtain high resolution mass spectrometric data. Conditions used in data acquisition were: capillary voltage of 45V, sheath gas flow rate of 40-50 arbitrary units, mass range of 100-2000 amu (maximum resolution of 30,000), and capillary temperature of 320 °C, spray voltage of 4.5 kV and an auxiliary gas flow rate between 10-20

arbitrary units. Separation on HPLC was done using a Phenomenex reversed-phase (C-18, 250 × 10 mm, L × d) column which was connected to an Agilent 1200 series binary pump. An Agilent photodiode array was used in monitoring and detection was carried out at a wavelength of 227 nm. Purification was performed using a Biphenyl column and elution was carried out using a solvent system of A= 80/20 (H₂O/ CH₃CN) and B= 95/5 (CH₃CN/ H₂O) in 30 minutes and held for 20 minutes. Column flow rate was set at 1.5 mL/min. Nuclear magnetic resonance (NMR) spectroscopy data was acquired on a 500 MHz Bruker spectrometer with deuterated methanol (CD₃OD) as the solvent. NMR experiments included ¹H-NMR, ¹³C-NMR, HSQC, COSY, HMBC and TOCSY.

3.4 ISOLATION AND STRUCTURE ELUCIDATION OF ANTITRYPANOSOMALS

About 1 mg each of the four Kupchan solvent partitioning fractions (FH, FD, FM and WB) from *Z. zanthoxyloides* and *B. pilosa* was submitted for high resolution electrospray ionization liquid chromatography tandem mass spectrometry (HRESI-LC-MSⁿ). Analysis of the data obtained for each solvent partitioning fraction in addition to antitrypanosomal activities suggested that the fraction of highest priority was FD.

The 600 mg FD fraction obtained from the *Z. zanthoxyloides* Kupchan solvent partitioning was divided into two 300 mg extracts. About 300 mg of this extract was loaded on a glass column (120 cm long and 2.5 cm wide) containing silica gel packed to the 80 cm mark. The column was subjected to gradient elution using a mixture of hexane and ethylacetate (90/10, 80/20, 70/30, 60/40, 50/50, 40/60, 30/70, 20/80 and 100%). The remaining compounds on the silica column were then flushed out using 100% methanol. The column fractions obtained were dried under vacuum and labeled ZRFD-C1 to C11. The antitrypanosomal activities of the column fractions were determined, after which fractions ZRFD-C3 (0.09 g) and ZRFD-C4 (0.25 g) were found to be the

most promising. Fraction ZRFD-C3 (0.09 g) was further purified by HPLC. HPLC separations were carried out using a Phenomenex Luna reverse-phase (C18 250 × 10 mm, L × i.d.) column connected to a Waters 1525 Binary HPLC pump Chromatograph with a 2998 PDA detector, column heater and in-line degasser. Detection was achieved on-line through a scan of wavelengths from 200 to 400 nm. Each injection took 60 minutes and started at time 0 minutes with solvent A (100% water) to 30 minutes with solvent B (100% acetonitrile) and hold at 100% acetonitrile for another 30 minutes. About 10.6 mg of the purified ZRFD-C3 was obtained after 48 hour injections and submitted for NMR data acquisition. Further purification of ZRFD-C4 (0.25 g) involved another silica gel gravity column chromatography using a gradient solvent elution system similar to that described above. This led to eleven sub-fractions that were labeled ZRFD-C4-C1 to C-11. Fraction ZRFD-C4-C3 was further fractionated into ZRFD-C4-CA to CH from which ZRFD-C4-CA to CD were found to be the most promising. Hence, ZRFD-C4-CA to CD were combined and further purified on HPLC using the standard and routine procedures as already described. This led to the isolation of 3.5 mg of the compound labeled ZRFD-AD-308.

The 0.3 g FD extract obtained for *B. pilosa* after Kupchan solvent partitioning was subjected to silica gel gravity column chromatography. The sample was loaded on the column as described earlier for ZR-FD and eluted with gradient solvent mixtures of hexane and ethylacetate (90/10, 80/20/, 60/40, 40/60, 20/80) after which 100% methanol was used to flush out all polar compounds. The eleven fractions obtained were labeled BPDF-C1-C11. The antitrypanosomal activities of these fractions were determined, and fractions BPDF-C2 and BPDF-C3 were found to be the most promising. BPDF-C3 was further fractionated and purified using HPLC, thereby resulting in 3.2 mg and 4.0 mg of the pure compounds labeled as BP-FD-HB and BP-FD-HC respectively. After

a determination of their antitrypanosomal activities, the structures of these compounds were determined by a combination of spectroscopic and spectrometric data.

3.5 CELL VIABILITY ASSAY

Determination of cell viability involved colorimetric analysis through the use of resazurin (alamar blue) (Vega-Avila and Pugsley 2011). *T. brucei* and human cell lines were each seeded at a cell density of 1.5×10^5 cells/ml on 96-well plates in a two-fold dilution of antitrypanosomals at 37°C and 5% CO₂. A 10% (v/v) alamar blue dye or resazurin (0.125 mg/ml) was employed for tracking changes in absorbance or fluorescence. Experiments were run in quadruplicates. Spectrophotometric absorbance was read at a wavelength of 540 nm using a reference wavelength of 595 nm. Fluorescence was read at wavelengths of 530 nm (excitation), 585 nm (emission), and 570 nm filter cut-off. Data was analysed with Graphpad Prism version 5 and Microsoft Excel. The concentration that caused a 50% reduction (or increase) in cell viability (or growth inhibition) was calculated as the half-maximal inhibitory concentration (IC₅₀) [(or half-maximal effective concentration (EC₅₀)]. All IC₅₀ and EC₅₀ values were calculated from non-linear regression analyses in the dose-response curves.

3.6 CELL DEATH ASSAY

Flow cytometry-based detection of apoptosis- and necrosis-like cell death using annexin-V and 7-aminoactinomycin-D was employed (Wlodkkowic et al., 2009). *T. brucei* cell lines were seeded at a density of 1.5×10^5 cells/ml on a 96-well plate in a two-fold dilution of antitrypanosomals for 24 hours. Cells were incubated with nexin reagent that contains annexin-v and 7-amino actinomycin-D (EMD, Millipore) in a volumetric ratio of 1:1 with gentle shaking for 20 minutes. Experiments were run in duplicates. Dot plots were recorded with the guava easycyte HT flow cytometer. Data was analysed with the guavaSoft software 2.1.

3.7 CELL CYCLE ASSAY

The cell cycle assay was based on a univariate analysis of DNA content upon staining with propidium iodide (Pozarowski and Darzynkiewicz, 2004). All centrifugation steps were performed at 1700 rpm for 10 minutes. *T. brucei* cell lines were seeded at a density of 1.5×10^5 cells/ml with or without antitrypanosomals for 24 hours and centrifuged. Cell pellets were suspended in 1.5 ml of 1x phosphate-buffered saline (PBS) with vortexing. Absolute ethanol was added (final concentration of 70%) to fix cells at -20°C for 1 hour and centrifuged. Cell pellets were suspended with guava cell cycle reagent that contained propidium iodide (EMD, Millipore). Suspended cells were added to wells containing the same volume of fresh guava cell cycle reagent in a 2-fold dilution. Cells were incubated for 30 minutes in darkness at room temperature. Distribution of cells at distinct cell cycle phases was measured with the BD LSFortessa X-20 flow cytometer. Data was analysed with BD FACSDiva 8.0.1, FlowJo V10, Microsoft Excel, and Graphpad Prism version 5.

3.8 FLUORESCENCE MICROSCOPY

All centrifugation steps were performed at 1700 rpm for 10 minutes. *T. brucei* cell lines were cultured with or without antitrypanosomals for 24 hours and centrifuged. Cell pellets were suspended in 375 μl of PBS and vortexed. Cell pellets were fixed with 125 μl of 16% paraformaldehyde (final concentration of 4%) for 5 minutes at room temperature and centrifuged. Cell pellets were suspended in 500 μl of PBS and 50 μl was incubated on a slide glass at room temperature for 1 hour. They were rinsed once in PBS for 5 minutes, followed by a second rinse in PBST (PBS with 0.1% Triton X) for 15 minutes. They were incubated with 4', 6-diamidino-2-phenylindole (DAPI) ($5\mu\text{g/ml}$ in PBS) for 10 minutes in the dark at room temperature. Cells were washed twice in PBS for 5 minutes each, followed by a second single wash in PBST for 5 minutes.

Cells were mounted with 90% glycerol in PBS using a cover slip, sealed with manicure, and observed with the Olympus DP72 reflected fluorescence microscope. Data was analysed with the CellSens standard imaging software and Adobe Photoshop CS6.

3.9 ANTITRYPANOSOMAL SENSIVITY ANALYSIS

The wildtype 2T1 strain of *T. b. brucei* was grown to a density of 2×10^6 cells/ml and split into fresh media with the antitrypanosomal compounds at 1.5×10^5 cells/ml. Cells were monitored and counted for 5 days, splitting into fresh media with the compounds at 1.5×10^5 cells/ml as and when was required by the growth of cells at a threshold of 5×10^5 cells/ml.

3.10 INDUCTION OF RNAI LIBRARY

An aliquot of approximately 1×10^6 cells/ml of the bloodstream-form RNAi library (Figure 3.2) (Alsford et al., 2011) was thawed in 100 ml HMI-9 with 10% v/v FBS. After 4 to 6 hours of growth, 1 μ g/ml of phleomycin (RNAi library) and 5 μ g/ml of blasticidin (TetR and T7 polymerase; Figure 3.2) were added. To ensure maintenance of library complexity, the RNAi library was grown between 2×10^5 cells/ml and 2×10^6 cells/ml. RNAi library expression was induced with 1 μ g/ml tetracycline for 24 hours. The antitrypanosomal was added to the culture medium at approximately $2 \times EC_{50}$ values. Cell density was monitored daily for approximately 8 days, splitting in fresh medium with blasticidin, phleomycin, tetracycline and the antitrypanosomal to obtain a resistant population of library strains as estimated from the cumulative growth curve.

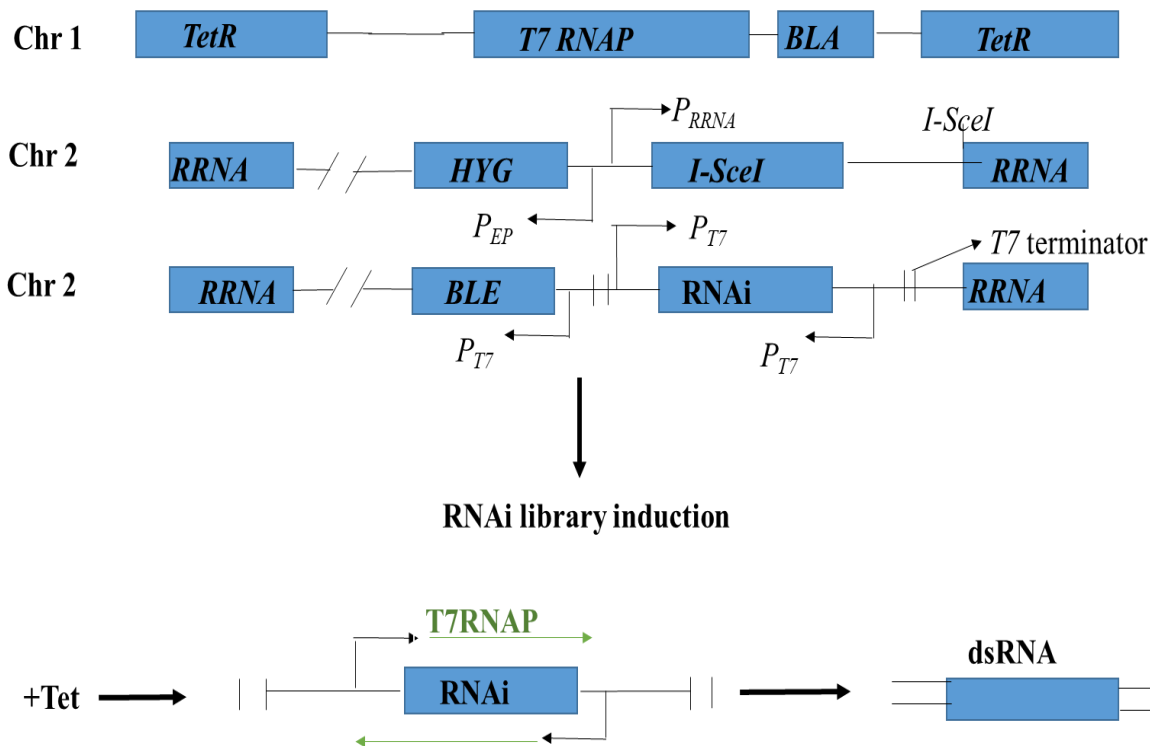


Figure 3.2: A simplified diagram of the genetic constitution of the RNAi library: The library strain is engineered to express the tetracycline repressor (*TetR*) and the phage T7 RNA polymerase (*T7 RNAP*) from the tubulin array locus on chromosome 1 (chr 1) (Glover et al., 2015). Also, a pZJM-based RNAi plasmid construct is employed to replace an inducible homing endonuclease (*I-SceI*) on chromosome 2 (chr 2) through a site-specific RNAi library integration at a tagged ribosomal RNA spacer locus (*RRNA*). TetR is constitutively expressed in the presence or absence of tetracycline (Tet). Tet competes with the tet operator for the binding of TetR (tet has a higher affinity for TetR and its binding leads to a conformational change in TetR). Hence, in the presence of tet, TetR dissociates from the operator enabling the uninterrupted expression of T7 RNAP. T7 RNAP binds to the phage promoter T7 (P_{T7}) on chromosome 2 and transcribes the integrated RNAi fragment (RNAi) in the form of its cognate double-stranded RNA (dsRNA). This results in the downregulation of the RNAi fragment through a canonical process of eukaryotic RNA interference. \emptyset =Tet-operator; *HYG*=Hygromycin-resistance gene; *BLE*=Phleomycin-resistance gene; *BLA*=Blasticidin-resistance gene; P_{RRNA} = RRNA promoter; EP=procyclin isoform with a glutamate (E)-proline (P) dipeptide repeat (Roditi et al., 1998; Roditi and Clayton, 1999); P_{EP} = EP promoter.

3.11 INDUCIBILITY ASSAY

The selected RNAi library and the antitrypanosomal under study were grown to a density of 1×10^6 cells/ml. Cells were seeded to 1×10^3 cells/ml for 72 hours in the presence of blasticidin (5 μ g/ml) and phleomycin (1 μ g/ml). Cells were split into two flasks (with and without tetracycline) at 1×10^5 cells/ml each for 24 hours. Each flask was then split into two flasks (with and without antitrypanosomal) at 1×10^5 cells/ml each for 24 hours in the presence of blasticidin (5 μ g/ml) and

phleomycin (1 µg/ml). Cells were monitored and counted in each flask for 72 hours with 24-hour splitting into fresh media with blasticidin, phleomycin and the antitrypanosomal.

3.12 EXTRACTION OF GENOMIC DNA FROM LIBRARY STRAINS

Extraction of genomic DNA from selected RNAi library (1×10^6 cells/ml) was carried out using the DNeasy Blood and Tissue Kit (Qiagen) according to the manufacturer's protocol. All centrifugation steps were carried out at room temperature (15-25 °C). Final elution volume of DNA was 50 µl.

3.13 AMPLIFICATION AND ELECTROPHORESIS OF RNAI TARGET FRAGMENTS

RNAi target fragments were amplified from the genomic DNA of selected RNAi library using a standard polymerase chain reaction (PCR) (Tables 3.1 and 3.2). The sequences of the forward (LibF) and reverse primers (LibR) were TAGCCCCTCGAGGGCCAGT and GGAATTCGATATCAAGCTTGGC respectively. The unique RNAi construct sequences used to track genuine RNAi fragments in the library strain were F-GTGAGGCCTCGCGA and R-TCGCGAGGCCTCAC, where F and R represent the forward and reverse orientations respectively. PCR products were separated on a 1% (w/v) agarose gel containing 1x Tris borate EDTA buffer (TBE). Ethidium bromide (final concentration of 1 µg/ml in TBE) was added for visualization of fragments through transillumination. Gel electrophoresis was carried out at 100V for 50 minutes. Gel pictures were captured and analysed using the GeneSnap software (version 7.12).

Table 3.1: PCR protocol for amplification of RNAi target fragments

COMPONENT	VOLUME (μ l)
Taq reaction buffer, To 1x	10
dNTPs, 10 mM	1
MgCl ₂ , 25 mM	5
Forward (LIB2F) primer, 200 μ M	1
Reverse (LIB2R) primer, 200 μ M	1
<i>T. brucei</i> genomic DNA, 0.1 μ g	1
Taq DNA polymerase, 1.25U	1
Distilled Water	To 50

Table 3.2: PCR cycle reactions for amplification of RNAi target fragments

CYCLE NUMBER	DENATURATION	ANNEALING	POLYMERIZATION
1	2 min at 90°C		
2-31	30 sec at 95°C	30 sec at 57°C	130 sec at 72°C
31			10 min at 72°C

3.14 PURIFICATION OF RNAI TARGET AMPLICONS

Purification of PCR products was performed using the QIAquick Gel Extraction Kit (Qiagen) with slight modifications. All centrifugation steps were performed at 13000 rpm in a conventional table-top microcentrifuge at 25 °C. DNA fragment was excised from the agarose gel, solubilized in a solubilization buffer of a volumetric ratio of 3:1 (100 mg of gel slice ~ 100 μ l) and incubated at 50°C for 10 minutes with regular vortexing. The sample was sequentially washed in isopropanol, solubilization buffer and wash buffer containing 80% v/v ethanol. Distilled water was used to elute the DNA.

3.15 MOLECULAR CLONING OF RNAI TARGET AMPLICONS

A ligation reaction was set up by preparing a mixture of a 5 μ l of a 2x ligation buffer (Promega), 1 μ l of 50 ng/ μ l pGEM-T Easy cloning vector (Promega), 2 μ l of RNAi PCR product and 1 μ l of a 3 U/ μ l ligase (Promega). After an overnight incubation at 4°C, 80 μ l of distilled water and 100 μ l of phenol-chloroform were added, vortexed for 5 seconds and spun at 13000 rpm for 2 minutes. Glycogen (0.2 μ l) and cold absolute ethanol (400 μ l) were added sequentially to the aqueous phase (supernatant). The mixture was precipitated for 10 minutes by keeping at -20°C, and centrifuged for 20 minutes at 13000 rpm. After resuspension of the precipitate in distilled water, an aliquot was used for electroporation. The ligation product (5 μ l) was added to the competent cells (24 μ l) (*Escherichia coli*, DH5 α strains) and the mixture was electroporated at 2.5 kV with time latency between 5.5 and 6 milliseconds. Electroporated cells were collected in 1 ml lysogeny broth (LB) media, centrifuged at 6000 x g for 60 seconds and resuspended in 50 μ l of the LB media before streaking on ampicillin agar plates containing 50 μ l mixture of 20 mg/mL X-gal (5-bromo-4-chloro-3-indolyl- β -D-galactopyranoside) and 100 mM of IPTG (isopropyl- β -D-1-thiogalactopyranoside) (Thermo Scientific) to enable the identification of individual colonies in a blue-white screening. Plates were incubated overnight at 37°C. LB media (5 ml) containing 50 μ g/ml ampicillin was inoculated with colonies containing the cloned RNAi target amplicons (white colonies). Strains were incubated overnight at 37°C with constant shaking.

3.16 PURIFICATION OF LIGATION PRODUCT

The ligation product was purified using the QIAprep Spin Miniprep Kit (Qiagen) with slight modification. All centrifugations, unless otherwise stated, were carried out at 13000 rpm at 25 °C. Briefly, the inoculated 5 ml bacterial overnight culture was pelleted by centrifugation at 8000 rpm for 5 minutes. Cell pellets were completely but gently resuspended in 250 μ l of an RNAase A-

containing resuspension buffer to which LyseBlue reagent has been added in a volumetric ratio of 1:1000. Lysis buffer (250 μ l) was added to the suspension, mixed gently until the solution turns completely blue before incubating for 5 minutes for lysis to proceed. Neutralization buffer (350 μ l) was added and mixed gently until the solution turns colorless. After a 10-minute centrifugation of the mixture and subsequent washing (wash buffer containing 80% v/v), the ligation product was eluted from the supernatant with an elution buffer.

3.17 RESTRICTION DIGESTION OF RECOMBINANT PLASMIDS

A restriction digestion reaction was set up by adding 1 μ l of 10x restriction enzyme buffer (New England BioLabs), 0.25 μ l of 10,000 U/ml Not I restriction enzyme (New England BioLabs), 3.75 μ l of distilled water and 5 μ l of purified plasmid DNA (ligation product). The reaction mixture was incubated at 37 °C for 2 hours to allow the digestion of ligation product by Not I. Digested products were separated on a 1% (W/V) agarose gel containing 1x Tris borate EDTA buffer (TBE). Ethidium bromide (final concentration of 1 μ g/ml in TBE) was added for visualization of fragments through transillumination. Gel electrophoresis was carried out at 100V for 50 minutes. Gel pictures were taken and analysed using the GeneSnap software (version 7.12).

3.18 SANGER SEQUENCING

The pGEM-T Easy vector (100 ng/ μ l) was prepared for capillary sequencing. Concentration of DNA fragments was determined using NanoDrop spectrophotometer (ND-1000 version 3.8.1). Fragments were submitted for capillary sequencing at Source BioScience (<https://www.sourcebioscience.com>). Forward and reverse sequencing primers employed were M13-F: 5'-d (GTTTTCCCAGTCACGAC)-3' and M13-R: 5'-d (CAGGAAACAGCTATGAC)-3' (Promega). Sequences were analysed using Chromas (version 2.6.5). Bioinformatics resources used included BLAST, InterPro, MMESAT-SVM, MMESAT-2, Phyre2 and SignalP.

3.19 STATISTICAL ANALYSIS

Data from cell viability assay was analysed with Graphpad Prism version 5 and Microsoft Excel. The half-maximal inhibitory concentration (IC_{50}) was calculated as the concentration that caused a 50% reduction in cell viability. The half-maximal effective concentration (EC_{50}) was calculated as the concentration that caused a 50% growth inhibition. All IC_{50} and EC_{50} values were calculated from a non-linear regression model as statistically appropriate. Dot plots from cell death and cell cycle assays were analysed with the guavaSoft software 2.1 and BD FACSDiva 8.0.1, respectively. Histograms for cell cycle were generated with FlowJo V10. Statistical analysis of percentage counts was carried out with Graphpad Prism version 5 using the unpaired t-test. P-values ≤ 0.05 were considered significant.

CHAPTER FOUR

4.0 RESULTS

4.1 ANTITRYPANOSOMAL ACTIVITY OF KUPCHAN FRACTIONS

In order to determine effects on general metabolism of parasites, hexane (BPFH, ZRFH), dichloromethane (ZRFD, BPDF), butanol (ZRWB, BPWB) and methanol (ZRFM, BPFM) fractions prepared using the modified Kupchan's method of solvent extraction were tested for their antitrypanosomal activities in a 48-hour alamar blue cell viability assay (Table 4.1). Potent fractions are expected to reduce the viability or metabolic activity of the parasites thereby resulting in low IC₅₀ values. The assay also included Jurkat cells (acute lymphoblastic leukaemia cells) and Chang liver cells (HeLa derivatives) in order to investigate potential selectivity and toxicity profiles of promising antitrypanosomal fractions.

Fractions ZRFM, ZRWB, ZRFD, BPDF, and BPFM stood out as the most promising antitrypanosomals with respective IC₅₀ values of 3.89 µg/ml, 4.02 µg/ml, 5.70 µg/ml, 3.29 µg/ml and 5.86 µg/ml (Table 4.1). Fractions were generally more selective to *T. brucei* as compared to Jurkat or Chang liver cells, though the selectivity was higher in the latter. With regards to *Z. zanthoxyloides*, ZRFD and ZRWB showed relatively higher toxicity against Jurkat cells with respective selectivity indices (SI) of 9.13 and 6.29 while ZRFM, ZRFD and ZRWB displayed lower toxicity profiles towards Chang liver cells with SI of 24.12, 15.78 and 93.43 respectively (Table 4.1). In respect of *B. pilosa*, BPDF and BPFM exhibited higher toxicity against Jurkat cells with respective SI values of 2.91 and 2.82, while displaying relatively lower toxicity profiles against Chang liver cells with SI of 35.09 and 25.10, respectively (Table 4.1).

Table 4.1: Effect of fractions on cell viability of *T. brucei*, Jurkat and Chang liver cells

FRACTIONS	MEAN IC ₅₀ ± SE (µg/ml)			SI	
	<i>T. brucei</i>	Jurkat	Chang liver	Jurkat	Chang liver
ZRC	3.41±0.06	NA	NA	NA	NA
ZRFD	5.70 ± 0.03	52.04 ± 0.04	89.93 ± 0.03	9.13	15.78
ZRFH	13.26 ± 0.11	NA	NA	NA	NA
ZRFM	3.89 ± 0.06	68.15 ± 0.05	93.84 ± 0.03	17.52	24.12
ZRWB	4.02 ± 0.06	25.28 ± 0.05	375.58 ± 0.07	6.29	93.43
BPC	6.72±0.04	NA	NA	NA	NA
BPFD	3.29±0.03	9.57±0.10	115.45±0.05	2.91	35.09
BPFM	5.86±0.04	16.52±0.03	147.10±0.03	2.82	25.10
BPFH	6.64±0.05	NA	NA	NA	NA
BPWB	12.97±0.12	NA	NA	NA	NA
DA	0.54 ± 0.05	NA	39.72 ± 0.03	NA	73.56
DX	NA	0.27 ± 0.28	145.22 ± 0.02	NA	NA

The effect of Kupchan's fractions on *T. brucei*, Jurkat cells and Chang liver cell lines was determined through alamar blue cell viability assay. Best-fit mean IC₅₀ values and standard errors (SE) were calculated from three distinct experiments. Selectivity index (SI) was calculated as the ratio of IC₅₀ in human cell lines (Jurkat or Chang liver) to IC₅₀ in *T. brucei*. ZR=*Z. zanthoxyloides*, root; ZRC=crude extract of ZR; BP=*B. pilosa*, whole plant; BPC= crude extract of BP; FD=Dichloromethane fraction; FM=methanol fraction; WB= butanol fraction; DA=Diminazene aceturate, (an antitrypanosomal drug); DX=Doxorubicin, (an antileukaemia drug); NA=Not applicable; DA and DX were used as positive controls.

4.2 EFFECTS OF KUPCHAN FRACTIONS ON CELL DEATH/CELL CYCLE OF *T. BRUCEI*

BRUCEI

By focusing on the most promising fractions, parasites challenged with or without fractions for 24 hours were then used in a cell death assay in order to investigate mechanisms of cell death (Figure 4.2.1). Since they are the best understood in eukaryotes, apoptosis and necrosis were the two types of cell death investigated. At the IC₅₀ values, ZRFD, ZRFM and ZRWB of *Z. zanthoxyloides* caused a significant induction of apoptosis-like cell death from 0.8% of cells in the untreated cells to 3.1%, 2.9% and 2.4% of cells respectively without practically inducing necrosis-like cell death. For *B. pilosa*, BPFH significantly induced apoptosis-like cell death in 3.0%, 27.4% and 1.9% of cells respectively. BPFM was the only fraction that also induced necrosis-like cell death in about 8.0% of cells (Figure 4.2.1).

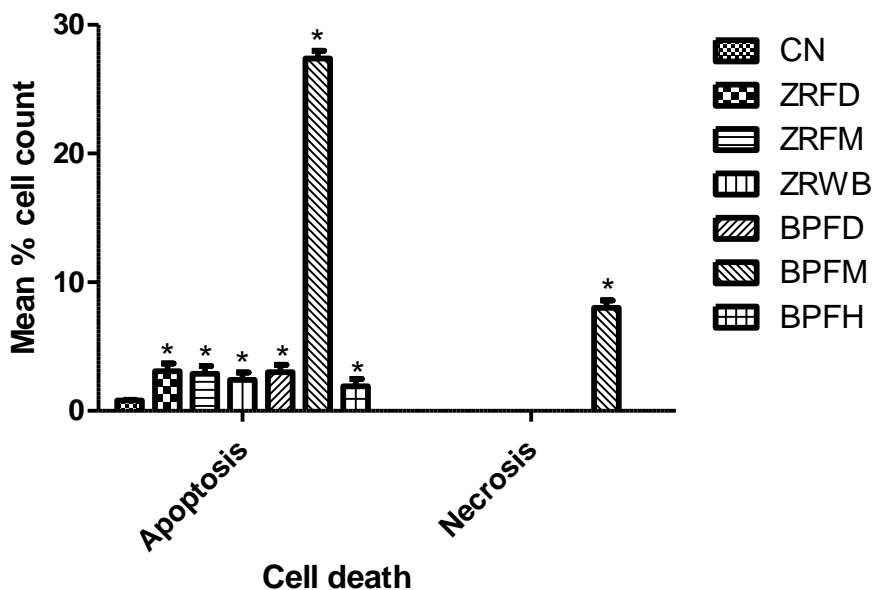


Figure 4.2.1: Effect of selected fractions on induction of cell death in *T. brucei*:

P-values were calculated from 3 distinct counts (n=4):[*:P<0.05]. Error bars originate from mean percentage count \pm standard deviation of the mean (Mean \pm SEM). ZR=*Z. zanthoxyloides* root; BP=*B. pilosa*, whole plant; WB=butanol fraction; FD=Dichloromethane fraction; FM=Methanol fraction; CN=Negative control

In order to identify any alterations in distinct cell cycle phases (G0-G1, S, and G2-M phases) of *T. brucei*, cell cycle assay was performed with parasites challenged with or without the fractions at the IC₅₀ values of the most promising fractions (Figure 4.2.2). The assay involved a flow cytometric analysis of parasites fixed and stained with propidium iodide. For *Z. zanthoxyloides*, there was a significant reduction of G0-G1 phase from 61.43% in the untreated cells to 50.30%, 52.60% and 55.25% in ZRFD, ZRFM, and ZRWB, respectively (Figure 4.2.2). Also, there was a significant increase of G2-M phase from 22.93% in the negative control to 31.48%, 29.18% and 30.18% in ZRFD, ZRFM and ZRWB, respectively (Figure 4.2.2). Moreover, ZRFD and ZRFM significantly increased the S-phase from 15.53% in the untreated cells to 19.08% and 19.03%, respectively (Figure 4.2.2). For *B. pilosa*, there was a significant reduction of G0-G1 phase from 61.43% in the negative control to 49.48% and 52.48% in BPDF and BPFM respectively (Figure 4.2.2). Also, there was a significant increase of G2-M phase in about 35.38% and 33.20% of cells in BPDF and BPFM, respectively (Figure 4.2.2). Fractions ZRWB, BPDF and BPFM did not cause any significant change in the S-phase.

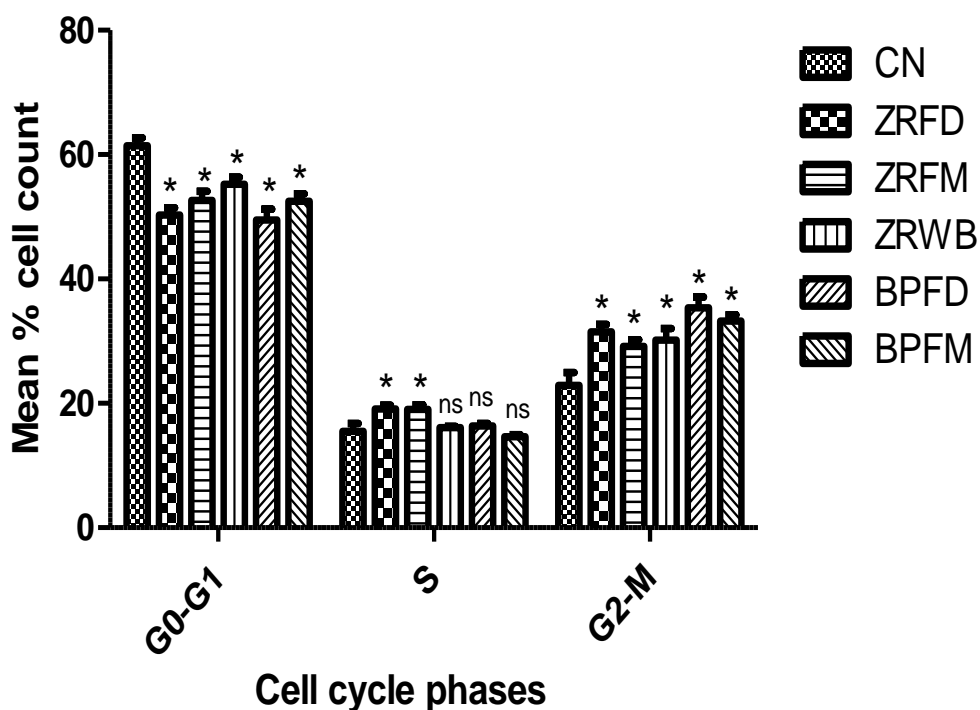


Figure 4.2.2: Effect of selected fractions on cell cycle of *T. brucei*: P-values were calculated from 4 distinct counts (n=4): [*: $P < 0.05$; ns: $P \geq 0.05$ =not significant]. Error bars originate from mean percentage count \pm standard deviation of the mean (Mean \pm SEM). ZR=*Z. zanthoxyloides* root; BP=*B. pilosa*, whole plant; WB=butanol fraction; FD=Dichloromethane fraction; FM=Methanol fraction; CN=Negative control.

4.3 EFFECTS OF KUPCHAN FRACTIONS ON CELL MORPHOLOGY OF *T. BRUCEI*

The morphological changes of parasites challenged with the most promising fractions were also observed by fluorescence microscopy using DAPI. Parasites were challenged for 24 hours at the IC_{50} values of the respective fractions. All the fractions induced severe distortion of parasite morphology thereby leading to the aggregation of a considerable number of the parasites (Figure 4.3). BPFM particularly gave rise to a remarkable clustering and distortion of parasites. Interestingly, in comparison to BPFM and BPFM, ZRFD and ZRFM led to a relative reduction in signal intensity of the kinetoplasts while the nuclei remained relatively intact (Figure 4.3).

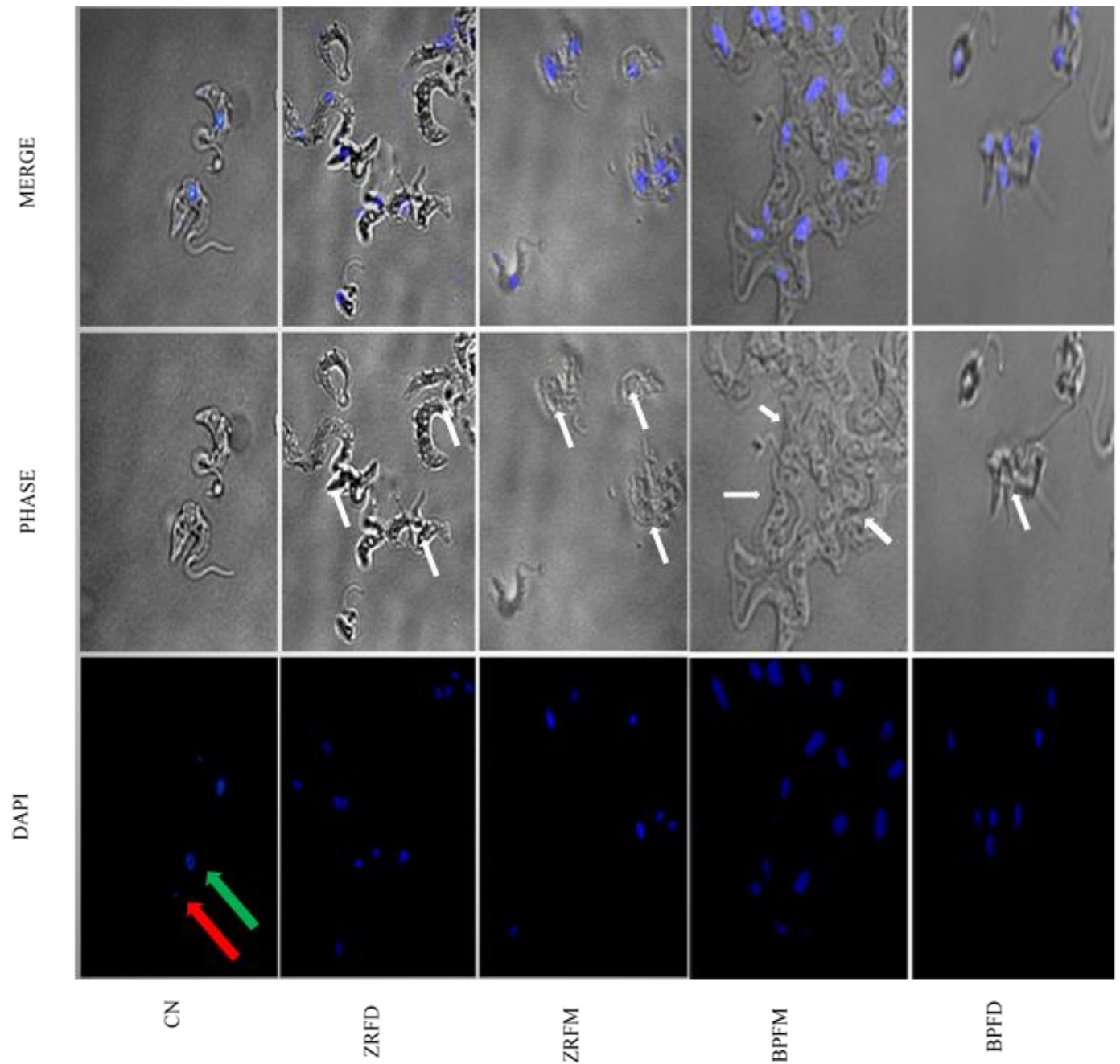


Figure 4.3: Effect of selected fractions on cell morphology and distribution of *T. brucei*: Cells were seeded (1.5×10^5 cells/ml) at the IC_{50} values of fractions. Experiment was conducted for 3 distinct times. Cells were mostly distorted or clustered as compared to the negative control (white arrows); red arrow=kinetoplast; green arrow=nucleus; ZR=*Z. zanthoxyloides* (root); BP=*B. pilosa*, whole plant; FD=Dichloromethane fraction; FM=Methanol fraction; CN=Negative control.

4.4 EFFECT OF COLUMN FRACTIONS ON CELL VIABILITY OF *T. BRUCEI*

Due to the usually high quantities of secondary metabolites found in dichloromethane fractions with polarities between that of hexane and methanol or butanol fractions (Figure 3.1), ZRFD and BPDFD were selected for chromatographic separation. Normal phase analytical TLCs were initially utilized to estimate levels of purity and polarity of each fraction. ZRFD and BPDFD were separated into column fractions via a gradient normal phase silica gel column chromatography using methanol-ethyl acetate solvent system. Profiles of TLCs were used as a guide to combine similar column fractions.

In order to select column fractions for subsequent purification, individual fractions were tested for their antitrypanosomal activities through the alamar blue cell viability assay (Table 4.4). The IC_{50} values of ZRFD ranged from 2.00 to 54.54 $\mu\text{g/ml}$ while that of BPDFD spun between 2.18 $\mu\text{g/ml}$ and 156.02 $\mu\text{g/ml}$ (Table 4.4). Column fractions 3 and 4 (ZRFD), as well as 2 and 3 (BPDFD) were selected for subsequent analysis and purification on the basis of purity, potency and quantity. Purification of column fractions was carried out by HPLC.

Table 4.4: Effect of column fractions on cell viability of *T. brucei*

ZRFD	MEAN IC ₅₀ ± SE (µg/ml)	BPDF	MEAN IC ₅₀ ± SE (µg/ml)
1	11.23± 0.71	1	39.83 ± 0.39
2	13.41±0.47	2	2.18 ±0.1
3	9.27± 1.73	3	5.89 ± 0.22
4	2.00± 0.20	4	7.54 ± 0.39
5	6.15±1.30	5	33.58 ± 11.32
6	9.74± 1.23	6	62.25 ± 1.92
7	17.18± 3.37	7	102.93 ± 2.64
8	8.88± 0.74	8	70.97 ± 12.13
9	19.48± 2.12	9	76.06 ± 6.41
10	28.32± 1.06	10	37.95 ± 0.45
11	54.54± 8.12	11	156.02 ± 5.69
DA	0.54 ± 0.05		0.54 ± 0.05

Eleven fractions each of ZRFD and BPDF (1-11) were tested for their antitrypanosomal activities. Best-fit mean IC₅₀ values and standard errors (SE) were calculated from three distinct experiments. SE was expressed in terms of the mean IC₅₀ values. DA=Diminazene aceturate, (an antitrypanosomal drug). FD=Dichloromethane fraction.

4.5 HIGH RESOLUTION ELECTROSPRAY IONIZATION MASS SPECTROMETRY

ANALYSIS OF KUPCHAN FRACTIONS

Kupchan fractions were analysed using high resolution electrospray ionization mass spectrometry (HRESI-LC-MSⁿ) in order to characterize potential metabolites of individual fractions through their masses. HRESI-LC-MS was utilized due to its ability to cause fragmentation through soft ionization, which may facilitate identification of molecular ions.

Even though the HRESI-LC-MSⁿ of ZRFH showed several interesting compounds, it was not further purified in the present study because the fraction did not exhibit relatively promising antitrypanosomal effects (Figure 4.5.1). Analysis of the HRESI-LC-MSⁿ data for ZRFH also

showed minute amounts of terpenes and alkaloids that were detected in the ZRFD fractions amongst other molecules that could not be identified outright (Figure 4.5.1).

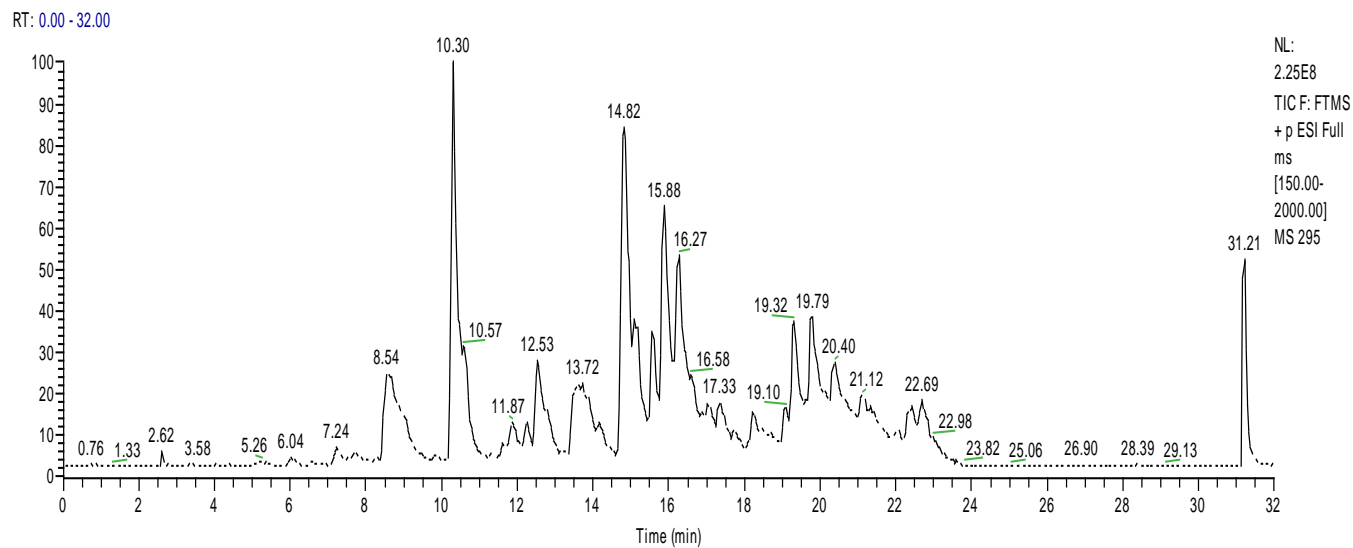
The HRESI-LC-MSⁿ data for ZRFD contained fewer compounds compared to that of ZRFH. There were two major compounds in this fraction with m/z 248.13 and 224.20 (Figure 4.5.2A). Since this fraction gave rise to promising antitrypanosomal activities, the two major compounds present in this fraction were targeted for isolation and structure elucidation. Furthermore, minute amounts of the known compound armatamide (m/z 325.15) (Kalia et al., 1999), were detected alongside other derivatives of this compound (Figure 4.5.2B). However, these compounds were not present in isolatable quantities compared to m/z 248.13 and 224.20.

The HRESI-LC-MSⁿ of ZRFM showed a similar profile to that of ZRFD but with relatively fewer compounds (Figure 4.5.3). Furthermore, this fraction also contained the two major compounds found in the ZRFD. It is not surprising therefore that the two fractions also exhibited similar antitrypanosomal effects. This also suggests that the two major compounds detected were the active principles responsible for the observed antitrypanosomal activities.

The ZRWB fraction contained several interesting compounds even though the antitrypanosomal activity was not as promising as that obtained for ZRFD and ZRFM (Figure 4.5.4). Hence, ZRWB was not further fractionated in this study.

E:\aboagye mass\295

03/18/17 17:50:53



295 #347-2160 RT: 5.08-31.42 AV: 604 NL: 1.26E6

F: FTMS + p ESI Full ms[150.00-2000.00]

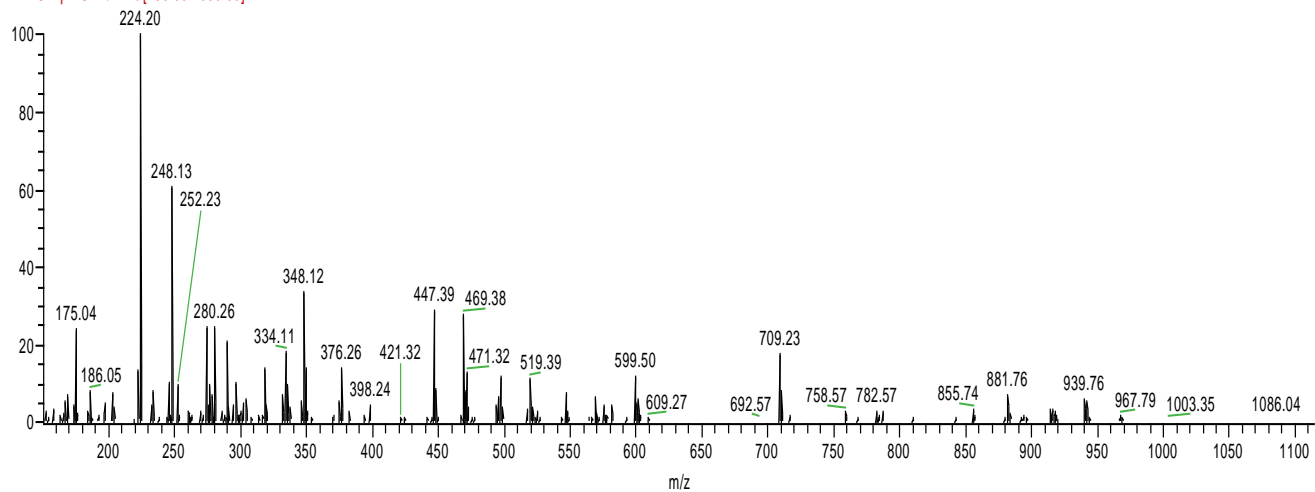


Figure 4.5.1: HRESI-LC-MSⁿ analysis of ZRFH showing several isolatable metabolites.

C:\Users\nepan\Desktop

11/29/16 08:30:56

RT: 0.00 - 35.00

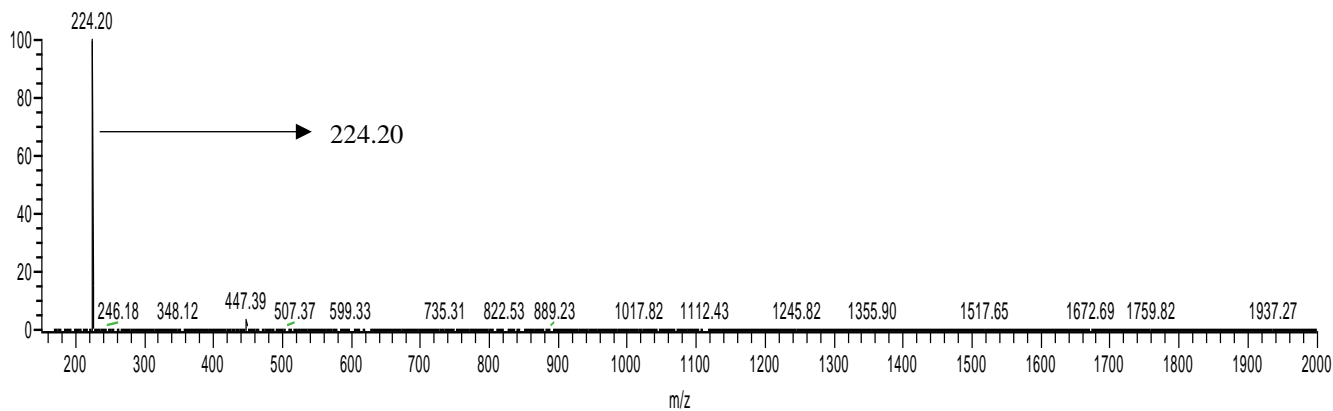
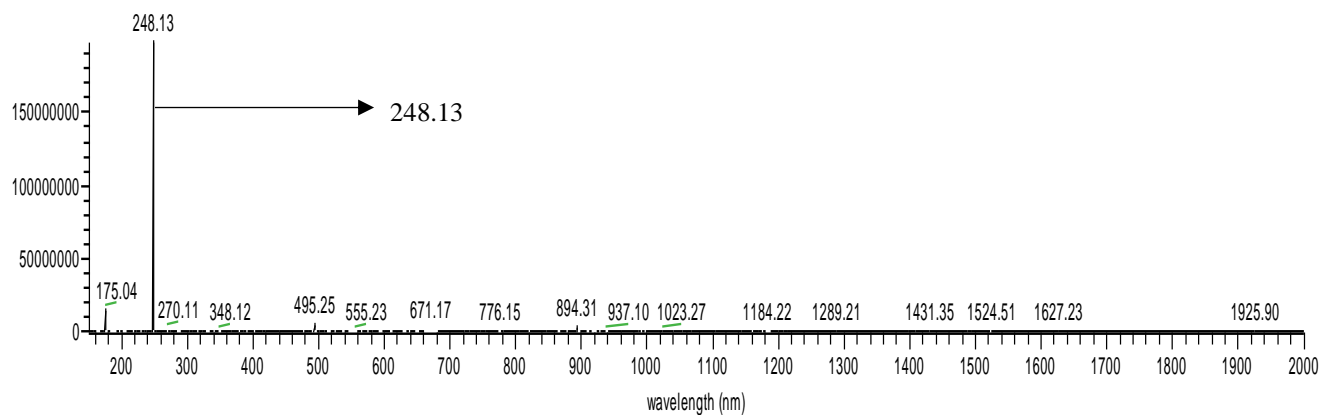
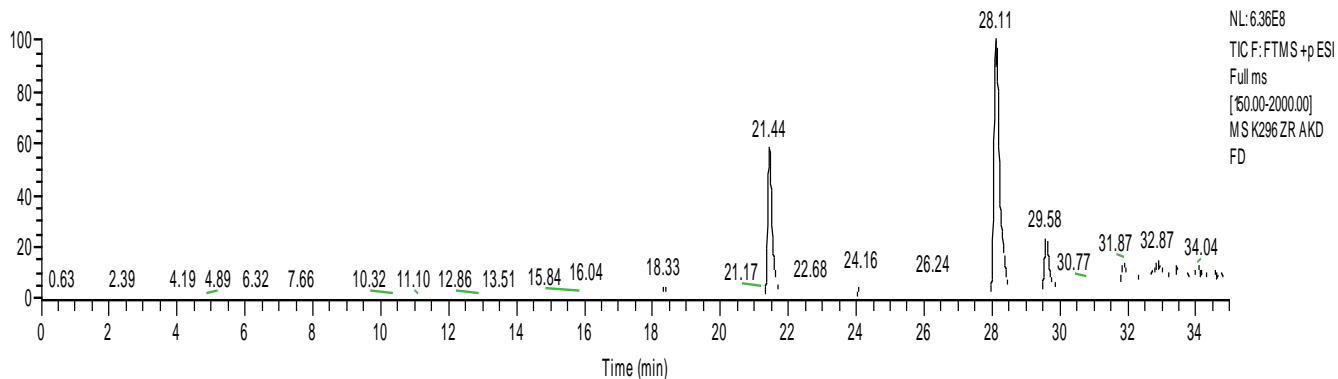
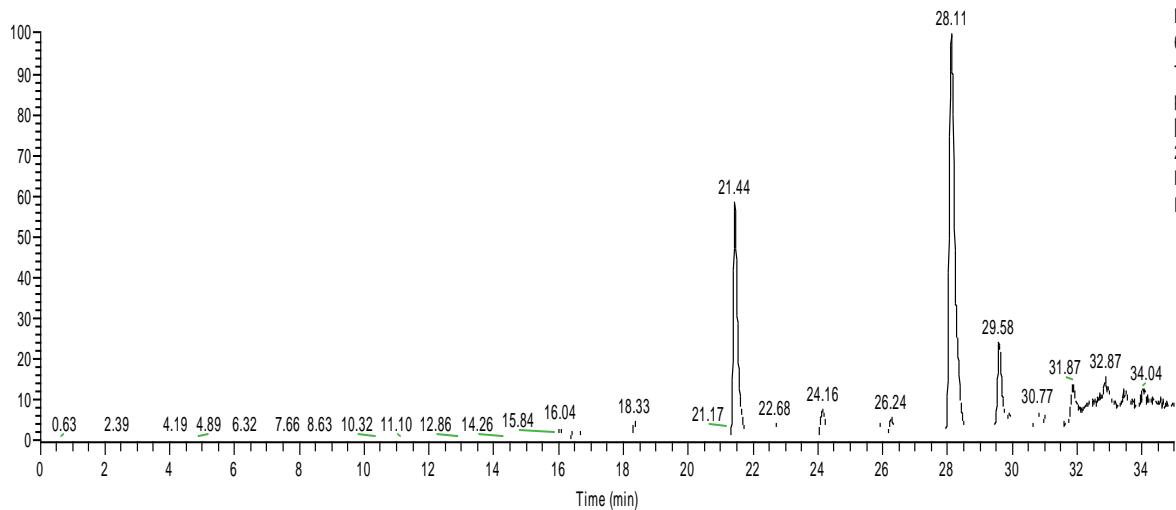


Figure 4.5.2A: HRESI-LC-MSⁿ analysis of ZRFD, version 1. It depicts two major metabolites with m/z 248.13 and 224.20

C:\Users\nepan\Desktop\K296.i

11/29/16 08:30:56

RT: 0.00 - 35.00



NL:
6.36E8
TIC F: FTMS +
p ESI Full ms
[150.00-
2000.00] MS
K296 ZR AKD
FD

K296 ZR AKD FD #2437 RT: 18.80 AV: 1 NL: 7.37E5

F: FTMS + p ESI Full ms [150.00-2000.00]

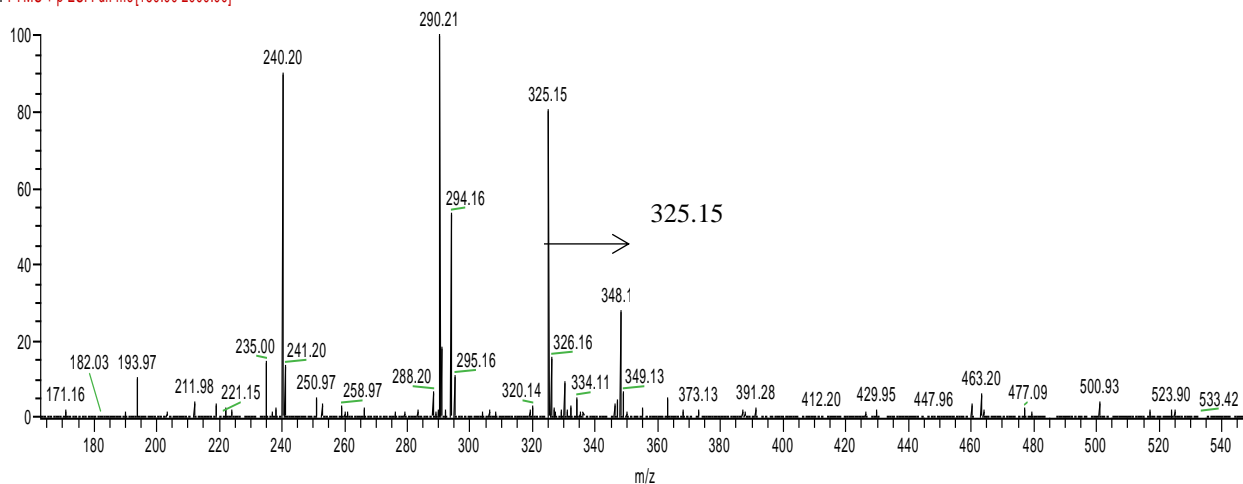


Figure 4.5.2B: HRESI-LC-MSⁿ analysis of ZRFD, version 2. It depicts the known compound armatamide with m/z 325.15, which was isolated from *Z. armatum* (Kalia et al., 1999). Derivatives of this compound are also shown.

E:\aboagye mass\297

03/18/17 18:27:55

RT: 0.00 - 32.04

NL:
5.48E8
TIC F: FTMS+p
ESI Full ms
[60.00-2000.00]
MS 297

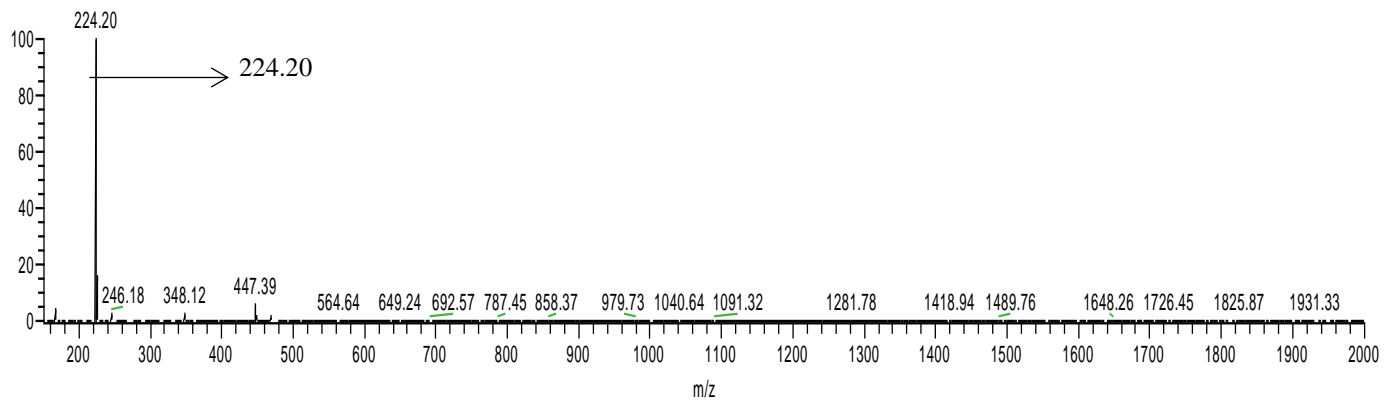
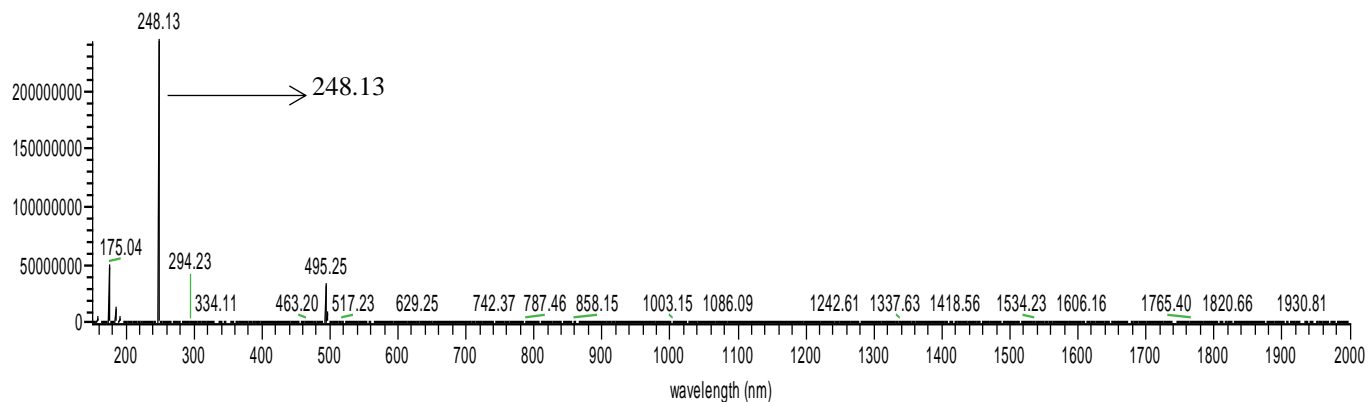
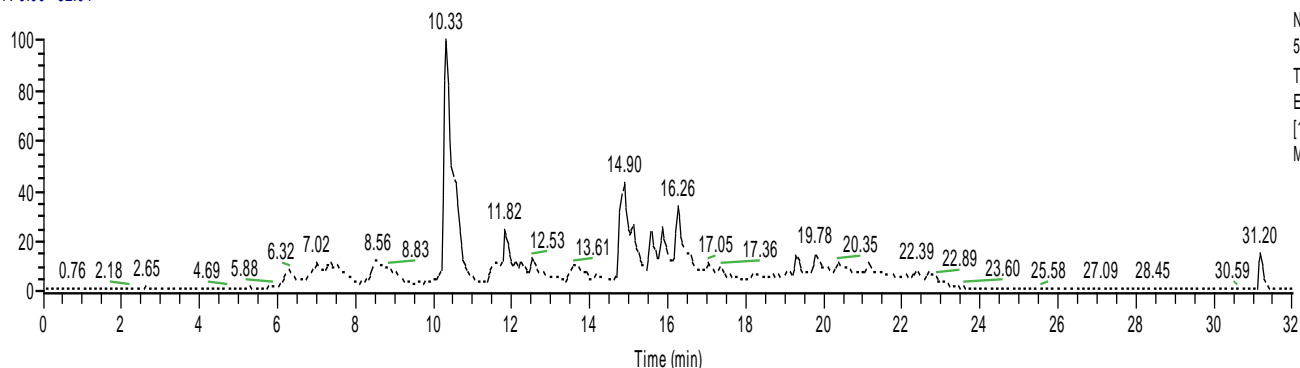
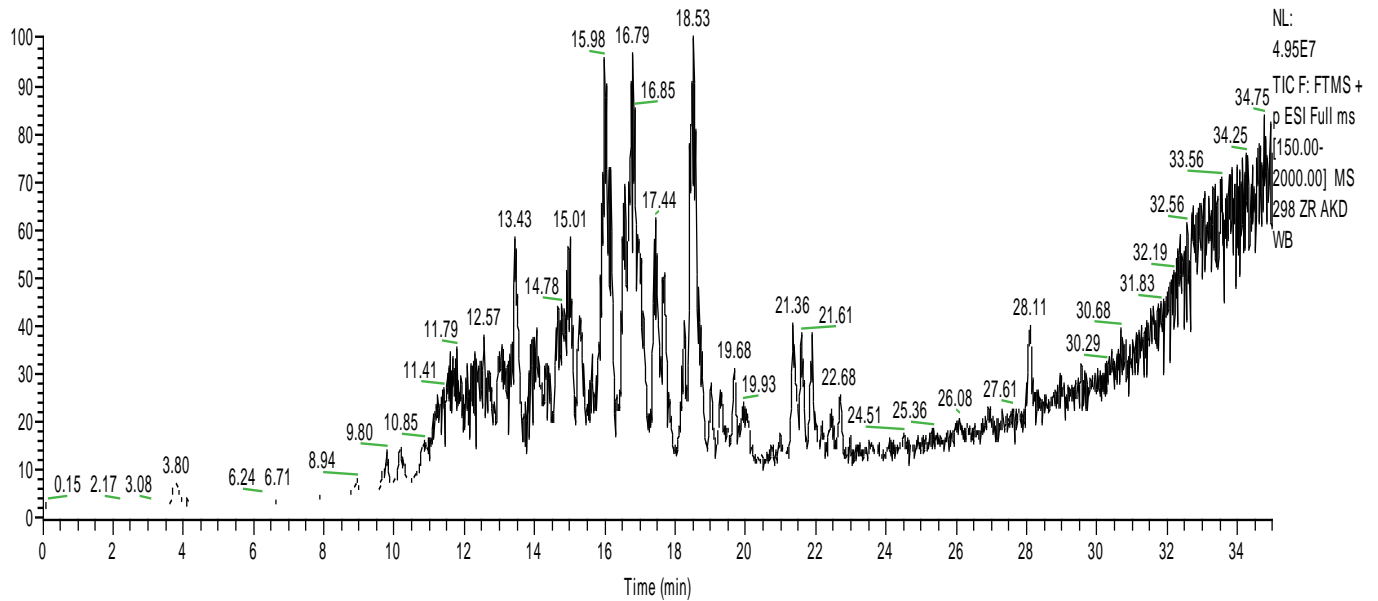


Figure 4.5.3: HRESI-LC-MSⁿ analysis of ZRFM. It shows the two major compounds with m/z 248.13 and 224.20 as observed for ZRFD

C:\Users\inepan\Desktop\298 ZF

01/11/17 12:37:54

RT: 0.00 - 35.01



298 ZR AKD WB #1314-3500 RT: 10.48-23.12 AV: 1093 NL: 7.73E5

F: FTMS + p ESI Full ms [150.00-2000.00]

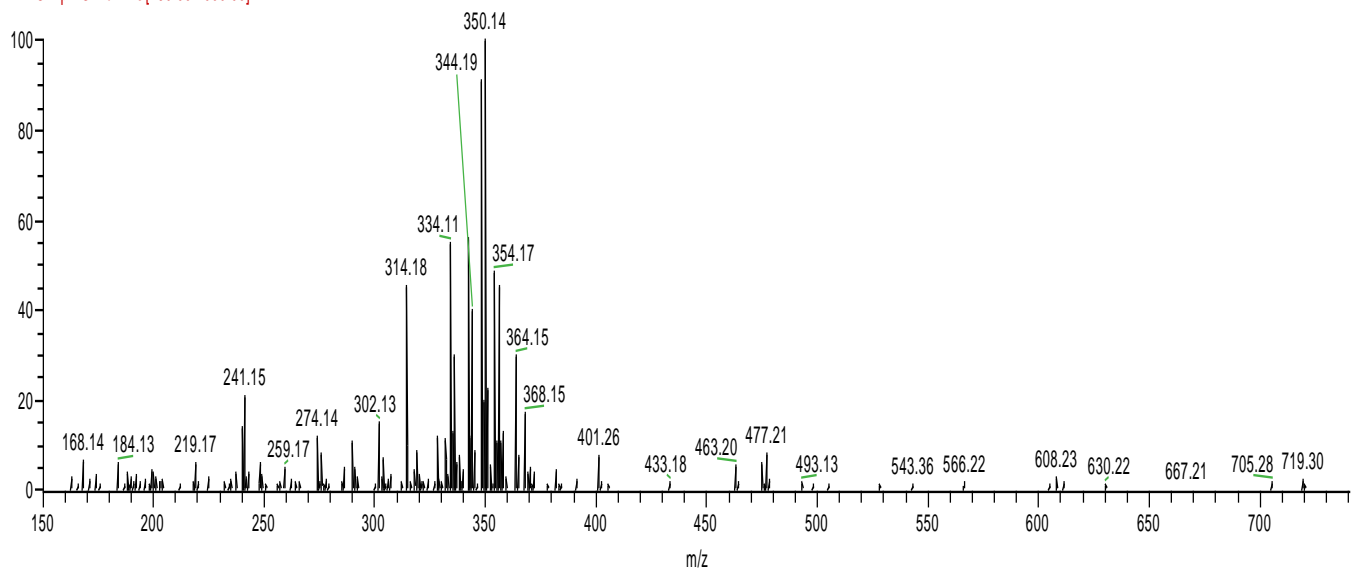


Figure 4.5.4: HRESI-LC-MSⁿ analysis of ZRWB

The HRESI-LC-MSⁿ data for the Kupchan fractions of *B. pilosa* was not as informative as those of *Z. zanthoxyloides*. Apart from BPFH which showed the presence of some compounds (Figure

4.5.5), the other Kupchan fractions did not show many distinguishable peaks in the mass spectrometry run. However, since BPDF (Figure 4.5.6) and BPFM (Figure 4.5.7) gave rise to promising antitrypanosomal activities, it is possible that the compounds present in these fractions do not ionize properly in the LC-MS run. Such situations exist for extracts that contain highly aliphatic and aromatic compounds, where the routine LC-MS run does not reveal these compounds. In order to see compounds for such samples, specialized LC-MS conditions are required to facilitate effective ionization and detection. BPDF was therefore prioritized for further fractionation and isolation of active antitrypanosomals.

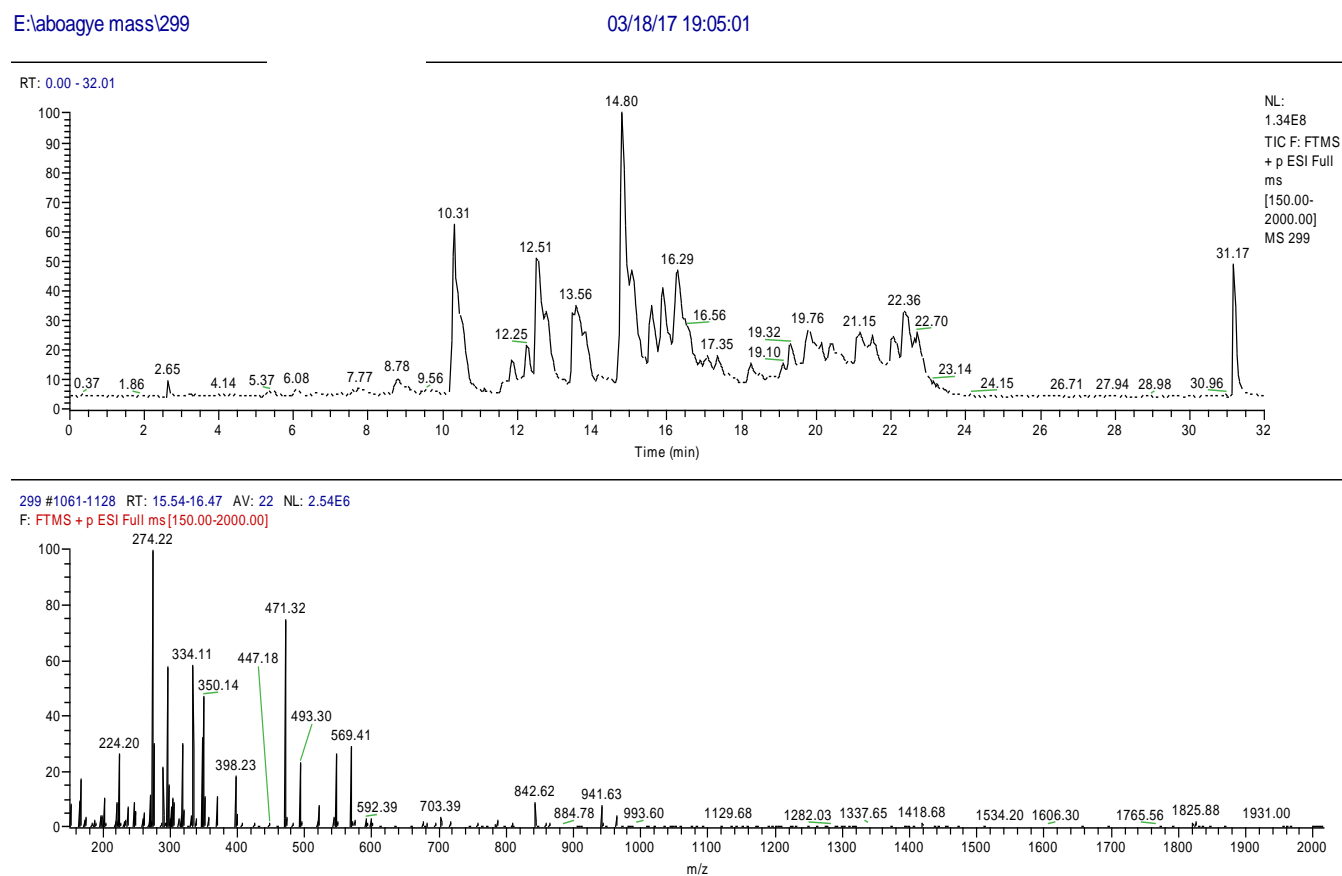
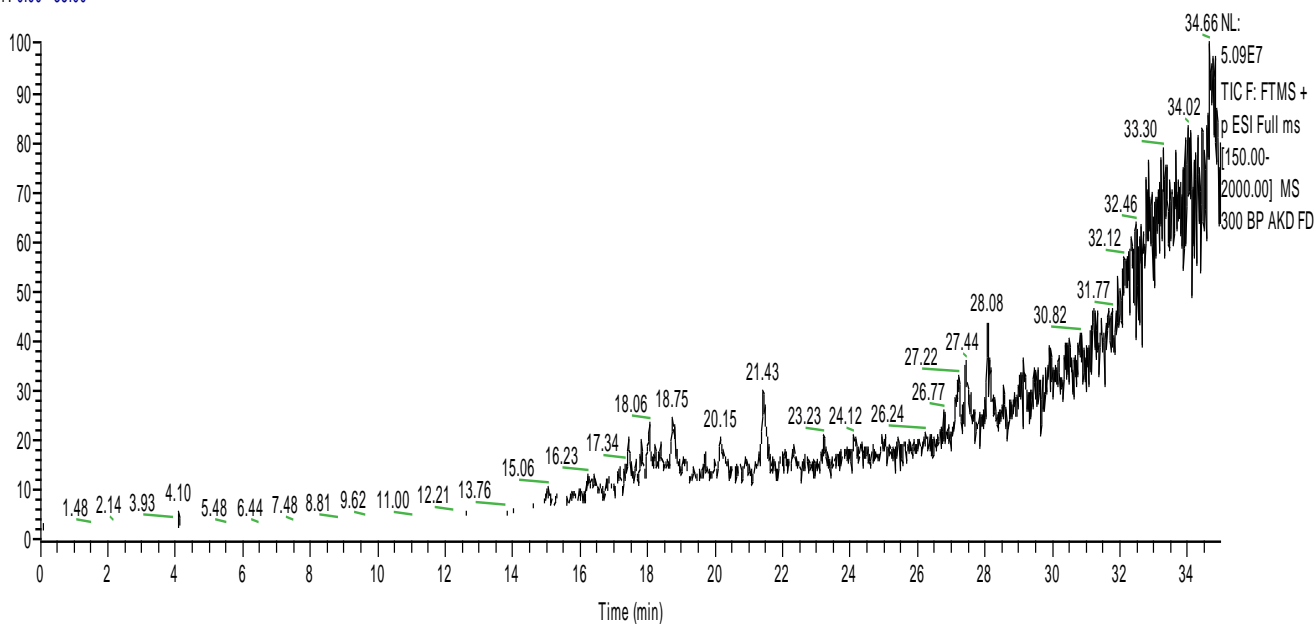


Figure 4.5.5: HRESI-LC-MSⁿ analysis of BPFH.

C:\Users\nepan\Desktop\300 BI

01/11/17 13:20:28

RT: 0.00 - 35.00



300 BP AKD FD #2121-3933 RT: 16.88-28.45 AV: 907 NL: 4.03E5

F: FTMS + p ESI Full ms [150.00-2000.00]

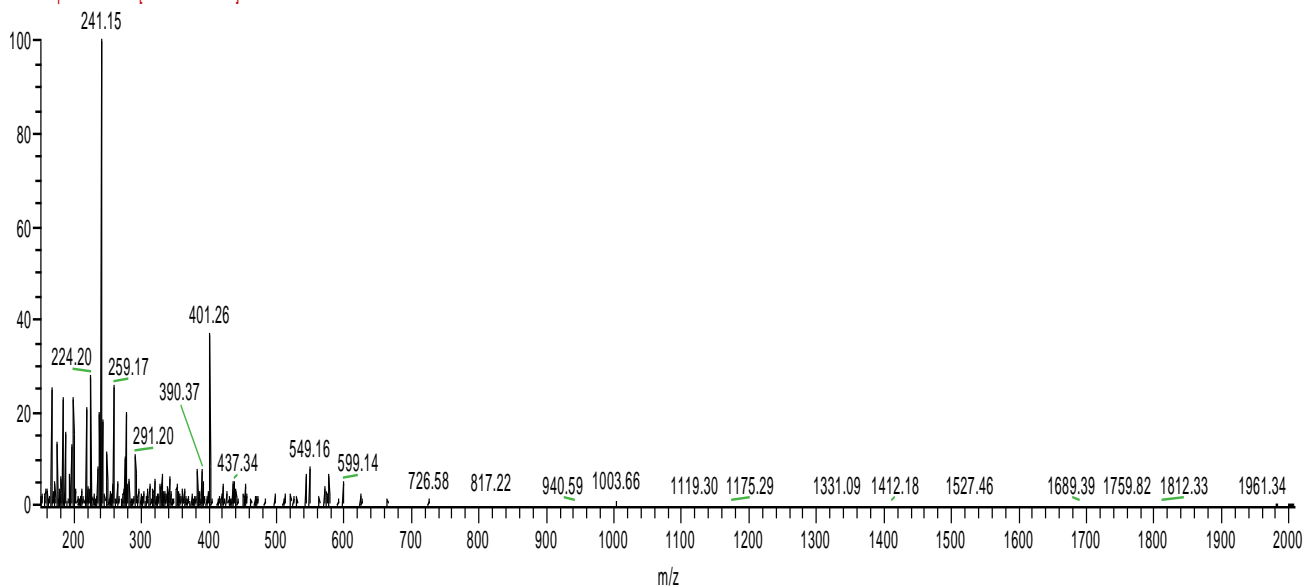
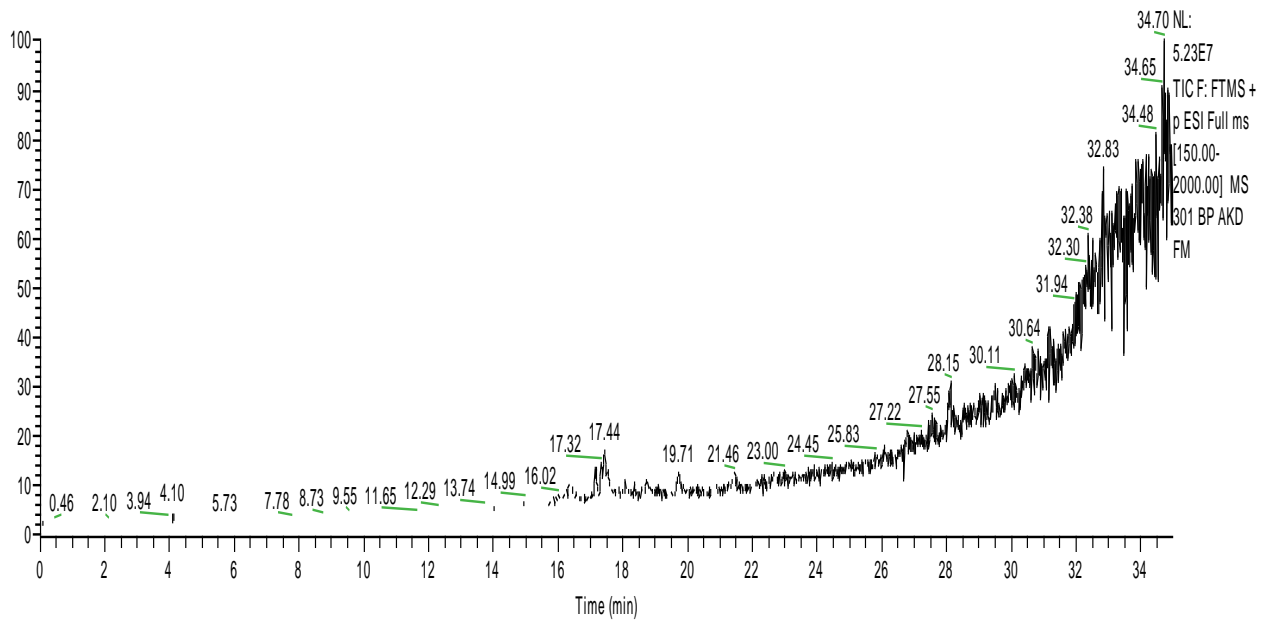


Figure 4.5.6: HRESI-LC-MSⁿ analysis of BPFD

C:\Users\nepan\Desktop\301 B1

01/11/17 14:03:03

RT: 0.00 - 35.00



301 BP AKD FM #4999 RT: 34.99 AV: 1 NL: 9.64E5

F: FTMS + p ESI Full ms [150.00-2000.00]

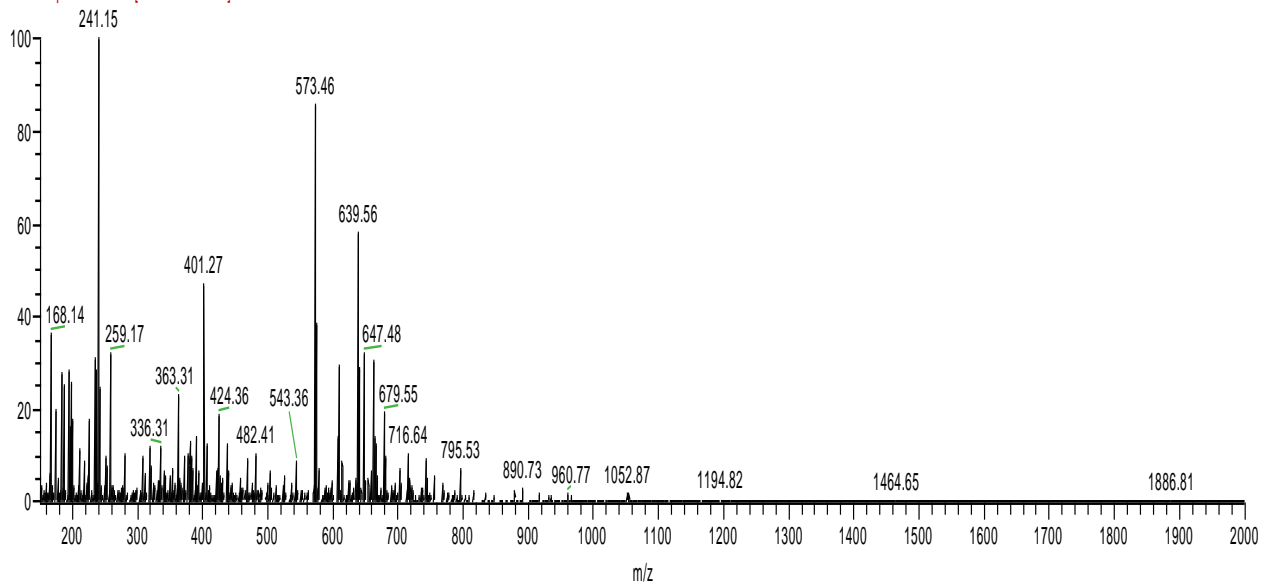


Figure 4.5.7: HRESI-LC-MSⁿ analysis of BPFM

4.6 STRUCTURE DETERMINATION OF A NEW COMPOUND FROM Z.

ZANTHOXYLOIDES

A new amide was isolated for the first time from ZR-FD-C3 after 48 hours of reverse phase HPLC injections using a gradient of acetonitrile and water. In reference to the genus of *Zanthoxylum*, and with respect to the fact that it is an amide, the name zanthoxylamide was assigned to this compound. Zanthoxylamide was isolated as a yellow oil that was readily soluble in both dichloromethane and methanol. The high resolution mass spectrometry data gave m/z 248.1281 $[M + H]^+$, which suggests a molecular formula of $C_{14}H_{18}NO_3^+$ with $\Delta = \pm 0.6$ ppm and 7 degrees of unsaturation. The ^{13}C -NMR of this compound gave rise to 14 carbons comprising 4 quaternary carbons, 6 methines, 2 methylenes and 2 methyls. A detailed analysis of the 1H , ^{13}C multiplicity-edited gHSQC spectrum showed that the protons were attached to the individual carbon atoms. 1H -NMR δ_H 7.49 (d, 15.5, 1H-D) and 6.33 (d, 15.5, 1H-G) confirmed the presence of a trans-alkene which was substituted by different groups. The δ_C 140.4 (D) and 119.2 (G) provided evidence for the substitution on the double bond. Also, δ_H 6.94 (d, 1.6, 1H-I), 6.90 (dd, 1.7, 8.1, 1H-F) and 6.71 (d, 8.0, 1H-H) along with δ_C 106.4, 123.7 and 108.4 ppm, respectively were direct indications of a tri-substituted benzene ring in which carbons H and F formed a spin system while I was isolated by virtue of substitution on the ring. The sp^3 hybridized carbon atom δ_C 101.4 (J) was unusual but literature search along with chemical shift predictors indicated that this carbon was a dioxol functionality that is known to be typical of isoflavones. HMBC correlations M-m along with gCOSY correlations from m-l indicated the presence of an isopropyl functionality whose spin system was further confirmed by the presence of isobutyl substructure. HMBC correlation A-k confirmed the attachment of the isobutyl to an amide. HMBC correlations A-g and A-d gave the

structure of zanthoxylamide as indicated below. The NMR and HRESI-LC-MSⁿ data analyses are summarized in Table 4.6.1, Figure 4.6.1 and Figure 4.6.2.

Table 4.6.1: NMR analysis of zanthoxylamide

#	$\delta^{13}\text{C}$ (ppm)	^{13}C mult	$\delta^1\text{H}$ (ppm)	Mult (Hz)	^1H - ^1H COSY	^1H - ^1H TOCSY	NOESY	HMBC
NH			2.00					
A	166.4	C						d, g, k
B	148.9	C						i, f
C	148.1	C						h
D	140.4	CH	7.49	d, 15.5	g	g	g	i, f, g
E	129.4	C						d, h, g
F	123.7	CH	6.90	dd, 1.7, 8.1	h	i, h		d, i
G	119.2	CH	6.33	d, 15.6	d	d	d	d
H	108.4	CH	6.71	d, 8.0	f	f		
I	106.4	CH	6.94	d, 1.6		f, h		d, f
J	101.4	CH ₂	5.92	S				
K	47.2	CH ₂	3.17	t, 6.4	NH, l	NH, l, m	l	l, m
L	28.7	CH	1.82	dh, 6.7, 13.3	k, m	NH, k, m	k, m	k, m
M	20.2	CH ₃	0.91	d, 6.7	l	NH, k, l	l	k, l, m

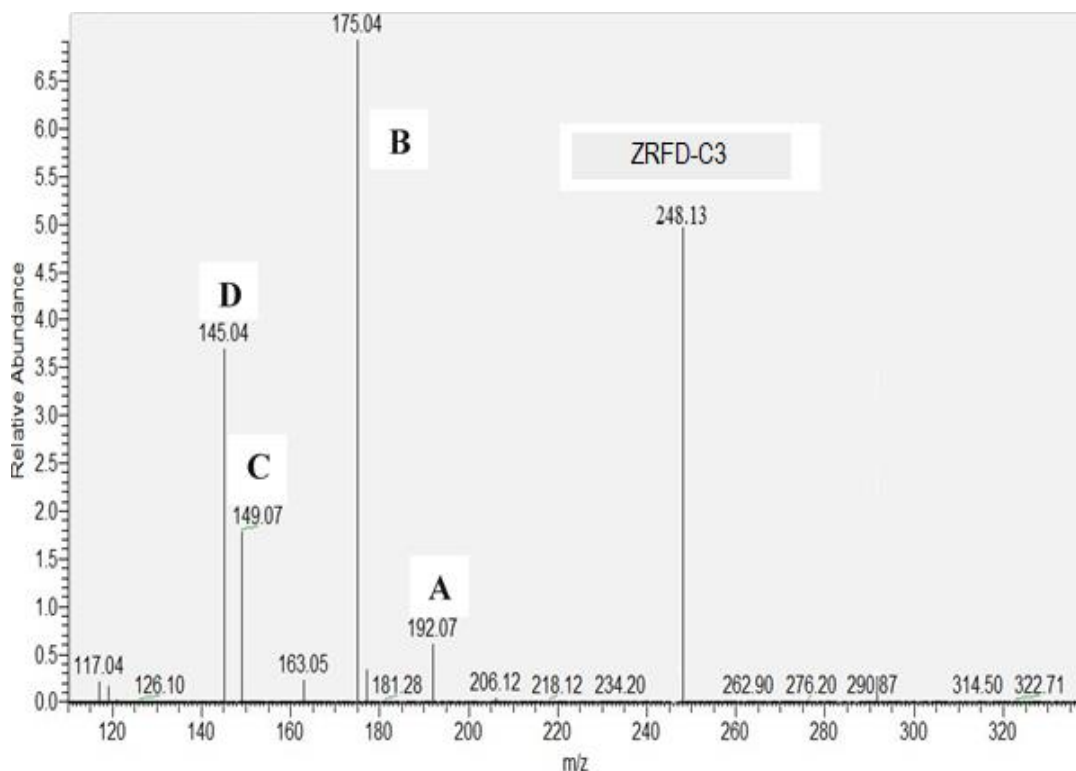


Figure 4.6.1: HRESI-LC-MSⁿ analysis of zanthoxylamide showing other fragmentation peaks (A, B, C, D)

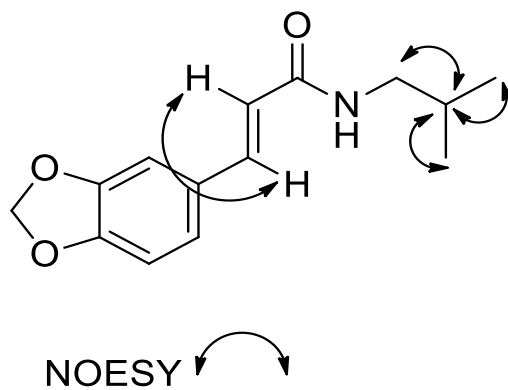
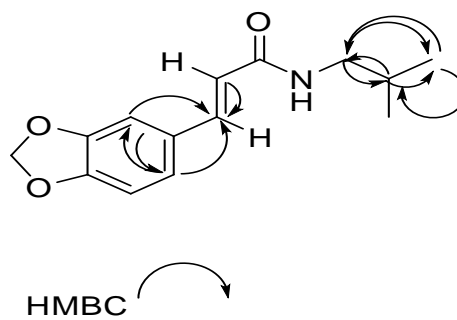
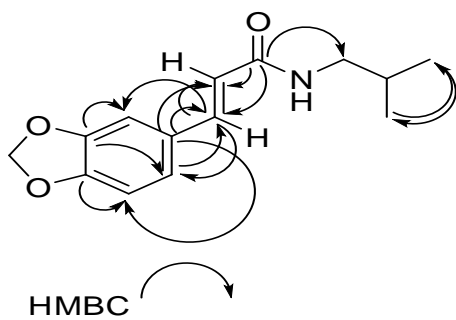
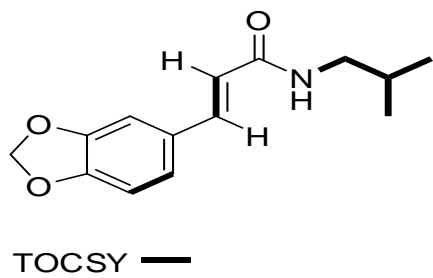
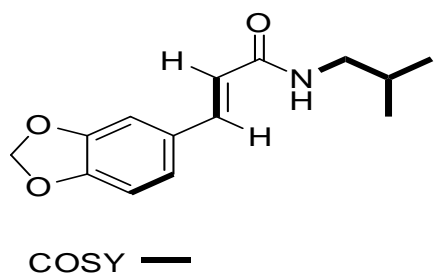
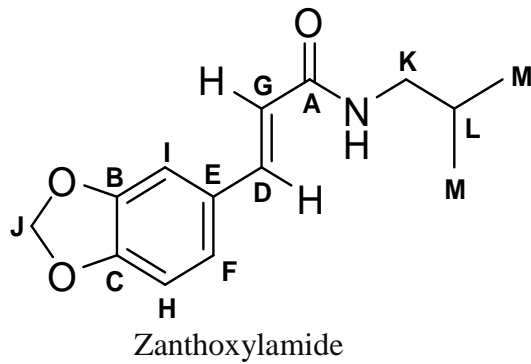




Figure 4.6.2: Structure of zanthoxylamide showing COSY —, TOCSY —, HMBC  and NOESY  correlations

From the analysis of the HRESI-LC-MSⁿ chromatogram (Figure 4.6.1), the structures for the fragmentation of zanthoxylamide based on the functional groups present in the compound were proposed as shown below (Figure 4.6.3).

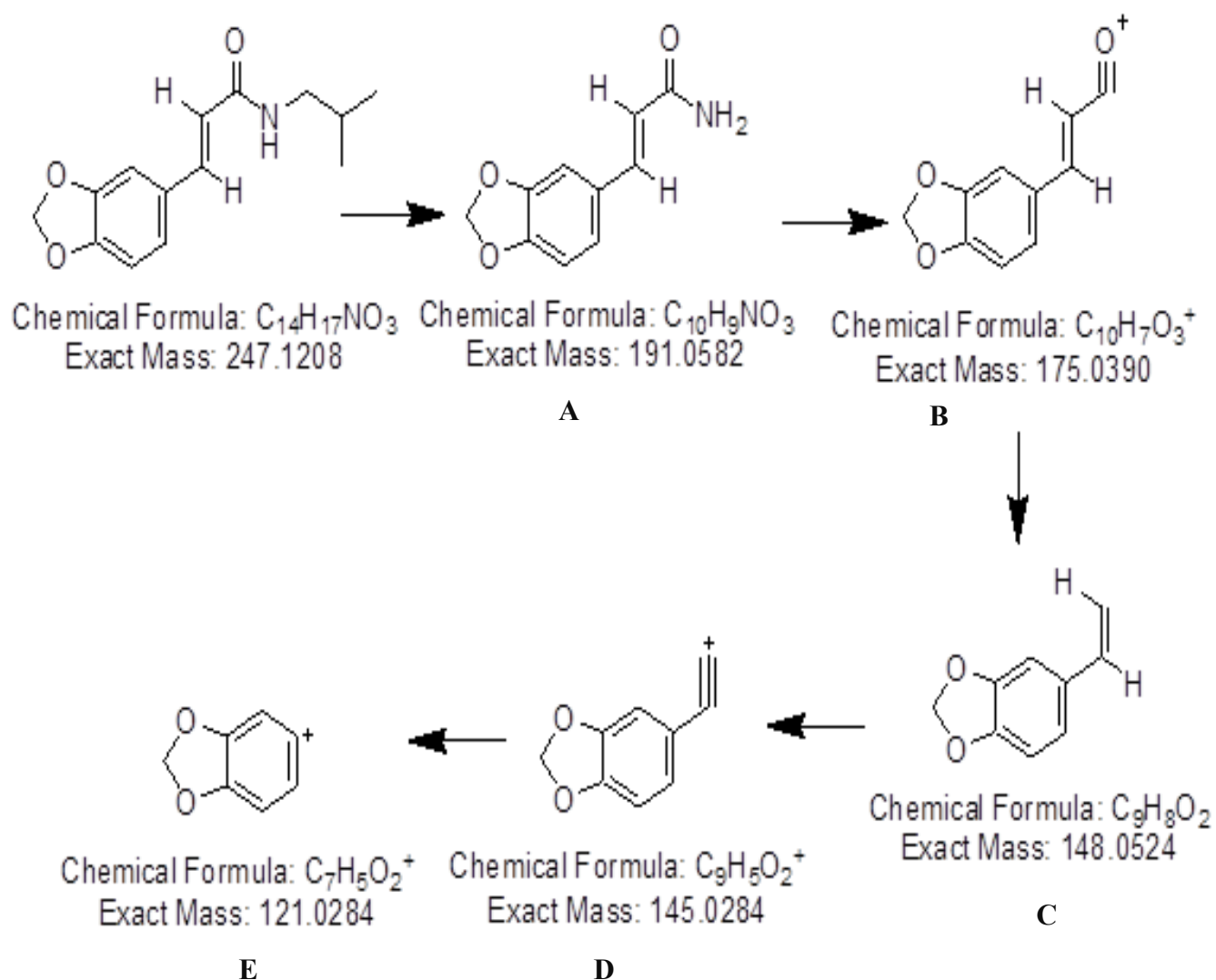


Figure 4.6.3: Fragmentation (A-E) of zanthoxylamide via labile bond cleavage

4.7 ISOLATION AND IDENTIFICATION OF THE STRUCTURAL FUNCTIONALITY OF ZR-FD-C4-C3

Compound ZR-FD-C4-C3 was consistently isolated within retention times of 32.95 to 34.48 minutes after 64 hours of reverse phase HPLC injections using a gradient of acetonitrile and water (Figures 4.7.1 and 4.7.2). ZR-FD-C4-C3 was isolated as yellow oil that was readily soluble in dichloromethane. The UV absorption (Figure 4.7.2) of this compound showed prominent absorption maxima at λ_{max} 308 nm in methanol. The HRESI-LC-MSⁿ analysis of ZR-FD-C4-C3 suggested an approximate m/z of 224.20, which was an inherently charged compound (Figure 4.7.3). The fragmentation pattern (Figure 4.7.4) which accounted for most of the peaks in the HRESI-LC-MSⁿ analysis suggested that ZR-FD.C4-C3 corresponded to the known acridine called xanthocridone.

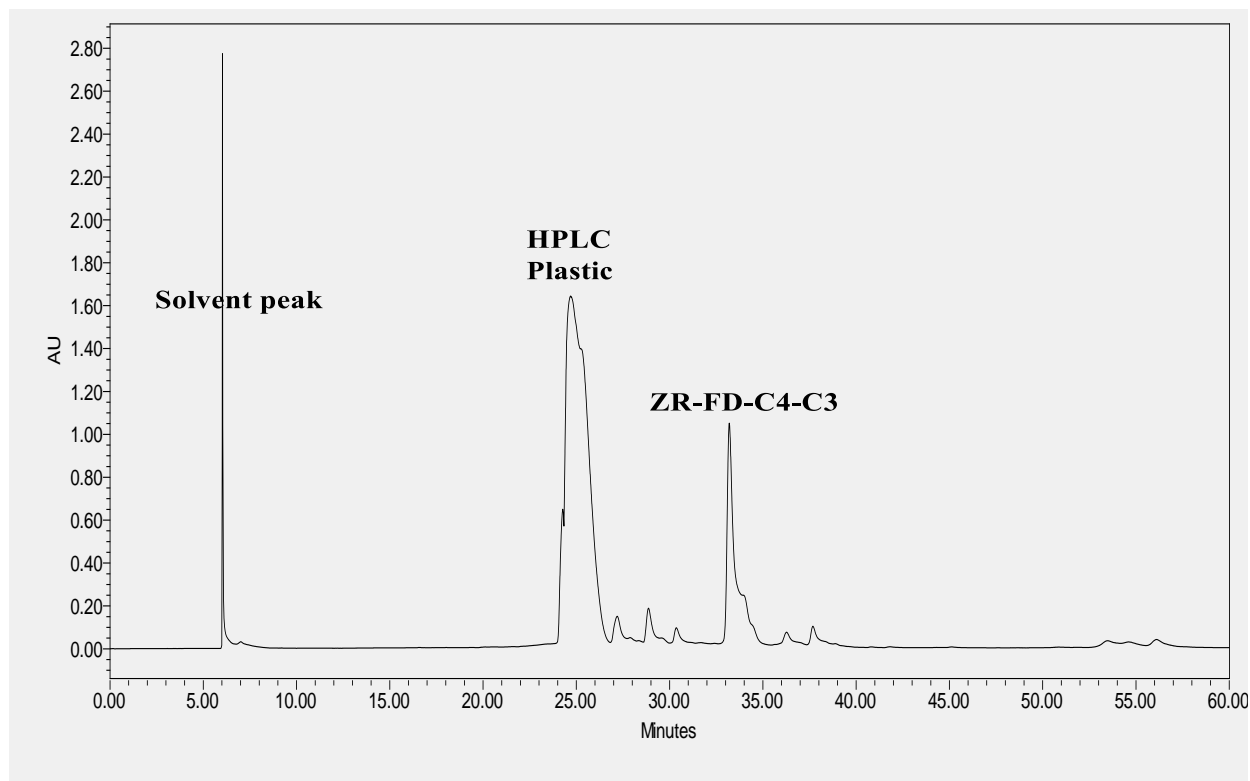


Figure 4.7.1: HPLC profile of ZRFD fraction showing the peak that yielded ZRFD-C4-C3

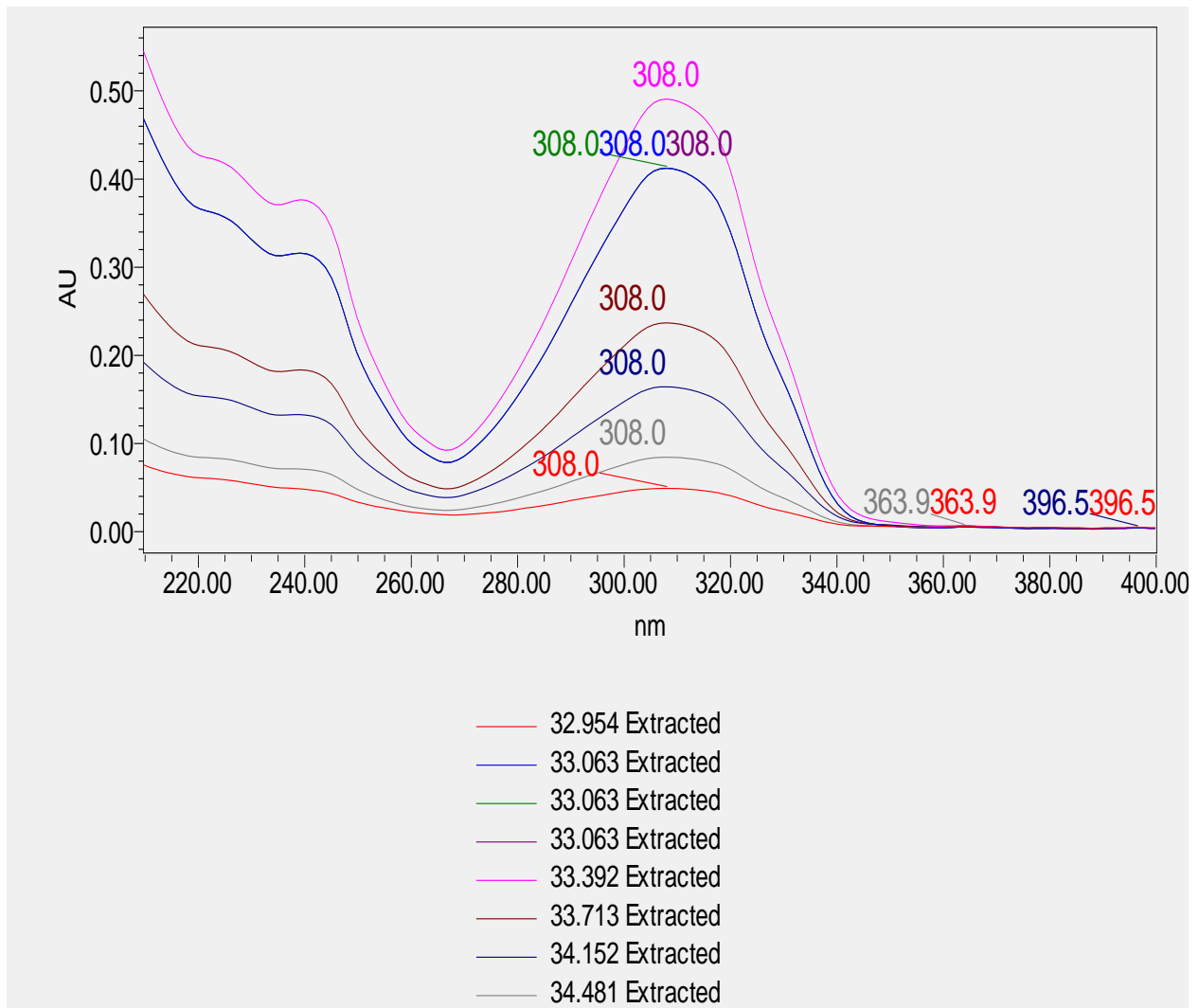


Figure 4.7.2: HPLC-UV spectrum of ZR-FD-C4-C3. It depicts prominent absorption maxima at λ_{max} 308nm

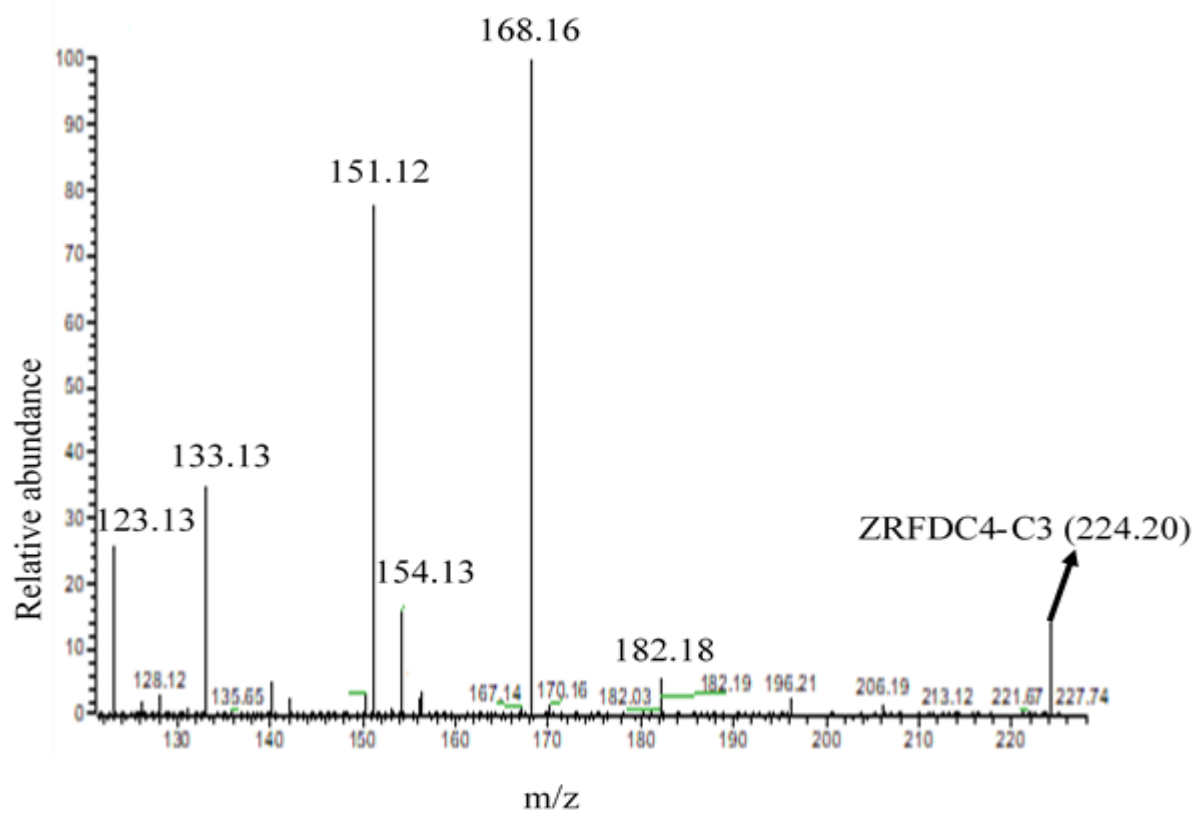


Figure 4.7.3: HRESI-LC-MSⁿ analysis of ZRFDC4-C3

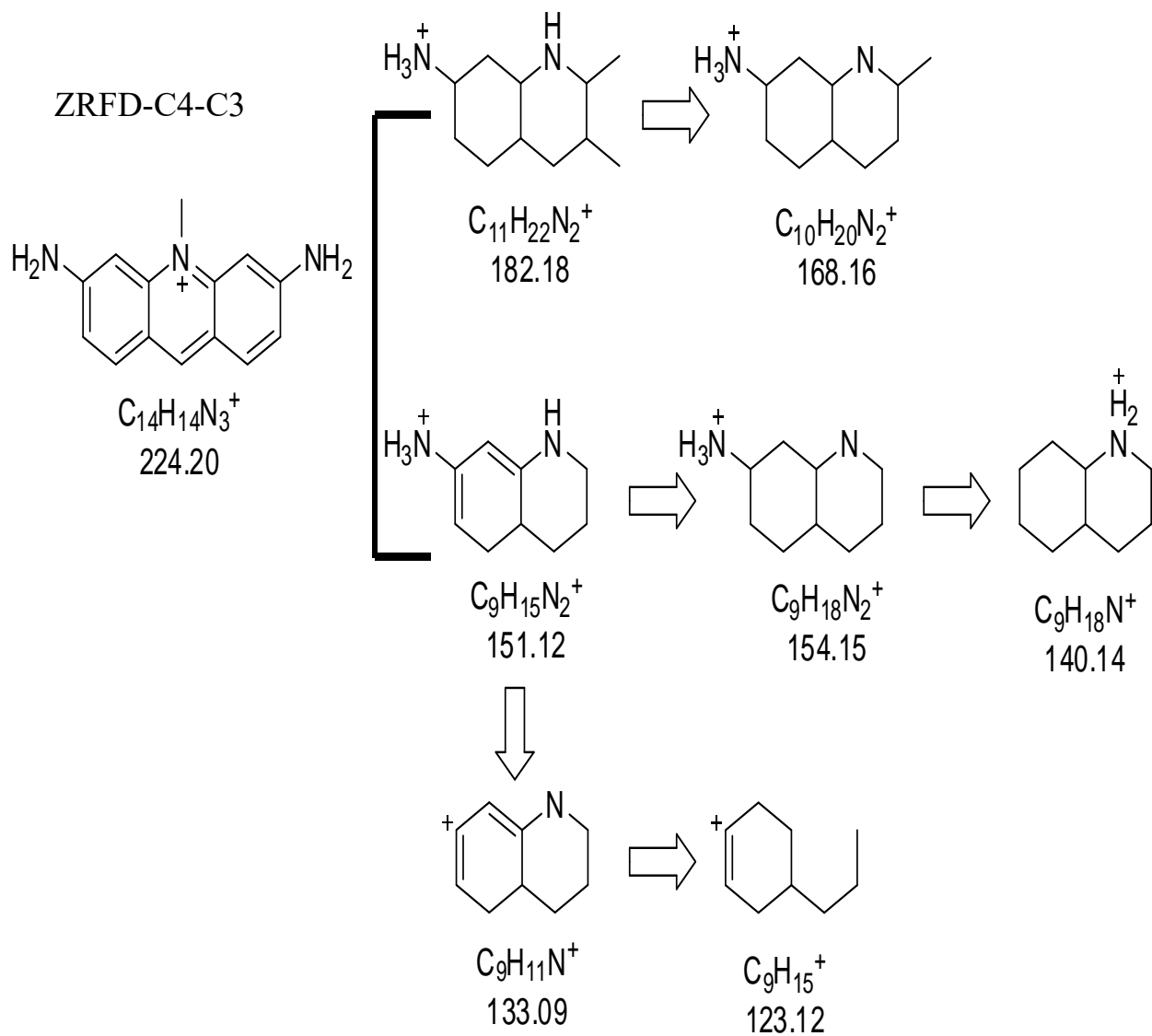


Figure 4.7.4: Fragmentation pattern of ZRFD4-C3 via labile bond cleavage analysis

4.8 ISOLATION AND IDENTIFICATION OF THE STRUCTURAL FUNCTIONALITY OF BP-FD-HB and BP-FD-HC

Compounds BP-FD-HB and BP-FD-HC were isolated at retention times of 33.38 and 34.65 minutes, respectively after 64 hours of reverse phase HPLC injections using a gradient of acetonitrile and water (Figure 4.8.1). Both BP-FD-HB and BP-FD-HC were isolated as colorless amorphous compounds that were readily soluble in methanol. The UV absorption spectrum (Figure 4.8.2) of BP-FD-HB indicated prominent absorption maxima at λ_{\max} 221.5, 271.1 and 287.7 nm in methanol. The fragmentation pattern of BP-FD-HB also suggested how BP-FD-HC could also be formed through alkylation via the backbone of tryptophan (Figures 4.8.3 and 4.8.4). BP-FD-HB and BP-FD-HC were thus identified as propyl and butyl esters of tryptophan, respectively.

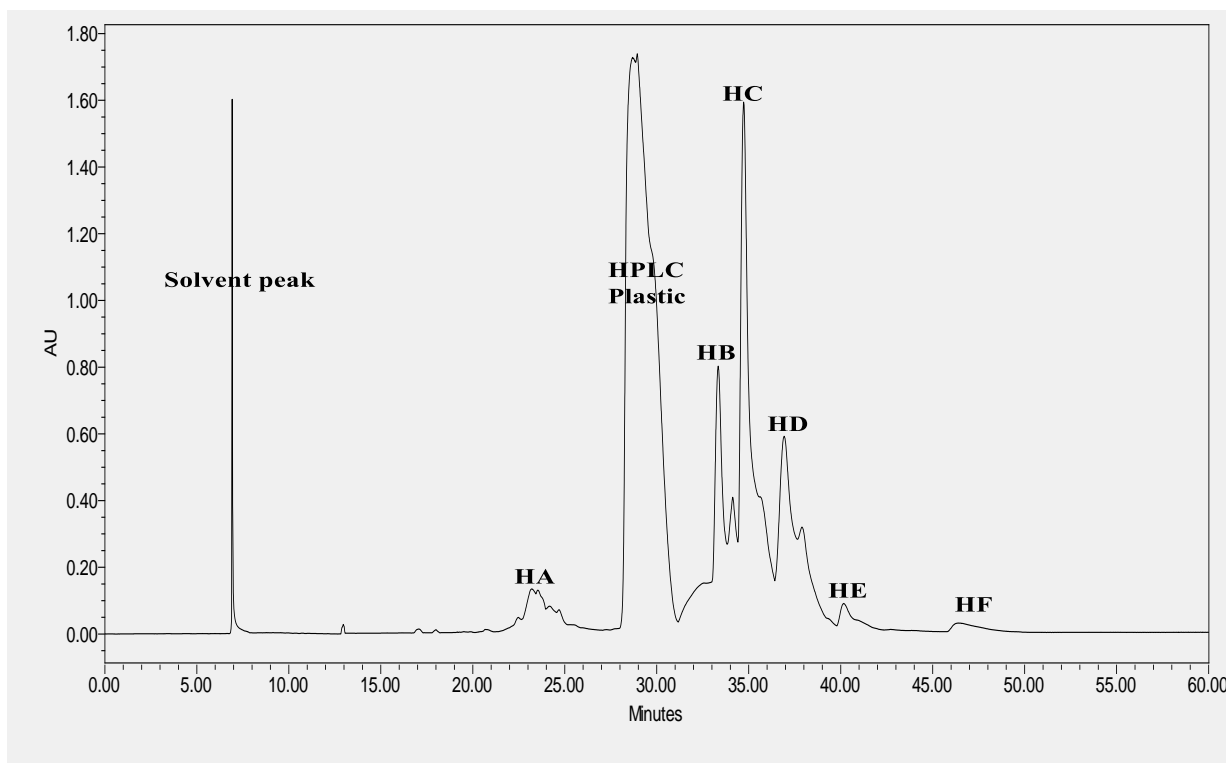


Figure 4.8.1: HPLC profile of BP-FD fraction. It depicts the peaks that yielded compounds BP-FD-HB and BP-FD-HC. Other peaks (HA, HD, HE, and HF) are also represented.

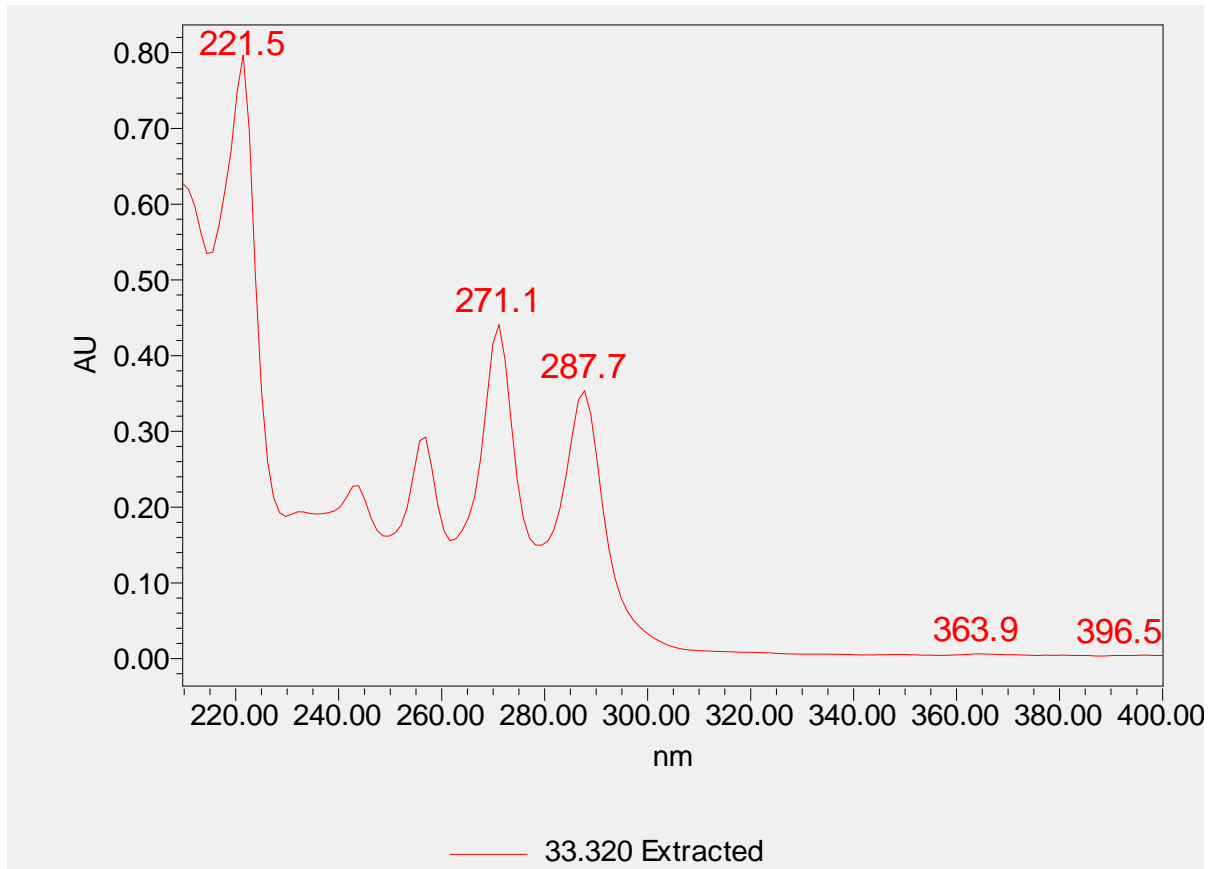


Figure 4.8.2: HPLC-UV spectrum of BP-FD-HB. It depicts the major absorption maxima at 221.5, 271.1 and 287.7 nm

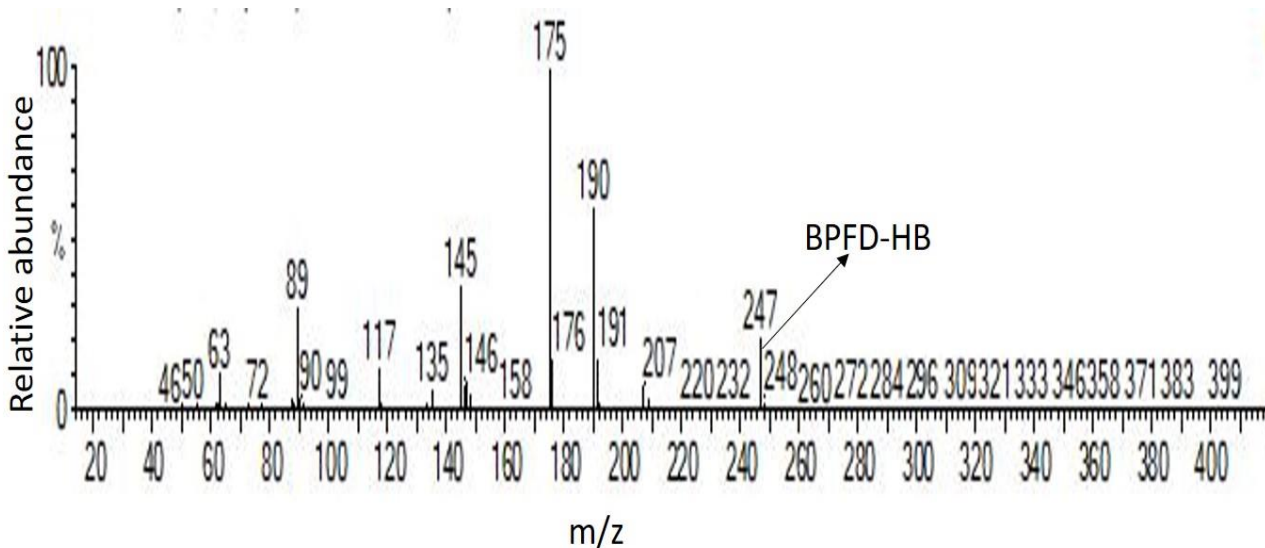


Figure 4.8.3: HRESI-LC-MSⁿ analysis of BPF-D-HB.

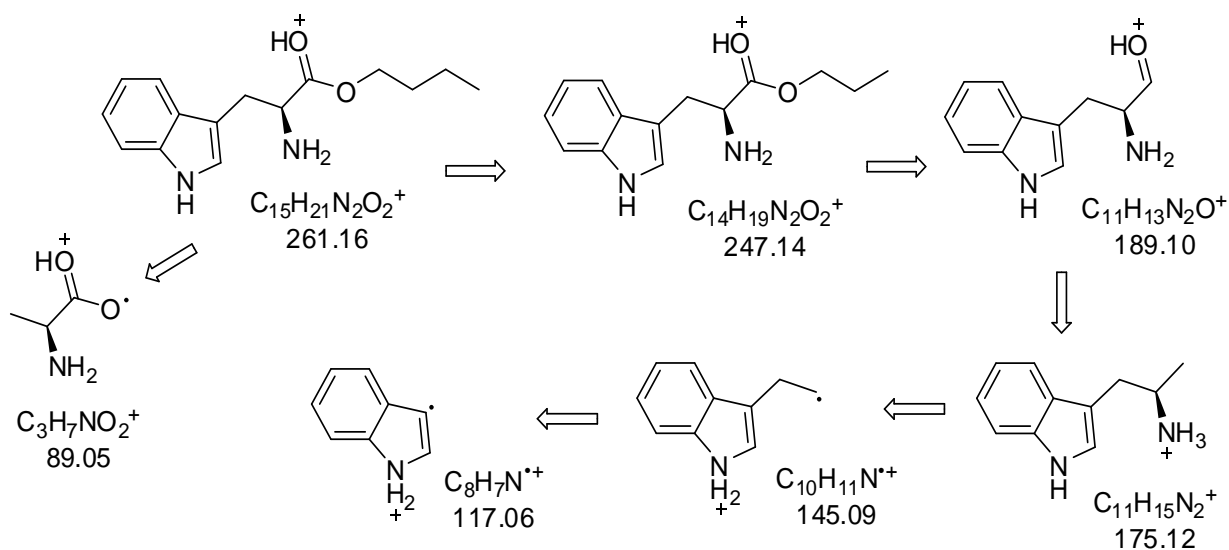


Figure 4.8.4: Fragmentation pattern of BPF-D-HB ($m/z=247.14$) and BPF-D-HC ($m/z=261.16$) via labile bond cleavage. The pattern also suggests the formation of a dehydroxylated form of tryptophan ($m/z=189.10$). BPF-D-HC and BPF-D-HB were respectively identified as butyl and propyl esters of tryptophan.

4.9 EFFECTS OF COMPOUNDS ON CELL VIABILITY OF *T. BRUCEI*

In order to determine effects on general metabolism of the parasites, the compounds were tested for their antitrypanosomal activities through the 48-hour alamar blue cell viability assay by employing the absorbance property of resazurin (Table 4.9). The assay also included ZRFDA11, an antitrypanosomal compound isolated from the root of *Z. zanthoxyloides* in preliminary screening studies (unpublished data). Chang liver cells were used to investigate potential selectivity and toxicity profiles of the compounds. BPF-D-C2 (BPF-D-HC), BPF-D-C3A (BPF-D-HB), ZRF-D-A11, ZRF-D-C4-C3 and ZRF-D-C3 (zanthoxylamide) exhibited antitrypanosomal activities with respective IC₅₀ values of 0.66, 1.17, 1.58, 1.64 and 1.93 µg/ml (Table 4.9). They also displayed low toxicity profiles with regards to their effects on Chang liver cells (Table 4.9). In the presence of Chang liver cells, BPF-D-C2 (SI=127.24) and ZRF-D-A11 (SI=20.87) respectively exhibited the highest and lowest selectivity towards *T. brucei* (Table 4.9). Compounds were more selective to the parasites as compared to Chang liver cells.

Table 4.9: Effect of compounds on cell viability of *T. brucei* and Chang liver cells

COMPOUNDS	MEAN IC ₅₀ ± SE (µg/ml)		SI
	<i>T. brucei</i>	Chang liver	
ZRF-D-C3	1.93±0.03	68.71±0.04	35.60
ZRF-D-C4	1.64±0.02	37.87±0.04	23.09
ZRF-D-A11	1.58± 0.04	32.98±0.05	20.87
BPF-D-C2	0.66±0.02	83.98 ±0.03	127.24
BPF-D-C3A	1.17±0.03	52.59±0.12	44.95
DA	0.54±0.05	39.72 ± 0.03	73.56

The activity of antitrypanosomal compounds on *T. brucei*, Jurkat cells and Chang liver cell lines was determined through alamar blue cell viability assay. Best-fit mean IC₅₀ values and standard errors (SE) were calculated from three distinct experiments. SE was expressed in terms of the mean IC₅₀ values. Selectivity indices (SI) were calculated as ratios of IC₅₀ values in Chang liver and *T. brucei* cells. DA=Diminazene aceturate, (an antitrypanosomal drug), used as a positive control.

4.10 EFFECTS OF COMPOUNDS ON CELL CYCLE OF *T. BRUCEI*

Effects of compounds on the cell cycle phases (G0-G1, S, and G2-M phases) of the parasites were also investigated through flow cytometry (Figure 4.10). There was a significant reduction of G0-G1 phase from 61.40% in the negative control to 51.96%, 51.83%, 55.0%, 38.17% and 42.23%, in ZRFD-C4-C3, ZRFD-A11, ZRFD-C3, BPDFD-C2 and BPDFD-C3A respectively (Figure 4.10). Again, there was a significant increase of S phase from 14.87% in the negative control to 18.83%, 17.70%, 18.80%, 27.60% and 26.20% in ZRFD-C4-C3, ZRFD-A11, ZRFD-C3, BPDFD-C2 and BPDFD-C3A respectively (Figure 4.10). Moreover, there was a significant increase of G2-M phase from 21.90% in the negative control to 28.63%, 28.93%, 25.83%, 42.47% and 39.50% in ZRFD-C4-C3, ZRFD-A11, ZRFD-C3, BPDFD-C2 and BPDFD-C3A respectively (Figure 4.10). Overall, BPDFD-C2 and BPDFD-C3A exhibited the most significant effects on the cell cycle phases in terms of G0-G1 inhibition or G2-M arrest (Figure 4.10).

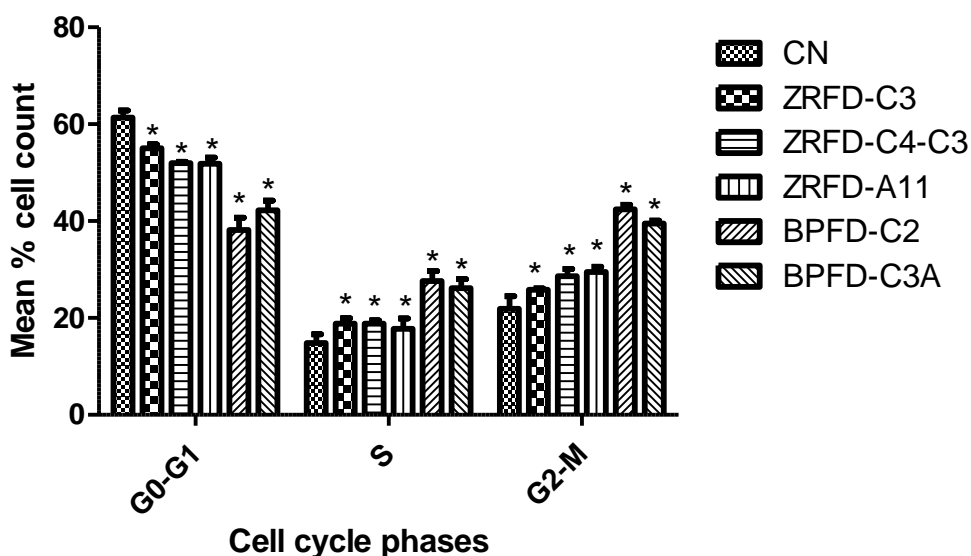


Figure 4.10: Effect of compounds on cell cycle of *T. brucei*: P-values were calculated from 3 distinct counts (n=3): [P < 0.05(*); ≥0.05 (ns=not significant)]. Error bars originate from mean percentage count ± standard error of the mean (Mean ± SEM). ZR=Z. *zanthoxyloides* root; FD=Dichloromethane fraction; CN=Negative control.

4.11 GROWTH INHIBITION OF *T. BRUCEI* BY COMPOUNDS

The effect of selected antitrypanosomal compounds (ZRFD-C4-C3, ZRFD-A11, ZRFD-C3, and BPDF-C2) from the dichloromethane fractions of *Z. zanthoxyloides* and *B. pilosa* on the growth inhibition of parasites was determined in a 72-hour alamar blue cell viability assay by employing the fluorescence property of resazurin (Figure 4.11). The assay also included a promising novel antitrypanosomal terpenoid (MLF52) isolated from *Morinda lucida* Benth (*M. lucida*) (Kwofie et al., 2016). MLF52 was included in order to determine potential similarities in the mechanisms of action and resistance between terpenoid and the isolated alkaloids. MLF52, ZRFD-C4-C3, ZRFD-C3, ZRFD-A11 and BPDF-C2 inhibited the growth of *T. brucei* at low cell density with respective EC₅₀ values of 0.17, 0.67, 0.49, 0.64, and 0.69 µg/ml (Figure 4.11). All the selected compounds also exhibited sigmoidal dose-response curves with Hill coefficients greater than 1 (Figure 4.11). The Hill slope was highest for MLF52 (3.29) and lowest for ZRFD-C3 (2.03).

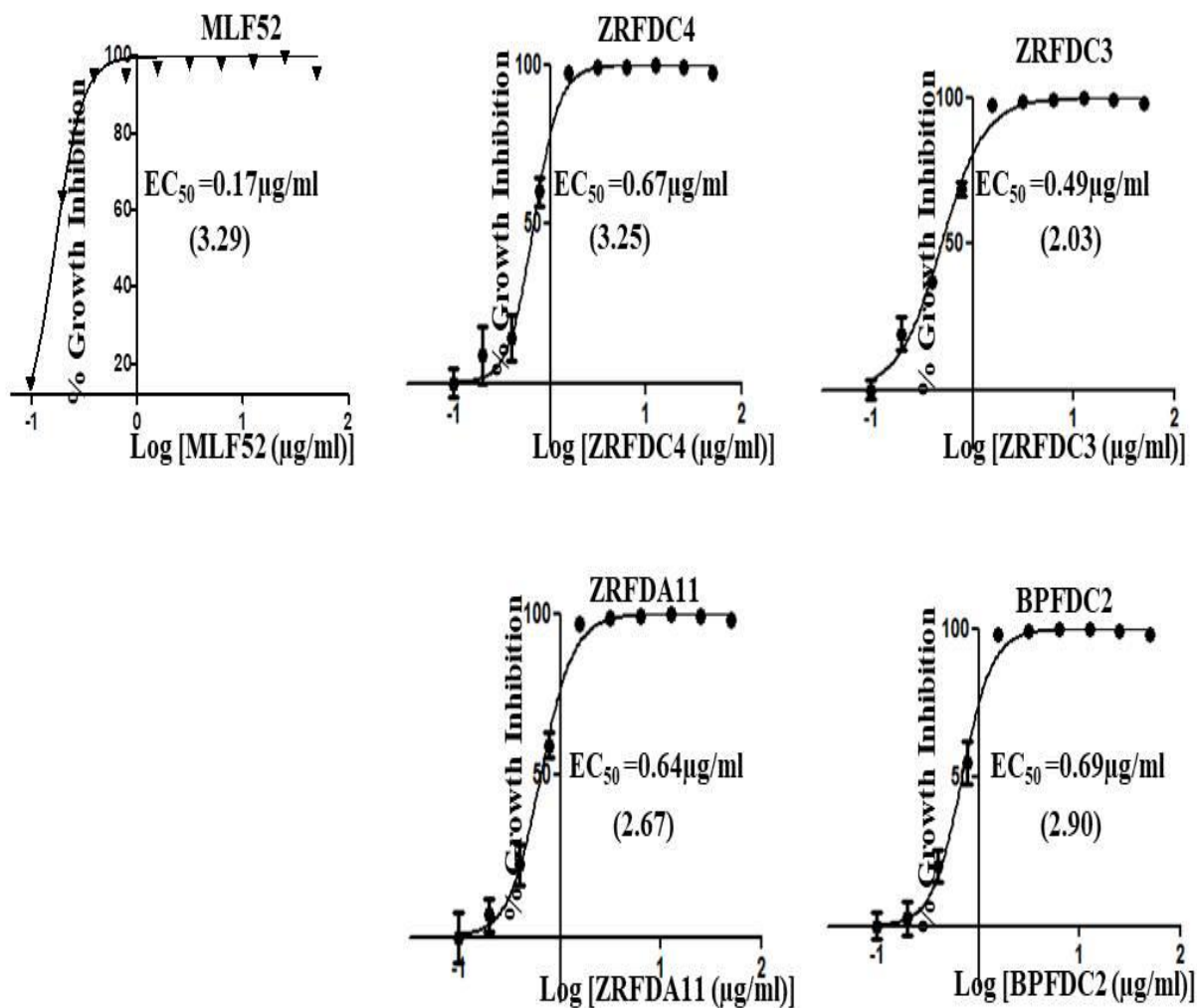


Figure 4.11: Inhibition of growth of *T. brucei* by antitrypanosomal compounds: The half-maximal effective concentration (EC_{50}) was calculated as the concentration that caused 50% growth inhibition of the parasites. The Hill slopes are indicated in parentheses. ML= *M. lucida*; ZR=*Z. zanthoxyloides*, root; BP=*B. pilosa*, whole plant; FD=Dichloromethane fraction.

4.12 EFFECTS OF COMPOUNDS ON INDUCTION OF RNAI LIBRARY

In order to facilitate the identification of potential targets involved in the mechanism of action and resistance through a RITseq approach, the effect of selected compounds on the induction of RNAi was first determined in a tetracycline-mediated library screening using the RNAi library

(Figure 4.12.1). The library was selected at $2 \times IC_{50}$ values of the compounds for approximately 8 days. The induction of RNAi was estimated through the selection of resistant strains as estimated via the generation of cumulative growth curves (Figure 4.12.1).

In comparison to the negative control, the growth curves of MLF52, ZRFD-A11 and BPF-D-C2 were generally consistent with the growth of resistant strains in the population, with ZRFD-A11 inducing the strongest resistance (Figure 4.12.1). However, ZRFD-C4-C3 and ZRFD-C3 resulted in relatively unstable strains that eventually collapsed the library at the tail end of induction (Figure 4.12.1). Moreover, PCR was carried out to identify the presence of selected library strains (Figure 4.12.2). BPF-D-C2 and ZRFD-A11 gave rise to relatively distinct though faint bands, as compared to MLF52 (Figure 4.12.2).

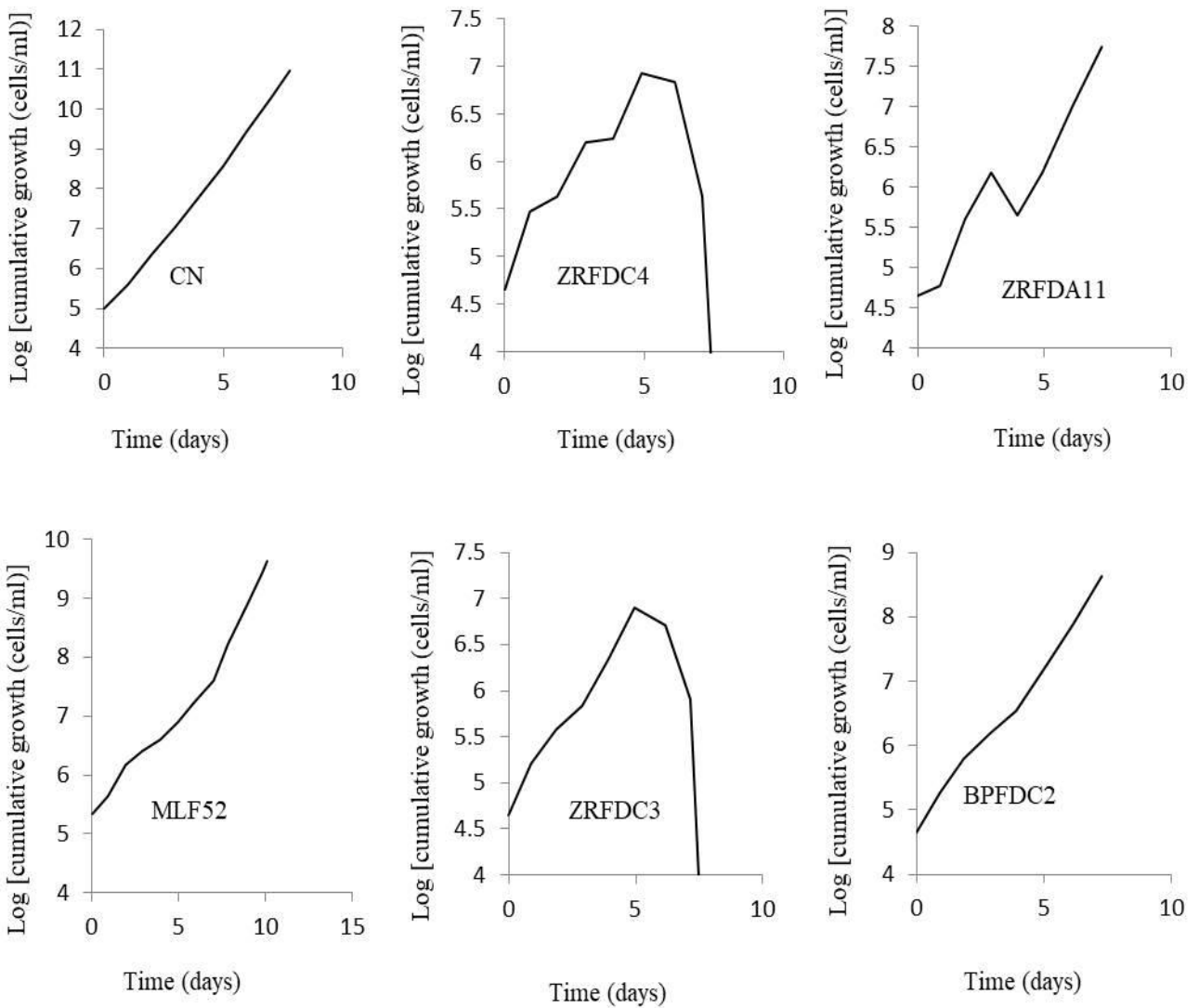


Figure 4.12.1: Induction of RNAi by antitrypanosomal compounds: Cumulative growth curves were generated from library strains selected at $2 \times IC_{50}$ values of the compounds in the presence of tetracycline for approximately 8 days. ML=*M. lucida*; ZR=*Z. zanthoxyloides*, root; BP=*B. pilosa*, whole plant; FD=Dichloromethane fraction; CN=Negative control.

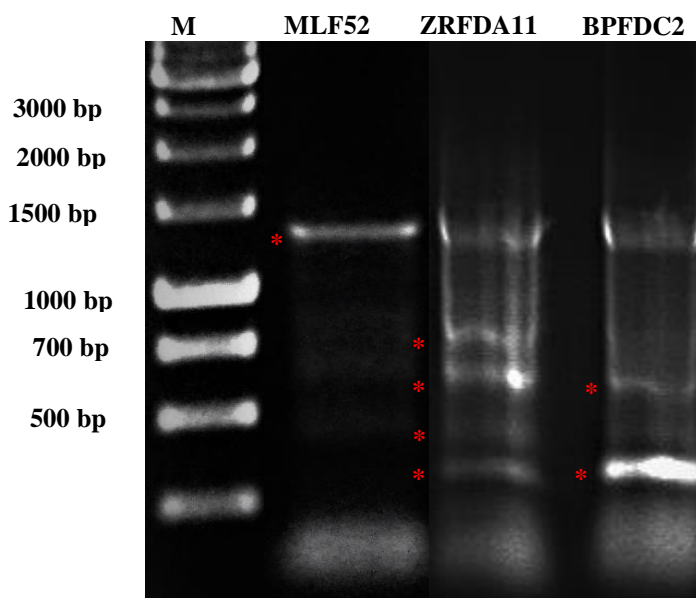


Figure 4.12.2: PCR of selected RNAi library strains: Selected strains obtained from the induction of the library were used for PCR. Experiment was carried out for 3 separate times. ML=*M. lucida*; ZR=*Z. zanthoxyloides*, root; BP=*B. pilosa*, whole plant; FD=Dichloromethane fraction; M=DNA ladder; Red stars: Bands selected for subsequent cloning and sequencing.

4.13 SENSITIVITY OF SELECTED COMPOUNDS AGAINST *T. BRUCEI*

To verify the apparent lack of library induction with regards to ZRFD-C4-C3 and ZRFD-C3, compound sensitivity analysis was carried out to assess relative metabolic stabilities of ZRFD-C4-C3 and ZRFD-C3 in *T. brucei* (Figure 4.13). Assays were carried out at $2 \times IC_{50}$ values of the compounds for approximately 5 days.

ZRFD-C4-C3 and ZRFD-C3 did not result in a persistent inhibition of parasites as estimated from the growth curves (Figure 4.13). This might have accounted for the apparent lack of library induction observed in Figure 4.12.1.

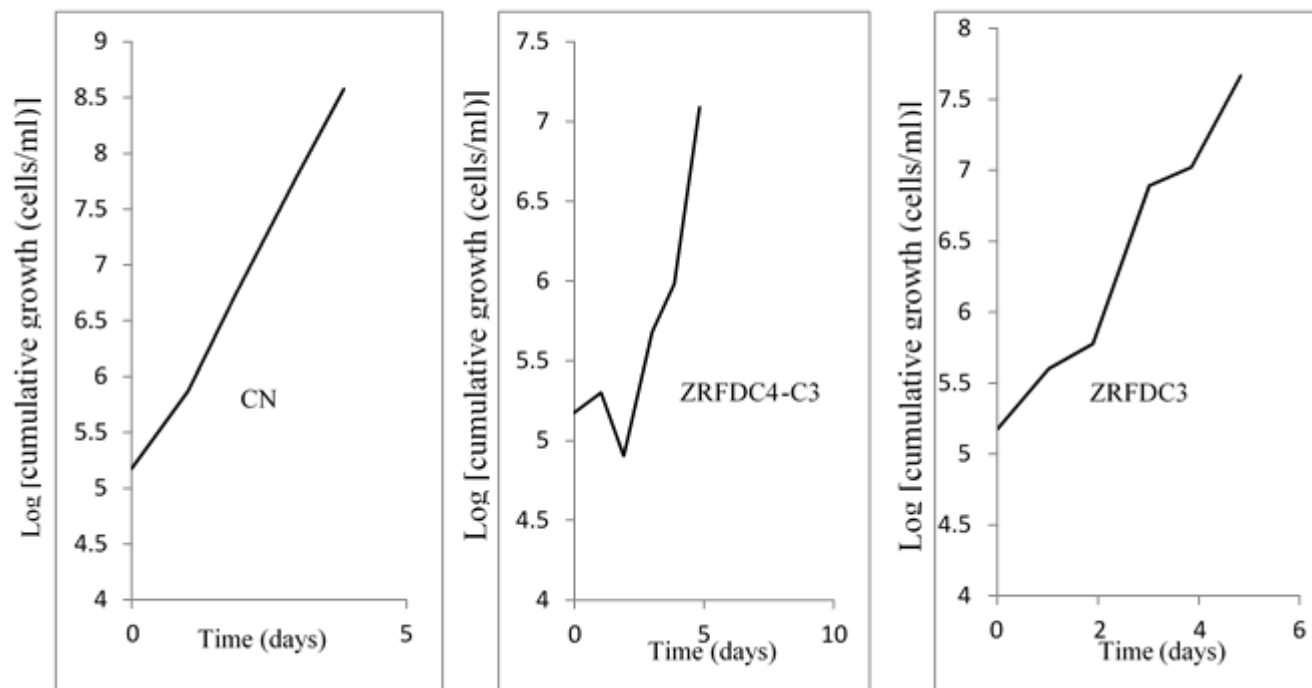


Figure 4.13.1: Antitrypanosomal sensitivity of compounds: Assays were carried out at $2xIC_{50}$ values of the compounds for approximately 5 days. ZR=*Z. zanthoxyloides*, root; FD=Dichloromethane fraction; CN=Negative control.

4.14 CLONING AND SEQUENCING OF RNAI FRAGMENTS

Compounds with promising effects on the induction and sensitivity of the RNAi library and wildtype *T. brucei* (MLF52, ZRFD-A11 and BPDF-C2) were then selected for cloning and subsequent sequencing of RNAi fragments to identify potential targets involved in the mechanism of action and resistance of respective compounds in *T. brucei* (Figure 4.14.1).

Capillary sequencing and analysis of cloned fragments of ZRFD-A11 and BPDF-C2 identified promising hit proteins with potential implications in the mode of action of the respective compounds (Figure 4.14.2). Promising hits of ZRFD-A11 and BPDF-C2 included putative leucine-rich repeat protein, putative receptor-type adenylate cyclase GRESAG 4 (gene-related

expression site associated genes), putative stumpy formation signaling pathway protein and hypothetical proteins (Figure 4.14.2). However, all the fragments of MLF52 gave rise to putative variant surface glycoprotein (VSG) pseudogene, thereby suggesting that MLF52 failed to induce the RNAi library (Figure 4.14.2). This is because the library genome is endowed with a vast array of VSG genes and pseudogenes that could be frequently expressed without any reflection of genuine inducibility. Hence, MLF52 was not considered in further analysis. Promising hits were mostly encoded on chromosomes 3, 4, and 11 (Figure 4.14.2).

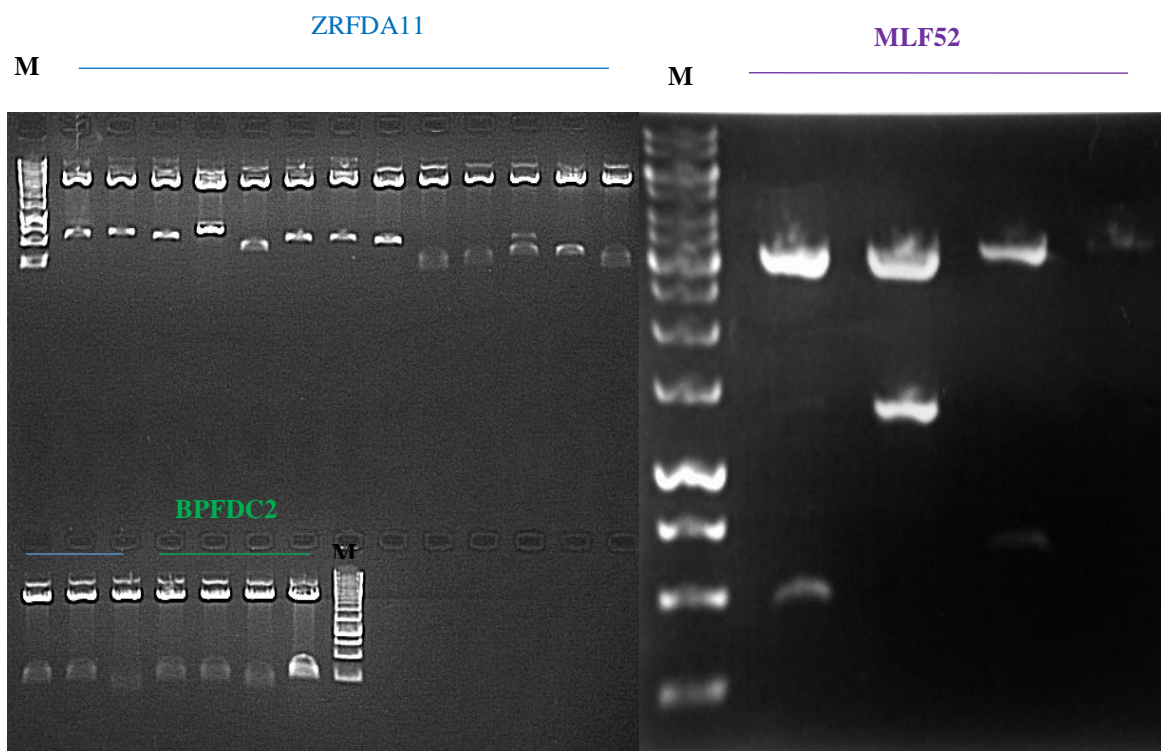


Figure 4.14.1: Cloning of selected RNAi fragments: RNAi fragments were cloned using pGEM-T Easy vector in a blue-white screening. ML= *M. lucida*; ZR=*Z. zanthoxyloides*, root; BP=*B. pilosa*; FD=Dichloromethane fraction; M=DNA ladder; Blue line=cloned ZRFDA11 fragments; Green line=cloned BPFDC6 fragments; Purple line= cloned MLF52 fragments. All cloned fragments were sequenced.

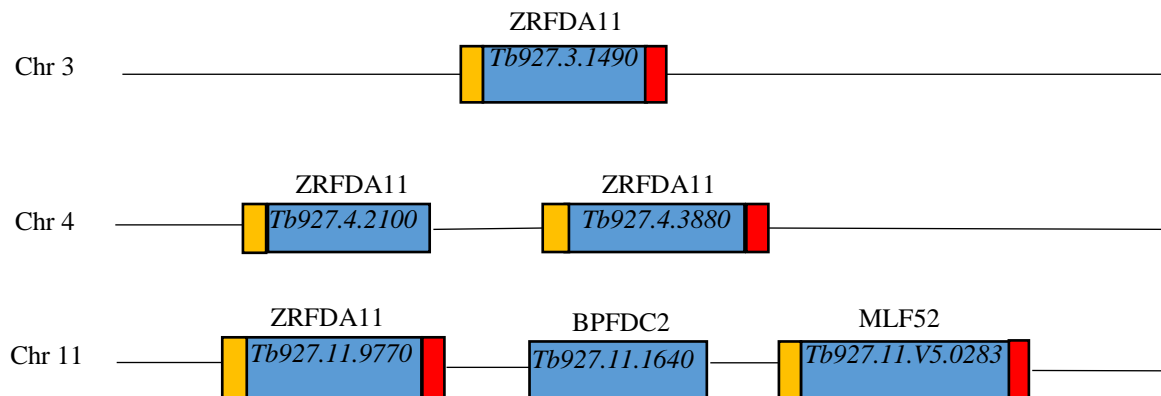


Figure 4.14.2: Capillary sequencing of RNAi fragments: Cloned RNAi fragments were sequenced and analysed to identify promising hits. Tb927.3.1490= leucine-rich repeat protein, putative; Tb927.4.2100=hypothetical protein; Tb927.4.3880= receptor-type adenylate cyclase (GRESAG 4), putative; Tb927.11.9770= hypothetical protein, conserved; Tb927.11.1640= stumpy formation signaling pathway protein, putative; Tb927.11.v5.0283= variant surface glycoprotein pseudogene, putative; orange and red bars are unique RNAi construct identifier sequences (14-mers used to track sequences that originate from the RNAi library): orange=GTGAGGCCTCGCGA; red=TCGCGAGGCCTCAC; Chr= chromosome; ML= *M. lucida*; ZR=*Z. zanthoxyloides*, root; BP=*B. pilosa*, whole plant; FD=Dichloromethane fraction.

4.15 INDUCIBILITY ANALYSIS OF COMPOUNDS

In order to confirm whether ZRFD-A11 and BPFDC-2 truly contributed towards the emergence of resistance strains in the cumulative growth curve experiments that eventually led to the identification of promising hits in the capillary sequencing, inducibility analysis was performed using the RNAi library strains recovered at the tail end of the cumulative growth curves (Figure 4.15). ZRFD-A11 exhibited percentage inducibility of 30.8%, 20.6% and 45.7%, while BPFDC-2 displayed percentage inducibility of 29.3%, 36.2% and 18.0% on day 1, 2, and 3, respectively (Figure 4.15). This confirmed that the emergence of resistance strains obtained from ZRFD-A11 and BPFDC-2 probably arose from interactions between the compounds and potential targets in the presence of tetracycline.

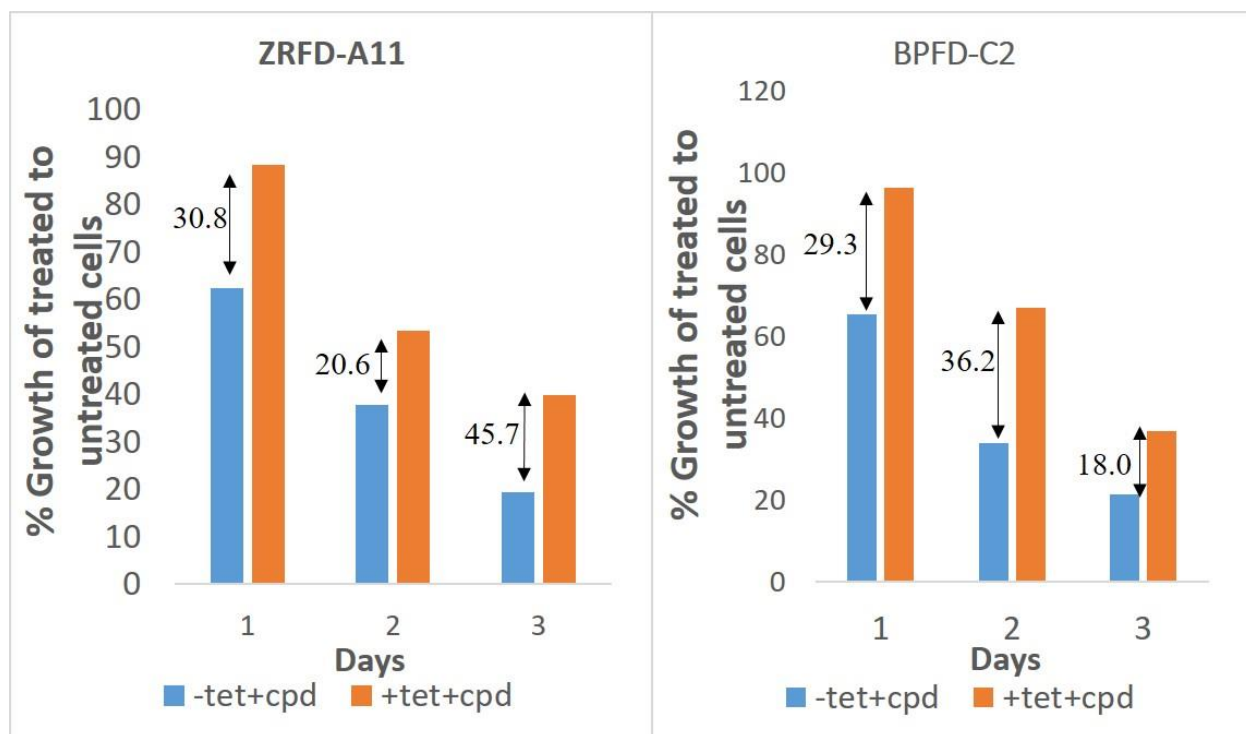


Figure 4.15: Inducibility analysis of selected compounds: Assay was carried out using the RNAi library strain. Strains were initially split into two based on the presence or absence of tetracycline, and subsequently into two based on the presence or absence of the compound under investigation. Cell density was then monitored for a period of 72 hours. If a compound contributes towards the emergence of resistance, the percentage growth of treated to untreated cells in the presence of tetracycline is expected to be greater than the corresponding growth in the absence of tetracycline. Percentage inducibility was calculated as the difference in percentage growth in the presence and absence of tetracycline. ZR=*Z. zanthoxyloides*, root; BP=*B. pilosa*, whole plant; FD=Dichloromethane fraction; tet=tetracycline; cpd= compound.

CHAPTER FIVE

5.0 DISCUSSION, CONCLUSIONS AND RECOMMENDATIONS

5.1 DISCUSSION

Zanthoxylum and *Bidens* are endowed with several pharmacological and phytochemical properties (Bartolome et al., 2013; Medhi et al., 2013). However, only a few studies have reported on the potential antitrypanosomal effects of these plants (Ogiti et al., 2009; Mann et al., 2011; Mann et al., 2012; Mwaniki et al., 2017). Even so, there is probably no reported data about the potential effects of these plants on the cell cycle, cell morphology and induction of cell death in African trypanosomes. Moreover, there is no reported data about the potential molecular targets involved in the mechanisms of their antitrypanosomal effects in African trypanosomes. The present study thus sought to determine the antitrypanosomal effects of the fractions of *Z. zanthoxyloides* and *B. pilosa* in the context of cell viability, cell death, cell cycle and cell morphology, as well as to isolate, identify, characterize and determine the mechanisms of action of antitrypanosomal compounds via chromatography, spectroscopy, cell cycle analysis and RITseq.

Fractions were prepared from the crude extracts of *Z. zanthoxyloides* and *B. pilosa* using the Kupchan method of solvent extraction. Fractions ZRFD, ZRFM, ZRWB, BPDF and BPFM were the most promising fractions with regards to their IC₅₀ values and selectivity indices towards *T. brucei* in comparison to Jurkat and Chang liver cells. In the presence of Chang liver cells, the highest selectivity was exhibited by ZRWB while the lowest was displayed by ZRFM in the presence of Jurkat cells. Moreover, in the presence of Jurkat cells, the highest and lowest selectivity was displayed by ZRFD and BPFM, respectively. However, the relatively low activity of these fractions towards Jurkat and Chang liver cells may not necessarily imply a generally low anticancer profile of *Z. zanthoxyloides* and *B. pilosa* because they may possess the required activity

of therapeutic significance towards other types of cancerous cell lines. Efforts to investigate anticancer activities in different cancerous cell lines are thus encouraged. In particular, anticancer properties of *B. pilosa* have been reported in a few studies (Sundararajan et al., 2006; Kumari et al., 2009; Shen et al., 2018). Cytotoxic activities in different mammalian cell lines have also been reported in other species of *Zanthoxylum* thereby serving to justify the need to investigate potential anticancer properties of *Z. zanthoxyloides* in different types of mammalian cell lines (Cordero et al., 2004; Da Silva et al., 2007; Ngoumfo et al., 2010; Kuetea et al., 2011; Misra et al., 2013). Moreover, even though the selectivity indices in the Chang liver cells may suggest that *Z. zanthoxyloides* and *B. pilosa* may be relatively less toxic for humans and other mammals, it is still important to investigate toxicity profiles in both *in vitro* and *in vivo* conditions because *in vitro* cytotoxicity studies are insufficient to completely assess safety profiles. Moreover, convincing data about *Zanthoxylum* and *Bidens* genera with regards to toxicity in different types of mammalian cells is limiting, and similar data about the *Z. zanthoxyloides* and *B. pilosa* species is even more scanty.

Distinct mechanisms of cell death such as apoptosis, necrosis and autophagy have been observed in *Trypanosoma* (Welburn et al., 1996; Schmidt and Bütikofer, 2014; De Silva Rodrigues et al., 2016; Sousa et al., 2017). Due to the degradation of DNA and flipping of phosphatidylserine across the plasmamembrane during apoptosis and the contrasting preservation of DNA during necrosis, a flow cytometry-based detection of apoptosis- and necrosis-like cell death using annexin-V and 7-aminoactinomycin-D was employed in the present study (Wlodkkowic et al., 2009). In this study, ZRFD, ZRFM, ZRWB, BPDF and BPFM significantly induced apoptosis-like cell death in *T. brucei*. However, BPFM was the only fraction that significantly induced necrosis-like cell death in *T. brucei*. This may indicate that while apoptosis could be therapeutically more important to *Z.*

zanthoxyloides, both apoptosis and necrosis might be therapeutically critical to *B. pilosa*. Even so, the importance of other potential mechanisms of cell death not investigated in the present study cannot be ruled out. The latter possibility is corroborated by the observation of autophagy in *T. brucei* (Schmidt and Bütikofer, 2014). Future studies that will consider the induction of other types of cell death by *Z. zanthoxyloides* should therefore be encouraged.

However, it is important to interpret with caution the induction of apoptosis and other mechanisms of cell death in unicellular protozoan parasites. This is because these unicellular protists do not encode caspases in their genome (Kaczanowski et al, 2011). Since caspases are generally pivotal to the classical pathways of apoptosis in most eukaryotes, the absence of caspases in protists raises interesting questions about the exact nature of the underlying mechanisms in this and other reported studies of apoptosis in other protozoan parasites. Even though caspase-independent mechanisms of cell death may play a role, reported data that could offer these mechanisms as alternative explanation have been contradictory and incomprehensive (Kaczanowski et al, 2011).

As in most other types of eukaryotes, the cell cycle of trypanosomes involves 4 main phases: G0-G1, S, G2 and M phases (Vaughan and Gull, 2008). *Zanthoxylum* has been reported to affect the cell cycle of different types of cell lines (Chou et al., 2011; Dung et al., 2012; Li et al., 2016). However, the present study is probably the first time *Zanthoxylum* is shown to affect the cell cycle of trypanosomes. At the IC₅₀ values, fractions ZRFD, ZRFM and ZRWB significantly altered the G0-G1 and G2-M phases. Moreover, both BPDF and BPFM significantly affected G0-G1 and G2-M but not the S-phase. The significant decrease in the cell count at the G0-G1 phase could suggest an inhibition of diploid cells while the corresponding increase at the G2-M phase may indicate the stimulation or proliferation of tetraploid cells. Furthermore, ZRFD and ZRFM of *Z. zanthoxyloides* significantly affected the S-phase of the parasite.

The effect on DNA content during the cell death and cell cycle was corroborated by morphological changes in which ZRFD, ZRFM, BPFM and BPFM led to clustering or distortion of parasites. BPFM particularly gave rise to a remarkable clustering and distortion of parasites. This appears to be in tune with the prominent induction of both apoptosis-like and necrosis-like cell deaths. Since molecular mechanisms of cell death and cell cycle overlap extensively, effects on the cell cycle of the parasite could also have contributed towards the aggregation and distortion of parasite distribution. Collectively, these may serve to emphasize the role played by the mechanisms of cell death and cell cycle as far as effects on cell morphology are concerned.

In the present study, ZRFD and BPFM were selected for the purification, identification and elucidation of their major antitrypanosomal compounds (ZRFD-C3, ZRFD-C4-C3, BPFM-C2 and BPFM-C3A) through chromatography and spectroscopy. ZRFD-C3 was isolated for the first time from *Z. zanthoxyloides* as a new alkaloid, with the name zanthoxylamide assigned to it. The present study, therefore, is the first time to report on the isolation and structural elucidation of this compound from any source of natural products. ZRFD-C4-C3, ZRFD-A11 and ZRFD-C3 stood out as the most potent antitrypanosomals with respect to their IC₅₀ values. In the presence of Chang liver cells, ZRFD-C4-C3 and BPFM-C2 exhibited the highest and lowest selectivity towards *T. brucei* respectively. Compounds were generally more selective to the parasites as compared to Chang liver cells, even though their SI values were below that of diminazine aceturate. Again, all the isolated compounds significantly inhibited the G₀-G₁ phase, stimulated the S-phase and arrested the G₂-M phase. In particular, BPFM-C2 and BPFM-C3A from *B. pilosa* exhibited the most significant effects on each of the phases.

RITseq is a loss-of-function screening technique capable of elucidating metabolic mechanisms of drug resistance and action (Alsford et al., 2013). In the application of RITseq to elucidate

mechanisms of action and resistance, the present study focused on the isolated alkaloids ZRFD-C4-C3, ZRFD-A11, ZRFD-C3, BPF-D-C2 and a novel antitrypanosomal terpenoid isolated from *M. lucida* (MLF52). MLF52 was included as an independent compound in order to highlight potential similarities in the mechanisms of action and resistance between the isolated alkaloids and terpenoids (Kwofie et al., 2016). All the compounds strongly inhibited the growth of *T. brucei*, with MLF52 and ZRFD-C3 exhibiting the most potent effects with regards to EC₅₀ values. Moreover, all the compounds displayed Hill coefficients above 1, thereby suggesting positively cooperative mechanisms of growth inhibition (Prinz, 2010). However, only ZRFD-A11 and BPF-D-C2 successfully induced the RNAi library, while ZRFD-C3 and ZRFD-C4-C3 resulted in a collapse of the library probably through destabilization. MLFF52 produced an outgrowth of library strains with the appearance of a successful RNAi library screen but without any changes in a parasite driven process as suggested by the detection of VSG pseudogenes during Sanger sequencing.

A structural and functional appreciation of MLF52 and BPF-D-C2 may be helpful in the understanding of their observed induction and growth inhibition properties, thereby providing insights into its potential mechanism of action. MLF52 belongs to the terpenoid group of plant secondary metabolites called iridoids (Kwofie et al., 2016). The pharmacological properties of a large number of iridoids may originate from their aglycone components (Ilc et al., 2016). MLF52 has an ethyl ester functional group attached to the glycone component (Kwofie et al., 2016). Esters are known to undergo enzymatic hydrolysis to the relatively stable cognate carboxyl groups which may contribute to their usefulness in commercially available drugs (Laizure et al., 2013). These drugs may be administered as esters so that they can be hydrolyzed to the cognate carboxylic acids, which could be more or less active than the parent ethyl ester depending on the nature of the

compound. Hence, MLF52 may be structurally unstable, thereby preventing any active interaction with potential transporters, activators or essential targets. This may have contributed to the lack of inducibility observed in the RNAi library screening. Moreover, due to the generally hydrophobic nature of esters, MLF52 may not require a transporter to gain entry into the parasite which might have also contributed to its inability to induce the RNAi library. Similarly, the presence of the butyl ester functional group in the alkaloid BPF-D-C2 might have reduced its stability even though the compound successfully induced the RNAi library.

Zanthoxylamide (ZRFD-C3) belongs to the sub-group of alkaloids known as N-alkylamides (Boonen et al., 2012). The mode of action of N-alkylamides may include regulation of lipid biosynthesis and the interference of quorum-sensing mechanisms in pathogens (Boonen et al., 2012). N-alkylamides may generally be inherently stable due to the amide functional groups. Hence, the observed effects of ZRFD-C3 could be partially explained from other biochemical characteristics. Due to their low critical micelle concentration, N-alkylamides have the tendency of forming micelles (Boonen et al., 2012). This property might contribute to some level of difficulty as far as the detection of potential targets are concerned due to the tendency to clump together instead of freely interacting with key metabolic proteins. Aggregation may also affect the long-term stability of parasites exposed to N-alkylamides. Collectively, these properties may partially provide insights with regards to the observed effects of ZRFD-C3 in the sensitivity and library screening.

Protein hits that were identified as potential targets included putative forms of leucine-rich repeats, receptor-type adenylate cyclase GRESAG 4, stumpy formation signaling pathway protein and other conserved hypothetical proteins encoded on chromosomes 3, 4, or 11 of *T. brucei*. These

proteins were mainly identified from ZRFD-A11 and BPDF-C2. Even though the receptor-type adenylate cyclase GRESAG 4 may only be predominantly useful in VSGs (Alexandre et al., 1996), they are nevertheless important to characterize in future studies because intact RNAi construct identifier sequences that are used to track genuine RNAi targets were present. Stumpy formation signaling proteins may be involved in the quiescence- and starvation-related morphological transformation to stumpy forms during survival and development of the parasites in the host (Mony and Matthews, 2015). However, the putative leucine-rich repeat and hypothetically conserved proteins were particularly interesting. Leucine-rich repeats are binding motifs known to be involved in various protein-protein interactions (Kedzierski et al., 2004). While leucine-rich repeats may be required for host defense systems of both plants and mammals, they may also be paradoxically involved in the interaction with host cells and establishment of infection (Kedzierski et al., 2004). Moreover, some of the hypothetical proteins identified also contained signal peptides, which are generally involved in secretory and localization pathways. Hence, the antitrypanosomals might act to interfere with the pathogenesis, growth, development and the secretory pathway of the parasite. The elucidation of the physical and chemical properties of these proteins, as well as the validation of these potential mechanisms of interaction with the antitrypanosomals might therefore contribute considerably to the development of novel chemotherapy in African trypanosomiasis.

5.2 CONCLUSIONS

In this study, the antitrypanosomal activities and mechanisms of action of *Z. zanthoxyloides* (root) and *B. pilosa* (whole plant) in the context of cell viability, cell death, cell cycle, morphology and distribution of *T. brucei* were investigated. The antitrypanosomal fractions and compounds of *Z. zanthoxyloides* (root) and *B. pilosa* (whole plant) were found to exhibit significant effects on apoptosis-like cell death and cell cycle of *T. brucei*. They also affected the morphology and induced aggregation of the parasites. The mechanisms of action and resistance of *Z. zanthoxyloides* (root) and *B. pilosa* (whole plant) were also investigated in the context of RITseq. Putative leucine-rich repeat proteins, stumpy formation signaling pathway proteins, putative receptor-type adenylate cyclase and hypothetically conserved proteins were identified as promising hits for selected compounds in the parasites, thereby shedding light on the antitrypanosomal mechanisms of resistance and action of the compounds.

5.3 RECOMMENDATIONS

It is recommended that attention be paid to natural products from plants as alternative sources of chemotherapy for African trypanosomiasis. In the same context, attention must also be paid to the metabolic sensitivities and stabilities of antitrypanosomals because these properties are crucial for the determination of mechanisms of action in *T. brucei*. Promising compounds with such limitations should therefore be structurally optimized in the drug discovery process before preclinical and clinical investigations. It is also important to investigate correlations between structure and various biological properties of antitrypanosomals. Studies into structure-potency, structure-stability, structure-resistance and structure-toxicity correlations could inform the design and synthesis of new drugs that may circumvent current challenges of side effects, resistance and physico-chemical limitations. These could also help in the structural modification and activity

optimization of lead compounds and available drugs. Moreover, it is recommended that the elucidation of the mode of action of antitrypanosomals be pursued comprehensively via the utilization of all available tools in genomics, transcriptomics, proteomics and computational studies that are of relevance to drug discovery and development.

REFERENCES

Abbasi K, DuBois KN, Leung KF, Dacks JB, Field MC (2011) A novel Rho-like protein TbRHP is involved in spindle formation and mitosis in trypanosomes. *PLoS One* 6: e26890.

Adam Y, Cecchi G, Kgori PM, Marcotty T, Mahama CI, Abavana M, Anderson B, Paone M, Mattioli R, Bouyer J (2013) The sequential aerosol technique: a major component in an integrated strategy of intervention against riverine tsetse in Ghana. *PLoS Neglected Tropical Diseases* 7(3): e2135.

Adebayo JO, Krettli AU (2011) Potential antimalarials from Nigerian Plants: a review. *Journal of Ethnopharmacology* 133(2): 289-302.

Adekunle AS, Kamdem JP, Rocha JBT (2012) Antioxidant Activity and HPLC Analysis of *Zanthoxylum zanthoxyloides*. *Report and Opinion* 4(3): 6–13.

Adesina SK (2005) The Nigerian *Zanthoxylum*; chemical and biological values. *African Journal of Traditional, Complementary and Alternative Medicine* 2(3): 282–301.

Ahua KM, Ioset JR, Ioset KN, Diallo D, Mauël J, Hostettmann K (2007) Antileishmanial activities associated with plants used in the Malian traditional medicine. *Journal of Ethnopharmacology* 110: 99–104.

Alexandre S, Painsavoine P, Hanocq-Quertier J, Paturiaux-Hanocq F, Tebabi P, Pays E (1996) Families of adenylate cyclase genes in *Trypanosoma brucei*. *Molecular and Biochemical Parasitology* 77: 173-182.

Al-Musayeb NM, Mothana RA, Al-Massarani S, Matheeussen A, Cos P, Maes L (2012) Study of the *in vitro* antiplasmodial, antileishmanial and antitrypanosomal activities of medicinal plants from Saudi Arabia. *Molecules* 17: 11379-11390.

Aloke C, Nwachukwu N, Ugwuja EI, Idenyi JN, Nwachi EU, Obasi IO, Oga O (2012) Effects of *Zanthoxylum zanthoxyloides* leaves on blood glucose, lipid profile and some liver enzymes in alloxan induces diabetic rats. *International Journal of Science and Nature* 3(3): 497–501.

Alsford S, Glover L, Horn D (2005) Multiplex analysis of RNA interference defects in *Trypanosoma brucei*. *Molecular and Biochemical Parasitology* 139(1): 129-132.

Alsford S, Turner DJ, Obado SO, Sanchez-Flores A, Glover L, Berriman M, Hertz-Fowler C, Horn D (2011) High-throughput phenotyping using parallel sequencing of RNA interference targets in the African trypanosome. *Genome Research* 21: 915–924.

Alsford S, Eckert S, Baker N, Glover L, Sanchez-Flores A, Leung KF, Turner DJ, Field MC, Berriman M, Horn D (2012) High-throughput decoding of antitrypanosomal drug efficacy and resistance. *Nature* 482: 232–236.

Alsford S, Kelly JM, Baker N, Horn D (2013) Genetic dissection of drug resistance in trypanosomes. *Parasitology* 140: 1478–1491.

Ambit A, Fasel N, Coombs GH, Mottram JC (2008) An essential role for the *Leishmania* major metacaspase in cell cycle progression. *Cell Death and Differentiation* 15: 113–122.

Amabeoku GJ, Kinyua CG (2010) Evaluation of the Anticonvulsant of *Zanthoxylum capense* (Thunb.) Harv. (Rutaceae) in Mice. *International Journal of Pharmacology* 6(6): 844-853.

Anne IO, Andrew OO, Idu M (2013) Phytochemistry and antimicrobial activity of *Zanthoxylum zanthoxyloides* root used as chewing stick in Nigeria. *The Journal of Phytopharmacology* 2(6): 1-7.

Araki H, Leem SH, Phongdara A, Sugino A (1995) Dpb11, which interacts with DNA polymerase II (epsilon) in *Saccharomyces cerevisiae*, has a dual role in S-phase progression and at a cell cycle checkpoint. *Proceedings of the National Academy of Sciences of the United States of America* 92: 11791–11795.

Aravin AA, Sachidanandam R, Bourc'his D, Schaefer C, Pezic D, Toth KF, Bestor T, Hannon GJ (2008) A piRNA Pathway Primed by Individual Transposons Is Linked to De Novo DNA Methylation in Mice. *Molecular Cell* 31(6): 785–799.

Arbonnier M (2004) Trees, shrubs and lianas of West African dry zones. CIRAD, Margraf Publishers Gmbh, MNHN, Paris, France: pp 573.

Archambault V, Glover DM (2009) Polo-like kinases: conservation and divergence in their functions and regulation. *Nature Reviews. Molecular Cell Biology* 10: 265–275.

Ashafa AOT, Afolayan AJ (2009) Screening the root extracts from *Biden pilosa* L. var. *radiata* (Asteraceae) for antimicrobial potentials. *Journal of Medicinal Plant Research* 3: 568–572.

Ayyanar M, Ignacimuthu S (2005) Traditional knowledge of Kani tribals in Kouthalai of Tirunelveli hills, Tamil Nadu, India. *Journal of Ethnopharmacology* 102: 246–255.

Azando EVB, Hounzangbé-Adoté MS, Oloundadé PA, Brunet S, Fabre N, Valentin A, Hoste H (2011) Involvement of tannins and flavonoids in the *in vitro* effects of *Newbouldia laevis* and

Zanthoxylum zanthoxyloides extracts on the exsheathment of third-stage infective larvae of gastrointestinal nematodes. *Veterinary Parasitology* 180: 292-297.

Baker N, Alsford S, Horn D (2011) Genome-wide RNAi screens in African trypanosomes identify the nifurtimox activator NTR and the eflornithine transporter AAT6. *Molecular and Biochemical Parasitology* 176: 55–57.

Barnabas BB, Man A, Ogunrinola TS, Anyanwu PE (2011) Screening for anthelmintic activities from extracts of *Zanthoxylum Zanthoxyloides*, *Neocaryamacrophylla* and *Celosia laxa* against *Ascaris* infection in rabbits. *International Journal of Applied Research in Natural Products* 3(4): 1-4.

Barrett MP, Burchmore RJ, Stich A (2003) The trypanosomiases. *Lancet* 362 (9394): 1469–1480.

Barrett MP, Vincent IM, Burchmore RJ, Kazibwe AJ, Matovu E (2011) Drug resistance in human African trypanosomiasis. *Future Microbiology* 6: 1037–1047.

Bartolome AP, Villaseñor IM, Yang WC (2013) *Bidens pilosa* L. (Asteraceae): Botanical properties, traditional uses, phytochemistry, and pharmacology. *Evidence-Based Complementary and Alternative Medicine* 2013 (340215): pp 51.

Bastos JK, Albuquerque S, Silva MLA (1999) Evaluation of the trypanocidal activity of lignans isolated from the leaves of *Zanthoxylum naranjillo*. *Planta Medica* 65: 541-544

Batool F, Mubashir S, Rocha JBT, Hussain A, Saied Z, Dilnawaz S (2010) Evaluation of antioxidant and free radical scavenging activities of fruit extract from *Zanthoxylum alatum*: A Commonly Used Spice from Pakistan. *Pakistan Journal of Botany* 42 (6): 4299-4311

Bauer B, Amsler-Delafosse S, Clausen PH, Kabore I, Petrich-Bauer J (1995) Successful application of deltamethrin pour-on to cattle in a campaign against tsetse flies (*Glossina* spp.) in the pastoral zone of Samorogouan, Burkina Faso. *Tropical Medicine and Parasitology* 46(3): 183–189.

Bauer B, Gitau D, Oloo FP, Karanja SM (2006) Evaluation of a preliminary title to protect zero-grazed dairy cattle with insecticide-treated mosquito netting in western Kenya. *Tropical Animal Health and Production* 38(1): 29–34.

Bauer B, H Bettina, Mahama CI, Baumann MPO, Mehlitz D, Clausen PH (2011) Managing tsetse transmitted trypanosomosis by insecticide treated nets: an affordable and sustainable method for resource poor pig farmers in Ghana. *PLoS Neglected Tropical Diseases* 5(10): e1343.

Benaim G, Lopez-Estrano C, Docampo R, Moreno SNJ (1993) A calmodulin-stimulated Ca²⁺ pump in plasma-membrane vesicles from *Trypanosoma brucei*: selective inhibition by pentamidine. *Biochemical Journal* 296: 759–763.

Benz C, Clayton CE (2007) The F-box protein CFB2 is required for cytokinesis of bloodstream-form *Trypanosoma brucei*. *Molecular and Biochemical Parasitology* 156: 217–224.

Benz C, Clucas C, Mottram JC, Hammarton TC (2012) Cytokinesis in bloodstream stage *Trypanosoma brucei* requires a family of katanins and spastin. *PLoS One* 7(3): e30367.

Berghe TV, Kaiser WJ, Bertrand MJM, Vandenabeele P (2015) Molecular crosstalk between apoptosis, necroptosis, and survival signaling. *Molecular and Cellular Oncology* 2(4): e975093.

Berger BJ, Carter NS, Fairlamb AH (1993) Polyamine and pentamidine metabolism in African trypanosomes. *Acta Tropica* 54(3-4): 215–224.

Berezikov E (2011) Evolution of microRNA diversity and regulation in animals. *Nature Reviews Genetics* 12(12): 846–860.

Berriman M, Ghedin E, Hertz-Fowler C, Blandin G, Renauld H, Bartholomeu DC, Lennard NJ et al., (2005) The genome of the African trypanosome *Trypanosoma brucei*. *Science* 309 (5733): 416–422.

Bertani S, Bourdy G, Landau I, Robinson JC, Esterre P, Deharo E (2005) Evaluation of French Guiana traditional antimalarial remedies. *Journal of Ethnopharmacology* 98: 45-54.

Beutler JA, Cardellina JH, Lin CM, Hamel E, G. M. Cragg GM, Boyd MR (1993) Centaureidin, a cytotoxic flavone from *Polymnia fruticosa*, inhibits tubulin polymerization. *Bioorganic and Medicinal Chemistry Letters* 3: 581–584.

Beutler JA, Hamel E, Vlietinck AJ et al., (1998) Structure-activity requirements for flavone cytotoxicity and binding to tubulin. *Journal of Medicinal Chemistry* 41: 2333–2338.

Blow JJ, Dutta A (2005) Preventing re-replication of chromosomal DNA. *Nature Reviews Molecular Cell Biology* 6: 476–486.

Blum B, Simpson L (1990) Guide RNAs in kinetoplastid mitochondria have a nonencoded 3' oligo (U) tail involved in recognition of the pre-edited region. *Cell* 62: 391-397.

Blum B, Bakalara N, Simpson L (1990) A model for RNA editing in kinetoplastid mitochondria: "guide" RNA molecules transcribed from maxicircle DNA provide the edited information. *Cell* 60: 189-198.

Boonen J, Bronselaer A, Nielandt J, Veryser L, Tre GD, Spiegeleer BD (2012) Alkamid database: Chemistry, occurrence and functionality of plant N-alkylamides. *Journal of Ethnopharmacology*: 142(3): 563-590.

Boothroyd JC, Cross GA (1982) Transcripts coding for variant surface glycoproteins of *Trypanosoma brucei* have a short, identical exon at their 5' end. *Gene* 20: 281-289.

Boulangé A, Serveau C, Brillard M, Minet C, Gauthier F, Diallo A (2001) Functional expression of the catalytic domains of two cysteine proteinases from *Trypanosoma congolense*. *International Journal for Parasitology* 31: 1435-1440.

Boye A, Koffuor GA, Boampong JN, Amoateng P, Ameyaw EO, Ansaah EO, Addai GM, Adjei CK, Addo J, Penu DKA (2012) Gastroprotective effect and safety assessment of *Zanthoxylum Zanthoxyloides* (Lam) Waterm root bark extract. *American Journal of Pharmacology and Toxicology* 7(2): 73–80.

Brennecke J, Aravin AA, Stark A, Dus M, Kellis M, Sachidanandam R, Hannon GJ (2007) Discrete small RNA-generating loci as master regulators of transposon activity in *Drosophila*. *Cell* 128(6): 1089–1103.

Calzada A, Hodgson B, Kanemaki M, Bueno A, Labib K (2005) Molecular anatomy and regulation of a stable replisome at a paused eukaryotic DNA replication fork. *Genes and Development* 19: 1905–1919.

Cano JH, Volpato G (2004) Herbal mixtures in the traditional medicine of Eastern Cuba. *Journal of Ethnopharmacology* 90: 293–316.

Capewell P, Clucas C, DeJesus E, Kieft R, Hajduk S, Veitch N, Steketee PC, Cooper A, Weir W, MacLeod A (2013) The TgsGP gene is essential for resistance to human serum in *Trypanosoma brucei gambiense*. PLoS Pathogens 9(10): e1003686.

Carmena M (2008) Cytokinesis: the final stop for the chromosomal passengers. Biochemical Society Transactions 36: 367–370.

Carnes J, Soares CZ, Wickham C, Stuart K (2011) Endonuclease associations with three distinct editosomes in *Trypanosoma brucei*. Journal of Biological Chemistry 286(22): 19320–19330.

Carter NS, Fairlamb AH (1993) Arsenical-resistant trypanosomes lack an unusual adenosine transporter. Nature 361: 173–176.

Carthew RW, Sontheimer EJ (2009) Origins and mechanisms of miRNAs and siRNAs Cell 136(4): 642–655.

Challier A, Laveissiere C (1973) Un nouveau piege pour la capture des glossines (*Glossina: Diptera: Muscidae*). Description et essais sur le terrain [A new trap for capturing tsetse (*Glossina: Diptera: Muscidae*). Description and field trials]. Cahiers ORSTOM: Série Entomologie Médicale et Parasitologie 11: 251–262.

Challier A et al (1977) Amelioration du rendement du piege biconique pour glossines (*Diptera, Glossinidae*), par l'emploi d'un cone inferieur bleu [Improved productivity of biconical traps for tsetse (*Diptera, Glossinidae*) with use of a blue lower cone]. Cahiers ORSTOM, Série Entomologie Médicale et Parasitologie 15: 283–286.

Chang JS, Chiang LC, Chen CC, Liu LT, Wang KC, Lin CC (2001) Atileukemic activity of *Bidens pilosa* L. var. *minor* (blume) sherff and *Houttuynia cordata* thumb. *American Journal of Chinese Medicine* 29: 303–312.

Chang SL, Chang CL, Chiang YM, Hsieh RH, Tzeng CR, Wu TK, Sytwu HK, Shyur LF, Yang WC (2004) Polyacetylenic compounds and butanol fraction from *Bidens pilosa* can modulate the differentiation of helper T cells and prevent autoimmune diabetes in non-obese diabetic mice. *Planta Medica* 70: 1045–1051.

Chang CL, Kuo HK, Chang SL, Chiang YM, Lee TH, Wu WM, Shyur LF, Yang WC (2005) The distinct effects of a butanol fraction of *Bidens pilosa* plant extract on the development of Th1-mediated diabetes and Th2-mediated airway inflammation in mice. *Journal of Biomedical Science* 12: 79–89.

Chang CL, Chang SL, Lee YM, Chiang YM, Chuang DY, Kuo HK, Yang WC (2007) Cytopyloine, a polyacetylenic glucoside, prevents type 1 diabetes in non-obese diabetic mice. *Journal of Immunology* 178: 6984–6993.

Chang SL, Chiang YM, Chang CL, Yeh HH, Shyur LF, Kuo YH, Wu TK, Yang WC (2007) Flavonoids, centaurein and centaureidin, from *Bidens pilosa*, stimulate IFN- γ expression. *Journal of Ethnopharmacology* 112: 232–236.

Chang SL, Yeh HH, Lin YS, Chiang YM, Wu TK, Yang WC (2007) The effect of centaurein on interferon- γ expression and *Listeria* infection in mice. *Toxicology and Applied Pharmacology* 219: 54–61.

Chang CLT, Liu HY, Kuo TF, Hsu YJ, Shen MY, Pan CY, Yang WC (2013) Anti-diabetic effect and mode of action of cytopiloyne. Evidence-Based Complementary and Alternative Medicine 2013: 1-13.

Charoenying P, Teerarak M, Laosinwattana C (2010) An allelopathic substance isolated from *Zanthoxylum limonella* Alston fruit. Scientia Horticulturae 125: 411-416.

Chen IS, Wu SJ, Tsai IL, Wu TS, Pezzuto JM, Lu MC, Chai H, Shu N, Teng CM (1994b) Chemical and bioactive constituents from *Zanthoxylum simulans*. Phytochemistry 57 (9): 1206-1211.

Chen JJ, Lin YH, Day SH, Hwang TL, Chen IS (2011) New benzenoids and anti-inflammatory constituents from *Zanthoxylum nitidum*. Food Chemistry 125: 282-287.

Chiang YM, Chuang DY, Wang SY, Kuo YH, Tsai PW, Shyur LF (2004) Metabolite profiling and chemopreventive bioactivity of plant extracts from *Bidens pilosa*. Journal of Ethnopharmacology 95: 409-419.

Chiang YM, Lo CP, Chen YP, Wang SY, Yang NS, Kuo YH, Shyur LF (2005) Ethyl caffeate suppresses NF- κ B activation and its downstream inflammatory mediators, iNOS, COX-2, and PGE2 *in vitro* or in mouse skin. British Journal of Pharmacology 146: 352-363.

Chiang YM, Chang CLT, Chang SL, Yang WC, Shyur LF (2007) Cytopiloyne, a novel polyacetylenic glucoside from *Bidens pilosa*, functions as a T helper cell modulator. Journal of Ethnopharmacology 110: 532-538.

Chien SC, Young PH, Hsu YJ, Chen CH, Tien YJ, Shiu SY, Li TH, Yang CW, Marimuthu P, Tsai LF, Yang WC (2009) Anti-diabetic properties of three common *Bidens pilosa* variants in Taiwan. Phytochemistry 70: 1246-1254.

Chou ST, Peng HY, Chang CT, Yang JS, Chung HK, Yang ST, Wood WG, Chung JG (2011) *Zanthoxylum ailanthoides* Sieb and Zucc. extract inhibits growth and induces cell death through G2/M-phase arrest and activation of apoptotic signals in colo 205 human colon adenocarcinoma cells. *Anticancer Research* 31(5): 1667-1676.

Clarkson AB, Bienen EJ, Bacchi CJ, McCann PP, Nathan HC, Hutner SH, Sjoerdsma A (1984) New drug combination for experimental late-stage African trypanosomiasis: DL-a-difluoromethylornithine (DFMO) with suramin. *American Journal of Tropical Medicine and Hygiene* 33: 1073–1077.

Chou ZT, Chan HH, Peng HY, Liou MJ, Wu TS (2011) Isolation of substances with antiproliferative and apoptosis-inducing activities against leukemia cells from the leaves of *Zanthoxylum ailanthoides* Sieb. & Zucc. *Phytomedicine* 18: 344-348.

Clayton C, Shapira M (2007) Post-transcriptional regulation of gene expression in trypanosomes and leishmanias. *Molecular and Biochemical Parasitology* 156: 93-101.

Cnops J, Magez S, De Trez C (2015) Escape mechanisms of African trypanosomes: why trypanosomosis is keeping us awake. *Parasitology* 142(3): 417-427.

Cordero CP, Gómez-González S, León-Acosta CJ, Morantes-Medina SJ, Aristizabal FA (2004) Cytotoxic activity of five compounds isolated from Colombian plants. *Fetoterapia* 75(2): 225-227.

Cordingley JS (1985) Nucleotide sequence of the 5S ribosomal RNA gene repeat of *Trypanosoma brucei*. *Molecular and Biochemical Parasitology* 17: 321-330.

Corrêa JR, Atella GC, Menna-Barreto RS, Soares MJ (2007) Clathrin in *Trypanosoma cruzi*: in silico gene identification, isolation and localization of protein expression sites. *Journal of Eukaryotic Microbiology* 54: 297-302.

Corrêa JR, Atella GC, Batista MM, Soares MJ (2008) Transferrin uptake in *Trypanosoma cruzi* is impaired by interference on cytosome-associated cytoskeleton elements and stability of membrane cholesterol, but not by obstruction of clathrin-dependent endocytosis. *Experimental Parasitology* 119: 58-66.

Courtin F, Sidibe I, Rouamba J, Jamonneau V, Gouro A, Solano P (2009) Impacts observes des evolutions demo-climatiques sur la repartition spatiale des hommes, des tse-tse et des trypanosomoses en Afrique de l'Ouest [Observed impacts of demo-climatic evolution on the spatial distribution of humans, tsetse and trypanosomiasis in West Africa]. *Parasite* 16: 3–10.

Courtin F, Rayaissé JB, Issa Tamboura I, Serdébéogo O, Koudougou Z, Solano P, Sidibé I (2010) Updating the northern tsetse limit in Burkina Faso (1949-2009): impact of global change. *International Journal of Environmental Research and Public Health* 7: 1708-1719.

Croteau R, Kutchan TM, Lewis NG (2000) Natural products (secondary metabolites). *Biochemistry and Molecular Biology of Plant* (24): 1250-1319.

D'Amours D, Amon A (2004) At the interface between signaling and executing anaphase: Cdc14 and the FEAR network. *Genes and Development* 18: 2581–2595.

Da Silva SL, Figueredo PMS, Yano T (2007a) Chemotherapeutic potential of the volatile oils from *Zanthoxylum rhoifolium* Lam leaves. *European Journal of Pharmacology* 576: 180-188.

Da Silva SL, Figueredo PM, Yano T (2007b) Cytotoxic evaluation of essential oil from *Zanthoxylum rhoifolium* Lam. leaves. *Acta Amazonica* 37 (2): 281-286.

Dalziel JM (1937) (reprinted 1955) The useful plants of West Tropical Africa. Crown Agents for Overseas Governments and Administration, London.

Dang HQ, Li Z (2011) The Cdc45/Mcm2-7/GINS protein complex in trypanosomes regulates DNA replication and interacts with two Orc1-like proteins in the origin recognition complex. *Journal of Biological Chemistry* 286: 32424–32435.

Daniels J, Gull K, Wickstead B (2010) Cell Biology of the Trypanosome Genome. *Microbiology and Molecular Biology Reviews* 74: 552-569.

Das A, Gale MJ, Carter V, Parsons M (1994) The protein phosphatase inhibitor okadaic acid induces defects in cytokinesis and organellar genome segregation in *Trypanosoma brucei*. *Journal of Cell Science* 107: 3477–3483.

Dawe HR, Farr H, Portman N, Shaw MK, Gull K (2005) The Parkin co-regulated gene product, PACRG, is an evolutionarily conserved axonemal protein that functions in outer-doublet microtubule morphogenesis. *Journal of Cell Science* 118: 5421–5430.

Dean S, Marchetti R, Kirk K, Matthews KR (2009) A surface transporter family conveys the trypanosome differentiation signal. *Nature* 459: 213-217.

Deba F, Xuan TD, Yasuda M, Tawata S (2007) Herbicidal and fungicidal activities and identification of potential phytotoxins from *Bidens pilosa* L. var. *radiata* Scherff. *Weed Biology and Management* 7: 77–83.

Deba F, Xuan TD, Yasuda M, Tawata S (2008) Chemical composition and antioxidant, antibacterial and antifungal activities of the essential oils from *Bidens pilosa* Linn. var. *radiata*. *Food Control* 19: 346–352.

Debatin KM, Krammer PH (2004) Death receptors in chemotherapy and cancer. *Oncogene* 23: 2950–2966.

Deborggraeve S, Koffi M, Jamonneau V (2008) Molecular analysis of archived blood slides reveals an atypical human *Trypanosoma* infection. *Diagnostic Microbiology and Infectious Disease* 61(4): 428–433.

De Graffenried CL, Ho HH, Warren G (2008) Polo-like kinase is required for Golgi and bilobe biogenesis in *Trypanosoma brucei*. *The Journal of Cell Biology* 181: 431–438.

De Koning, HP (2001) Uptake of pentamidine in *Trypanosoma brucei brucei* is mediated by three distinct transporters: Implications for cross-resistance with arsenicals. *Molecular Pharmacology* 59: 586–592.

De Melo LD, Sant'Anna C, Reis SA, Lourenço D, De Souza W, Lopes UG, Cunha-e-Silva NL (2008) Evolutionary conservation of actin-binding proteins in *Trypanosoma cruzi* and unusual subcellular localization of the actin homologue. *Parasitology* 135: 955-965.

De Silva Rodrigues JH, Stein J, Strauss M, Rivarola HW, Ueda-Nakamura T, Nakamura CV, Duszenko M (2016) Clomipramine kills *Trypanosoma brucei* by apoptosis. *International Journal of Medical Microbiology* 306(4): 196-205.

Dewick PM (2002) *Medicinal Natural Products: A Biosynthetic Approach*, 2nd edition, John Wiley and Sons, Chichester.

De Souza W, Meyer H (1974) On the fine structure of the nucleus in *Trypanosoma cruzi* in tissue culture forms. Spindle fibers in the dividing nucleus. *Journal of Protozoology* 21: 48-52.

Dimo T, Nguenefack TB, Kamtchouing P, Dongo E, Rakotonirina A, Rakotonirina SV (1999) Hypotensive effects of methanol extract from *Bidens pilosa* Linn on hypertensive rats. *Comptes Rendus de l'Academie des Sciences* 322: 323–329.

Docampo R (1990) Sensitivity of parasites to free radical damage by antiparasitic drugs. *Chemico-Biological Interactions* 73: 1–27.

Dung TD, Chang HC, Binh TV, Lee MR, Tsai CH, Tsai FJ, Kuo WW, Chen LM, Huang CY (2012) *Zanthoxylum avicennae* extracts inhibit cell proliferation through protein phosphatase 2A activation in HA22T human hepatocellular carcinoma cells *in vitro* and *in vivo*. *International Journal of Molecular Medicine* 29(6): 1045-1052.

Dutertre S, Cazales M, Quaranta M, Froment C, Trabut V, Dozier C, Mirey G, Bouché JP, Theis-Febvre N, Schmitt E, Monsarrat B, Prigent C, Ducommun B (2004) Phosphorylation of CDC25B by Aurora-A at the centrosome contributes to the G2-M transition. *Journal of Cell Science* 117: 2523–2531.

Elias MC, Marques-Porto R, Freymüller E, Schenkman S (2001) Transcription rate modulation through the *Trypanosoma cruzi* life cycle occurs in parallel with changes in nuclear organisation. *Molecular and Biochemical Parasitology* 112: 79-90.

Erdmann M, Scholz A, Melzer IM, Schmetz C, Wiese M (2006) Interacting protein kinases involved in the regulation of flagellar length. *Molecular Biology of the Cell* 17: 2035–2045.

Eulalio A, Huntzinger E, Izaurralde E (2008) GW182 interaction with Argonaute is essential for miRNA mediated translational repression and mRNA decay. *Nature Structural and Molecular Biology* 15(4): 346–353.

Fang J, Ruiz FA, Docampo M (2007) Overexpression of a Zn²⁺- sensitive soluble exopolyphosphate from *Trypanosoma cruzi* depletes polyphosphate and affects osmoregulation. *Journal of Biological Chemistry* 282: 32501-32510.

Fairlamb AH, Bowman IB (1980) Uptake of the trypanocidal drug suramin by bloodstream forms of *Trypanosoma brucei* and its effect on respiration and growth rate *in vivo*. *Molecular and Biochemical Parasitology* 1: 315–333.

Fairlamb AH, Cerami A (1992) Metabolism and functions of trypanothione in the Kinetoplastida. *Annual Review of Microbiology* 46: 695–729.

Fairlamb AH (2003) Chemotherapy of human African trypanosomiasis: current and future prospects. *Trends in Parasitology* 19: 488-494.

Ferreira ME, Rojas A, Torres S, Inchausti A, Nakayama H, Thouvenel C, Hocquemiller R, Fournet A (2002) Leishmanicidal activity of two canthin-6-one alkaloids, two major constituents of *Zanthoxylum chiloperone* var. *angustifolium*. *Journal of Ethnopharmacology* 80: 199-202.

Ferreira MH, Nakayama H, Rojas A, Schinini A, Vera N, Serna E, Lagoutte D, Soriano-Agatón F, Poupon E, Hocquemiller R, Fournet A (2007) Effects of canthin-6-one alkaloids from *Zanthoxylum chiloperone* on *Trypanosoma cruzi*-infected mice. *Journal of Ethnopharmacology* 109: 258-263.

Ferreira M E, Cebrián-Torrejón G, Corrales AS, Vera N, Rolón M, Vega C, Leblanc K, Yaluf G, Schinini A, Torres S, Serna E, Rojas A, Poupon E, Fournet A (2011) *Zanthoxylum chiloperone* leaves extract: First sustainable Chagas disease treatment. *Journal of Ethnopharmacology* 133: 986-993.

Festjens N, Vanden Berghe T, Vandenabeele P (2006) Necrosis, a well-orchestrated form of cell demise: signalling cascades, important mediators and concomitant immune response. *Biochimica et Biophysica Acta* 1757: 1371-1387.

Fisk JC, Zurita-Lopez C, Sayegh J, Tomasello DL, Clarke SG, Read LK (2010) TbPRMT6 is a type I protein arginine methyltransferase that contributes to cytokinesis in *Trypanosoma brucei*. *Eukaryotic Cell* 9: 866–877.

Ford J, Nash TAM, Welch JR (1970) Control by clearing of vegetation. In: Mulligan HW, ed. *The African trypanosomiasis*. London, George Allen and Unwin, 543–563.

Fuentes-Prior P, Salvesen GS (2004) The protein structures that shape caspase activity, specificity, activation and inhibition. *Biochemical Journal* 384: 201-232.

Fogang HPD, Tapondjou LA, Womeni HM, Quassinti L, Bramucci M, Vitali LA, Petrelli D, Lupidi G, Maggi F, Papa F, Vittori S, Barboni (2012) Characterization and biological activity of essential oils from fruits of *Zanthoxylum xanthoxyloides* Lam. and *Z. Leprieurii* Guill. & Perr, two culinary plants from Cameroon. *Flavour and Fragrance Journal* 27(2): 171–179.

Franco JR, Simarro PP, Diarra A, Ruiz-Postigo JA, Samo M, Jannin JG (2012) Monitoring the use of nifurtimox-eflornithine combination therapy (NECT) in the treatment of second stage

gambiense human African trypanosomiasis. *Research and Reports in Tropical Medicine* 3: 93–101.

Fries DS, Fairlamb AH (2003) Antiprotozoal agents. In *Burger's Medicinal Chemistry and Drug Discovery: Chemotherapeutic Agents*, 6th edn, (Abraham, D.J. ed.), John Wiley & Sons, City, State, pp 1033-1087.

Gadelha C, Wickstead B, McKean PG, Gull K (2006) Basal body and flagellum mutants reveal a rotational constraint of the central pair microtubules in the axonemes of trypanosomes. *Journal of Cell Science* 119: 2405–2413.

Gambus A, Jones RC, Sanchez-Diaz A, Kanemaki M, van Deursen F, Edmondson RD, Labib K (2006) GINS maintains association of Cdc45 with MCM in replisome progression complexes at eukaryotic DNA replication forks. *Nature Cell Biology* 8: 358–366.

Ganders FR, Berbee M, Persiyedi M (2000) ITS base sequence phylogeny in *Bidens* (Asteraceae): Evidence for the continental relatives of Hawaiian and Marquesan *Bidens*. *Systematic Botany* 25(1): 122-133.

Gansane A, Sanon S, Ouattara PL, Hutter S, Ollivier E, Azas N, Traore A, Traore AS, Guissou IP, Nebie I, Sirima BS (2010) Antiplasmodial activity and cytotoxicity of semi purified fractions from *Zanthoxylum zanthoxyloides* Lam. *Bark of Trunk. International Journal of Pharmacology* 6 (6): 921-925.

García-Salcedo JA, Perez-Morga D, Gijon P, Dilbeck V, Pays E, Nolan DP (2004) A differential role for actin during the life cycle of *Trypanosoma brucei*. *EMBO Journal* 23: 780-789.

- Gaur U, Showalter M, Hickerson S, Dalvi R, Turco SJ, Wilson ME, Beverley SM (2009) *Leishmania donovani* lacking the Golgi GDP-Man transporter LPG2 exhibit attenuated virulence in mammalian hosts. *Experimental Parasitology*: 122: 182-191.
- Ge C (1990) Cytologic study of *Bidens bipinnata* L, *Zhongguo Zhong Yao Za Zhi* 15(2): 72–125.
- Geissberger P, Sequin U (1991) Constituents of *Bidens pilosa* L.: do the components found so far explain the use of this plant in traditional medicine? *Acta Tropica* 48: 251–261.
- Gilbert IH (2014) Target-based drug discovery for human African trypanosomiasis: selection of molecular target and chemical matter. *Parasitology* 141: 28–36.
- Glotzer M (2005) The molecular requirements for cytokinesis. *Science* 307: 1735–1739.
- Glover L, Alford S, Baker N, Turner DJ, Sanchez-Flores A, Hutchinson S, Hertz-Fowler C, Berriman M, Horn D (2015) Genome-scale RNAi screens for high-throughput phenotyping in bloodstream-form African trypanosomes. *Nature Protocols* 10(1): 106-133.
- Gourguechon S, Savich JM, Wang CC (2007) The multiple roles of cyclin E1 in controlling cell cycle progression and cellular morphology of *Trypanosoma brucei*. *Journal of Molecular Biology* 368: 939–950.
- Gourguechon S, Wang CC (2009) CRK9 contributes to regulation of mitosis and cytokinesis in the procyclic form of *Trypanosoma brucei*. *BMC Cell Biology* 10: 68.
- Gray MW (1992) The endosymbiont hypothesis revisited. *International Review of Cytology* 141: 233-357.

Green CH, Cosens D (1983) Spectral responses of the tsetse fly *Glossina morsitans morsitans*. *Journal of Insect Physiology* 29: 795–800.

Green DR, Kroemer G (2004) The pathophysiology of mitochondrial cell death. *Science* 305: 626-629.

Gruneberg U, Nigg EA (2003) Regulation of cell division: stop the SIN! *Trends in Cell Biology* 13: 159–162.

Gull K (1999) The cytoskeleton of trypanosomatid parasites. *Annual Review of Microbiology* 53: 629-655.

Gull K (2003) Host-parasite interactions and trypanosome morphogenesis: a flagellar pocketful of goodies. *Current Opinion in Microbiology* 6: 365-370.

Haile S, Papadopoulou B (2007) Developmental regulation of gene expression in trypanosomatid parasitic protozoa. *Current Opinion in Microbiology* 10: 569-577.

Hall DR, Beevor PS, Cork A, Nesbitt BF (1984) 1-Octen-3-ol: a potent olfactory stimulant and attractant for tsetse isolated from cattle odours. *Insect Science and its Application* 5: 335–339.

Hall BS, Gabernet-Castello C, Voak A, Goulding D, Natesan SK, Field MC (2006) TbVps34, the trypanosome orthologue of Vps34, is required for Golgi complex segregation. *Journal of Biological Chemistry* 281: 27600–27612.

Hammarton TC, Clark J, Douglas F, Boshart M, Mottram JC (2003) Stage-specific differences in cell cycle control in *Trypanosoma brucei* revealed by RNA interference of a mitotic cyclin. *Journal of Biological Chemistry* 278: 22877–22886.

Hammarton TC, Engstler M, Mottram JC (2004) The *Trypanosoma brucei* cyclin, CYC2, is required for cell cycle progression through G1 phase and maintenance of procyclic form cell morphology. *Journal of Biological Chemistry* 279: 24757–24764.

Hammarton TC, Lillico SG, Welburn SC, Mottram JC (2005) *Trypanosoma brucei* MOB1 is required for accurate and efficient cytokinesis but not for exit from mitosis. *Molecular Microbiology* 56: 104–116.

Hammarton TC (2007) Cell cycle regulation in *Trypanosoma brucei*. *Molecular and Biochemical Parasitology* 153: 1–8.

Hammarton TC, Kramer S, Tetley L, Boshart M, Mottram JC (2007) *Trypanosoma brucei* Polo-like kinase is essential for basal body duplication, kDNA segregation and cytokinesis. *Molecular Microbiology* 65: 1229–1248.

Hargrove JW, Vale GA (1979) Aspects of the feasibility of employing odourbaited traps for controlling tsetse flies (Diptera; Glossinidae). *Bulletin of Entomological Research* 69: 283–290.

Harper JV, Brooks G (2005) The mammalian cell cycle: an overview. *Methods in Molecular Biology* 296: 113–153.

Hassan AK, Deogratus O, Nyafuono JF, Francis O, Engeu OP (2011) Wound healing potential of the ethanolic extracts of *Bidens pilosa* and *Ocimum suave*. *African Journal of Pharmacy and Pharmacology* 5: 132–136.

Hassanali A, McDowell PG, Owaga MLA, Saini RK (1986) Identification of tsetse attractants from excretory products of a wild host animal, *Syncerus caffer*. *Insect Science and its Application* 7(1): 5–9.

He CY, Pypaert M, Warren G (2005) Golgi duplication in *Trypanosoma brucei* requires Centrin2. *Science* 310: 1196–1198.

Helms MJ, Ambit A, Appleton P, Tetley L, Coombs GH, Mottram JC (2006) Bloodstream form *Trypanosoma brucei* depend upon multiple metacaspases associated with RAB11-positive endosomes. *Journal of Cell Science* 119: 1105–1117.

Hendrichs J, Vreysen MJB, Enkerlin WR, Cayol JP (2005) Strategic options in using sterile insects for area-wide integrated pest management. In: Dyck VA, Hendrichs J, Robinson AS (eds). *Sterile insect technique. Principles and practice in area-wide integrated pest management*. Dordrecht, Springer, pp563–600.

Hirumi H, Hirumi K (1989) Continuous cultivation of *Trypanosoma brucei* bloodstream forms in a medium containing a low concentration of serum protein without feeder cell layers. *Journal of Parasitology* 75: 985-989.

Hirumi H, Hirumi K (1994) Axenic culture of african trypanosome bloodstream forms. *Parasitology Today* 10: 80-84.

Hisatomi E, Matsui M, Kobayashi A, Kubota K (2000) Antioxidative activity in the pericarp and seed of Japanese pepper (*Xanthoxylum piperitum* DC). *Journal of Agricultural and Food Chemistry* 48: 4924-4928.

Hoet S, Opperdoes F, Brun R, Adjakidjé V, Quetin-Leclercq J (2004) *In vitro* antitrypanosomal activity of ethnopharmacologically selected Beninese plants. *Journal of Ethnopharmacology* 91: 37–42.

Horiuchi M, Seyama Y (2008) Improvement of the anti-inflammatory and antiallergic activity of *Bidens pilosa* L. var. radiata SCHERFF treated with enzyme (Cellulosine). *Journal of Health Science* 54: 294–301.

Horn D, McCulloch R (2010) Molecular mechanisms underlying the control of antigenic variation in African trypanosomes. *Current Opinion in Microbiology* 13(6): 700–705.

Hsu YJ, Lee TH, Chang CLT, Huang YT, Yang WC (2009) Anti-hyperglycemic effects and mechanism of *Bidens pilosa* water extract. *Journal of Ethnopharmacology* 122: 379–383.

Hu L, Hu H, Li Z (2012) A kinetoplastid-specific kinesin is required for cytokinesis and for maintenance of cell morphology in *Trypanosoma brucei*. *Molecular Microbiology* 83: 565–578.

Humphrey T, Pearce A (2005) Cell cycle molecules and mechanisms of the budding and fission yeasts. *Methods in Molecular Biology* 296: 3–29.

Hsu YJ, Lee TH, Chang CLT, Huang YT, Yang WC (2009) Anti-hyperglycemic effects and mechanism of *Bidens pilosa* water extract. *Journal of Ethnopharmacology* 122: 379–383.

Ibrahim HM, Ogbadoyi EO, Adamu KY, Bello MU, Yemisi IJ (2012) Evaluation of antitrypanosomal activity of ethyl acetate extract of *Adansonia digitata* seed extraction in *T. b. brucei* infected albino mice. *International Journal of Drug Research and Technology* 2(7): 454-460.

Ilc T, Parage C, Boachon B, Navrot N, Werck-Reichhart D (2016) Monoterpenol Oxidative Metabolism: Role in Plant Adaptation and Potential Applications. *Frontiers in Plant Science* 7: e509

Ilgoutz SC, McConville MJ (2001) Function and assembly of the *Leishmania* surface coat. *Internal Journal for Parasitology* 31: 899-908.

Ilves I, Petojevic T, Pesavento JJ, Botchan MR (2010) Activation of the MCM2-7 helicase by association with Cdc45 and GINS proteins. *Molecular Cell* 37: 247–258.

Jiang X, Wang X (2004) Cytochrome C-mediated apoptosis. *Annual Review of Biochemistry* 73: 87-106.

Jordan AM (1986) Trypanosomiasis control and African rural development. London, Longman.

Jullian V, Bourdy G, Georges S, Maurel S, Sauvain M (2006) Validation of use of a traditional remedy from French Guiana, *Zanthoxylum rhoifolium* Lam. *Journal of Ethnopharmacology* 106: 348-352.

Kaczanowski S, Sajid M, Reece SE (2011) Evolution of apoptosis-like programmed cell death in unicellular protozoan parasites. *Parasites and Vectors* 4: 44.

Kandaswami C, Middleton E (1994) Free radical scavenging and antioxidant activity of plant flavonoids. *Advances in Experimental Medicine and Biology* 366: 351–376.

Karis PO, Ryding O (1994) Asteraceae Cladistics and Classification, Bremer K. (Eds), Timber press, Portland, Ore, USA, pp 559–569.

Kassim OO, Loyevsky M, Elliott B, Geall A, Amonoo H, Gordeuk VR (2005) Effects of Root Extracts of *Fagara zanthoxyloides* on the *in vitro* growth and stage distribution of *Plasmodium falciparum*. *Antimicrobial Agents and Chemotherapy* 49(1): 264–268.

Kaufmann D, Gassen A, Maiser A, Leonhardt H, Janzen CJ (2012) Regulation and spatial organization of PCNA in *Trypanosoma brucei*. *Biochemical and Biophysical Research Communications* 419: 698–702.

Kaur K, Jain M, Kaur T, Jain R (2009) Antimalarials from nature. *Bioorganic and Medicinal Chemistry* 17: 3229-3256.

Kędzierski L, Montgomery J, Curtis J, Handman E (2004) Leucine-rich repeats in host-pathogen interactions. *Archivum Immunologiae et Therapiae Experimentalis* 52: 104–112.

Keiser J, Ericsson O, Burri C (2000) Investigations of the metabolites of the trypanocidal drug melarsoprol. *Clinical Pharmacology and Therapeutics* 67: 478–488.

Kgori P, Modo S, Torr SJ (2006) The use of aerial spraying to eliminate tsetse from the Okavango delta of Botswana. *Acta Tropica* 99: 184–199.

Kgori PM, Orsmond G, Phillemon-Motsu TK (2009) Integrating GIS and GPS-assisted navigation systems to enhance the execution of a SAT-based tsetse elimination project in the Okavango delta (Botswana). In: Cecchi G, Mattioli RC (eds). *Geospatial datasets and analyses for an environmental approach to African trypanosomiasis*. Rome, Food and Agriculture Organization of the United Nations, (Technical and Scientific Series, No. 9) pp 61–67.

Kieft R, Capewell P, Turner CMR, Veitch JN, Annette MacLeod A, Hajduk S (2010) Mechanism of *Trypanosoma brucei gambiense* (group 1) resistance to human trypanosome lytic factor. *Proceedings of the National Academy of Sciences of the United States of America* 107: 16137–16141.

Kohl L, Robinson D, Bastin P (2003) Novel roles for the flagellum in cell morphogenesis and cytokinesis of trypanosomes. *EMBO Journal* 22: 5336–5346.

Kim JS, Lee HJ, Lee MH, Kim JC, Jin C, Ryu JH (2006) Luteolin inhibits LPS-stimulated inducible nitric oxide synthase expression in BV-2 microglial cells. *Planta Medica* 72: 65–68.

Kim YK, Kim VN (2007) Processing of intronic microRNAs. *EMBO Journal* 26(3): 775–783.

Klingbeil MM, Shapiro TA (2009) Unraveling the secrets of regulating mitochondrial DNA replication. *Molecular Cell* 35: 398–400.

Knipling EF (1955) Possibilities of insect control or eradication through the use of sexually sterile males. *Journal of Economic Entomology* 48(4): 459–466.

Kosec G, Alvarez VE, Agüero F, Sánchez D, Dolinar M, Turk B, Turk V, Cazzulo JJ (2006) Metacaspases of *Trypanosoma cruzi*: possible candidates for programmed cell death mediators. *Molecular and Biochemical Parasitology* 145: 18–28

Kuetea V, Krusche B, Youns M, Voukeng I, Fankama AG (2011) Cytotoxicity of some Cameroonian spices and selected medicinal plant extracts. *Journal of Ethnopharmacology* 134: 803-812.

Kumar P, Wang CC (2006) Dissociation of cytokinesis initiation from mitotic control in a eukaryote. *Eukaryotic Cell* 5: 92–102.

Kumari P, Misra K, Sisodia BS, Faridi U, Srivastava S, Luqman S, Darokar MP, Negi AS, Gupta MM, Singh SC, Kumar JK (2009) A promising anticancer and antimalarial component from the leaves of *Bidens pilosa*. *Planta Medica* 75(1): 59-61.

Kupchan MS, Britton RW, Zeigler MF, Sigel CW (1973) Bruceantin, a new potent antileukemic simaroubolide from *Brucea antidysenterica*. *Journal of Organic Chemistry* 38(1): 178-179.

Kviecinski MR, Felipe KB, Schoenfelder T, de Lemos Wiese LP, Rossi MH, Gonzalez E, Felicio JD, Filho DW, Pedrosa RC (2008) Study of the antitumor potential of *Bidens pilosa* (Asteraceae) used in Brazilian folkmedicine. *Journal of Ethnopharmacology* 117: 69–75.

Kwofie KD, Tung NH, Suzuki-Ohashi M, Amoa-Bosompem M, Adegle R, Sakyiamah MM, Ayertey F, Owusu KB, Tuffour I, Atchoglo P, Frempong KK, Anyan WK, Uto T, Morinaga O, Yamashita T, Aboagye F, Appiah AA, Appiah-Opong R, Nyarko AK, Yamaguchi Y, Edoh D, Koram KA, Yamaoka S, Boakye DA, Ohta N, Shoyama Y, Ayi I (2016) Antitrypanosomal Activities and Mechanisms of Action of Novel Tetracyclic Iridoids from *Morinda lucida Benth.* *Antimicrobial Agents and Chemotherapy* 60(6): 3283-3290.

La Greca F, Magez S (2011) Vaccination against trypanosomiasis. Can it be done or is the trypanosome truly the ultimate immune destroyer and escape artist? *Human Vaccines* 7(11): 1225-1233.

Labib K (2010) How do Cdc7 and cyclin-dependent kinases trigger the initiation of chromosome replication in eukaryotic cells? *Genes and Development* 24: 1208–1219.

Lai PK, Roy J (2004) Antimicrobial and chemopreventive properties of herbs and spices. *Current Medicinal Chemistry* 11 (11): 1451–1460.

Laizure (SC), Herring V, Hu Z, Witbrodt K, Parker RB (2013) The role of human carboxylesterases in drug metabolism: have we overlooked their importance? *Pharmacotherapy* 33(2): 210–222.

Lança AS, de Sousa KP, Atouguia J, Prazeres DM, Monteiro GA, Silva MS (2011) *Trypanosoma brucei*: immunization with plasmid DNA encoding invariant surface glycoprotein gene is able to induce partial protection in experimental African trypanosomiasis. *Experimental Parasitology* 127: 18-24.

Landfear SM, Ignatushchenko M (2001) The flagellum and flagellar pocket of trypanosomatids. *Molecular and Biochemical Parasitology* 115: 1-17.

Landfear SM, Ullman B, Carter NS, Sanchez MA (2004) Nucleoside and nucleobase transporters in parasitic protozoa. *Eukaryotic Cell* 3: 245-254.

Landfear SM (2008) Drugs and transporters in kinetoplastid protozoa. *Advances in Experimental Medicine and Biology* 625: 22-32.

Landfear SM (2010) Transporters for drug delivery and as drug targets in parasitic protozoa. *Clinical Pharmacology and Therapeutics* 87: 122-125.

Langousis G, Kent LH (2014) Motility and more: the flagellum of *Trypanosoma brucei*. *Nature Reviews Microbiology* 12: 505-518.

Lans C (2007) Comparison of plants used for skin and stomach problems in Trinidad and Tobago with Asian ethnomedicine. *Journal of Ethnobiology and Ethnomedicine* 3:3.

Lee WJ, Wu LF, Chen WK, Wang CJ, Tseng TH (2006) Inhibitory effect of luteolin on hepatocyte growth factor/scatter factor-induced HepG2 cell invasion involving both MAPK/ERKs and PI3K-Akt pathways. *Chemico-Biological Interactions* 160: 123–133.

Lee SJ, Lim KT (2008) Glycoprotein of *Zanthoxylum piperitum* DC has a hepatoprotective effect via anti-oxidative character *in vivo* and *in vitro*. *Toxicology in Vitro* 22: 376-385.

Liang X, Haritan A, Uliel S, Michaeli S (2003) Trans and cis splicing in trypanosomatids: mechanism, factors, and regulation. *Eukaryotic Cell* 2: 830-840.

Liu B, Liu Y, Motyka SA, Agbo EE, Englund PT (2005) Fellowship of the rings: the replication of kinetoplast DNA. *Trends in Parasitology* 21: 363-369.

Liu Y, Englund PT (2007) The rotational dynamics of kinetoplast DNA replication. *Molecular Microbiology* 64: 676-690.

Levine B, Yuan J (2005) Autophagy in cell death: an innocent convict? *Journal of Clinical Investigation* 115: 2679–2688.

Levine B, Kroemer G (2008) Autophagy in the pathogenesis of disease. *Cell* 132: 27-42.

Li SQ, Fung MC, Reid SA, Inoue N, Lun ZR (2007) Immunization with recombinant beta-tubulin from *Trypanosoma evansi* induced protection against *T. evansi*, *T. equiperdum* and *T. b. brucei* infection in mice. *Parasite Immunology* 29: 191-199.

Li SQ, Yang WB, Ma LJ, Xi SM, Chen QL, Song XW (2009) Immunization with recombinant actin from *Trypanosoma evansi* induces protective immunity against *T. evansi*, *T. equiperdum* and *T. b. brucei* infection. *Parasitology Research* 104: 429-435.

Li K, Zhou R, Jia WW, Li Z, Li J, Zhang P, Xiao T (2016) *Zanthoxylum bungeanum* essential oil induces apoptosis of HaCaT human keratinocytes. *Journal of Ethnopharmacology* 186: 351-361.

Li Z, Wang CC (2003) A PHO80-like cyclin and a B-type cyclin control the cell cycle of the procyclic form of *Trypanosoma brucei*. *Journal of Biological Chemistry* 278: 20652-20658.

Li Z, Wang CC (2006) Changing roles of aurora-B kinase in two life cycle stages of *Trypanosoma brucei*. *Eukaryotic Cell* 5: 1026–1035.

Li Z, Wang CC (2008) KMP-11, a basal body and flagellar protein, is required for cell division in *Trypanosoma brucei*. *Eukaryotic Cell* 7: 1941–1950.

Li Z, Gourguechon S, Wang CC (2007) Tousled-like kinase in a microbial eukaryote regulates spindle assembly and S-phase progression by interacting with Aurora kinase and chromatin assembly factors. *Journal of Cell Science* 120: 3883–3894.

Li Z, Lindsay ME, Motyka SA, Englund PT, Wang CC (2008) Identification of a bacterial-like HslVU protease in the mitochondria of *Trypanosoma brucei* and its role in mitochondrial DNA replication. *PLOS Pathogens* 4: e1000048.

Liang XH, Haritan A, Uliel S, Michaeli S (2003) Trans and cis splicing in trypanosomatids: mechanism, factors, and regulation. *Eukaryotic Cell* 2: 830-840.

Liu Y, Tidwell RR, Leibowitz MJ (1994) Inhibition of *in vitro* splicing of a group I intron of *Pneumocystis carinii*. *Journal of Eukaryotic Microbiology* 41: 31–38.

Liu Y, Englund PT (2007) The rotational dynamics of kinetoplast DNA replication. *Molecular Microbiology* 64: 676-690.

Liu B, Wang J, Yaffe N, Lindsay M, Zhao Z, Zick A, Shlomai J, Englund PT (2009) Trypanosomes have six mitochondrial DNA helicases with one controlling kinetoplast maxicircle replication. *Molecular Cell* 35: 490–501.

Lopes AH, Padrón TS, Dias FA, Gomes MT, Rodrigues GC, Zimmermann LT, Silva TLA, Vermelho AB (2010) Trypanosomatids: Odd Organisms, Devastating Diseases. *The Open Parasitology Journal* 4: 30-59.

Los M, Wesselborg S, Schulze-Osthoff K (1999) The role of caspases in development, immunity, and apoptotic signal transduction: lessons from knockout mice. *Immunity* 10: 629-639.

Lu M, Zhang Q, Deng M, Miao J, Guo Y (2008) An analysis of human microRNA and disease associations. *PLoS ONE* 3(10): e3420.

Lubega GW, Byarugaba DK, Prichard RK (2002) Immunization with a tubulin-rich preparation from *Trypanosoma brucei* confers broad protection against African trypanosomiasis. *Experimental Parasitology* 102: 9-22.

Lund E, Dahlberg JE (2006) Substrate selectivity of exportin 5 and Dicer in the biogenesis of microRNAs. *Cold Spring Harbor Symposia on Quantitative Biology* 71: 59–66.

Ma J, Benz C, Grimaldi R, Stockdale C, Wyatt P, Frearson J, Hammarton TC (2010) Nuclear DBF-2-related kinases are essential regulators of cytokinesis in bloodstream stage *Trypanosoma brucei*. *Journal of Biological Chemistry* 285: 15356–15368.

MacRae IJ, Ma E, Zhou M, Robinson CV, Doudna JA (2008) *In vitro* reconstitution of the human RISC-loading complex. *Proceedings of the National Academy of Science of the United States of America* 105(2): 512–517.

Mahama CI, Mohammed HA, Abavana M, Sidibe I, Kone A, Geerts S (2003) Tsetse and trypanosomes in Ghana in the twentieth century: a review. *Revue d'élevage et de médecine vétérinaire des pays tropicaux* 56: 27-32.

Mahama CI, Desquesnes M, Dia ML, Losson B, De Deken R, Geerts S (2004) A cross-sectional epidemiological survey of bovine trypanosomosis and its vectors in the Savelugu and West Mamprusi districts of Northern Ghana. *Veterinary Parasitology* 122: 1-13.

Maiuri MC, Zalckvar E, Kimchi A, Kroemer G (2007) Self-eating and self-killing: crosstalk between autophagy and apoptosis. *Nature Reviews Molecular Cell Biology* 8: 741-752.

Mann A, Ifarajimi OR, Adewoye AT, Ukam C, Udeme EE, Okorie II, Sakpe MS, Ibrahim DR, Yahaya YA, Kabir AY, Ogbadoyi EO (2011) *In vivo* antitrypanosomal effects of some ethnomedicinal plants from Nupeland of north central Nigeria. *African Journal of Traditional, Complementary and Alternative Medicines* 8(1): 15-21.

Mann A, Ogbadoyi EO (2012) Evaluation of medicinal plants from Nupeland for their *in vivo* antitrypanosomal activity. *American Journal of Biochemistry* 2(1): 1-6.

Márquez L, Agüero J, Hernández I, Garrido G, Martínez I, Diéguez R, Prieto S, Rivas Y, Molina-Torres J, Curini M, Delgado R (2005) Anti-inflammatory evaluation and phytochemical characterization of some plants of the *Zanthoxylum* genus. *Acta Farmaceutica Bonaerense* 24 (3): 325-330.

Martinez-Calvillo S, Vizuet-de-Rueda JC, Florencio-Martinez (2010) Gene expression in trypanosomatid parasites. *Journal of Biomedicine and Biotechnology* 2010 (525241): pp 15.

Masai H, Taniyama C, Ogino K, Matsui E, Kakusho N, Matsumoto S, Kim JM, Ishii A, Tanaka T, Kobayashi T, Tamai K, Ohtani K, Arai K (2006) Phosphorylation of MCM4 by Cdc7 kinase facilitates its interaction with Cdc45 on the chromatin. *Journal of Biological Chemistry* 281: 39249–39261.

- Matovu E, Geiser F, Schneider V, Maser P, Enyaru JC, Kaminsky R, Gallati S, Seebeck T (2001) Genetic variants of the TbAT1 adenosine transporter from African trypanosomes in relapse infections following melarsoprol therapy. *Molecular and Biochemical Parasitology* 117: 73–81.
- May SF, Peacock L, Almeida Costa CI, Gibson WC, Tetley L, Robinson DR, Hammarton TC (2012) The *Trypanosoma brucei* AIR9-like protein is cytoskeleton-associated and is required for nucleus positioning and accurate cleavage furrow placement. *Molecular Microbiology* 84: 77–92.
- Mbaze LM, Poumale HMP, Wansi JD, Lado JA, Khan SN, IqbalMC, Ngadjui BT, Laatsch H (2007) α -glucosidase inhibitory pentacyclic triterpenes from the stem bark of *Fagara tessmannii* (Rutaceae). *Phytochemistry* 68: 591-595.
- McKean PG (2003) Coordination of cell cycle and cytokinesis in *Trypanosoma brucei*. *Current Opinion in Microbiology* 6: 600–607.
- Medhi K, Deka M, Bhau BS (2013) The Genus *Zanthoxylum*-A Stockpile of Biological and Ethnomedicinal Properties. *Scientific Reports* 2 (3): 697.
- Melaku A, Birasa B (2013) Drugs and Drug Resistance in African Animal Trypanosomosis: A Review. *European Journal of Applied Sciences* 5 (3): 84-91.
- Melino G, Knight RA, Nicotera P (2005) How many ways to die? How many different models of cell death? *Cell Death and Differentiation* 12: 1457-1462.
- Michels PA, Hannaert V, Bringaud F (2000) Metabolic aspects of glycosomes in *Trypanosomatidae* - new data and views. *Parasitology Today* 16: 482-489.

Misra LN, Wouatsa NA, Kumar S, Venkatesh KR, Tchoumboungang F (2013) Antibacterial, cytotoxic activities and chemical composition of fruits of two Cameroonian *Zanthoxylum* species. *Journal of Ethnopharmacology* 148(1): 74-80.

Mkunza F, Olaho WM, Powell CN (1995) Partial protection against natural trypanosomiasis after vaccination with a flagellar pocket antigen from *Trypanosoma brucei rhodesiense*. *Vaccine* 13: 151-154.

Mony BM, Matthews KR (2015) Assembling the components of the quorum sensing pathway in African trypanosomes. *Molecular Microbiology* 96(2): 220–232.

Moreno B, Urbina JA, Oldifield E, Bailey BN, Rodrigues CO, Docampo R (2000) ³¹P NMR spectroscopy of *Trypanosoma brucei*, *Trypanosoma cruzi* and *Leishmania major*. Evidence for high levels of condensed inorganic phosphates. *Journal of Biological Chemistry* 275: 28356-28362.

Morrison LJ, Vezza L, Rowan T, Hope JC (2016). Animal African Trypanosomiasis: Time to Increase Focus on Clinically Relevant Parasite and Host Species. *Trends in Parasitology* 32(8): 599-607.

Motta MC (1999) Endosymbiosis in protozoa of the *Trypanosomatidae* family. *FEMS Microbiology Letters* 173: 1-8.

Moyer SE, Lewis PW, Botchan MR (2006) Isolation of the Cdc45/ Mcm2-7/GINS (CMG) complex, a candidate for the eukaryotic DNA replication fork helicase. *Proceedings of the National Academy of Sciences of the United States of America* 103: 10236–10241.

Moyersoer J, Choe J, Fan E, Hol WG, Michels PA (2004) Biogenesis of peroxisomes and glycosomes: trypanosomatid glycosome assembly is a promising new drug target. *FEMS Microbiology Review* 28: 603-643.

Mshana NR, Abbiw, DK, Addae-Mensah I, Adjanouhoun E, Ahyi MRA, Ekpere JA, Enow-Orock EG, Gbile ZO, Noamesi, GK, Osei MA, Odunlami H, Oteng-Yeboah AA, Sarpong K, Sofowora A, Tackie AN (2000) Traditional medicine and pharmacopeia contributing to the revision of ethnobotanical floristic studies in Ghana. Organisation of African unity/scientific, technical and research commission: p 537.

Muchuweti M, Mupure C, Ndhlala A, Murenje T, Benhura MAN (2007) Screening of antioxidant and radical scavenging activity of *Vigna unguiculata*, *Bidens pilosa* and *Cleome gynandra*. *American Journal of Food Technology* 2: 161–168.

Mueller AK, Hammerschmidt-Kamper C, Kaiser A (2014) RNAi in Plasmodium. *Current Pharmaceutical Design* 20 (2): 278-283.

Murray AW (2004) Recycling the cell cycle: cyclins revisited. *Cell* 116: 221–234.

Mwaniki LM, Mose JM, Mutwiri T, Mbithi JM (2017) Evaluation of trypanocidal activity of *Bidens pilosa* and *Physalis peruviana* against *Trypanosoma brucei rhodesiense*. *American Journal of Laboratory Medicine* 2: 69-73.

Nacoulma O (1996) Plantes médicinales et pratiques médicales traditionnelles au Burkina Faso Cas du plateau central. TOME II. Thèse d'Etat. Univ Ouaga.

Nakayasu ES, Yashunsky DV, Nohara LL (2009) GPIomics: global analysis of glycosylphosphatidylinositol-anchored molecules of *Trypanosoma cruzi*. *Molecular Systems Biology* 5: 261-279.

Nakayima J, Nakao R, Alhassan A, Mahama C, Afakye K, Sugimoto C (2012) Molecular epidemiological studies on animal trypanosomiasis in Ghana. *Parasites and vectors* 5: 1-7.

Namukobe J, Kasenene JM, Kiremire BT, Byamukama R, Kamatenesi-Mugisha M, Krief S, Dumontet V, Kabasa JD (2011) Traditional plants used for medicinal purposes by local communities around the Northern sector of Kibale National Park, Uganda. *Journal of Ethnopharmacology* 136: 236–245.

Newstead R (1911) A revision of the tsetse flies (*Glossina*) based on a study of the male genital armature. *Bulletin of Entomological Research* 2: 9–36.

Ngane AN, Biyiti L, Zollo PH, Bouchet P (2000) Evaluation of antifungal activity of extracts of two Cameroonian Rutaceae, *Zanthoxylum leprieurii* Guill. et Perr. and *Zanthoxylum xanthoxyloides* Waterm. *Journal of Ethnopharmacology* 70: 335–342.

Ngassoum, MB, Essia-ngang JJ, Tatsadjieu, LN (2003) Antimicrobial study of essential oils of *Ocimum gratissimum* leaves and *Zanthoxylum xanthoxyloides* fruits from Cameroon. *Fitoterapia* 74(03): 284–287.

Ngo H, Tschudi C, Gull K, Ullu E (1998) Double stranded RNA induces mRNA degradation in *Trypanosoma brucei*. *Proceedings of the National Academy of Sciences of the United States of America* 95: 14687–14692.

Ngoumfo RM, Jouda JB, Mouafo FT, Komguem J, Mbazoa CD (2010) *In vitro* cytotoxic activity of isolated acridones alkaloids from *Zanthoxylum leprieurii* Guill. et Perr. Bioorganic and Medicinal Chemistry 18: 3601-3605.

Nguelefack TB, Dimo T, Nguelefack Mbuyo EP, Tan PV, Rakotonirina SV, Kamanyi A (2005) Relaxant effects of the neutral extract of the leaves of *Bidens pilosa* Linn on isolated rat vascular smooth muscle. Phytotherapy Research 19: 207–210.

Nguyen VQ, Co C, Irie K, Li JJ (2000) Clb/Cdc28 kinases promote nuclear export of the replication initiator proteins Mcm2-7. Current Biology 10: 195–205.

Norhayati I, Getha K, Haffiz JM, Ilham AM, Sahira HL, Syarifah MMS, Syamil AM (2013) *In vitro* antitrypanosomal activity of Malaysian plants. Journal of Tropical Forest Science 25(1): 52–59.

Noumi E, Houngue F, Lontsi D (1999) Traditional medicines in primary health care: plants used for the treatment of hypertension in Bafia, Cameroon. Fitoterapia 70: 134–139.

Ogoti P, Magiri E, Auma J, Magoma G, Imbuga M, Murilla G (2009) Evaluation of *in vivo* antitrypanosomal activity of selected medicinal plant extracts. Journal of Medicinal Plants Research 3(11): 849-854.

Olatunji OA (1983) The Biology of *Zanthoxylum Linn* (Rutaceae) in Nigeria. “Anti-infective agents of Higher Plants origin”. In: Essien, Adebajo, Adewunmi, Odebiyi (Eds.), Proceedings of the Fifth International Symposium on Medicinal Plants: pp 56-59.

Oli MW, Cotlin LF, Shiflett AM, Hajduk SL (2006) Serum resistance-associated protein blocks lysosomal targeting of trypanosome lytic factor in *Trypanosoma brucei*. *Eukaryotic Cell* 5: 132–139.

Oliver-Bever B (1982) Medicinal plants in tropical West Africa I, plants acting on cardiovascular system. *Journal of Ethnopharmacology* 5: 1-17.

Omar M, Khan F (2007) Trypanothione reductase: A viable chemotherapeutic target for antitrypanosomal and antileishmanial drug design. *Drug Target Insights* 2: 129–146.

Opperdoes FR, Szikora JP (2006) In silico prediction of the glycosomal enzymes of *Leishmania major* and trypanosomes. *Molecular and Biochemical Parasitology* 147: 193-206.

Orrenius S, Zhivotovsky B, Nicotera P (2003) Regulation of cell death: the calcium-apoptosis link. *Nature Reviews Molecular Cell Biology* 4: 552–565.

Ouattara B, Angenot L, Guissou P, Fondou P, Dubois J, Frédérick M, Jansen O, Van Heugen JC, Wauters JN, Tits M (2004) LC/MS/NMR analysis of isomeric divanilloylquinic acids from the root bark of *Fagara zanthoxyloides* Lam. *Phytochemistry* 65 (8): 1145–1151.

Panthi MP, Chaudhary RP (2006) Antibacterial Activity of Some Selected Folklore Medicinal Plants from West Nepal. *Scientific World* 4(4): 16-21.

Parsons M (2004) Glycosomes: parasites and the divergence of peroxisomal purpose. *Molecular Microbiology* 53: 717-724.

Patino LOJ, Prieto RJA, Cuca SLE (2012) *Zanthoxylum* Genus as potential source of bioactive compounds. *Bioactive Compounds in Phytomedicine* 26037: 185-218. doi 10.5772/26037.

Pereira RLC, Ibrahim T, Lucchetti L, Da Silva AJR, De Moraes VLG (1999) Immunosuppressive and anti-inflammatory effects of methanolic extract and the polyacetylene isolated from *Bidens pilosa* L. *Immunopharmacology* 43: 31–37.

Pereira SS, Lopes LS, Marques RB, Figueiredo KA, Costa DA, Chaves MH, Almeida FRC (2010) Antinociceptive effect of *Zanthoxylum rhoifolium* Lam (Rutaceae) in models acute pain in rodents. *Journal of Ethnopharmacology* 129: 227-231.

Peter ME, Budd RC, Desbarats J, Hedrick SM, Hueber AO, Newell MK, Owen LB, Pope RM, Tschopp J, Wajant H, Wallach D, Wiltout RH, Zornig M, Lynch DH (2007) The CD95 receptor: apoptosis revisited. *Cell* 129: 447-450.

Poinar G Jr, Poinar R (2004) Evidence of vector-borne disease of early cretaceous reptiles. *Vector Borne Zoonotic Diseases* 4: 281-284.

Poinar G Jr, Poinar R (2005) Fossil evidence of insect pathogens. *Journal of Invertebrate Pathology* 89: 243-250.

Portman N, Gull K (2010) The paraflagellar rod of kinetoplastid parasites: from structure to components and function. *International Journal for Parasitology* 40: 135-148.

Potts WH, Jackson CHN (1952) The Shinyanga game destruction experiment. *Bulletin of Entomological Research* 53: 365–374.

Poulin R, Lu L, Ackermann B, Bey P, Pegg AE (1992) Mechanism of the Irreversible inactivation of mouse ornithine decarboxylase by α -Difluoromethylornithine, characterization of sequences at the inhibitor and coenzyme binding sites. *Journal of Biological Chemistry* 267 (1): 150–158.

Pozharitskaya ON, Shikov AN, Makarova MN, Kosman VM, Faustova NM, Tesakova SV, Makarov VG, Galambosi B (2010) Anti-inflammatory activity of a HPLC-fingerprinted aqueous infusion of aerial part of *Bidens tripartita* L. *Phytomedicine* 17: 463–468.

Pozarowski P, Darzynkiewicz Z (2004) Analysis of cell cycle by flow cytometry. *Methods in Molecular Biology* 281: 301-311.

Pradel LC, Bonhivers M, Landrein N, Robinson DR (2006) NIMA-related kinase TbNRKC is involved in basal body separation in *Trypanosoma brucei*. *Journal of Cell Science* 119: 1852–1863.

Prempeh ABA, Mensah-Attipoe J (2008) Analgesic activity of crude aqueous extract of the root bark of *Zanthoxylum xanthoxyloides*. *Ghana Medical Journal* 42(2): 79-84.

Prempeh ABA, Mensah-Attipoe J (2009) Inhibition of vascular response in inflammation by crude aqueous extract of the root bark of *Zanthoxylum xanthoxyloides*. *Ghana Medical Journal* 43(2): 77–81.

Price HP, Peltan A, Stark M, Smith DF (2010) The small GTPase ARL2 is required for cytokinesis in *Trypanosoma brucei*. *Molecular and Biochemical Parasitology* 173: 123–131.

Prinz H (2010) Hill coefficients, dose–response curves and allosteric mechanisms. *Journal of Chemical Biology* 3: 37-44.

Ouattara B, Angenot L, Guissou P, Fondu P, Dubois J, Frédérick M, Jansen O, Van Heugen JC, Wauters JN, Tits M (2004) LC/MS/NMR analysis of isomeric divanilloylquinic acids from the root bark of *Fagara zanthoxyloides* Lam. *Phytochemistry* 65(8): 1145–1151.

Radwanska M, Magez S, Dumont N, Pays A, Nolan D, Pays E (2000) Antibodies raised against the flagellar pocket fraction of *Trypanosoma brucei* preferentially recognize HSP60 in cDNA expression library. *Parasite Immunology* 22: 639-650.

Ralston KS, Kabututu ZP, Melehani JH, Oberholzer M, Hill KL (2009) The *Trypanosoma brucei* flagellum: moving parasites in new directions. *Annual Review of Microbiology* 63: 335-62.

Ramey K, Eko FO, Thompson WE, Armah H, Igietseme JU, Stiles JK (2009) Immunolocalization and challenge studies using a recombinant *Vibrio cholera* ghost expressing *Trypanosoma brucei* Ca²⁺ ATPase (TBCA2) antigen. *American Journal of Tropical Medicine and Hygiene* 81: 407-415.

Raper J, Portela MP, Lugli E, Frevert U, Tomlinson S (2001) Trypanosome lytic factors: novel mediators of human innate immunity. *Current Opinion in Microbiology* 4: 402-408.

Robertson AG (1983) The feeding habits of tsetse flies in Zimbabwe (formerly Rhodesia) and their relevance to some tsetse control measures. *Smithersia* 1: 1-72.

Rodgers MJ, Albanesi JP, Phillips MA (2007) Phosphatidylinositol 4-kinase III-beta is required for Golgi maintenance and cytokinesis in *Trypanosoma brucei*. *Eukaryotic Cell* 6: 1108-1118.

Roditi I, Furger A, Ruepp S, Schürch N, Bütikofer P (1998) Unravelling the procyclin coat of *Trypanosoma brucei*. *Molecular and Biochemical Parasitology* 91: 117-130.

Roditi I, Clayton C (1999) An unambiguous nomenclature for the major surface glycoproteins of the procyclic form of *Trypanosoma brucei*. *Molecular and Biochemical Parasitology* 103: 99-100.

Rohloff P, Rodrigues CO, Docampo R (2003) Regulatory volume decrease in *Trypanosoma cruzi* involves amino acid efflux and changes in intracellular calcium. *Molecular and Biochemical Parasitology* 126: 219-230.

Ross SA, Sultana GNN, Burandt CL, ElSohly MA, Marais JPJ, Ferreira D (2004) Syncarpamide, a new antiplasmodial (+)-norepinephrine derivative from *Zanthoxylum syncarpum*. *Journal of Natural Products* 67: 88-90.

Ross SA, Al-Azeib MA, Krishnavei KS, Fronczek FR, Burandt CL (2005) Alkamides from the Leaves of *Zanthoxylum syncarpum*. *Journal of Natural Products* 68: 1297-1299.

Ruiz FA, Marchesini N, Seufferheld M, Govindjee, Docampo R (2001) The polyphosphate bodies of *Clamydomonas reinhardtii* possess a proton-pumping pyrophosphate and are similar to acidocalcisomes. *Journal of Biological Chemistry* 276: 46196-46203.

Saini RK (1990) Responses of tsetse flies *Glossina* spp. (*Diptera: Glossinidae*) to phenolic kairomones in a wind tunnel. *Insect Science and its Application* 11: 369–375.

Saini RK (1992) Olfactory sensitivity of tsetse flies to phenolic kairomones. *Insect Science and its Application* 13: 95–104.

Saini RK, Hassanali A, Ahuya P, Andoke J, Nyandat E (1993) Close range responses of tsetse flies *Glossina morsitans morsitans* Westwood (*Diptera: Glossinidae*) to host body kairomones. *Discovery and Innovation* 5: 149–153.

Saini HK, Griffiths-Jones S, Enright AJ (2007) Genomic analysis of human microRNA transcripts. *Proceedings of the national academy of sciences of the United States of America* 104(45): 17719–17724.

Saleem M (2009) Lupeol, a novel anti-inflammatory and anti-cancer dietary triterpene. *Cancer Letters* 285: 109-115.

Salmon D, Bachmaier S, Krumbholz C, Kador M, Gossmann JA, Uzureau P, Pays E, Boshart M (2012) Cytokinesis of *Trypanosoma brucei* bloodstream forms depends on expression of adenylyl cyclases of the ESAG4 or ESAG4-like subfamily. *Molecular Microbiology* 84: 225-242.

Schenkman S, Jiang MS, Hart GW, Nussenzweig V (1991) A novel cell surface trans-sialidase of *Trypanosoma cruzi* generates a stage-specific epitope required for invasion of mammalian cells. *Cell* 65: 1117-1125.

Schenone M, Dančík V, Wagner BK, Clemons PA (2013) Target identification and mechanisms of action in chemical biology and drug discovery. *Nature Chemical Biology* 9: 232-240.

Schmidt RS, Bütikofer P (2014) Autophagy in *Trypanosoma brucei*: Amino acid requirement and regulation during different growth phases. *PLOS ONE* 9(4): e93875.

Schneider A, Bursac D, Lithgow T (2008) The direct route: a simplified pathway for protein import into the mitochondrion of trypanosomes. *Trends in Cell Biology* 18: 12-18.

Schwarz DS, Hutvagner G, Du T, Xu Z, Aronin N, Zamore PD (2003) Asymmetry in the assembly of the RNAi enzyme complex. *Cell* 115(2): 199–208.

Schweichel JU, Merker HJ (1973) The morphology of various types of cell death in prenatal tissues. *Teratology* 7: 253–266.

Scott AG, Tait A, Turner CM (1996) Characterisation of cloned lines of *Trypanosoma brucei* expressing stable resistance to MelCy and suramin. *Acta Tropica* 60: 251–262.

Seelinger G, Merfort I, Wölfle U, Schempp CM (2008) Anticarcinogenic effects of the flavonoid luteolin. *Molecules* 13: 2628-2651.

Sen R, Chatterjee M (2011) Plant derived therapeutics for the treatment of Leishmaniasis. *Phytomedicine* 18(12): 1056-1069.

Seki A, Coppinger JA, Jang CY, Yates JR, Fang G (2008) Bora and the kinase Aurora A cooperatively activate the kinase Plk1 and control mitotic entry. *Science* 320: 1655–1658.

Shapiro TA, Englund PT (1990) Selective cleavage of kinetoplast DNA minicircles promoted by antitrypanosomal drugs. *Proceedings of the National Academy of Sciences of the United States of America* 87: 950–954.

Shaw AP, Torr SJ, Waiswa C, Cecchi G, Wint GR, Mattioli RC, Robinson TP (2013) Estimating the costs of tsetse control options: an example for Uganda. *Preventive Veterinary Medicine* 110: 290–303.

Shen Y, Sun Z, Shi P, Wang G, Wu Y, Li S, Zheng Y, Huang L, Lin L, Lin X, Yao H (2018) Anticancer effect of petroleum ether extract from *Bidens pilosa* L and its constituent's analysis by GC-MS. *Journal of Ethnopharmacology* 217: 126-133.

Sheu YJ, Stillman B (2006) Cdc7-Dbf4 phosphorylates MCM proteins via a docking site-mediated mechanism to promote S phase progression. *Molecular Cell* 24: 101–113.

Sheu YJ, Stillman B (2010) The Dbf4-Cdc7 kinase promotes S phase by alleviating an inhibitory activity in Mcm4. *Nature* 463: 113–117.

Shi H, Djikeng A, Mark T, Wirtz E, Tschudi C, Ullu E (2000) Genetic interference in *Trypanosoma brucei* by heritable and inducible double-stranded RNA. *RNA* 6: 1069–1076.

Silva MS, Prazeres DM, Lanca A, Atouguia J, Monteiro GA (2009) Trans-sialidase from *Trypanosoma brucei* as a potential target for DNA vaccine development against African trypanosomiasis. *Parasitology Research* 105: 1223-1229.

Silva FL, Fischer DC, Tavares JF, Silva MS, de Athayde-Filho PF, Barbosa-Filho JM (2011) Compilation of secondary metabolites from *Bidens pilosa* L. *Molecules* 16(2): 1070-1102.

Simarro PP, Giuliano Cecchi, Franco JR, Paone M, Diarra A, Ruiz-Postigo JA, Fèvre EM, Mattioli RC, Jannin JG (2012) Estimating and mapping the population at risk of sleeping sickness. *PLOS Neglected Tropical Diseases* 6(10): e1859.

Simpson AG, Stevens J, Lukes J (2006) The evolution and diversity of kinetoplastid flagellates. *Trends in Parasitology* 22: 168-174.

Solari AJ (1995) Mitosis and genome partition in trypanosomes. *Biocell* 19: 65-84.

Sousa PL, Souza RODS, Tessarolo LD, de Menezes RRPPB, Sampaio TL, Canuto JA, Martins AMC (2017) Betulinic acid induces cell death by necrosis in *Trypanosoma cruzi*. *Acta Tropica* 174: 72-75.

Stijlemans B, Baral TN, Guilliams M, Brys L, Korf J, Drennan M (2007) A glycosylphosphatidylinositol-based treatment alleviates trypanosomiasis-associated immunopathology. *Journal of Immunology* 179: 4003–4014.

Steverding D (2010) The development of drugs for treatment of sleeping sickness: a historical review. *Parasites and Vectors* 3: 15.

Stuart K, Panigrahi AK (2002) RNA editing: complexity and complications. *Molecular Microbiology* 45: 591-596.

Stuart KD, Schnauffer A, Ernst NL, Panigrahi AK (2005) Complex management: RNA editing in trypanosomes. *Trends in Biochemical Sciences* 30: 97-105.

Sun T, Zhang Y (2008) Pentamidine binds to tRNA through non-specific hydrophobic interactions and inhibits aminoacylation and translation. *Nucleic Acids Research* 36(5): 1654–1664.

Sundararajan P, Dey A, Smith A, Doss AG, Rajappan M, Sridhar Natarajan S (2006) Studies of anticancer and antipyretic activity of *Bidens pilosa* whole plant. *African Health Sciences* 6(1): 27–30.

Szallies A, Kubata BK, Duszenko M (2002) A metacaspase of *Trypanosoma brucei* causes loss of respiration competence and clonal death in the yeast *Saccharomyces cerevisiae*. *FEBS Letters* 517: 144–150.

Tagboto S, Townson S (2001) Antiparasitic properties of medicinal plants and other naturally occurring products. *Advances in Parasitology* 50: 199–295.

Tan PV, Dimo T, Dongo E (2000) Effects of methanol, cyclohexane and methylene chloride extracts of *Bidens pilosa* on various gastric ulcer models in rats. *Journal of Ethnopharmacology* 73: 415–421.

Tanaka S, Umemori T, Hirai K, Muramatsu S, Kamimura Y, Araki H (2007) CDK-dependent phosphorylation of Sld2 and Sld3 initiates DNA replication in budding yeast. *Nature* 445: 328-332.

Tatsadjieu LN, Essia Ngang JJ, Ngassoum MB, Etoa FX (2003) Antibacterial and antifungal activity of *Xylopiya aethiopica*, *Monodora myristica*, *Zanthoxylum xanthoxyloides* and *Zanthoxylum leprieurii* from Cameroon. *Fitoterapia* 74: 469-472.

Taylor RC, Cullen SP, Martin SJ (2008) Apoptosis: controlled demolition at the cellular level. *Nature Reviews Molecular Cell Biology* 9: 231-241.

Tewtrakul S, Miyashiro H, Nakamura N, Hattori M, Kawahata T, Otake T, Yoshinaga T, Fujiwara T, Supavita T, Yuenyongsawad S, Rattanasuwon P, Dej-Adisai S (2003) HIV-1 integrase inhibitory substances from *Coleus parvifolius*. *Phytotherapy Research* 17: 232–239.

Tillequin F (2007) Rutaceous alkaloids as models for the design of novel antitumor drugs. *Phytochemical Reviews* 6: 65-70.

Tobinaga S, Sharma MK, Aalbersberg WG, Watanabe K, Iguchi K, Narui K, Sasatsu M, Waki S (2009) Isolation and identification of a potent antimalarial and antibacterial polyacetylene from *Bidens pilosa*. *Planta Medica* 75: 624–628.

Torii S, Yamamoto T, Tsuchiya Y, Nishida E (2006) ERK MAP kinase in G(1) cell cycle progression and cancer. *Cancer Science* 97: 697–702.

Tour SJ, Hall DR, Smith JL (1995) Responses of tsetse flies (*Diptera: Glossinidae*) to natural and synthetic odours. *Entomological Research* 85: 157–166.

Trinkle-Mulcahy L, Lamond AI (2006) Mitotic phosphatases: no longer silent partners. *Current Opinion in Cell Biology* 18: 623–631.

Tu X, Wang CC (2004) The involvement of two cdc2-related kinases (CRKs) in *Trypanosoma brucei* cell-cycle regulation and the distinctive stage-specific phenotypes caused by CRK3 depletion. *Journal of Biological Chemistry* 279: 20519–20528.

Tu X, Wang CC (2005) Pairwise knockdowns of cdc2-related kinases (CRKs) in *Trypanosoma brucei* identified the CRKs for G1/S and G2/M transitions and demonstrated distinctive cytokinetic regulations between two developmental stages of the organism. *Eukaryotic Cell* 4: 755–764.

Tu X, Kumar P, Li Z, Wang CC (2006) An Aurora kinase homologue is involved in regulating both mitosis and cytokinesis in *Trypanosoma brucei*. *Journal of Biological Chemistry* 281: 9677–9687.

Ubillas RP, Mendez CD, Jolad SD, Luo J, King SR, Carlson TJ, Fort DM (2000) Antihyperglycemic acetylenic glucosides from *Bidens pilosa*. *Planta Medica* 66: 82–83.

Ullu E, Djikeng A, Shi H, Tschudi C (2002) RNA interference: Advances and questions. *Philosophical transactions of the Royal Society B: Biological Sciences* 357: 65–70.

Van Hellemond JJ, Neuville P, Schwarz RT, Matthews KR, Mottram JC (2000) Isolation of *Trypanosoma brucei* CYC2 and CYC3 cyclin genes by rescue of a yeast G1 cyclin mutant: functional characterization of CYC2. *Journal of Biological Chemistry* 275: 8315–8323.

Van Vugt MA, Bras A, Medema RH (2004) Polo-like kinase-1 controls recovery from a G2 DNA damage-induced arrest in mammalian cells. *Molecular Cell* 15: 799–811.

Vaughan S, Gull K (2008) The structural mechanics of cell division in *Trypanosoma brucei*. *Biochemical Society Transactions* 36: 421–424.

Vaughan S, Kohl L, Ngai I, Wheeler RJ, Gull K (2008) A repetitive protein essential for the flagellum attachment zone filament structure and function in *Trypanosoma brucei*. *Protist* 159: 127–136.

Vega-Avila E, Pugsley MK (2011). An overview of colorimetric assay methods used to assess survival or proliferation of mammalian cells. *Proceedings of the Western Pharmacology Society* 54: 10-14.

Vercammen D, Declercq W, Vandenabeele P, Breusegem FV (2007) Are metacaspases caspases? *Journal of Cell Biology* 179: 375–380.

Vercesi, AE, Docampo R (1992) Ca²⁺ transport by digitonin permeabilized *Leishmania donovani*. Effects of Ca²⁺, pentamidine and WR-6026 on mitochondrial membrane potential in situ. *Biochemical Journal* 284: 463–467.

Villalba MA, Carmo MI, Leite MN, Sousa OV (2007) Atividades farmacológicas dos extratos de *Zanthoxylum chiloperone* (Rutaceae). *Revista Brasileira de Farmacognosia* 17(2): 236-241.

Vickerman K (1994) The evolutionary expansion of the trypanosomatid flagellates. *International Journal for Parasitology* 24: 1317-1331.

Vreysen MJ, Saleh KM, Ali MY, Abdulla AM, Zhu ZR, Juma KG, Dyck VA, Msangi AR, Mkonyi PA, Feldmann HU (2000) *Glossina austeni* (Diptera: Glossinidae) eradicated on the island of Unguja, Zanzibar, using the sterile insect technique. *Journal of Economic Entomology* 93: 123–135.

Vreysen MJB (1996) Evaluation of sticky panels to monitor populations of *Glossina austeni* (Diptera: Glossinidae) on Unguja island of Zanzibar. *Bulletin of Entomological Research* 86: 289–296.

Vreysen MJB (2005) Monitoring sterile and wild insects in area-wide integrated pest management programmes. In: Dyck VA, Hendrichs J, Robinson AS (Eds), Sterile insect technique. Principles and practice in area-wide integrated pest management. Dordrecht, Springer, pp 325–361.

Waller RF, McConville MJ, McFadden GI (2004) More plastids in human parasites? Trends in Parasitology 20: 54-57.

Wang HQ, Lu SJ, Li H, Yao ZH (2007) EDTA-enhanced phytoremediation of lead contaminated soil by *Bidens maximowicziana*. Journal of Environmental Sciences 19: 1496–1499.

Welburn SC, Dale C, Ellis D, Beecroft R, Pearson TW (1996) Apoptosis in procyclic *Trypanosoma brucei rhodesiense* in vitro. Cell Death and Differentiation 3(2): 229-236.

Were PS, Kinyanjui P, Gicheru MM, Mwangi E, Ozwara HS (2010) Prophylactic and curative activities of extracts from *Warburgia ugandensis* Sprague (Canellaceae) and *Zanthoxylum usambarense* (Engl.) Kokwaro (Rutaceae) against *Plasmodium knowlesi* and *Plasmodium berghei*. Journal of Ethnopharmacology 130: 158-162.

Wirtz E, Leal S, Ochatt C, Cross GA (1999) A tightly regulated inducible expression system for conditional gene knock-outs and dominant-negative genetics in *Trypanosoma brucei*. Molecular and Biochemical Parasitology 99: 89–101.

Wlodkowic D, Skommer J, Darzynkiewicz Z (2009) Flow cytometry-based apoptosis detection. Methods in Molecular Biology 559: 1-14.

Wouatsa VN, Misra L, Kumar S, Prakash O, Khan F, Tchoumboungang F, Venkatesh RK (2013) Aromatase and glycosyl transferase inhibiting acridone alkaloids from fruits of Cameroonian *Zanthoxylum* species. Chemistry Central Journal 7(1): 125.

Wu LW, Chiang YM, Chuang HC, Wang SY, Yang GW, Chen YH, Lai LY, Shyur LF (2004) Polyacetylenes function as anti-angiogenic agents. *Pharmaceutical Research* 21: 2112–2119.

Wu LW, Chiang YM, Chuang HC, Lo CP, Yang KY, Wang SY, Shyur LF (2007) A novel polyacetylene significantly inhibits angiogenesis and promotes apoptosis in human endothelial cells through activation of the CDK inhibitors and caspase-7. *Planta Medica* 73: 655–661.

Xia L, You J, Li G, Sun Z, Suo Y (2011) Compositional and antioxidant analysis of *Zanthoxylum bungeanum* seed oil obtained by supercritical CO₂ fluid extraction. *Journal of the American Oil Chemists' Society* 88 (1): 23-32.

Xong HV, Vanhamme L, Chamekh M, Chimfwembe CE, Van Den Abbeele J, Pays A (1998) A VSG expression site-associated gene confers resistance to human serum in *Trypanosoma rhodesiense*. *Cell* 95: 839-846.

Yit CC, Das NP (1994) Cytotoxic effect of butein on human colon adenocarcinoma cell proliferation. *Cancer Letters* 82: 65–72.

Yoshida N, Kanekura T, Higashi Y, Kanzaki T (2006) *Bidens pilosa* suppresses interleukin-1 β -induced cyclooxygenase-2 expression through the inhibition of mitogen activated protein kinases phosphorylation in normal human dermal fibroblasts. *Journal of Dermatology* 33: 676–683.

Young PH, Hsu YJ, Yang WC (2010) ‘*Bidens pilosa* L. and its medicinal use,’ in *Recent Progress in Medicinal Plants Drug Plant II*, A.S. Awaad, V.K. Singh, and J.N. Govil, (Eds), Standium Press, Houston, Texas, USA.

Zahoui SO, Zirihi NG, Soro YT, Traore F (2010) Effet hypotenseur d'un extrait aqueux de *Zanthoxylum zanthoxyloides* (Lam.) Waterman (Rutaceae). *Phytothérapie* 8(6): 359-369.

Zamudio JR, Mitra B, Chattopadhyay A (2009) *Trypanosoma brucei* spliced leader RNA maturation by the cap 1 2'-O-ribose methyltransferase and SLA1 H/ACA snoRNA pseudouridine synthase complex. *Molecular and Cellular Biology* 29: 1202-1211.

Zegerman P, Diffley JF (2007) Phosphorylation of Sld2 and Sld3 by cyclin-dependent kinases promotes DNA replication in budding yeast. *Nature* 445: 281–285.

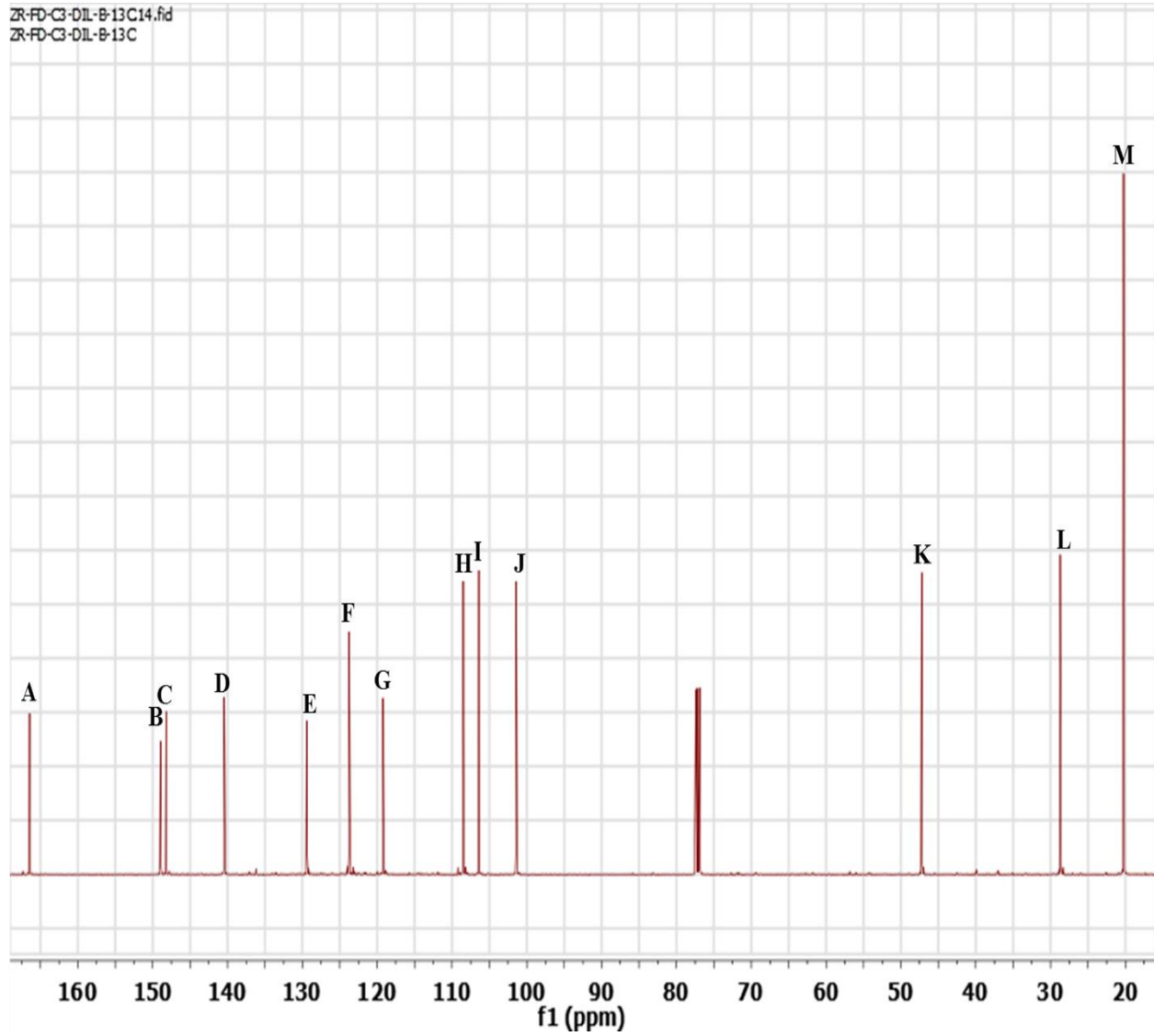
Zhang Y, Li Z, Pilch DS, Leibowitz MJ (2002) Pentamidine inhibits catalytic activity of group I intron Ca. LSU by altering RNA folding. *Nucleic Acids Research* 30: 2961–2971.

Zirihi GN, N'guessan K, Etien DT, Serikouassi B (2009) Evaluation *in vitro* of antiplasmodial activity of ethanolic extracts of *Funtumia elastica*, *Rauvolfia vomitoria* and *Zanthoxylum gillettii* on *Plasmodium falciparum* isolates from Côte d'Ivoire. *Journal of Animal and Plant Sciences* 5 (1): 406-413.

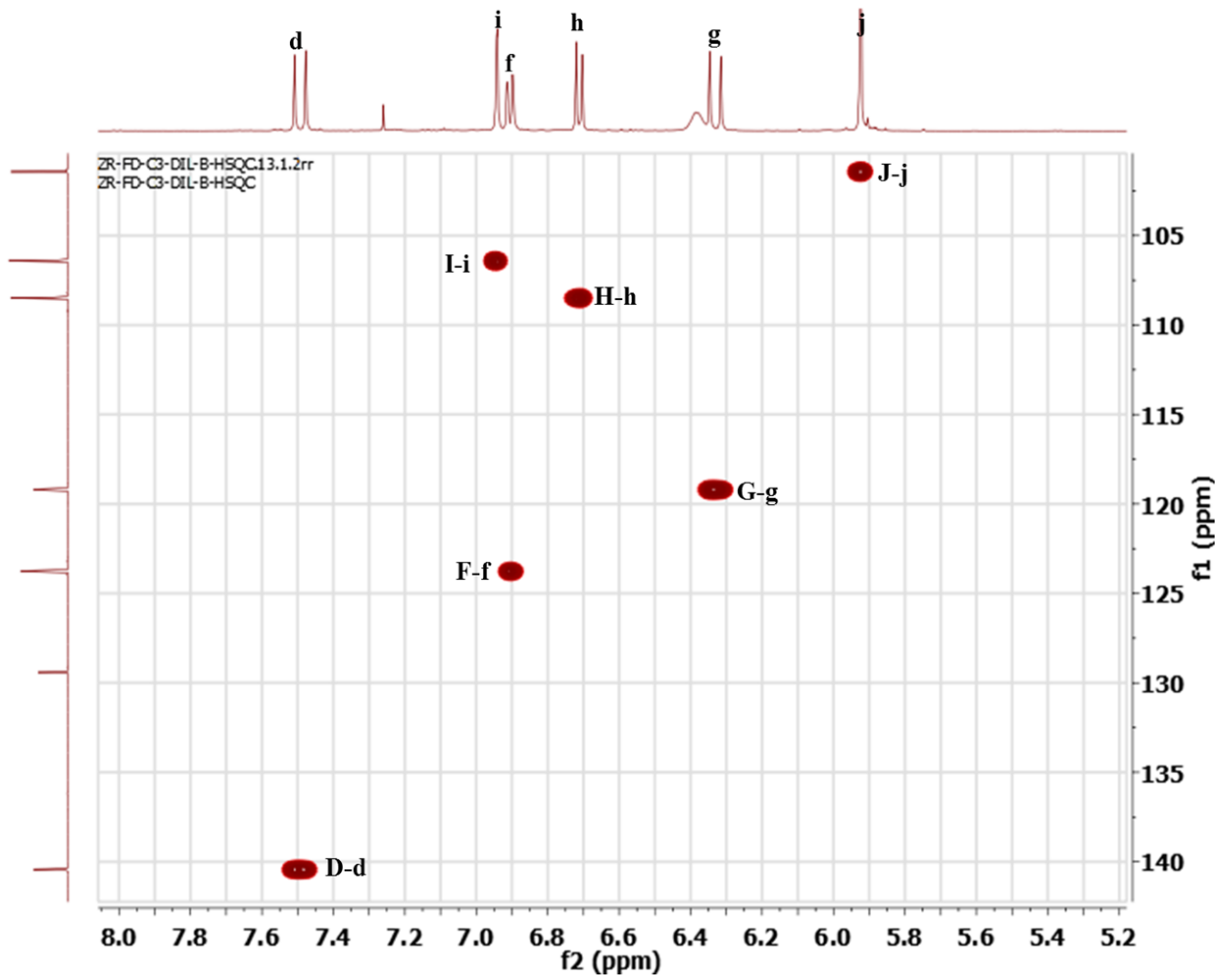
Zou L, Stillman B (2000) Assembly of a complex containing Cdc45p, replication protein A, and Mcm2p at replication origins controlled by S-phase cyclin-dependent kinases and Cdc7p-Dbf4p kinase. *Molecular and Cellular Biology* 20: 3086–3096.

APPENDICES

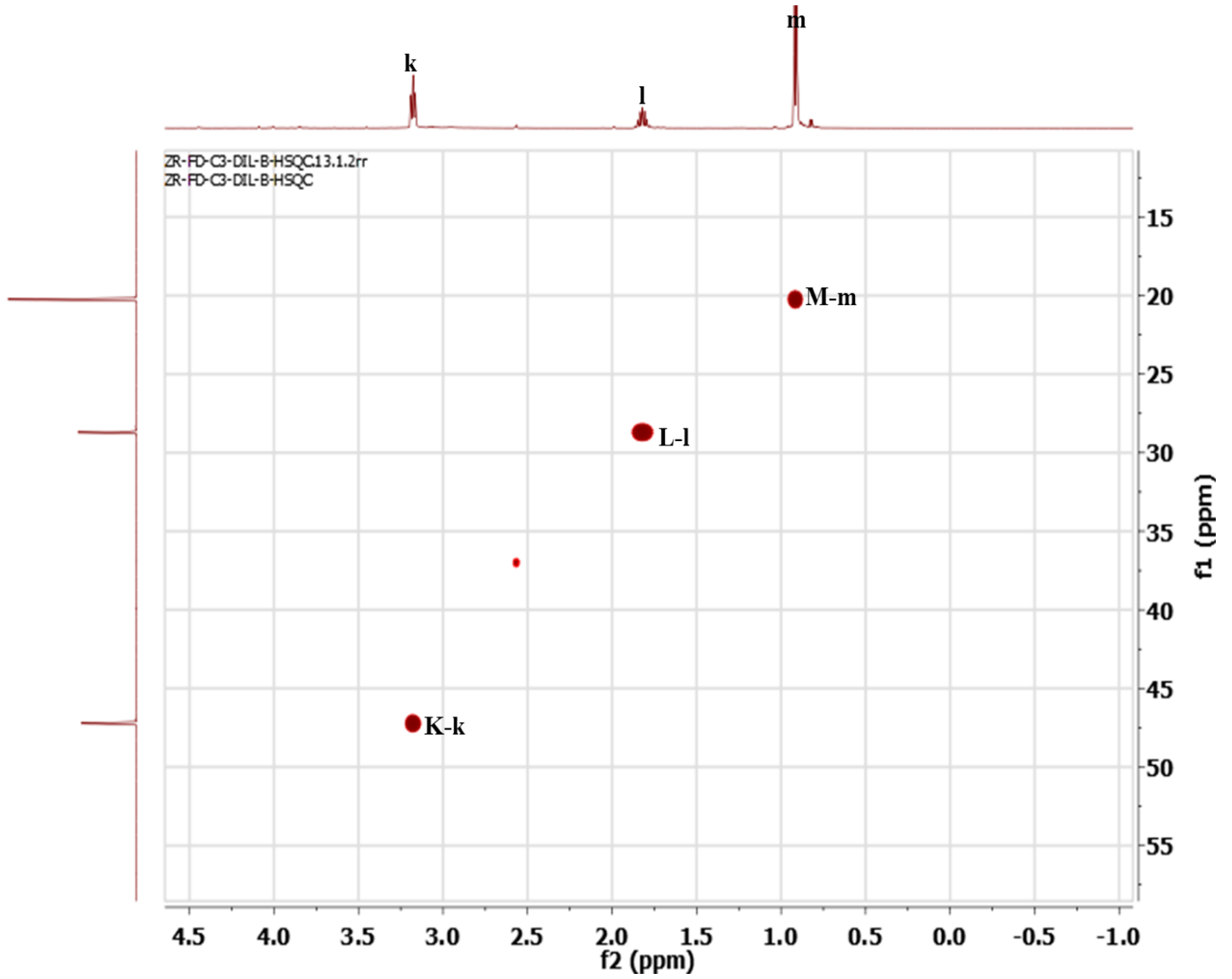
Appendix 1: Full ^{13}C -NMR spectrum of zanthoxylamide



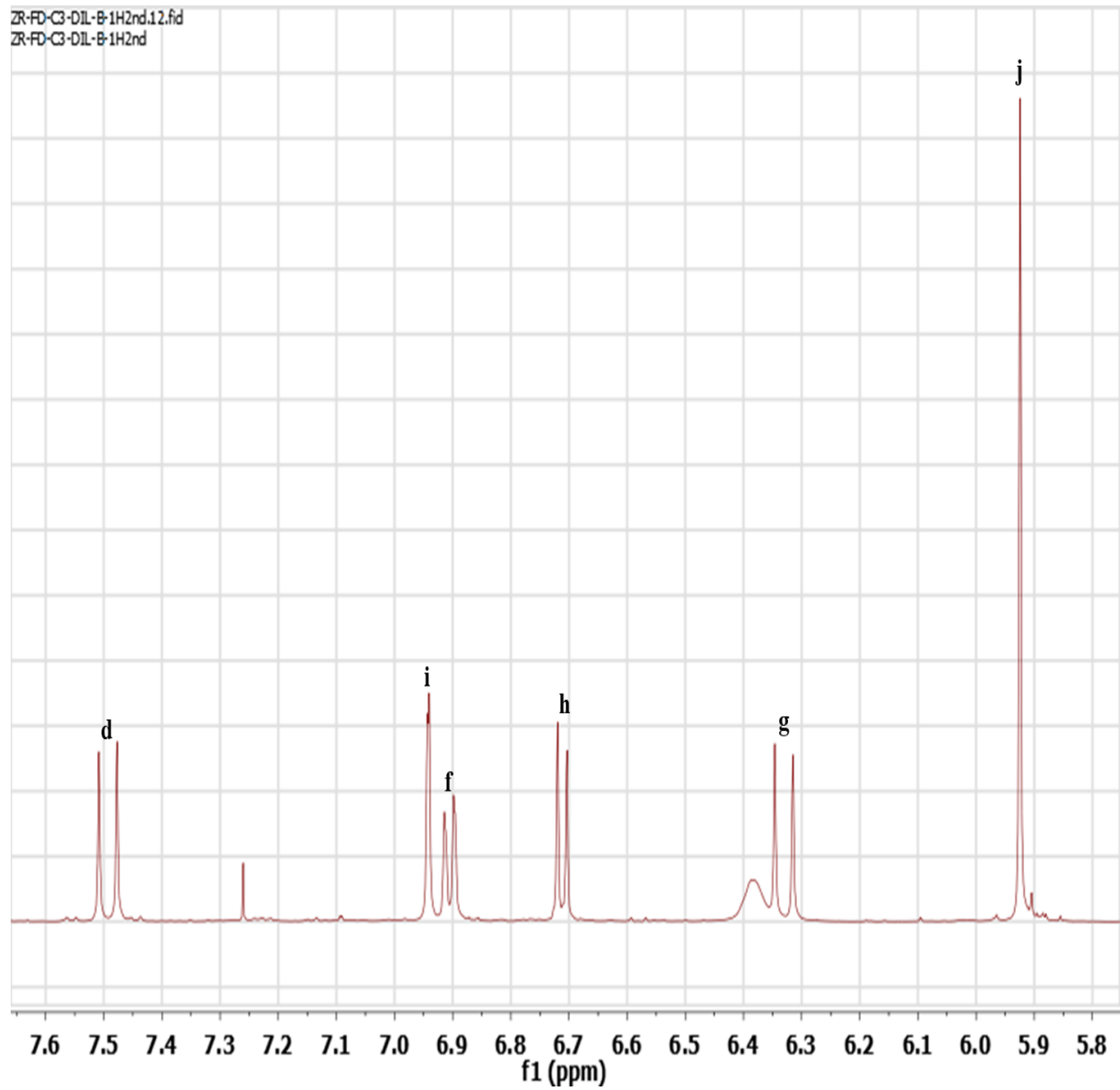
Appendix 2: gHSQC NMR spectrum of zanthoxylamide



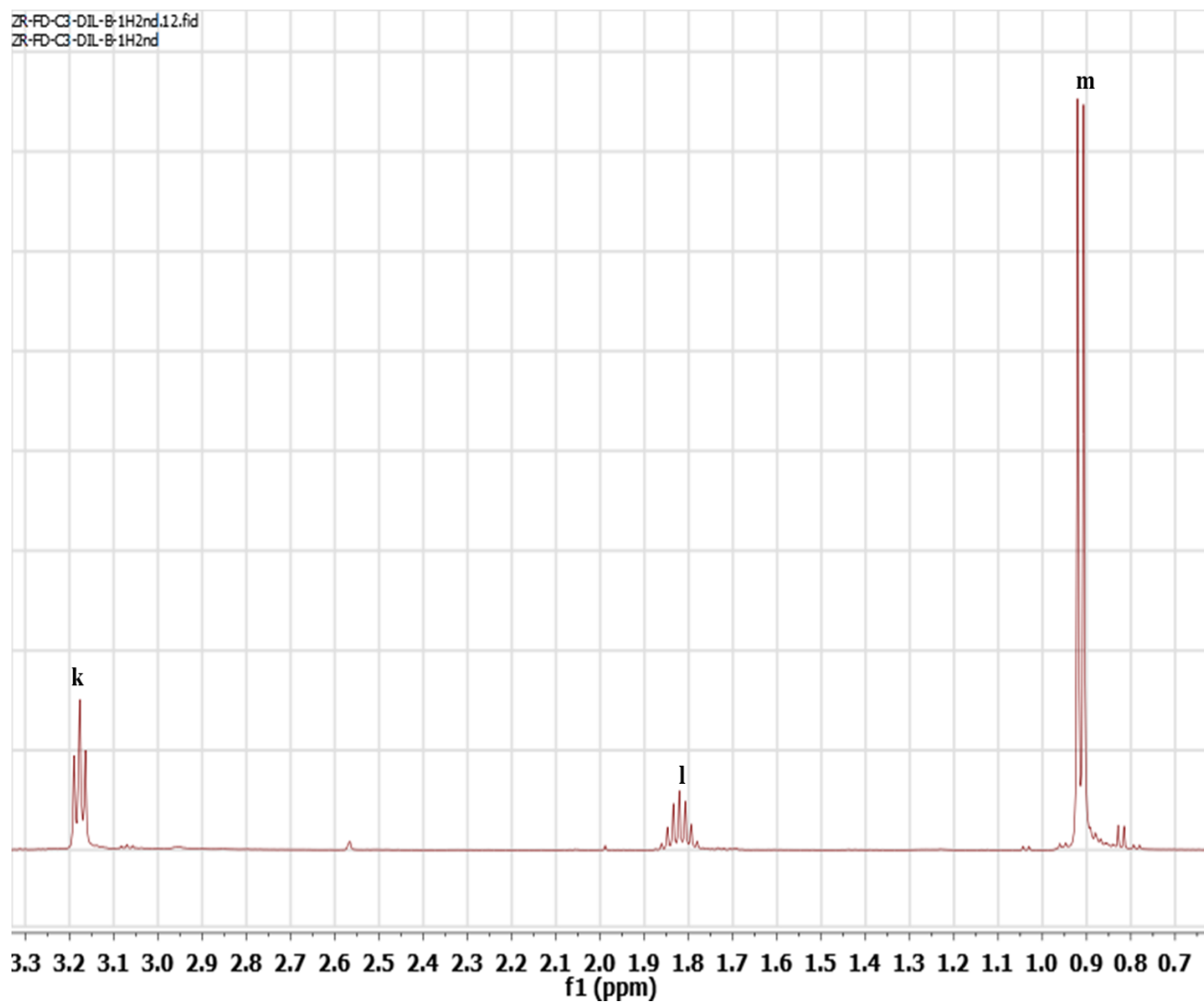
Appendix 3: gHSQC NMR spectrum of zanthoxylamide



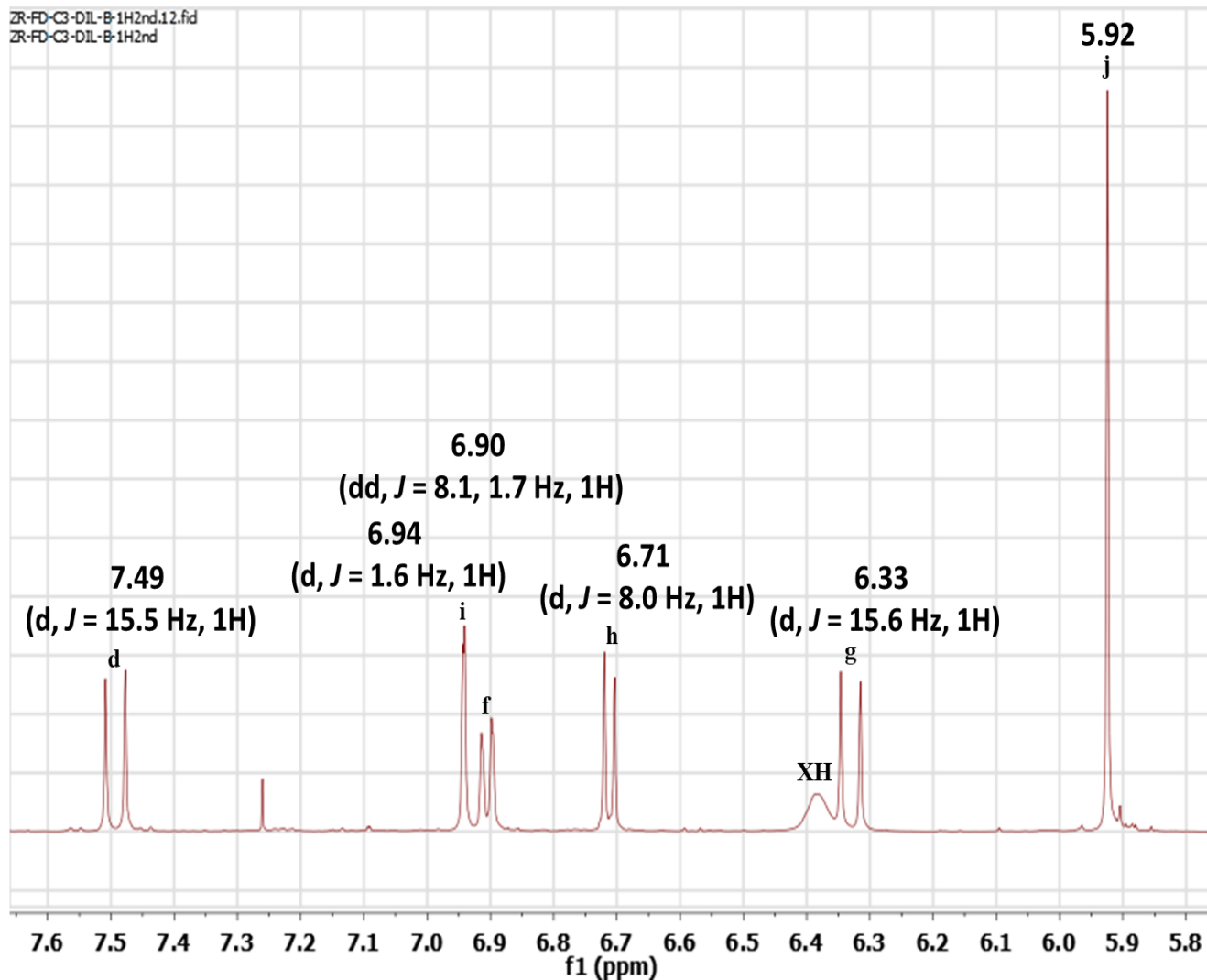
Appendix 4: Expanded ^1H -NMR spectrum of zanthoxylamide, version 1



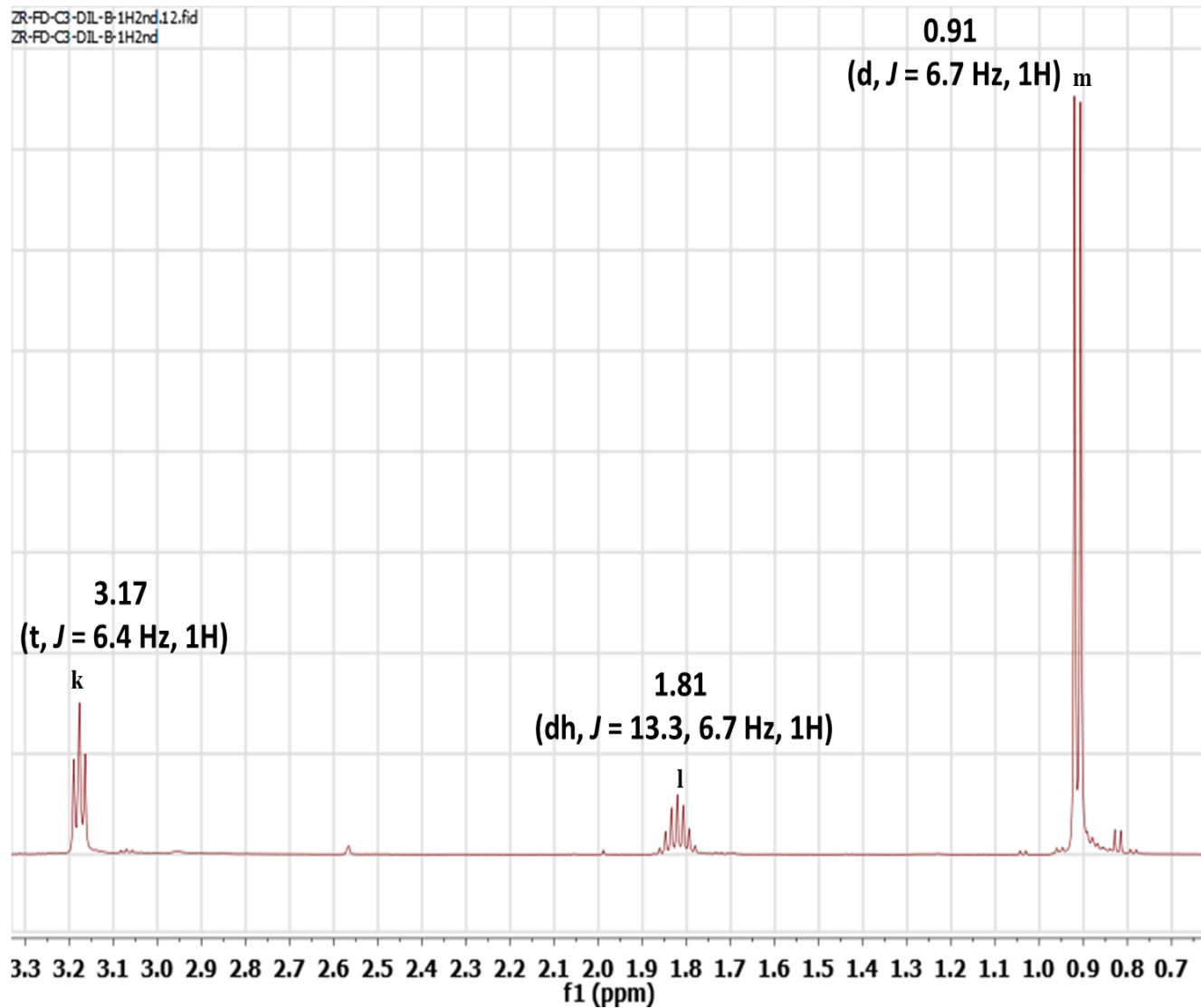
Appendix 5: Expanded ^1H -NMR spectrum of zanthoxylamide, version 2



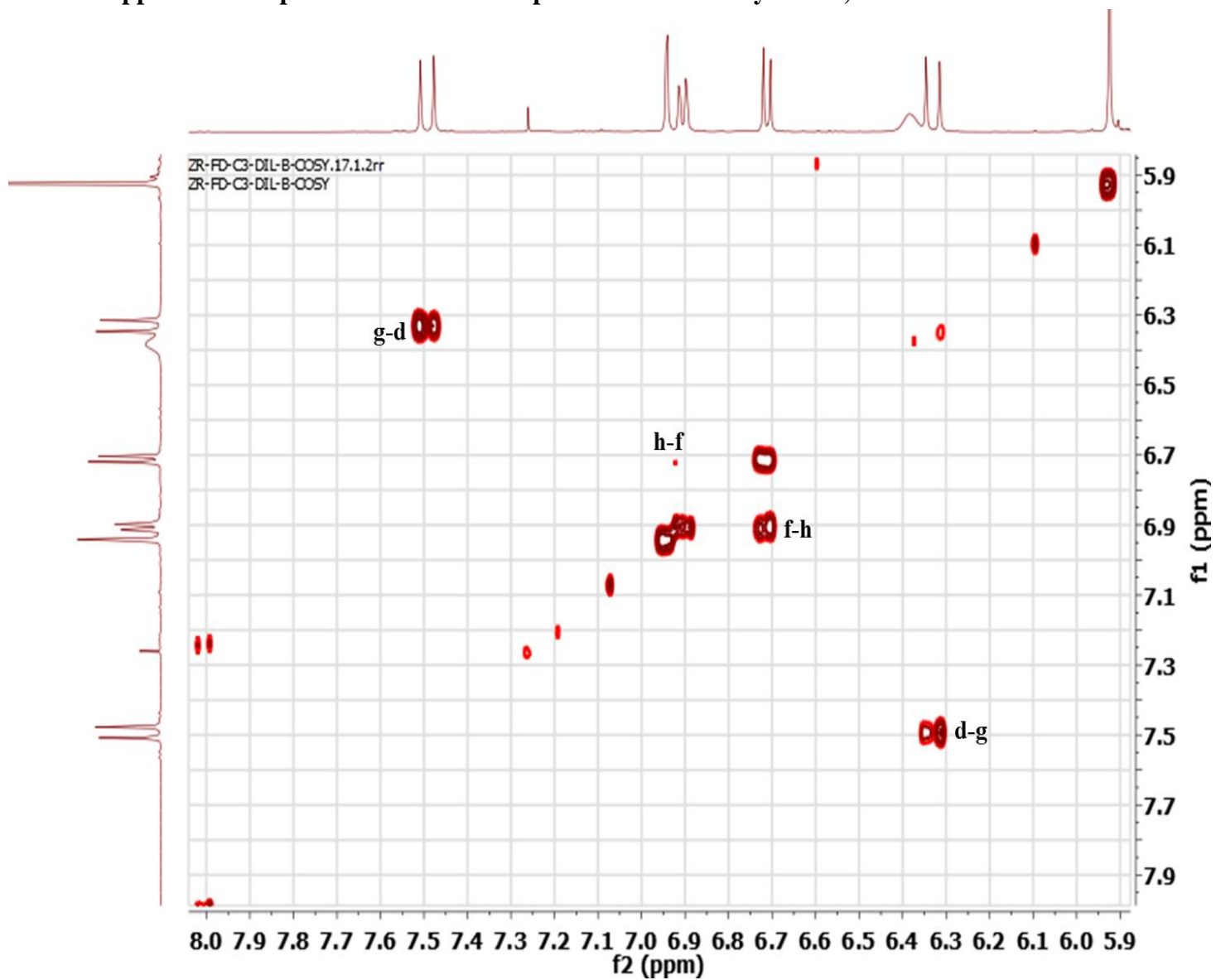
Appendix 6: Expanded ^1H -NMR spectrum of zanthoxylamide, version 3



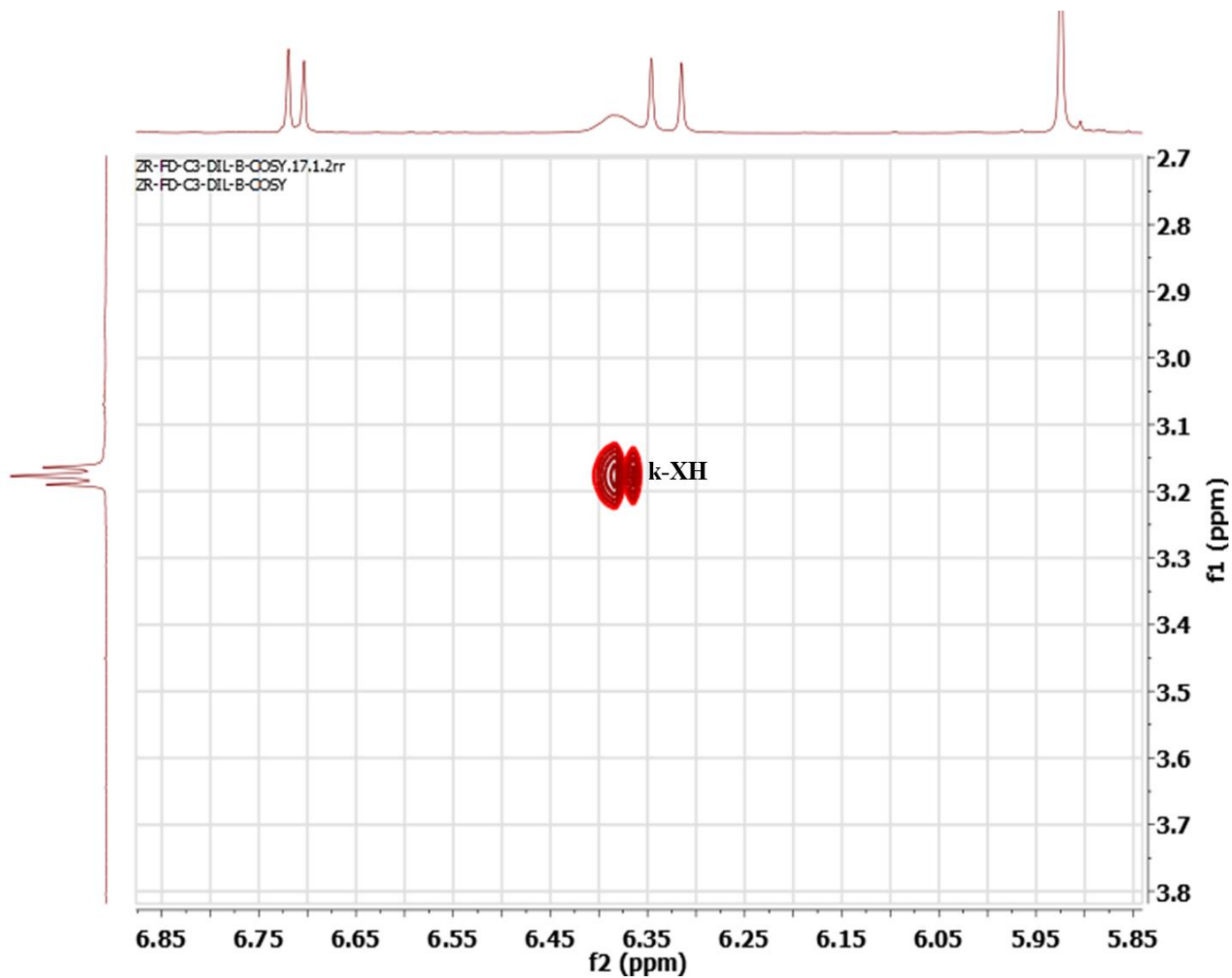
Appendix 7: Expanded ^1H -NMR spectrum of zanthoxylamide, version 4



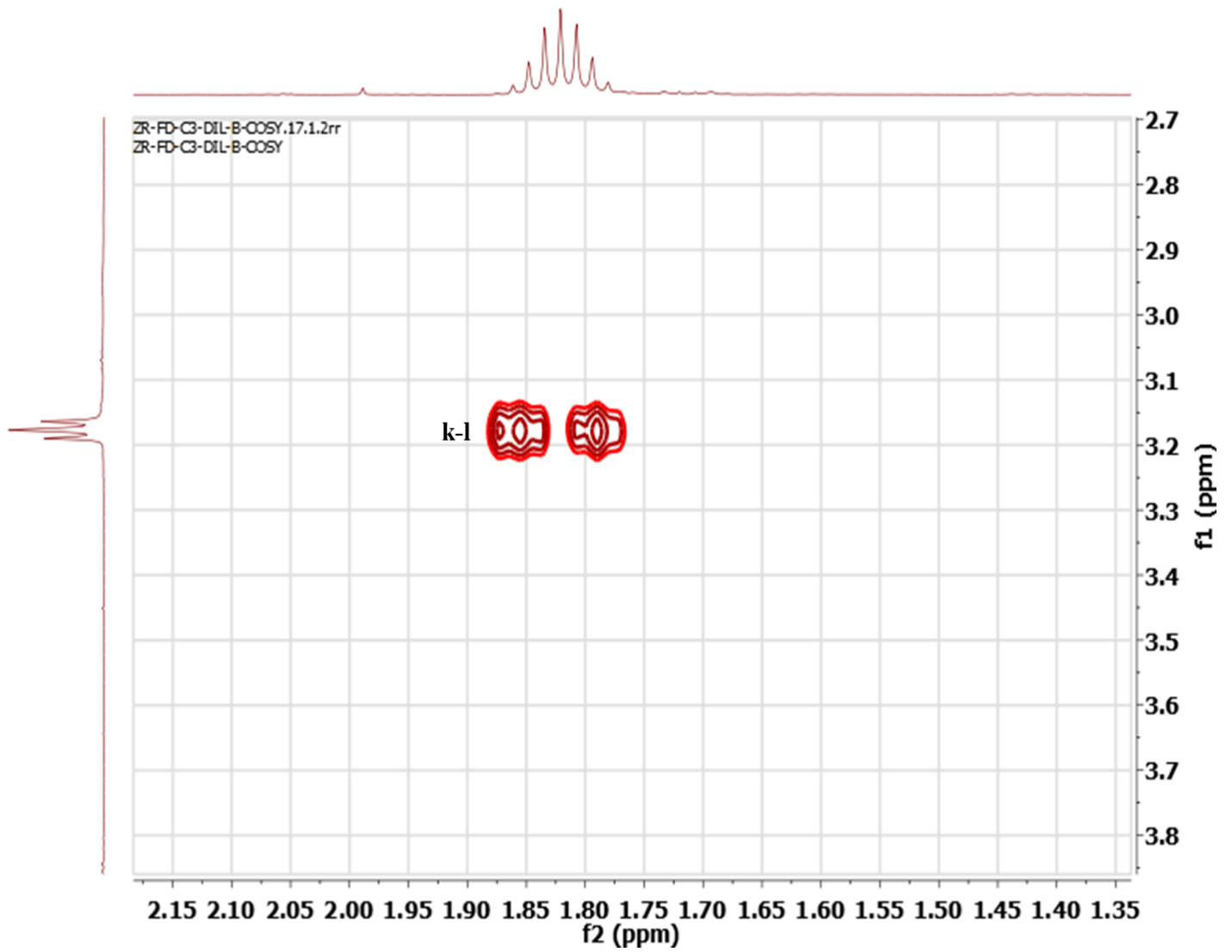
Appendix 8: Expanded COSY-NMR spectrum of zanthoxylamide, version 1



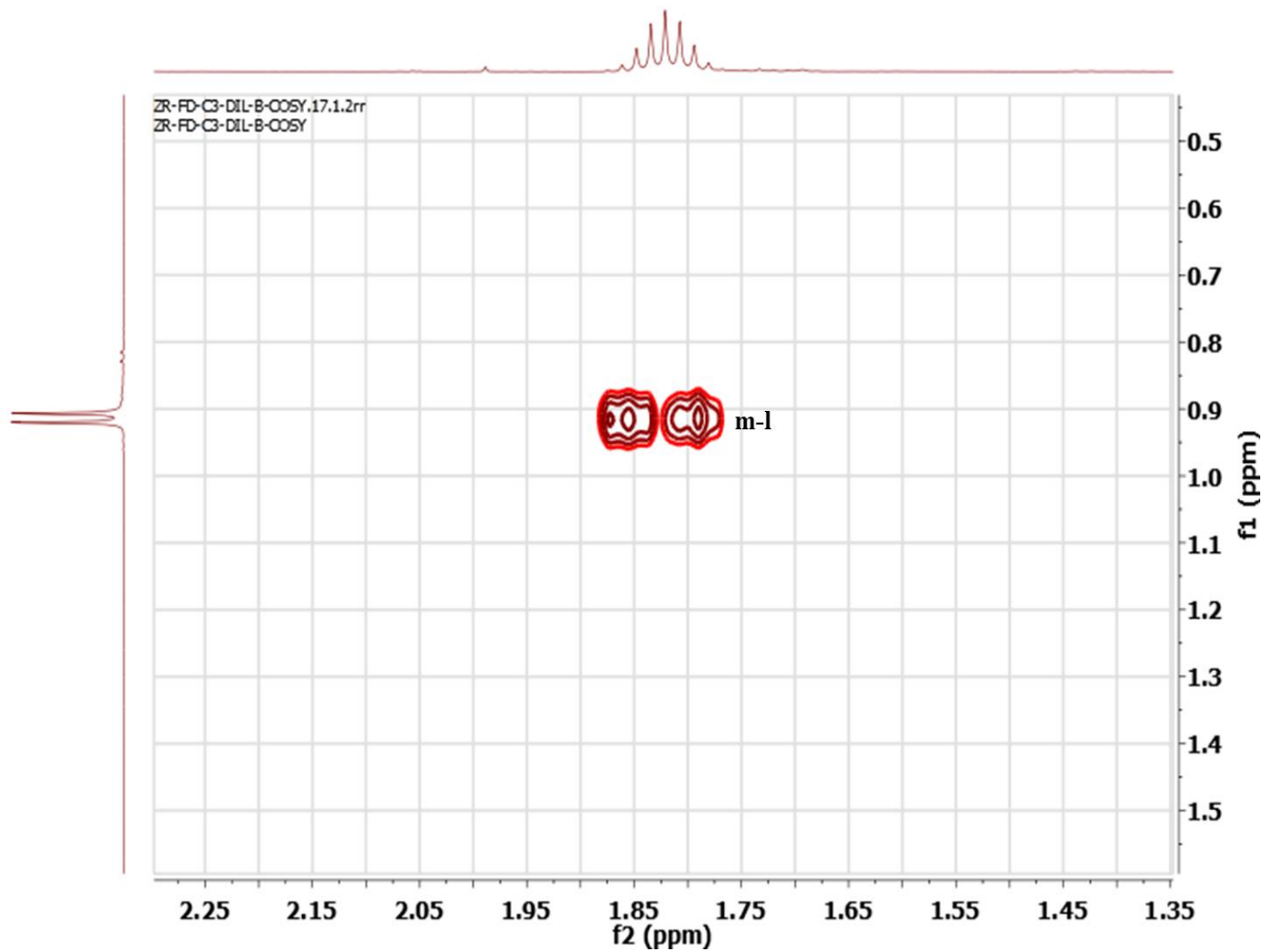
Appendix 9: Expanded COSY-NMR spectrum of zanthoxylamide, version 2



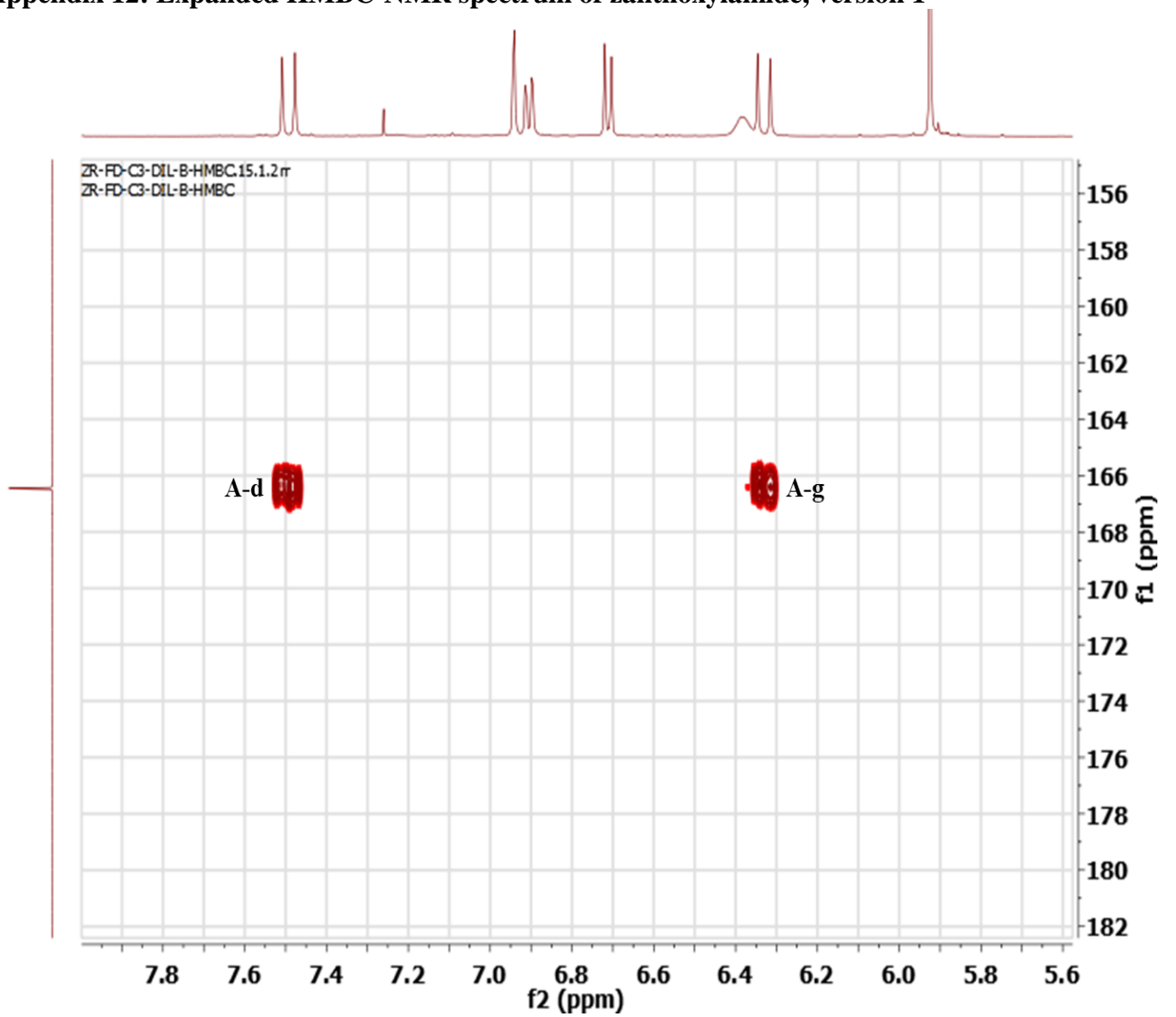
Appendix 10: Expanded COSY-NMR spectrum of zanthoxylamide, version 3



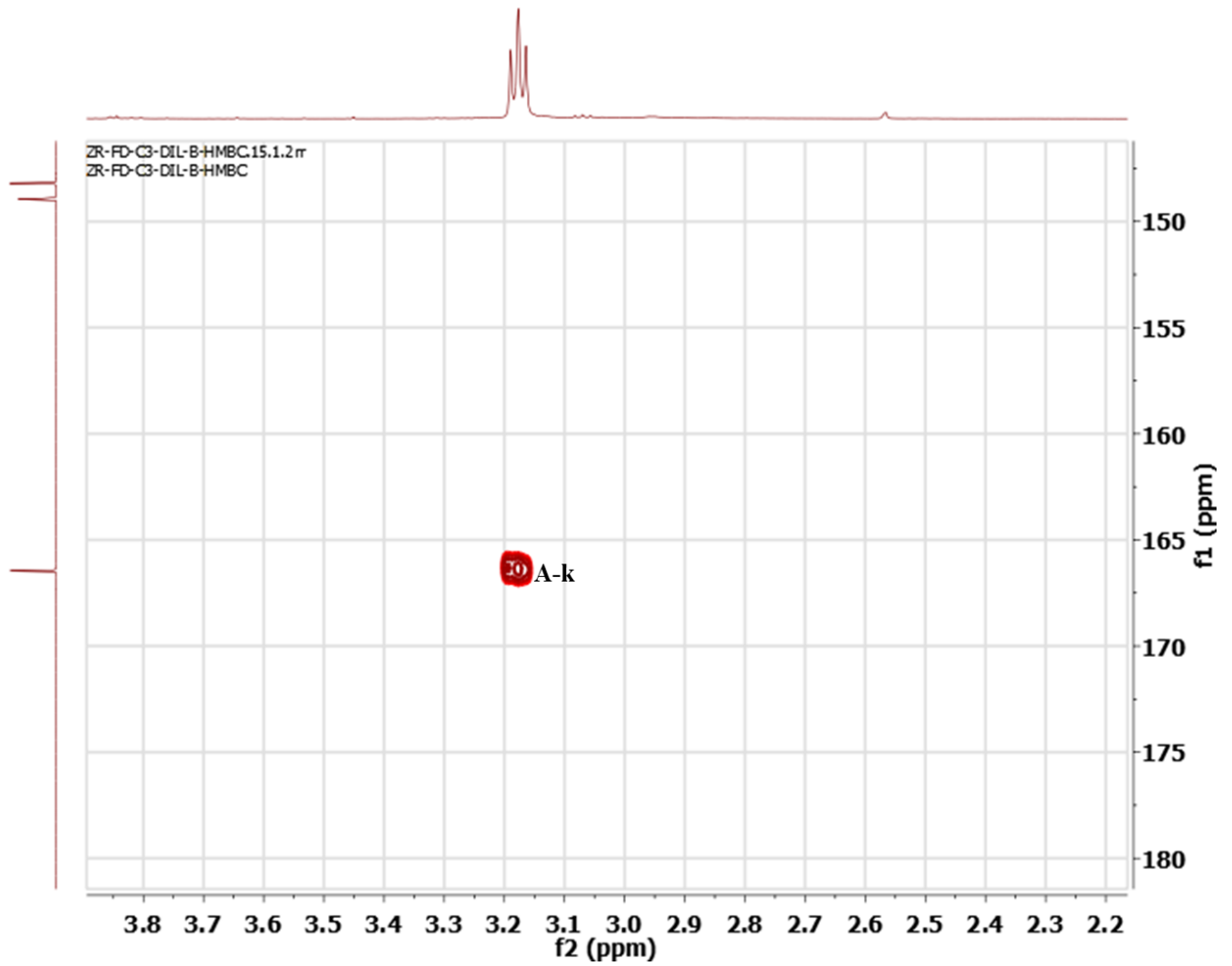
Appendix 11: Expanded COSY-NMR spectrum of zanthoxylamide, version 4



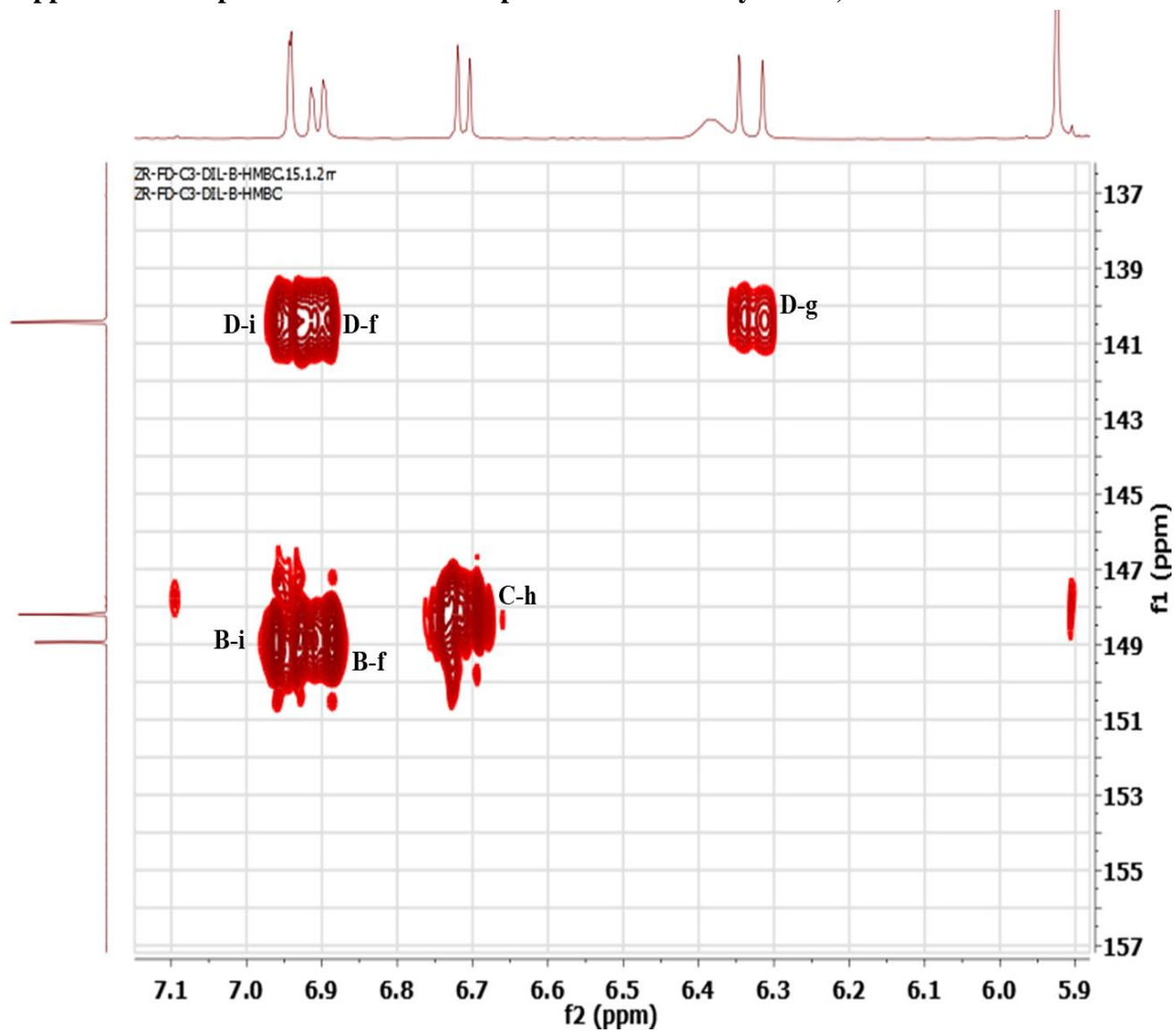
Appendix 12: Expanded HMBC-NMR spectrum of zanthoxylamide, version 1



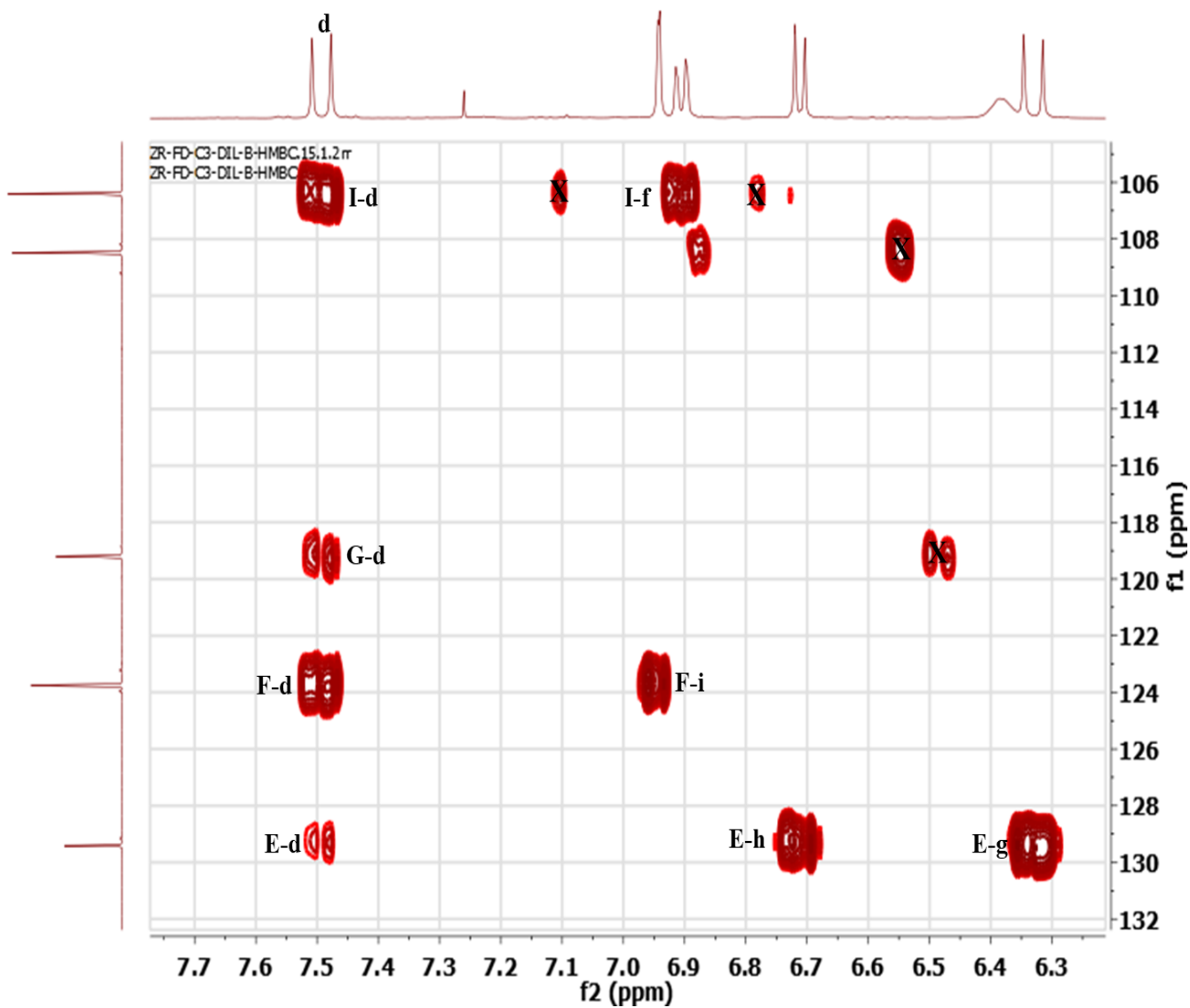
Appendix 13: Expanded HMBC-NMR spectrum of zanthoxylamide, version 2



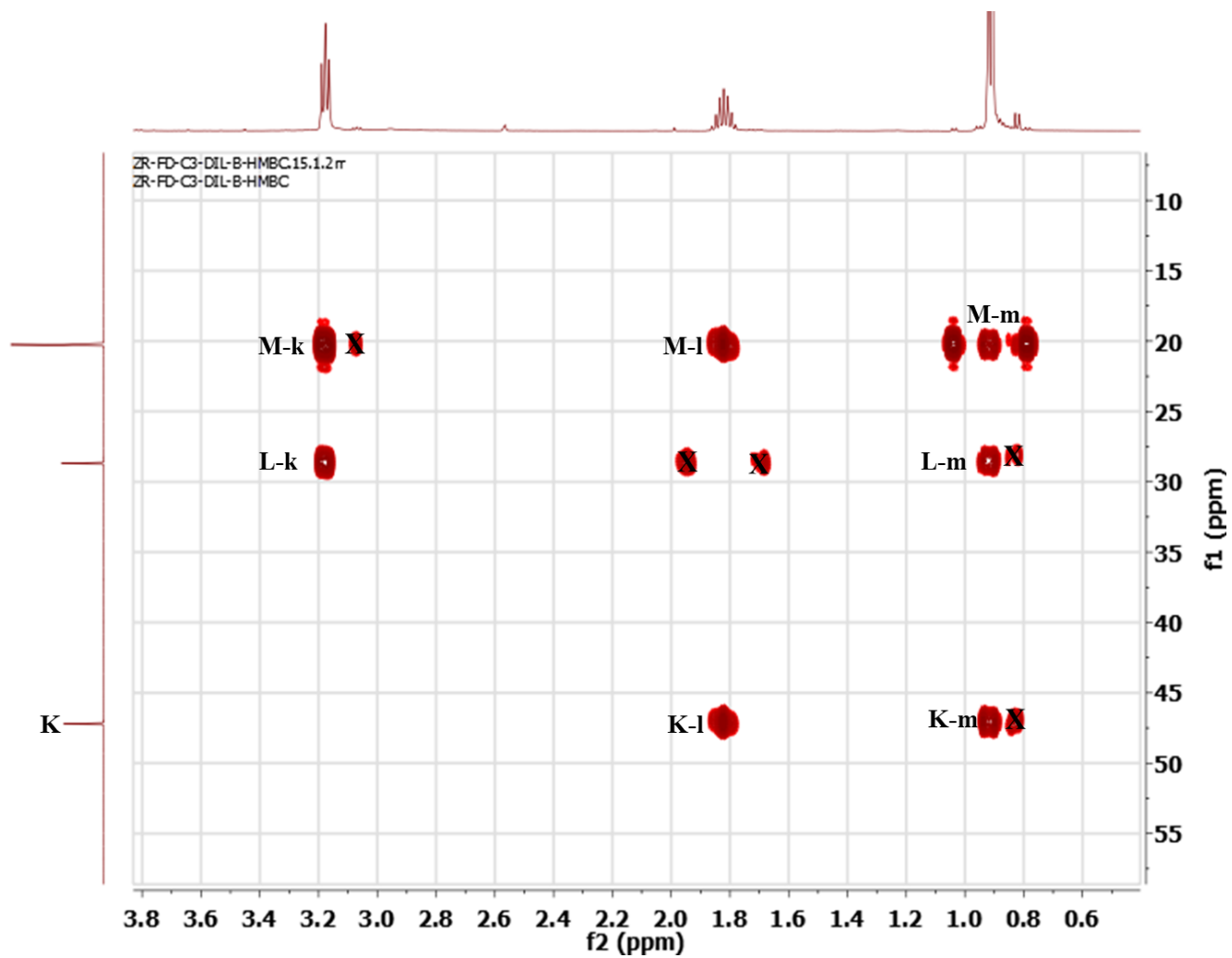
Appendix 14: Expanded HMBC-NMR spectrum of zanthoxylamide, version 3



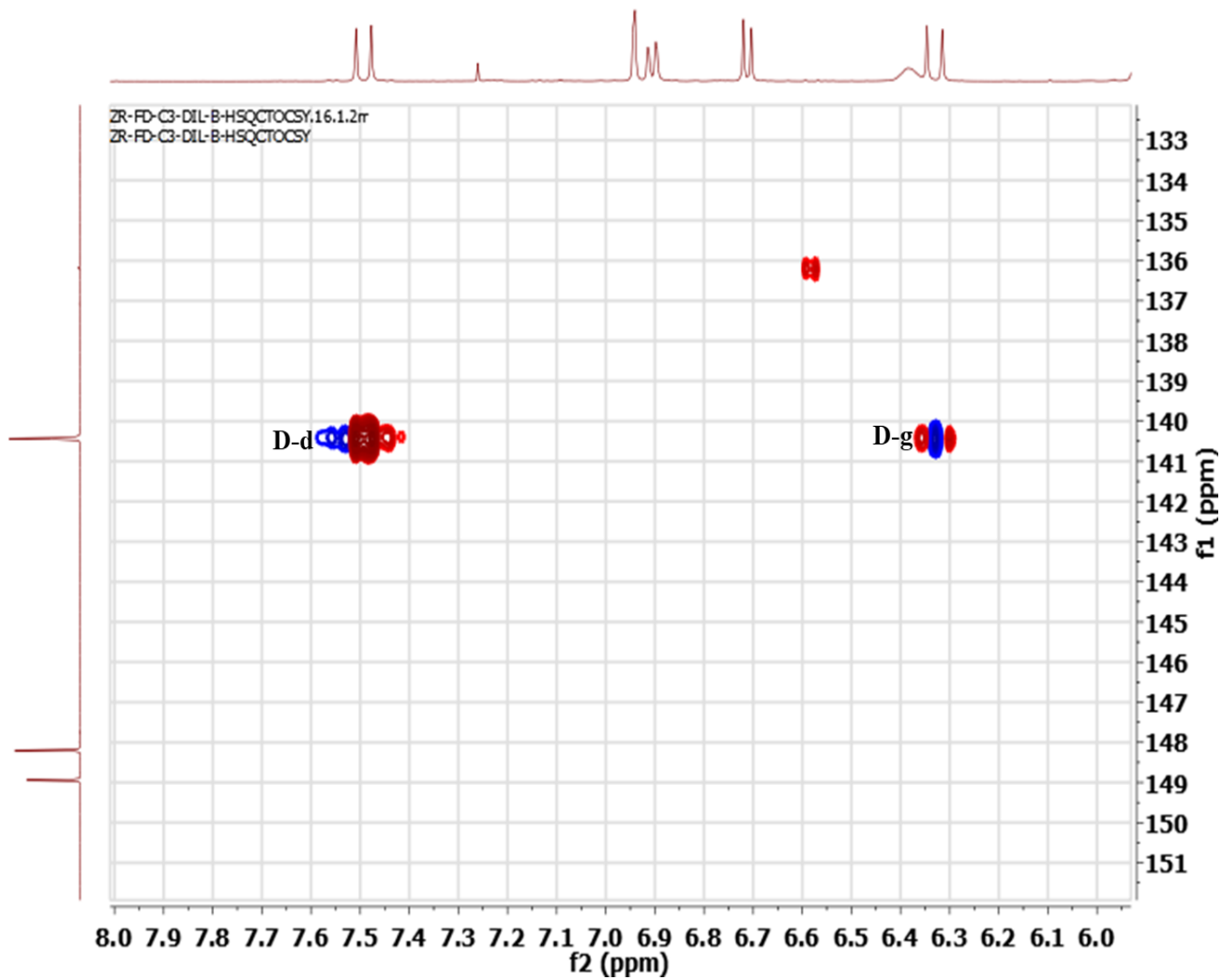
Appendix 15: Expanded HMBC-NMR spectrum of zanthoxylamide, version 4



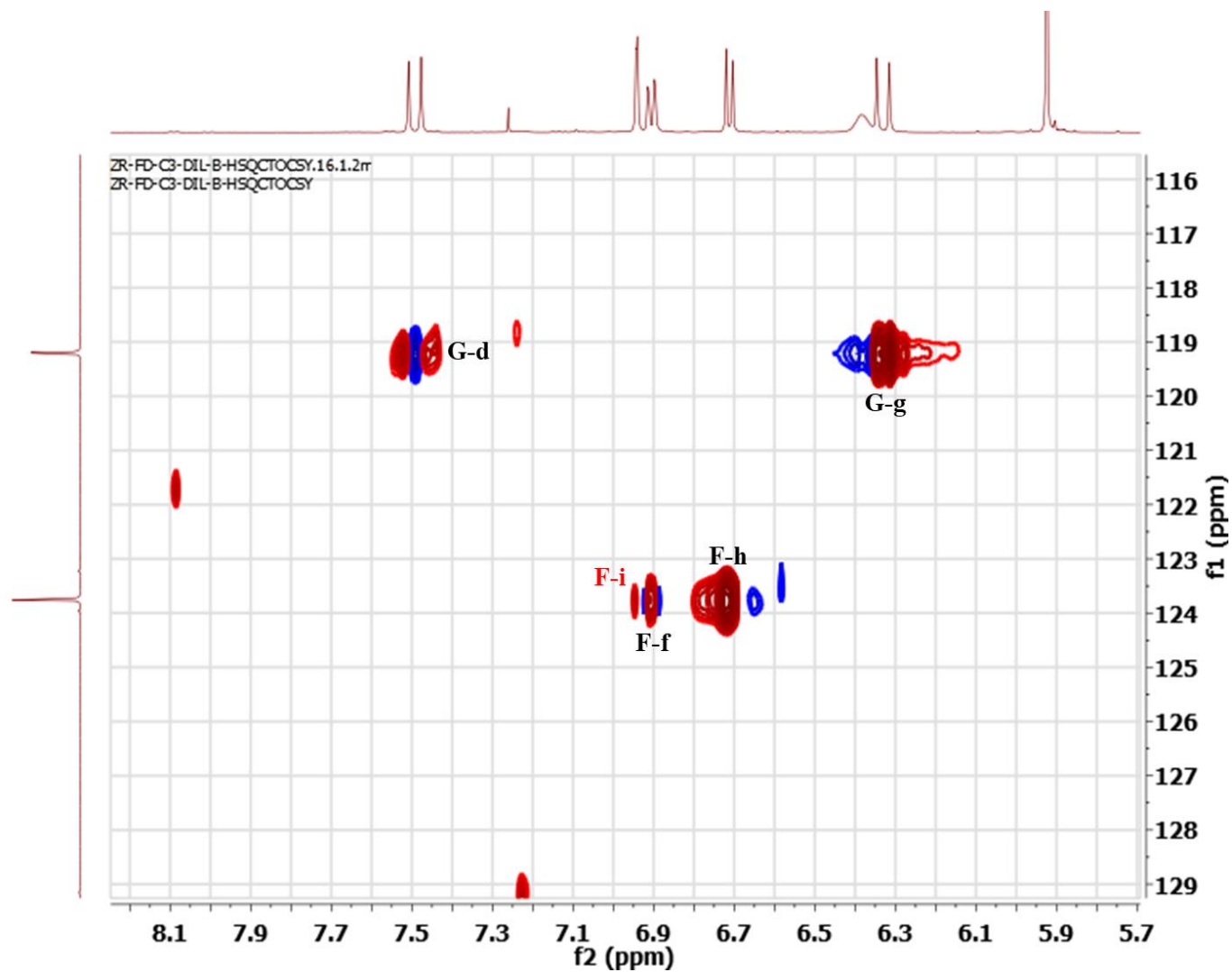
Appendix 16: Expanded HMBC-NMR spectrum of zanthoxylamide, version 5



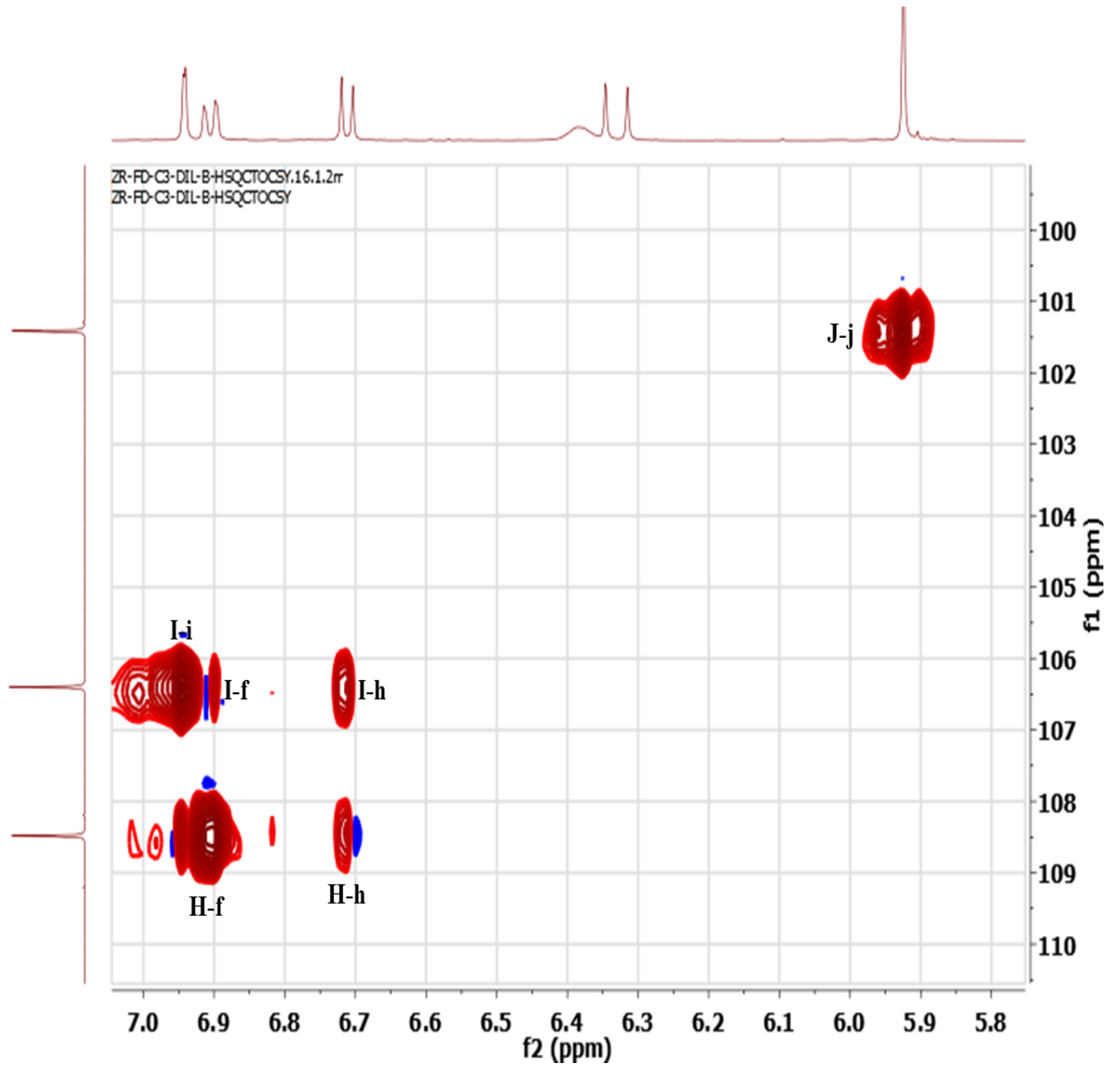
Appendix 17: Expanded HSQCTOCSY-NMR spectrum of zanthoxylamide



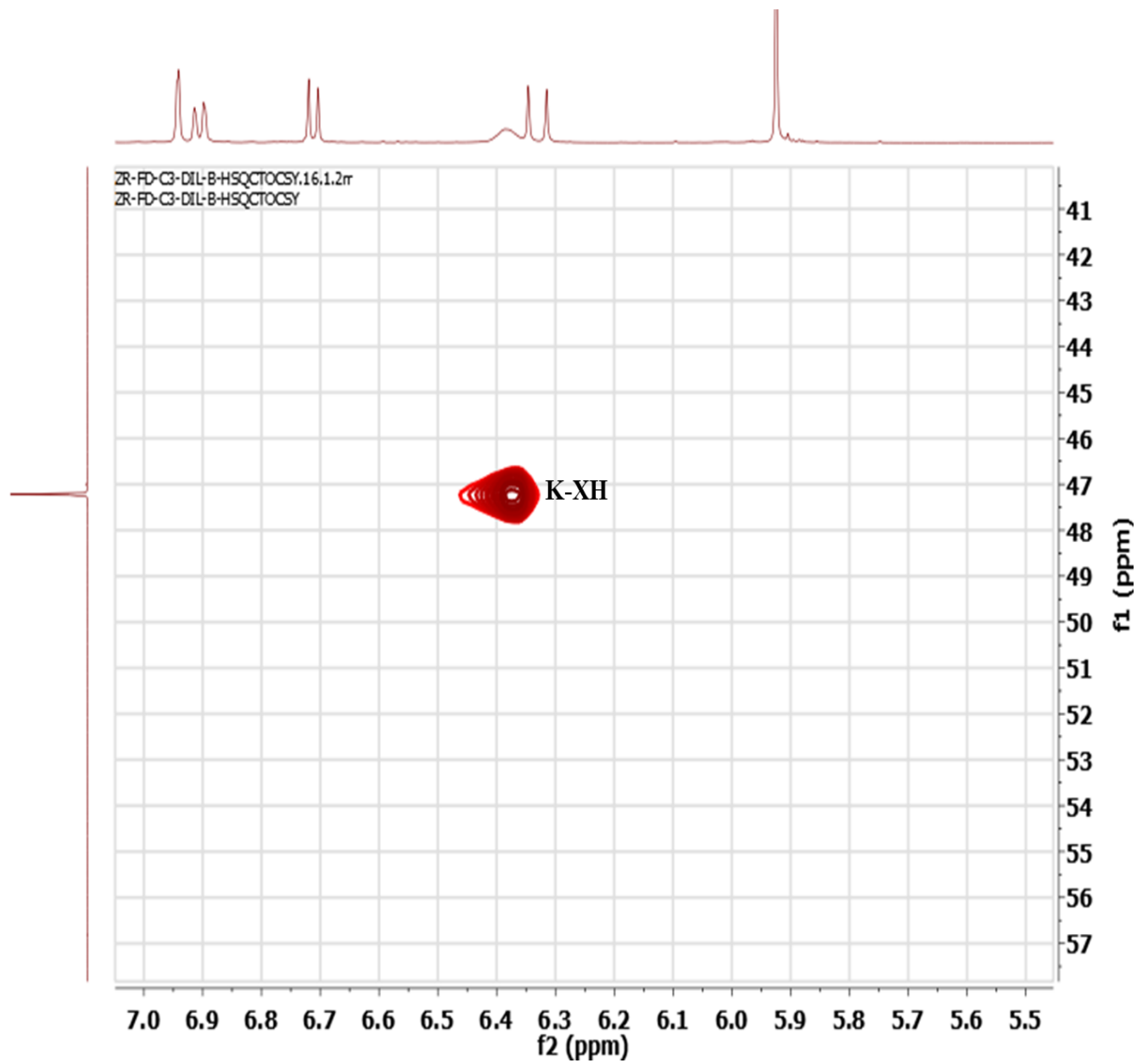
Appendix 18: HSQCTOCSY-NMR spectrum of zanthoxylamide



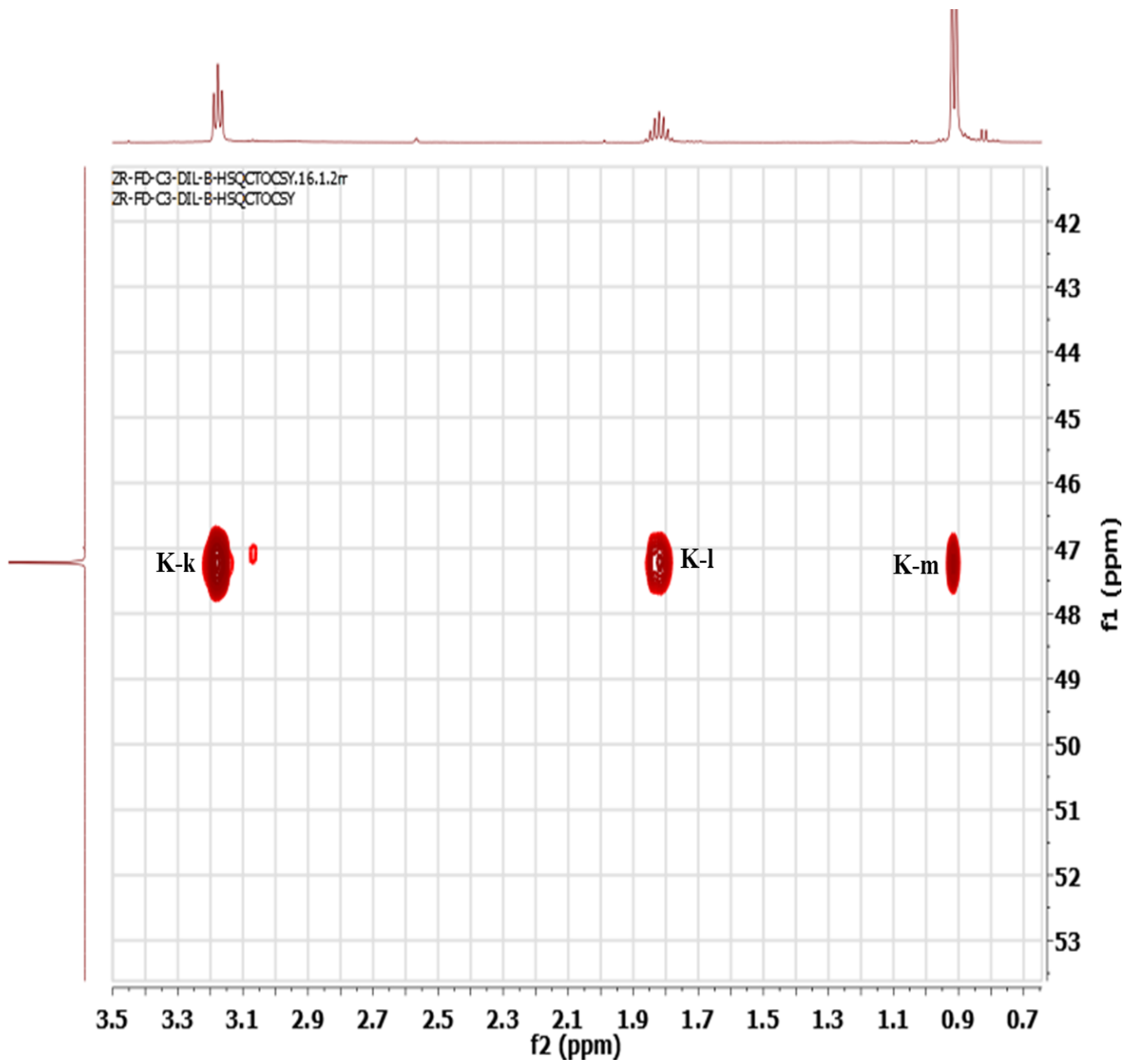
Appendix 19: Expanded HSQCTOCSY-NMR spectrum of zanthoxylamide, version 1



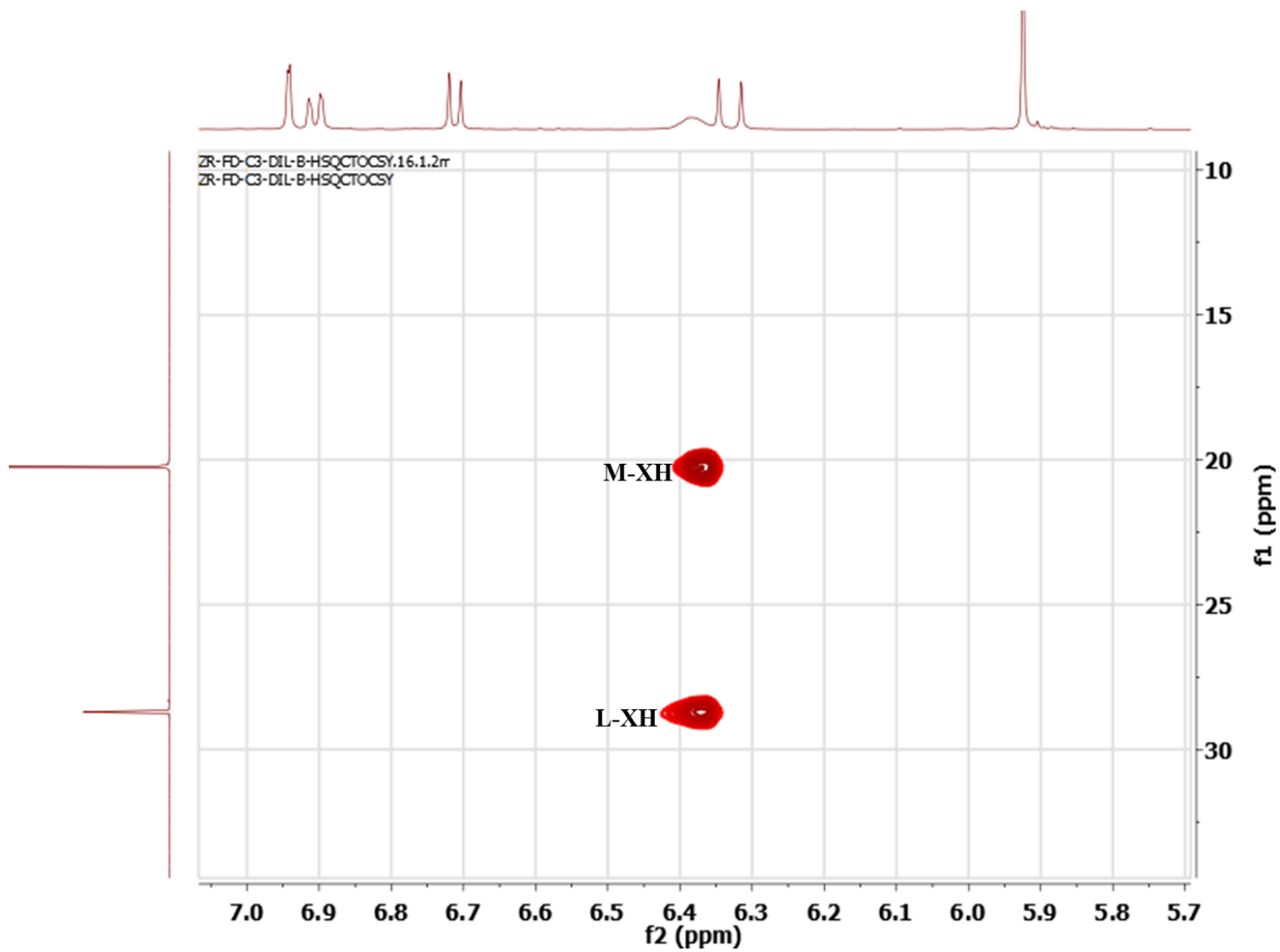
Appendix 20: Expanded HSQCTOCSY-NMR spectrum of zanthoxylamide, version 2



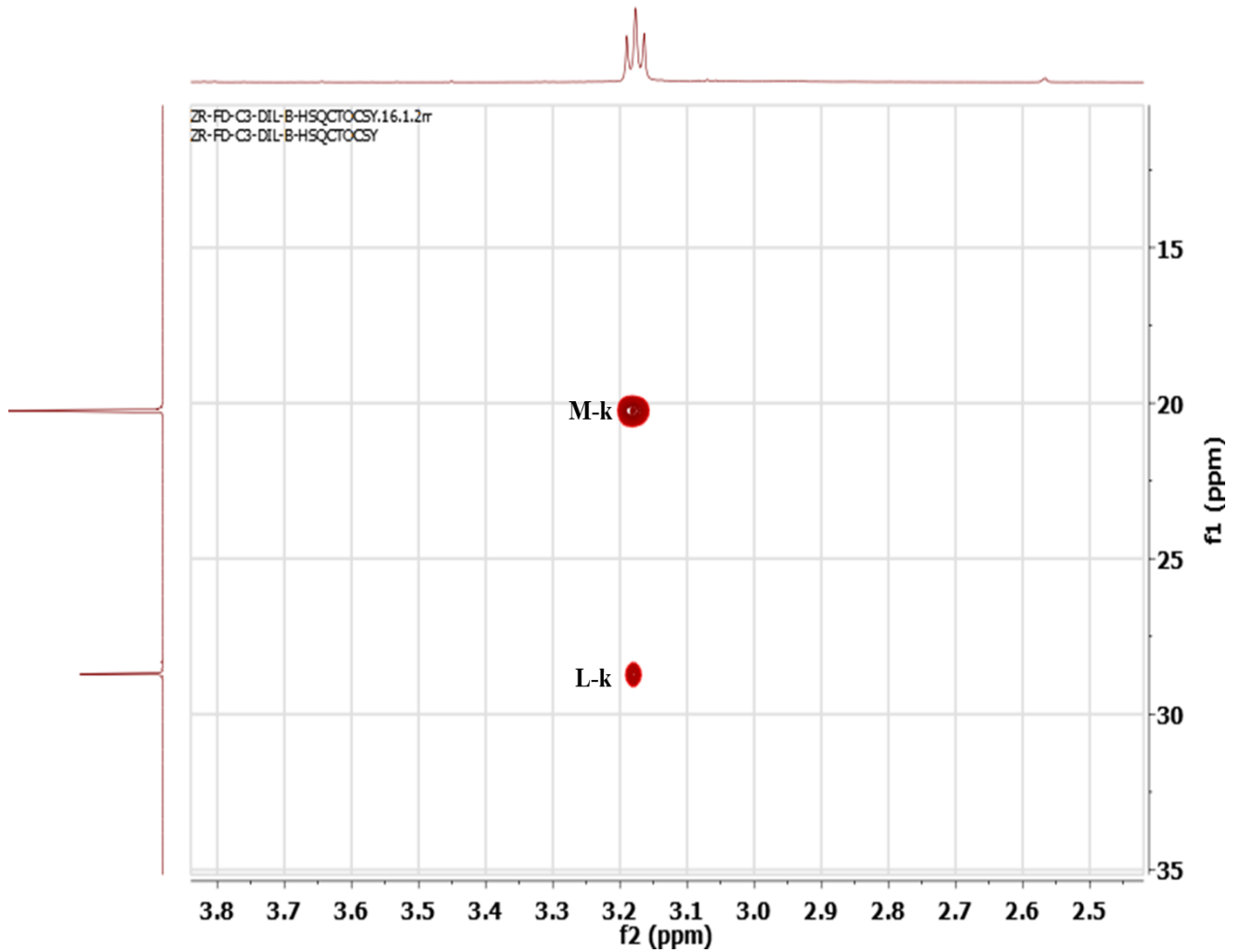
Appendix 21: Expanded HSQCTOCSY-NMR spectrum of zanthoxylamide, version 3



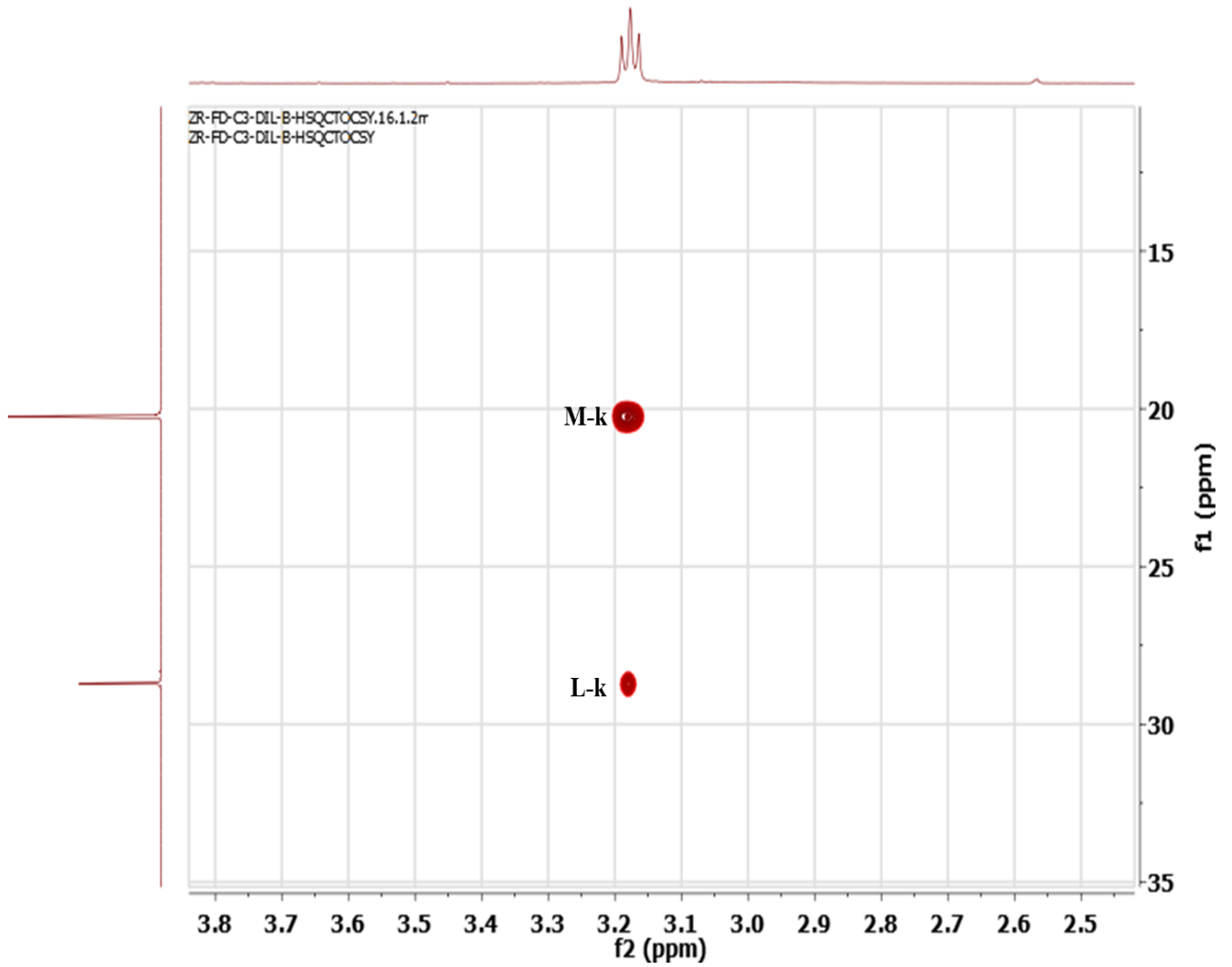
Appendix 22: Expanded HSQCTOCSY-NMR spectrum of zanthoxylamide, version 4



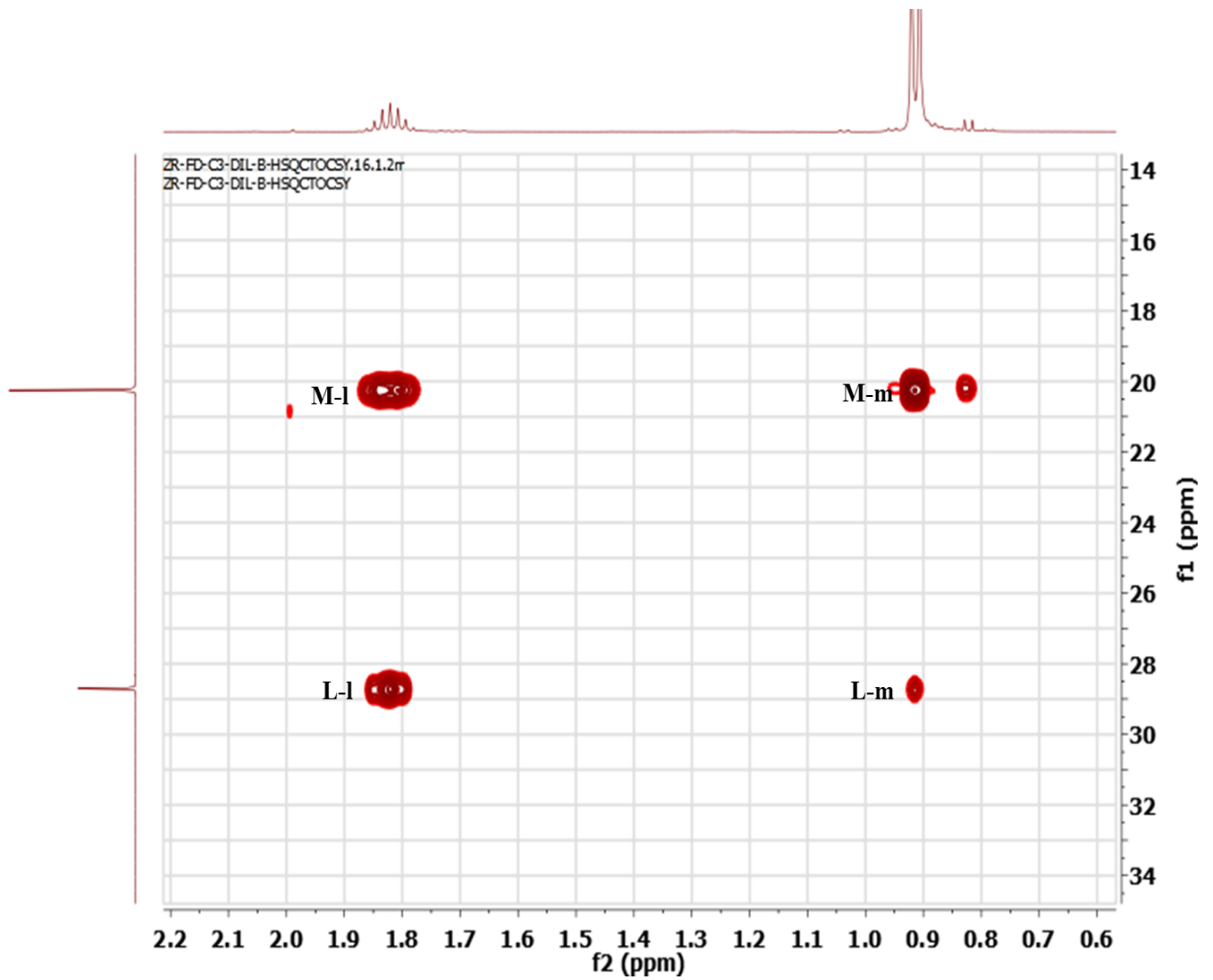
Appendix 23: Expanded HSQCTOCSY-NMR spectrum of zanthoxylamide, version 5



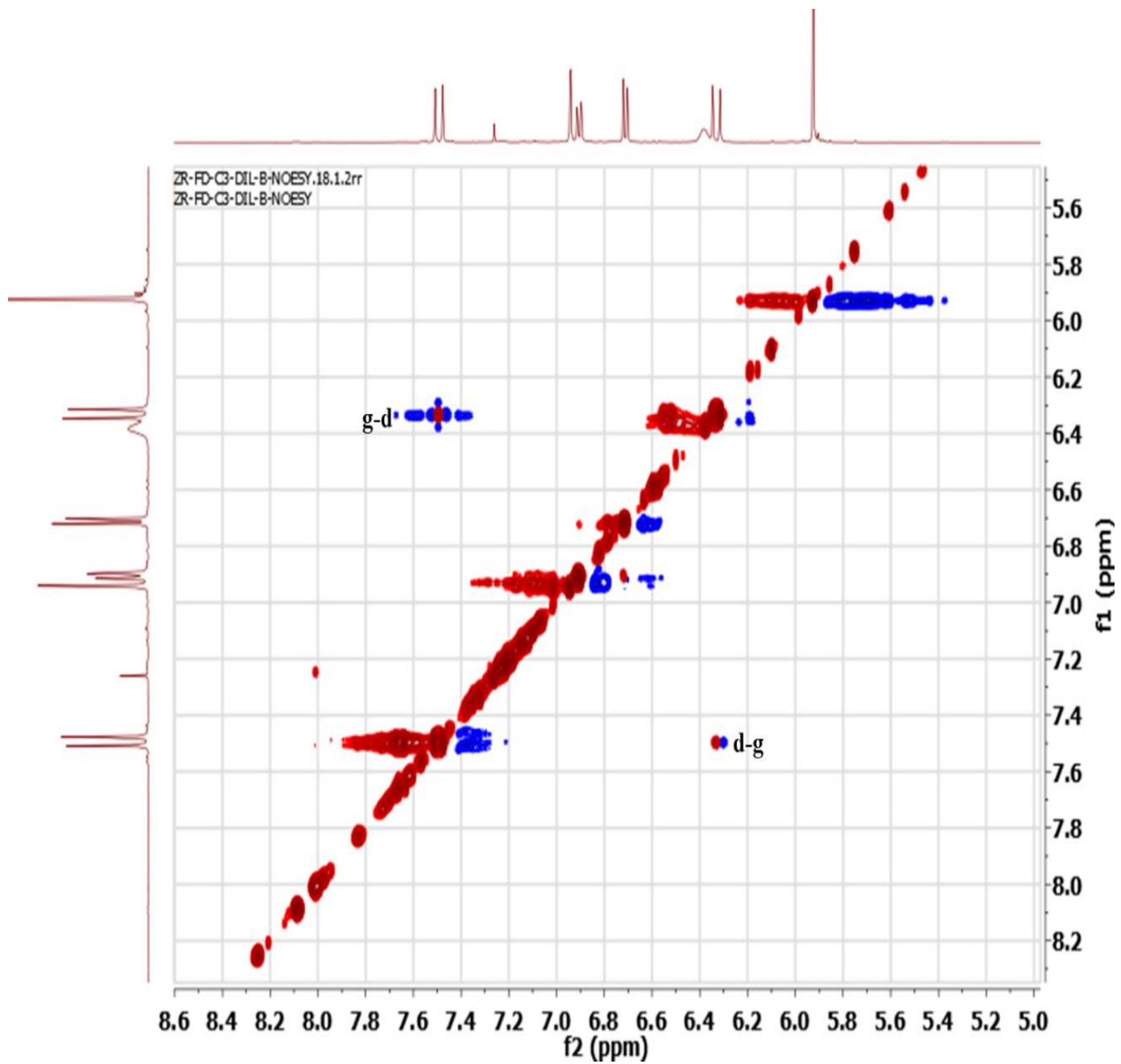
Appendix 24: Expanded HSQCTOCSY-NMR spectrum of zanthoxylamide, version 6



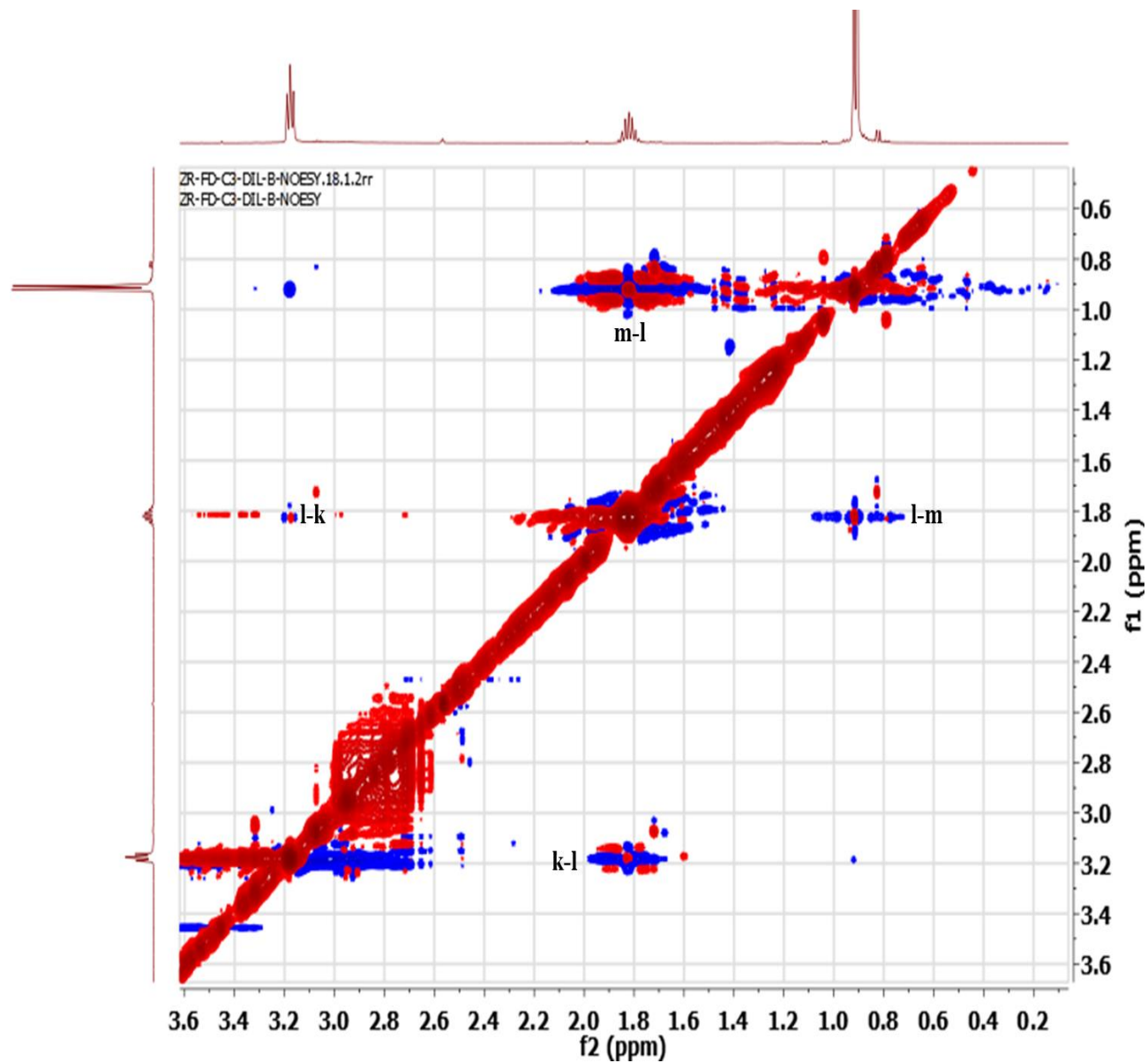
Appendix 25: Expanded HSQCTOCSY-NMR spectrum of zanthoxylamide, version 7



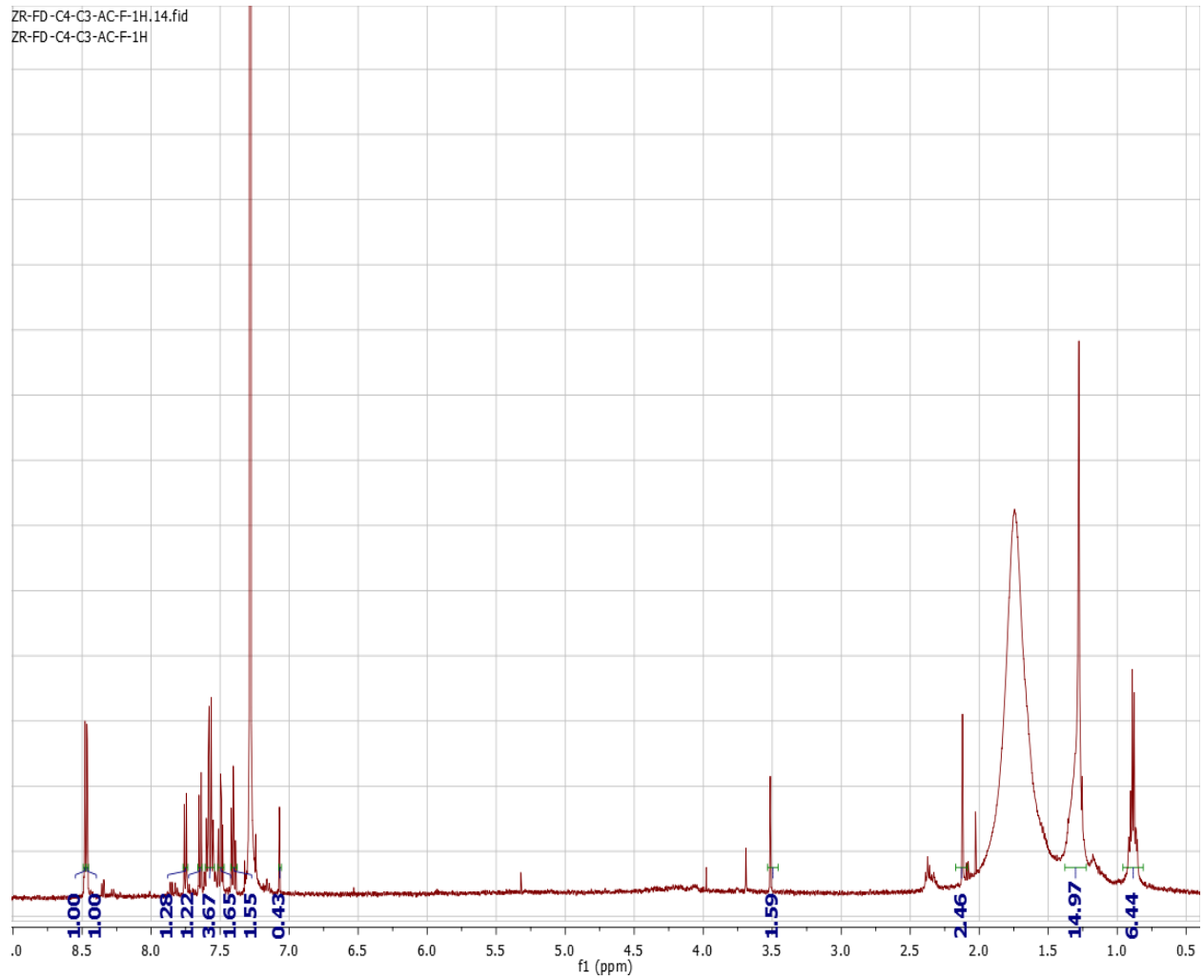
26: Expanded NOESY-NMR spectrum of zanthoxylamide, version 1



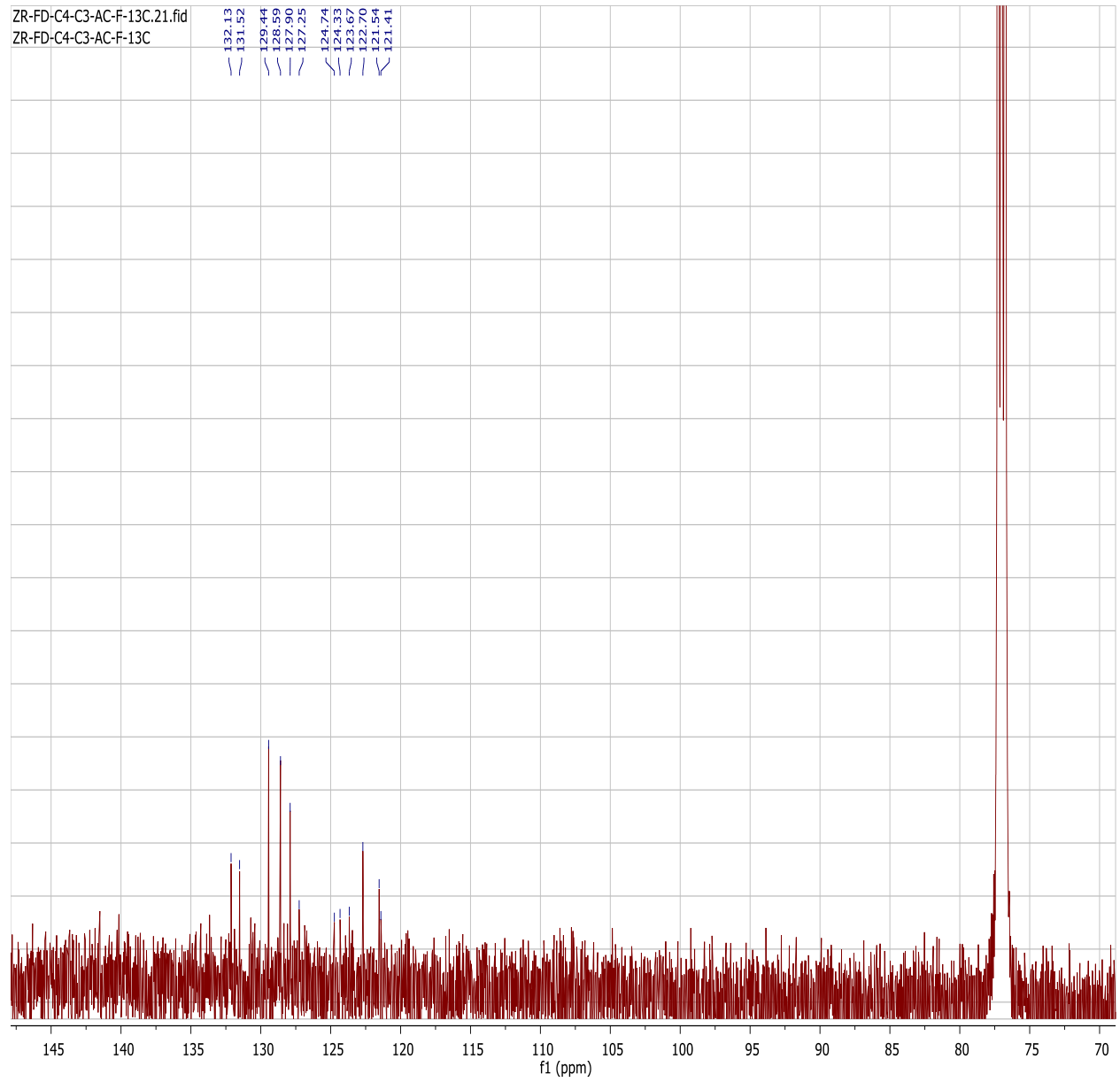
Appendix 27: Expanded NOESY-NMR spectrum of zanthoxylamide, version 2



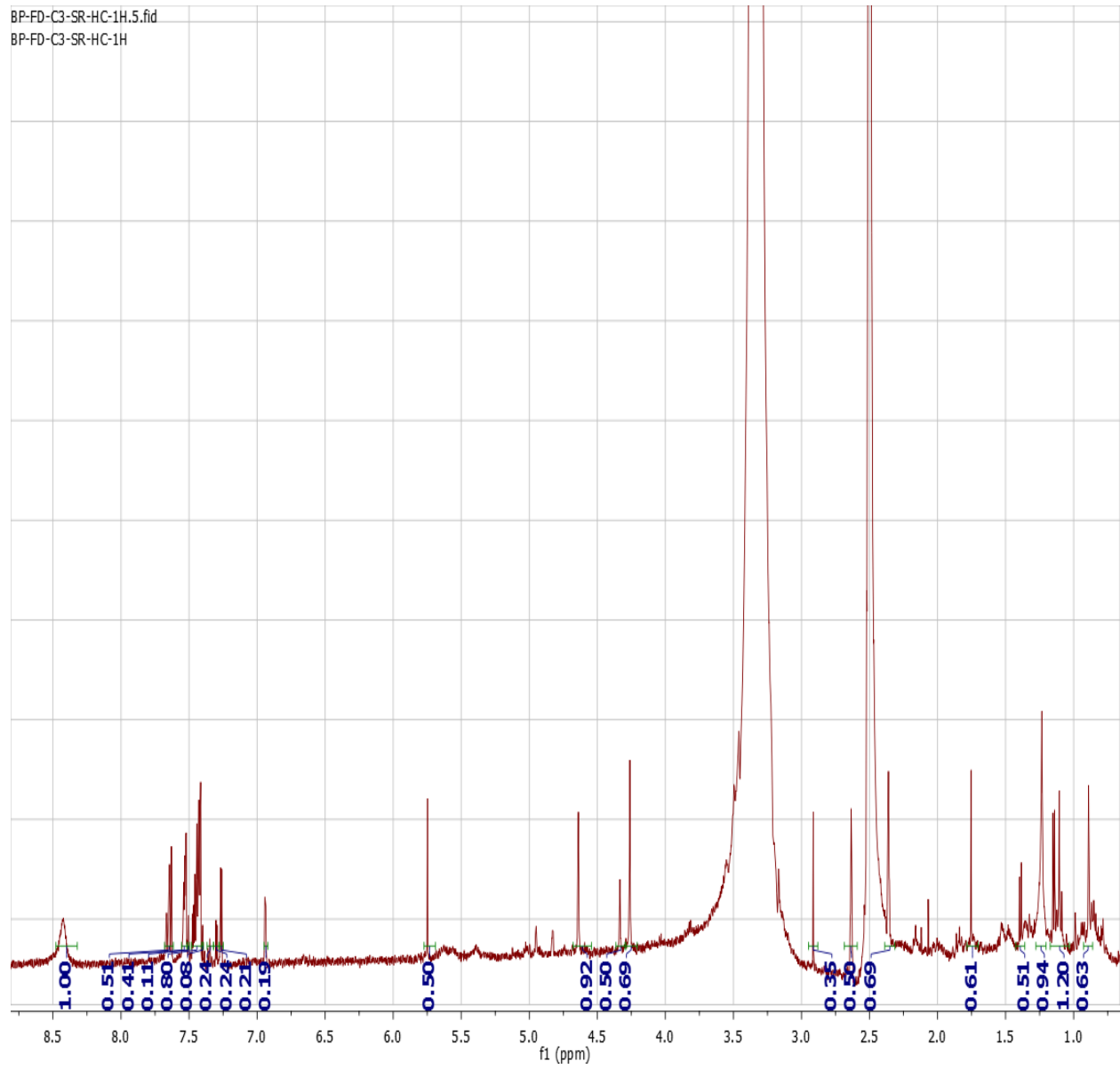
Appendix 28: ^1H NMR spectrum of ZRFD-C4-C3



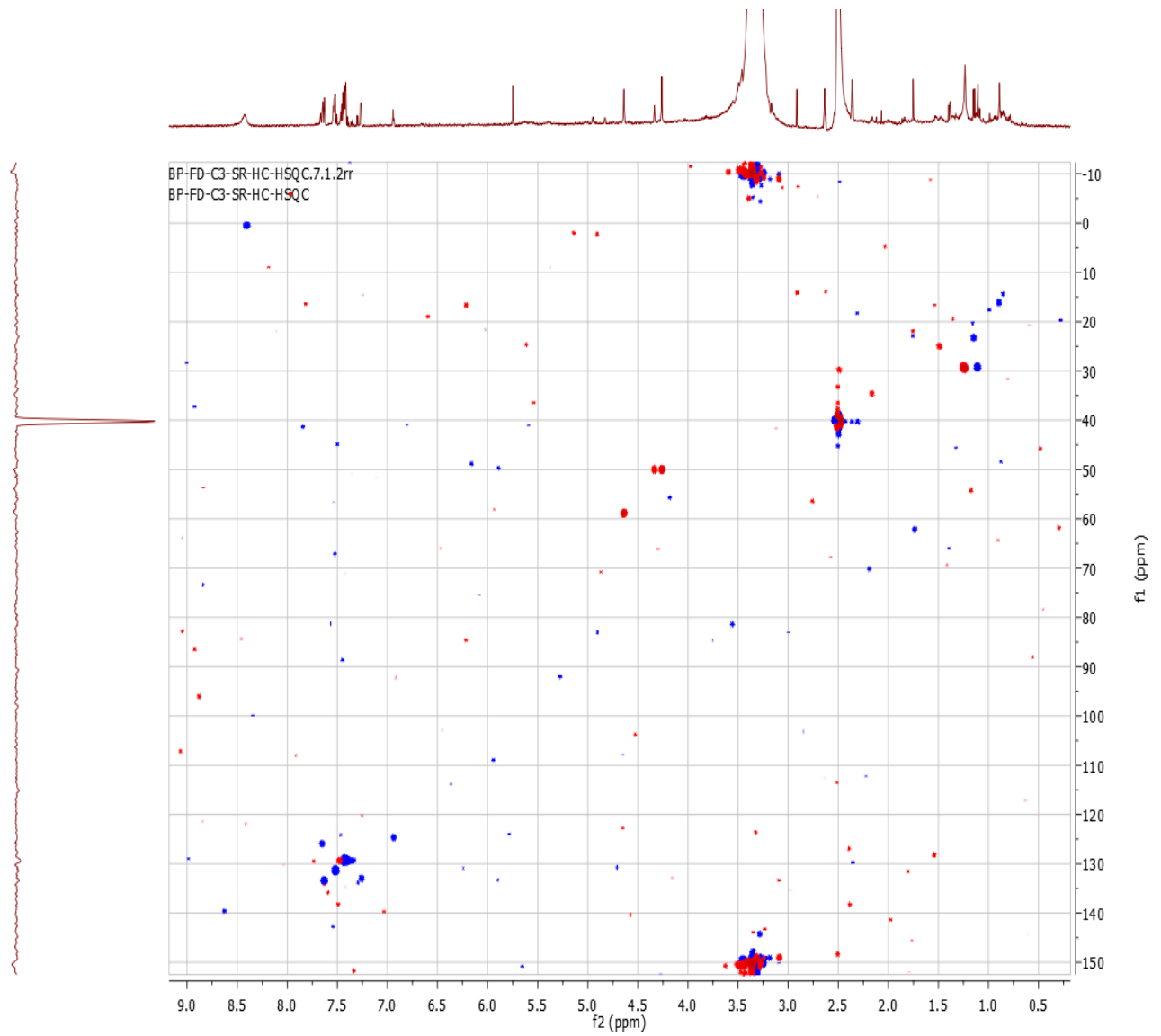
Appendix 29: ^{13}C NMR spectrum of ZRFD-C4-C3



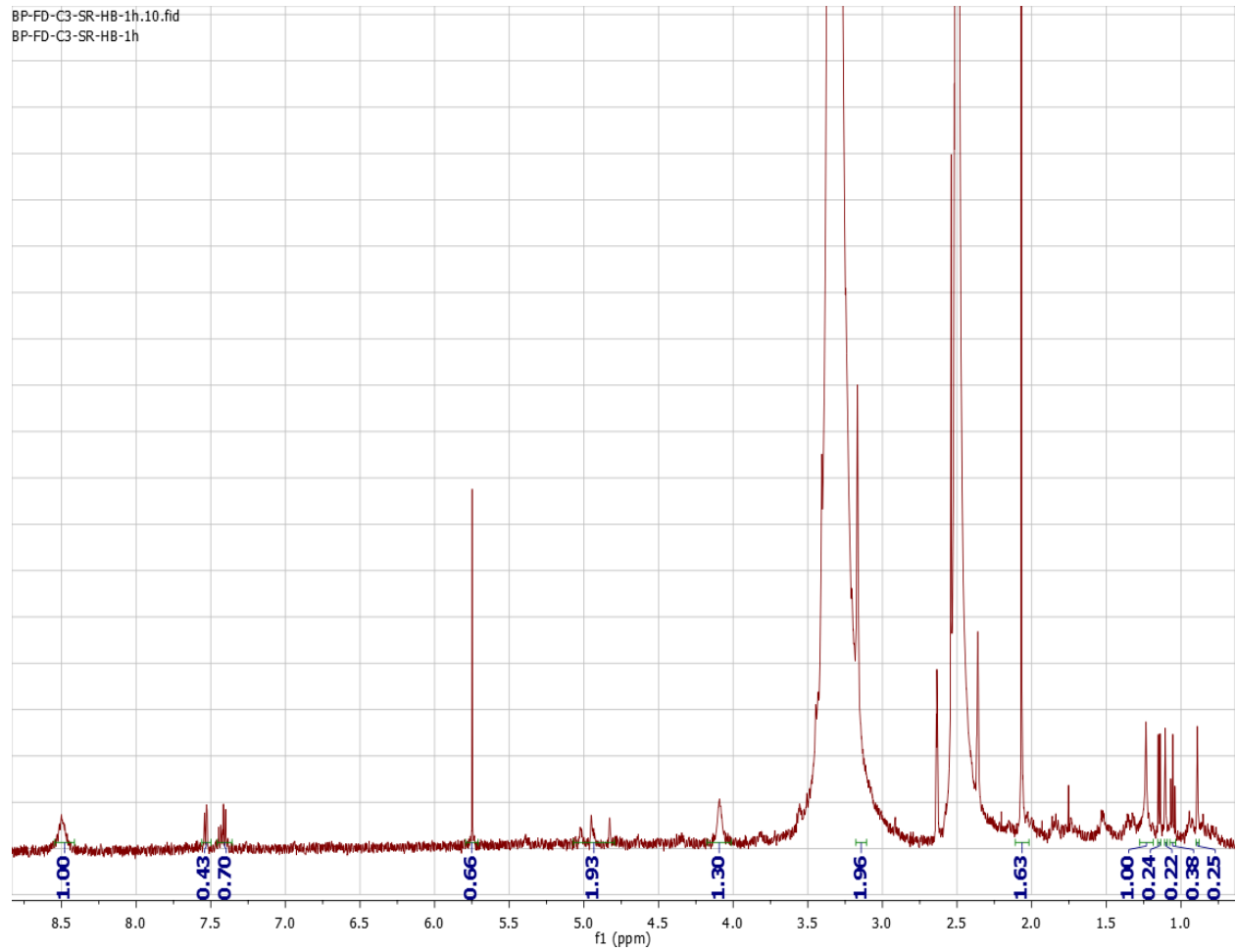
Appendix 30: ^1H NMR spectrum of BPFD-HC



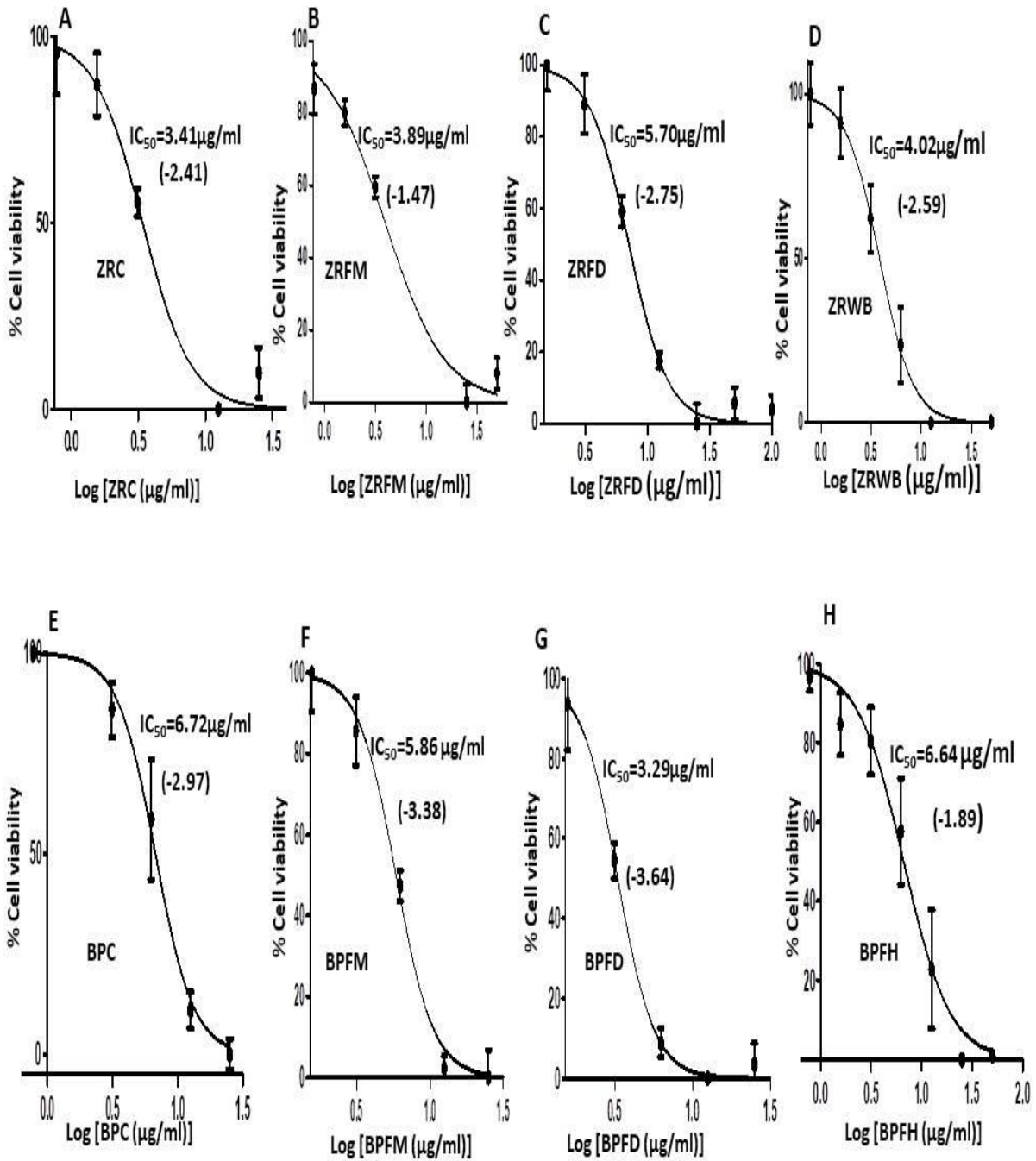
Appendix 31: gHSQC spectrum of BP-FD-HC



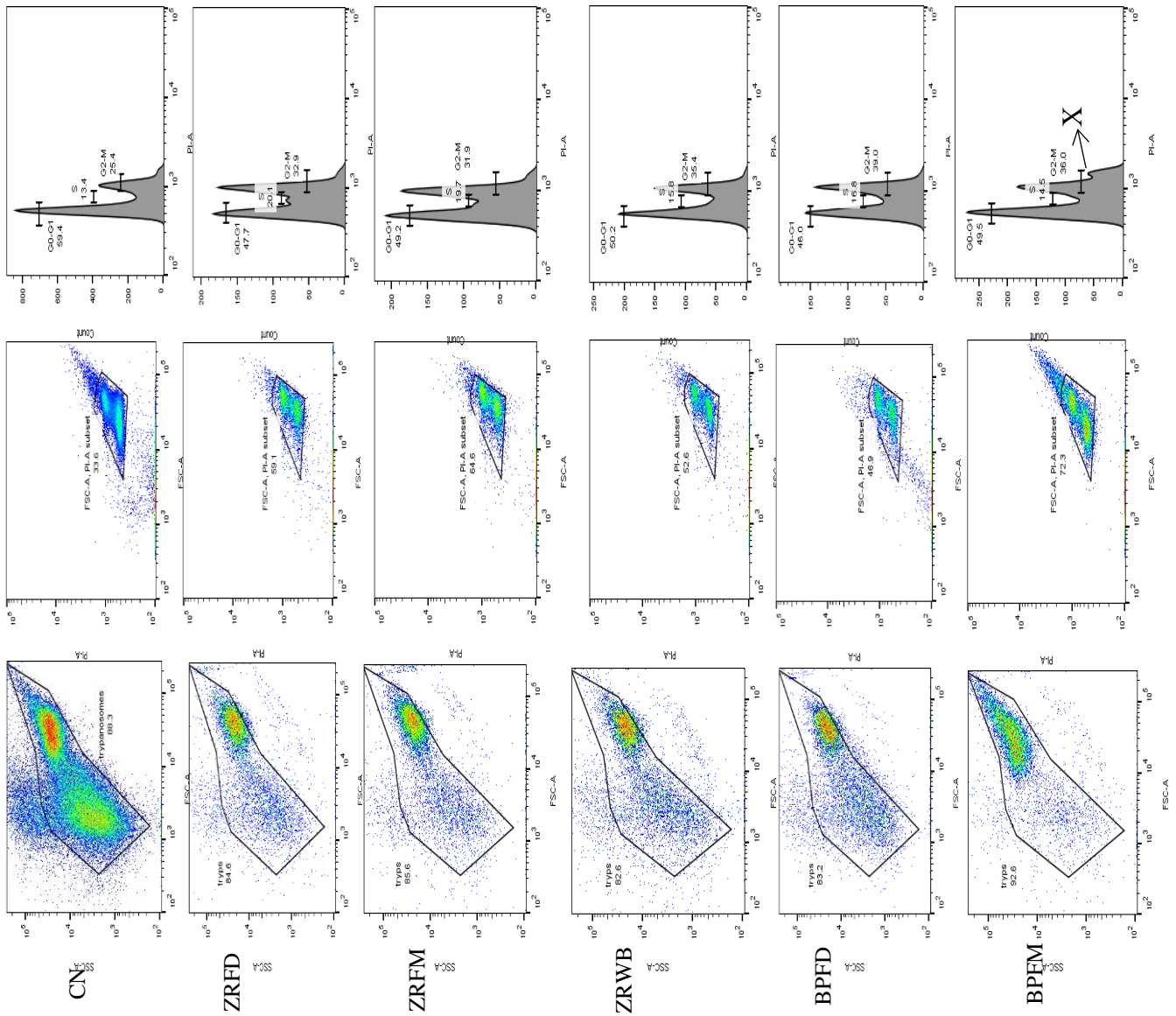
Appendix 32: ^1H NMR spectrum of BPFD-HB



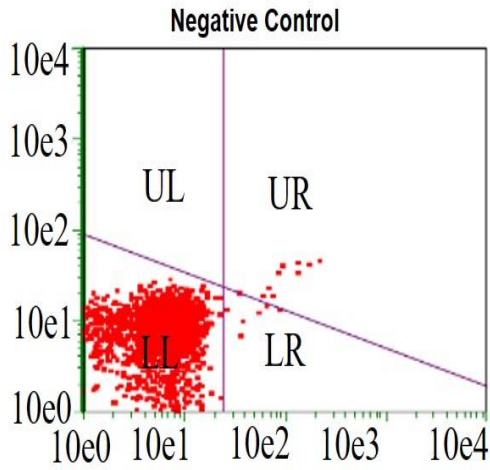
Appendix 33: Dose-response curves of Kupchan fractions



Appendix 34: Effect of Kupchan fractions on cell cycle of *T. brucei*



Appendix 35: Effects of Kupchan fractions on induction of cell death in *T. brucei*



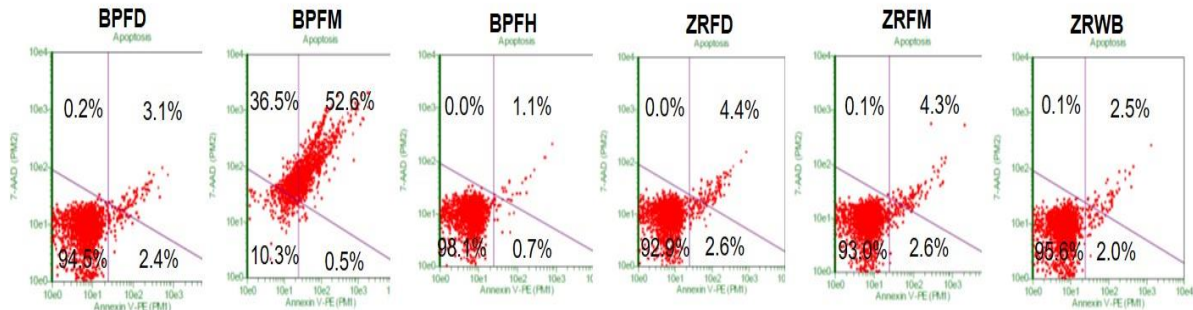
LL= Viable cells

LR= Early apoptosis

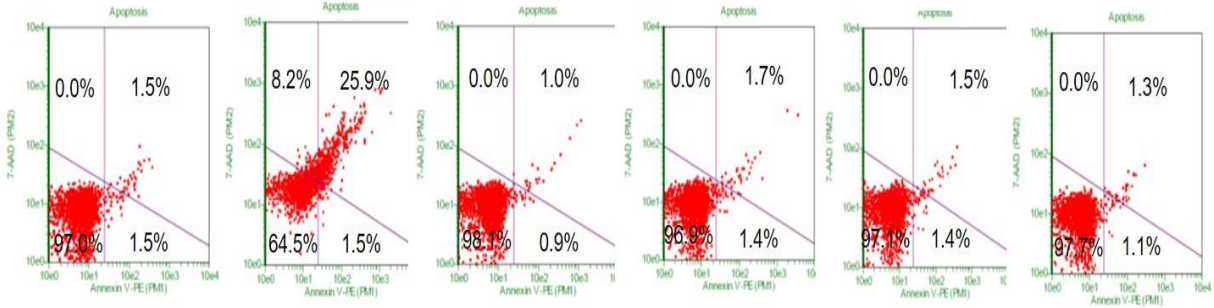
UR= Late apoptosis

UL= Necrosis

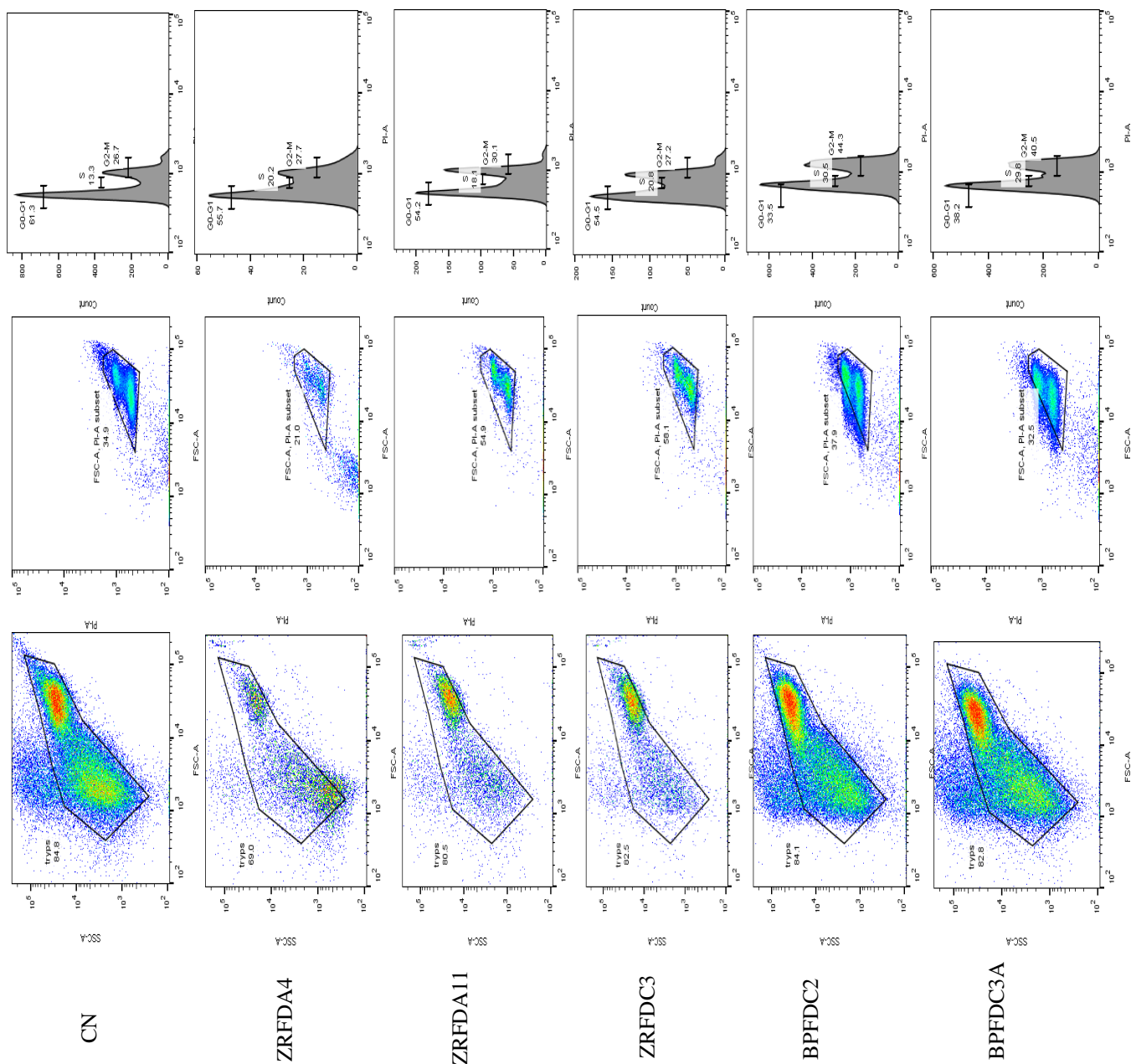
Fraction concentration = 12.5µg/ml



Fraction concentration = 6.25µg/ml



Appendix 36: Effects of compounds on cell cycle of *T. brucei*



Appendix 37: Protein sequence: Tb927.4.2100, hypothetical

MTVIHLFLYVKMYFVALCFPMQLDVVITQDFCCCGITPIGAVFLVRLDTIDFAVTLPLSE
YGAAAYVDIVGRTGDCRRENGVVGASAAEYLNGAHHVDSVVYVGNVRTLWMRYRSAT
QTFELSCLSSPTKIASYLLGKAWNCTASQKEKGRY

Appendix 38: Protein sequence: Tb927.3.1490, leucine-rich repeat protein, putative

MATQLNSDTVTDSFPKSGEQSRSDSGLGERMNAARNKGWKELDISYFKEVEDVGNLC
EVAGLFLEDLNFWSCTNIRTTGLEKICTVECFPSLQRLYLNGTGTNDRCIDKLSRGNLRV
LECGYCRNITDVRPLERNETLEVLSLRGCQNIVHGLEDVCGRWLINLRELYLSDMVAVT
DACIEAIGNSKKSLVRLECENCERITNVSALGNVKTLLKVLNLSHNSKNIAEGVSNIFEISEL
QDLGFRGFAKITQVNLMPWQRCASLTTLDSLGCCKKVTNLNLGGECRKLVCCLKLSECPQ
LREVDITGCESLTALNISGRWHLKVVKLNKGCKELKSIDLSVCPHLEDVYGVCDCCKNLEIF
NLCFCSRLTKLELVELEKLMNLNLCGCKDLEDIGSPSRWGKNLVELNVSMCRKLNLYMD
LSGRVKLEKLNLSQCDSLVEVNLSGCQNLSSLLDLSNSRELEILNLCNCGELPALNVDGC
VNLQILILSGCRSLSTMKLSECNLRETDFSGCAKLSAIKLSSRRGIKLVKLDGCIDLMSL
DLSECVSLKDLIGVSGCTQLKSLNLSGCSRLADVAALKDLKGLVRLNLSRLVEVVDLSM
LTGHEDLEELNLSQCNALADISGLKGECSTKLISLNVSWCRSLSAICVLSECCRNLTTLDI
SGCWNLDDMSVLGSLKSLSVLNLSWCSQLTDINMLAGLNCLAVLNLSWCNQLVDASV
VSELESIAILNLSYCCELARLNLSGCIKCLKCLDICGCVSLKHLTGLRKCTNLES LFACGYR
DAAEDVRDEFLNIPCSATLHIDESTDREVIQELMGWGVRVKTI

Appendix 39: Protein sequence: Tb927.4.3880, receptor-type adenylate cyclase GRESAG 4, putative

MIYHSETDGPHTPAASKSAGSAVWHCRLSTVMALLFSNVLP AHSEGNIKVKVYSFSL
QRLPLRLTEAINAGLNASFAARQWTVAPNVTQVPPPPNNV SFMETLHDTINQNGKF
IIIIGPMGDVETLHALPLLEREDLVAFAPITGSDSVRGWNPNIYFIRASPTAELIALVRYAV
SQLRLLRIGFMYLQDISFGDREHEHAVELF SHMGRELCGVFTVKSSMEAFADDRAFEAA
WEFAKTRPQGVILFAPPAARDTVKFITKMVADKRTRDAYVLAPSALEFVVEVTWRFA
LAAAGKQLKPGQVILGTNPLAADIRYQAIRRFQDHMRSYLSANPGVTVFNGTDNFHH
DDVDGELMVYGW IAGEVLSQALSSREWLT SRKAFMESLYNQRRYVIDDLVIGDFGGDC
KGGAGERGAACNCNQGGSVVYVKQFAENYKLLPAKNPVKVIQHGMCDADGIILYAPL
NGLFILSNESHRRKKINREIHKSASATNRNADMTQFHRLFFHSMASSSAESARTLQHQLD
TRSVTAVFGVDDAMLSIAEVA FVDPVMLTPRLHHRGKNVIQLSPTLEQQLFVVVGYV
TNTSASAPMSAIVRGADATIEVALRKIVWMHGGTLQTVAVLDDNATLVGRLPNRGNA
FVIGLAPGDPSLLAAHLDRNPDRVLPFFDVALMYDELVS AFNGNPNAERVQFATSLP
HWADANTSSEIVREFHTALPDSSAWKPLPLLG YAAARFAQAVLPRMEYVTPKTLTLDTIY
MQSIITADEMRYGPFEEEEKECFTANDPVPEQGEVCVVNYGATRISMWSLARALNASV
PPLTSPVTPLIRYADPNAIKLSSAQLAGVIVGSLVALALFAAPLVVVLVYVLRRGARDNDS
APKEPVEPVTLIFTDIESSTAQWAAHPELMPDAVSTHRLIRSLIVQYGCYEVKTVGDSF
MIACKKPFAAAQLASDLQRCFLRHEWGTTAFD DSYREFERQRADDDNEYKAPSARLDP
EVYRQLWNGLRVRVGVHTGLCDIRHDEVTKGYDYYGR TSNMAARTESVANGGQVLLT
RAAYLSLSNSERGLDVTALGMSLRGVPEPVEMYQLNAV VGRSFAALRLDHEAGEDG
DLSSTSFSDTGSLRGSINASAQKFSISIKAVFGAFAPAHQQQLLMPLCERWQVSLPPSSKA
TWNEEYCEGVIRRIAVKVGRVADHCAASGSEHSVSTLGSASLIISNHGLERELHGN

Appendix 40: Protein sequence: Tb927.11.9770, hypothetical, conserved

MAIARTTVTTVLDGLYFADRAVKMTHAAHRGCSFVCTPALLACTCPGTSVAVRLTPLS
TGRPPLARMELLGQCAVSLFRAQRLAFHCAGEEGRAQMHELTLKRGDVIAVLGGCELD
RDWGSVERTLKSVAHADLEYMAEEMLLELGRGTRRTGGGNGEVVSNSTCVMTVVQD
RPSGLLPQPPSCLG

Appendix 41: Protein sequence: Tb927.11.1640, stumpy formation signaling pathway, putative

MSGQRNSLRDAPVEAVSRRPRTNDIVDNNQGEREVLYVKAPLTFDPTPRVLPQSGYNQ
QYQSPPRVQRRRRGGGKTLYVRTDDSESEKEGSSDGRNGMRQLVTAAEQPEGSDSDVG
EEEDSSSFMGKLAACGDAFLRVANSIPGTVFGVCQKWHVTGILIFLFFFLCFMFFLMLSA
KQAQYAAKVIEHDNRQSLLFTASLVDQHLMAANEARKLMGSDSQRSAAALKEAKLHV
EELAELCDGSIKQLHSRILYPGPVEDIKFLEEHVAYEANLVRLIKEEVEWFERHVHDHK
KVTTGPQTGVGNASSKKKERTPKHRQGQKFTLTKTGFYLGAGDGPEANSKDLLPFFRV
FLGLLGNRVIVAVALLALVVLYRRLS